C10G-E070

SHIMADZU
Excellence in Science

Solutions for

Electronics & Chemicals

Application Notebook

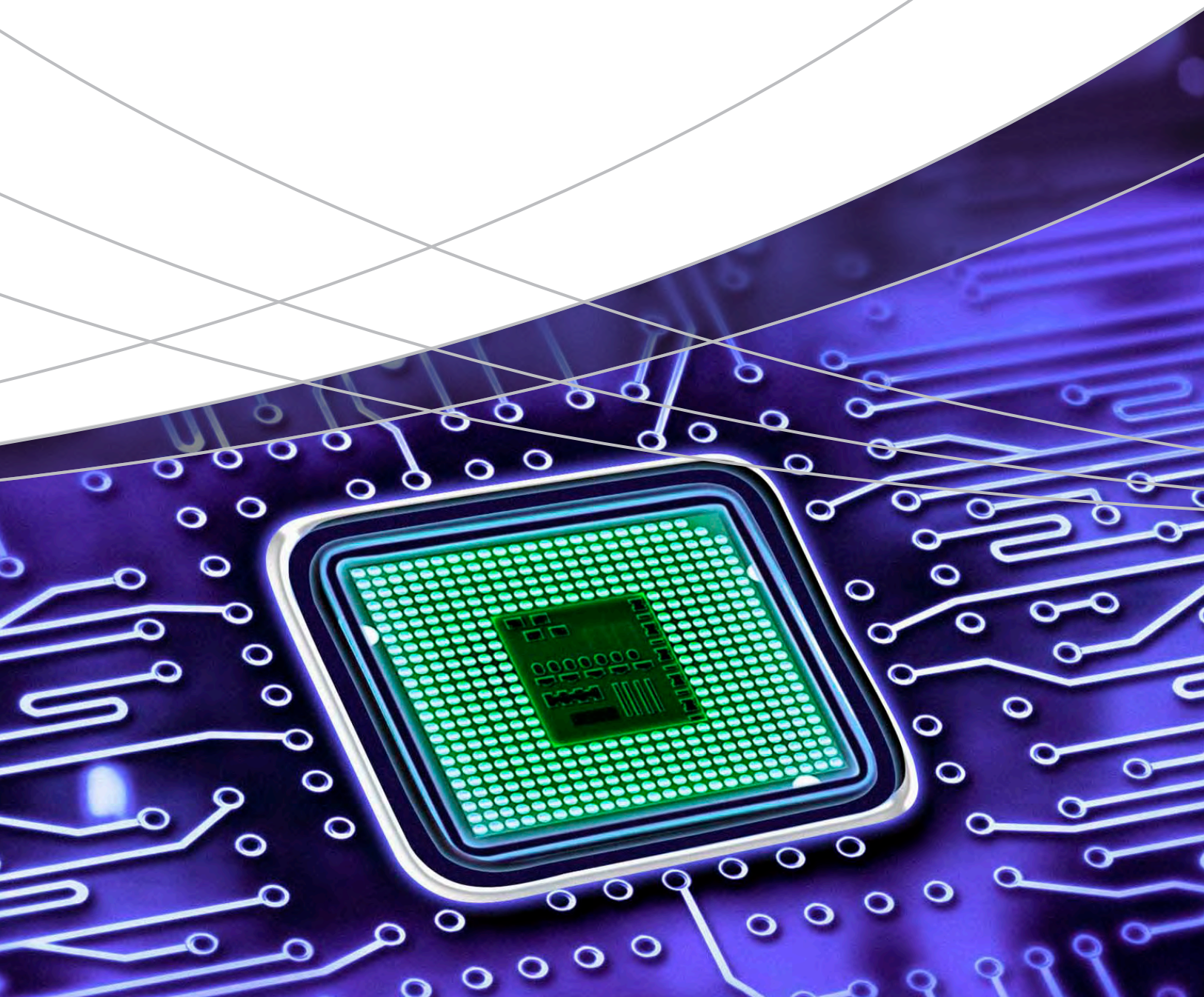

Solutions for

Electronics & Chemicals

Application Notebook

Introduction

Both inorganic and organic analyses are indispensable for electronics industry and related chemical industries. Purposes of analysis are wide ranging, and data generated can give much insight for research/development, reduction of defects, conforming to regulations and increasing productivity, all of which will contribute to delivering better products to consumers with diminished impact on our environment.

This application handbook is a compilation of case studies where analytical techniques are playing critical roles in various parts of electronics industries. It demonstrates the range of analytical solutions provided by Shimadzu, from simple evaluation test to combinatorial use of inorganic and organic analytical methods. We are hoping that you will find the solution that addresses your needs.

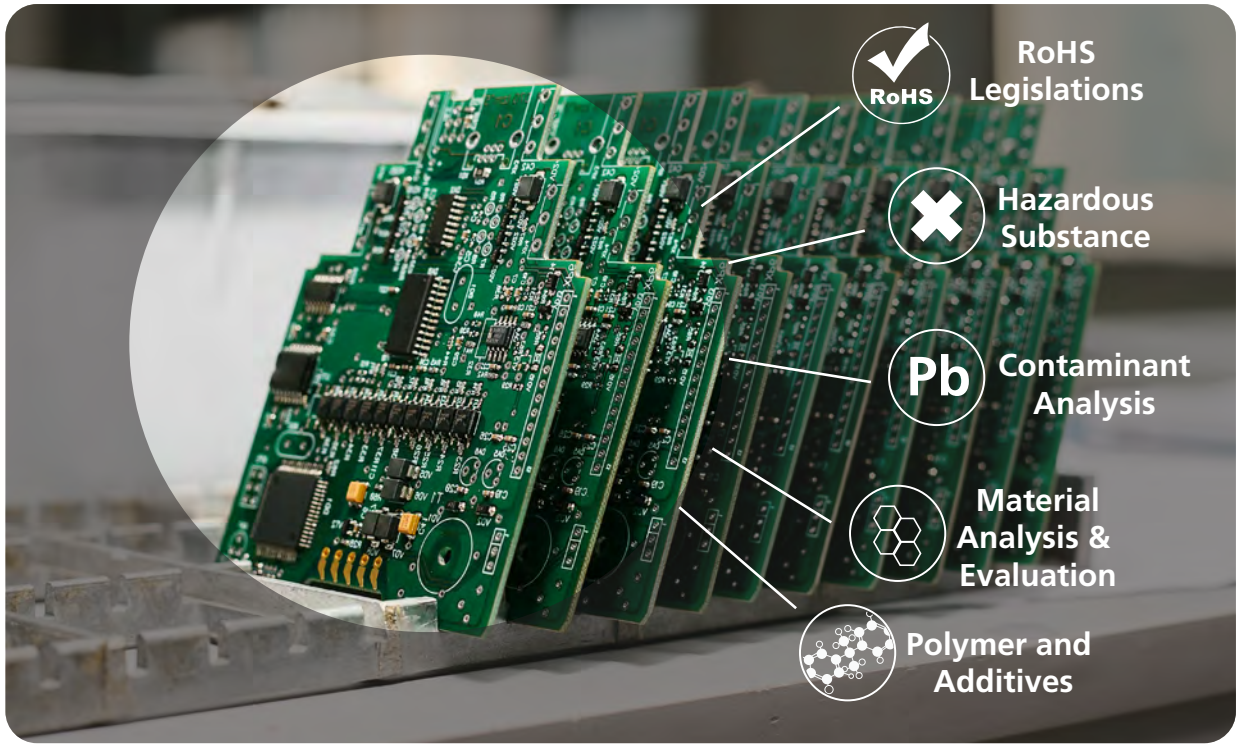

RoHS Legislation

Analysis of Phthalate Esters Using the Py-Screener (1)

This application data sheet introduces measurements of phthalate ester standard samples using the Py-Screener.

Analysis of Phthalate Esters Using the Py-Screener (2)

This application data sheet introduces an example of the analysis of phthalate esters and brominated flame retardants using the Py-Screener.

Screening Analysis of Phthalate Esters and Qualitative Analysis of Other Additives in Medical Supplies Using the Py-GC/MS Screening System

A simultaneous Scan/SIM analysis method was paired with Py-Screener's high-speed scanning mode to perform a highly sensitive screening analysis for phthalate esters using SIM and, perform a qualitative analysis of other additives based on scan information.

A Pyrolysis-GC/MS Screening System for Analysis of Phthalate Esters and Brominated Flame Retardants

In this application note, a PY-GC/MS method has been used to screen for seven phthalate esters and 11 brominated flame retardants.

Hazardous Substance Analysis

Simultaneous Analysis of Lower Aldehydes That Do Not Require Derivatization

This data sheet introduces the analyzing lower aldehydes in water using HS-20 headspace sampler and Tracera high sensitivity gas chromatograph system (GC-BID).

Analysis of Organic Solvents and Specified Chemical Substances in a Working Environment Using Two Different Columns (1)

This article investigates the analysis of 58 organic solvents (including some specified chemical substances) subject to the working environment measurement.

Analysis of Organic Solvents and Specified Chemical Substances in a Working Environment Using Two Different Columns (2)

This application data sheet introduces the results of investigating the quantitative analysis of 58 organic solvents using the Twin Line MS system.

Test Methods for Certain Aromatic Amines Derived from Azo Colorants

This data sheet provides an overview of inspection methods for certain aromatic amines derived from azo colorants, as well as a description on separation of certain aromatic amines.

Analysis of Naphthalene in a Working Environment

In this article, an investigation was performed using a gas chromatograph mass spectrometer (GC-MS), in accordance with the naphthalene standard measurement analysis method.

Analysis of Leachate from Water Supply Equipment Using Purge and Trap GC/MS

The purge and trap GC/MS system enabled the measurement of components in the leachate from water supply equipment with high sensitivity and high accuracy.

Off - Flavor Analysis in Chemical Material Using a Thermal Desorption Method

In order to narrow down the candidate off-flavor causing substances, the quantitative values for the defective product were compared to the quantitative values for the normal product.

Analysis of VOC and SVOC Emissions from Automotive Interior Materials in Accordance with VDA278 Using the Thermal Desorption Method

After evaluating TD-GC/MS method for standard samples, the automotive interior materials (rubber, plastic, and leather) were sliced thinly and analyzed using this method.

EDXRF Analysis of Arsenic and Lead in Dietary Supplement

Using an energy dispersive X-ray fluorescence spectrometer, the quantitative analysis of As and Pb in a dietary supplement was conducted and their LOQ/LOD were evaluated.

Contaminant Analysis

Material Analysis and Evaluation

Polymer and Additives

SHIMADZU
Excellence in Science

Application Data Sheet

No.110

GC-MS
Gas Chromatograph Mass Spectrometer

Analysis of Phthalate Esters Using the Py-Screener (1)

BACK TO CONTENTS

In the RoHS directive (directive on the restriction of the use of certain hazardous substances in electrical and electronic equipment), four phthalate esters: diisobutyl phthalate (DIBP), dibutyl phthalate (DBP), benzyl butyl phthalate (BBP), and bis(2-ethylhexyl)phthalate (DEHP), will be added to the six conventionally limited substances starting in 2019.

Of these, the substances that can be measured with GC-MS are the brominated flame retardants, PBBs and PBDEs, and phthalate esters. The Soxhlet extraction-GC/MS method, while an accurate quantitation method, requires time-consuming pretreatment and uses organic solvents. In contrast, the pyrolysis-GC/MS (Py-GC/MS) method does not require complicated pretreatment and is therefore expected to be used as a screening method. The “Py-Screener” is a screening system for phthalate esters using Py-GC/MS. It consists of polymer standard samples containing phthalate esters, a sample preparation sampling kit, and Py-GC/MS analysis files.

This Application Datasheet introduces measurements of phthalate ester standard samples using the Py-Screener.

Standard Samples Used in the Py-Screener

The Py-Screener uses the Phthalate Esters Polymer Standards for Py-GC/MS (P/N: S225-31003-91). These polymer standard samples can be prepared easily, without using organic solvents, by using a special sampling toolkit (P/N: PY1-K101 from Frontier Laboratories).

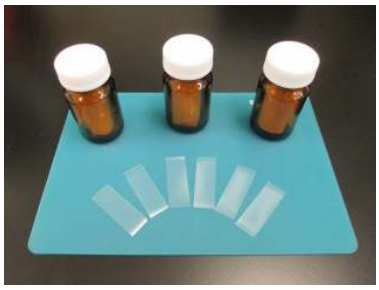

Fig. 1: Phthalate Esters Polymer Standards for Py-GC/MS (S225-31003-91), including seven phthalate esters
(Three types: Blank, 100 mg/kg, and 1000 mg/kg)

Preparing the Phthalate Ester Standard Samples

The phthalate ester resin standard samples are ribbon shaped and of uniform thickness. As a result, samples can be prepared just by placing two fragments of the sample (approximately 0.5 mg) in the Py Eco-cup using the 1.25 mm diameter micro puncher included in the special sampling toolkit. Fig. 1 shows the standard samples. Table 1 shows the repeatability for the weight of samples prepared seven times. The RSD is a favorable 2.24 %, and it is evident that the thickness is uniform.

Table 1: Sampling Weight Repeatability for the 100 mg/kg Phthalate Ester Standard

	1st	2nd	3rd	4th	5th	6th	7th	%RSD
Sample Weight (mg)	0.49	0.50	0.52	0.50	0.50	0.51	0.52	2.24

Analytical Conditions

The conditions registered in the Py-Screener were used as the GC-MS analysis conditions (Table 2).

Table 2: Analytical Conditions

Pyrolizer	:Multi-Shot Pyrolizer EGA/PY-3030D		
GC-MS	:GCMS-QP2010 Ultra		
Column	:Ultra ALLOY-PBDE (Length 15 m, 0.25 mm I.D., df = 0.05 Hm)		
[Pyrolyzer]			
Furnace Temp.	:200 °C→(20 °C/min)→300 °C →(5 °C /min)→340 °C(1min)	[MS]	
Interface Temp.	:Manual (300 °C)	Interface Temp.	:320 °C
[GC]		Ion Source Temp.	:230 °C
Injection Temp.	:320 °C	Measurement Mode	:FASST (Scan/SIM mode)
Column Oven Temp.	:80 °C→(20 °C /min)→300 °C (5min)	Scan Mass Range	:*m/z* 50-1000
Injection Mode	:Split	Scan Event Time	:0.15 sec
Carrier Gas	:He	Scan Speed	:10,000 *u*/sec
Flow Control Mode	:Linear velocity (52.1cm/sec)	SIM Event Time	:0.3 sec
Purge Flow	:3.0 mL/min	SIM Micro Scan Width	:0.3 *u*
Split Ratio	:50		

Results

Fig. 2 shows the mass chromatograms for the phthalate esters obtained by measuring the 100 mg/kg phthalate ester standard sample. They were detected with sufficient sensitivity even at a concentration of 1/10th the prescribed concentration. Table 3 shows the repeatability and MDL calculated after measuring the 100 mg/kg phthalate ester standard sample seven times. The repeatability for the quantitative values obtained (% RSD) ranged from 4.1 % to 5.7 %, and the MDL was 12.3 mg/kg to 16.3 mg/kg, which are favorable results.

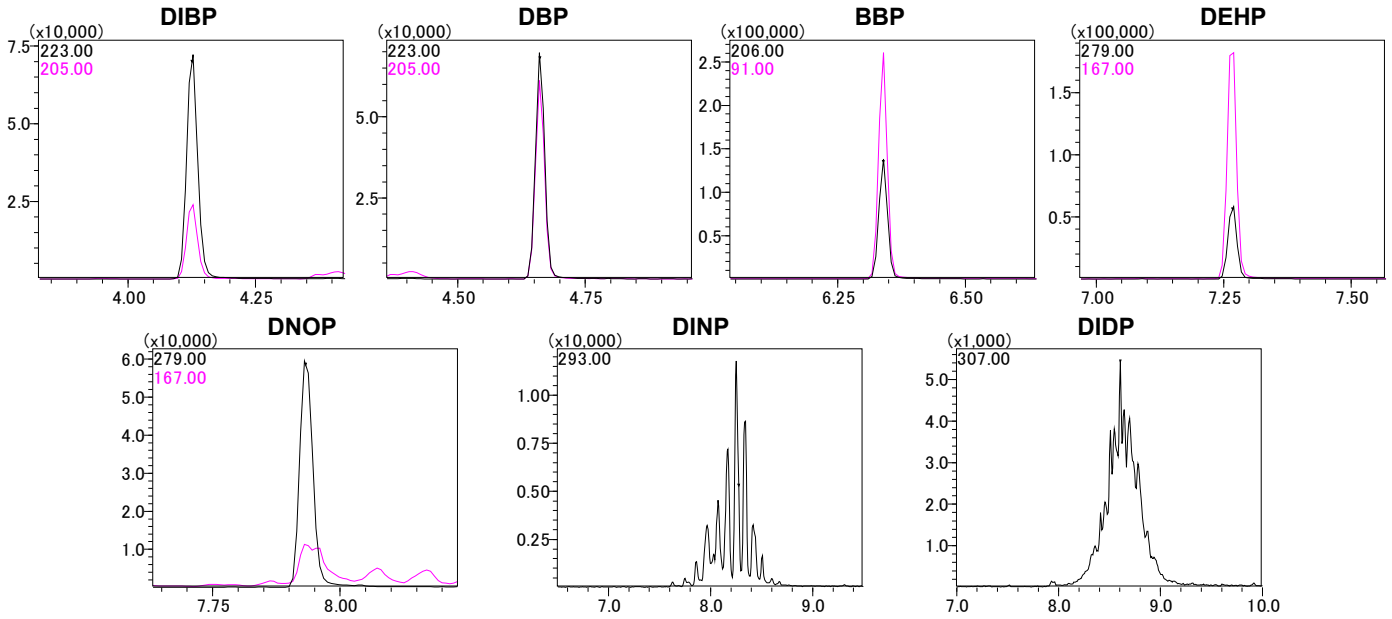

Fig. 2: Mass Chromatograms for the Phthalate Esters Measured in the 100 mg/kg Phthalate Ester Standard Sample

Table 3: Repeatability and MDL for the 100 mg/kg Phthalate Ester Standard Sample (n=7)

	Quantitation Value (mg/kg)							%RSD	MDL (mg/kg)
	1st	2nd	3rd	4th	5th	6th	7th		
DIBP	104.1	102.9	98.6	95.2	103.2	109.3	101.5	4.4	14.0
DBP	107.0	105.2	100.7	98.7	105.9	113.8	106.6	4.6	15.3
BBP	95.5	94.3	91.0	87.9	96.3	100.1	95.1	4.1	12.3
DEHP	110.7	108.5	101.1	101.5	111.2	115.3	108.4	4.8	16.3
DOP	101.2	101.9	93.9	90.3	99.3	103.9	99.1	4.8	15.0
DINP	94.3	95.7	87.4	84.8	92.8	96.8	92.5	4.8	13.7
DIDP	93.3	94.2	83.1	80.9	89.2	91.6	87.3	5.7	15.9

First Edition: Apr, 2015

Shimadzu Corporation
www.shimadzu.com/an/

SHIMADZU
Excellence in Science

Application Data Sheet

No.111

GC-MS
Gas Chromatograph Mass Spectrometer

Analysis of Phthalate Esters Using the Py-Screener (2)

BACK TO CONTENTS

In the RoHS directive (directive on the restriction of the use of certain hazardous substances in electrical and electronic equipment), four phthalate esters: diisobutyl phthalate (DIBP), dibutyl phthalate (DBP), benzyl butyl phthalate (BBP), and bis(2-ethylhexyl)phthalate (DEHP), will be added to the six conventionally limited substances starting in 2019.

Of these, the substances that can be measured with GC-MS are the brominated flame retardants, PBBs and PBDEs, and phthalate esters. The Soxhlet extraction-GC/MS method, while an accurate quantitation method, requires time-consuming pretreatment and uses organic solvents. In contrast, the pyrolysis-GC/MS (Py-GC/MS) method does not require complicated pretreatment and is therefore expected to be used as a screening method. The “Py-Screener” is a screening system for phthalate esters. It consists of resin standard samples containing phthalate esters, a sample preparation sampling kit, and Py-GC/MS analysis files.

This Application Datasheet introduces an example of the analysis of phthalate esters and brominated flame retardants using the Py-Screener.

Analytical Conditions

The conditions registered in the Py-Screener were used as the GC-MS analysis conditions. For the detailed analysis conditions, refer to GC-MS Application Datasheet No.110, "Analysis of Phthalate Esters Using the Py-Screener (1)."

Results

A calibration curve was created using the 1000 mg/kg phthalate ester resin standard sample. KRISS CRM113-03-006, which is sold as a phthalate ester certified standard sample, was then measured and quantified based on this calibration curve. Fig. 1 shows the mass chromatograms obtained. Table 1 shows the results of a comparison of the quantified values and the CRM certified values. The yield using the certified values as reference was in the range of 92.9 % to 109.0 %, so the quantitation results obtained were favorable with a view to screening.

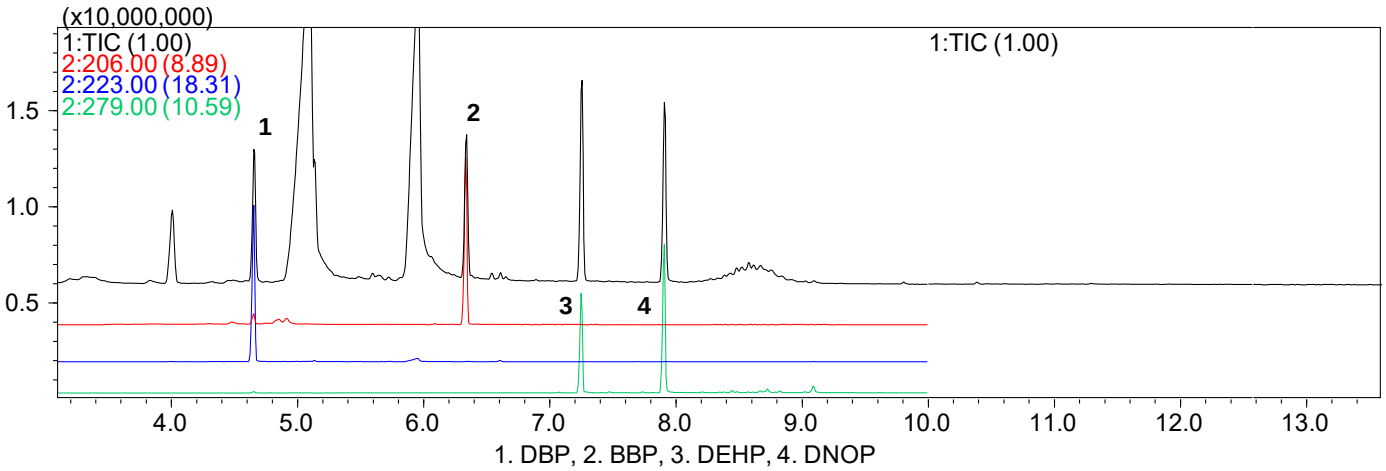

Fig. 1: Mass Chromatograms for the Phthalate Esters Measured in KRISS CRM113-03-006

Table 1: Comparative Results for the Certified Values and the Quantitation Results

	Quantitation Results (mg/kg)	Certified Values (mg/kg)	Yield (%) with the Certified Values as Reference
DBP	1059	972	109.0
BBP	894	962	92.9
DEHP	1015	989	102.6
DNOP	993	967	102.7

Figs. 2 and 3 show the mass chromatograms for a PVC cable and PBT resin measured as testing samples. DBP, DEHP, DINP, and DIDP were detected in the PVC cable, and DEHP and Deca-BDE were detected in the PBT resin. This system can accommodate screening for phthalate esters and brominated flame retardants with a single measurement cycle.

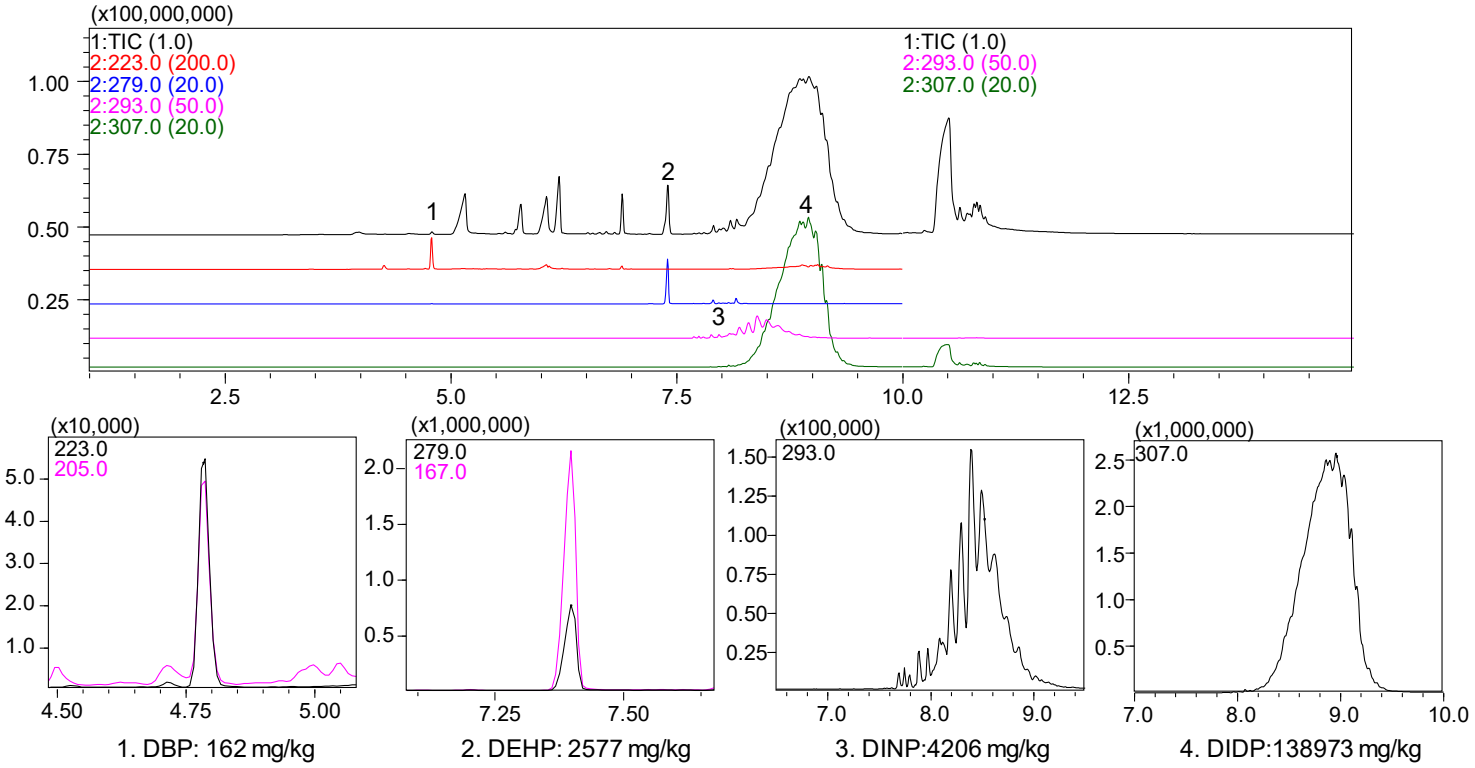

Fig. 2: Mass Chromatograms for Compounds Detected in a PVC Cable

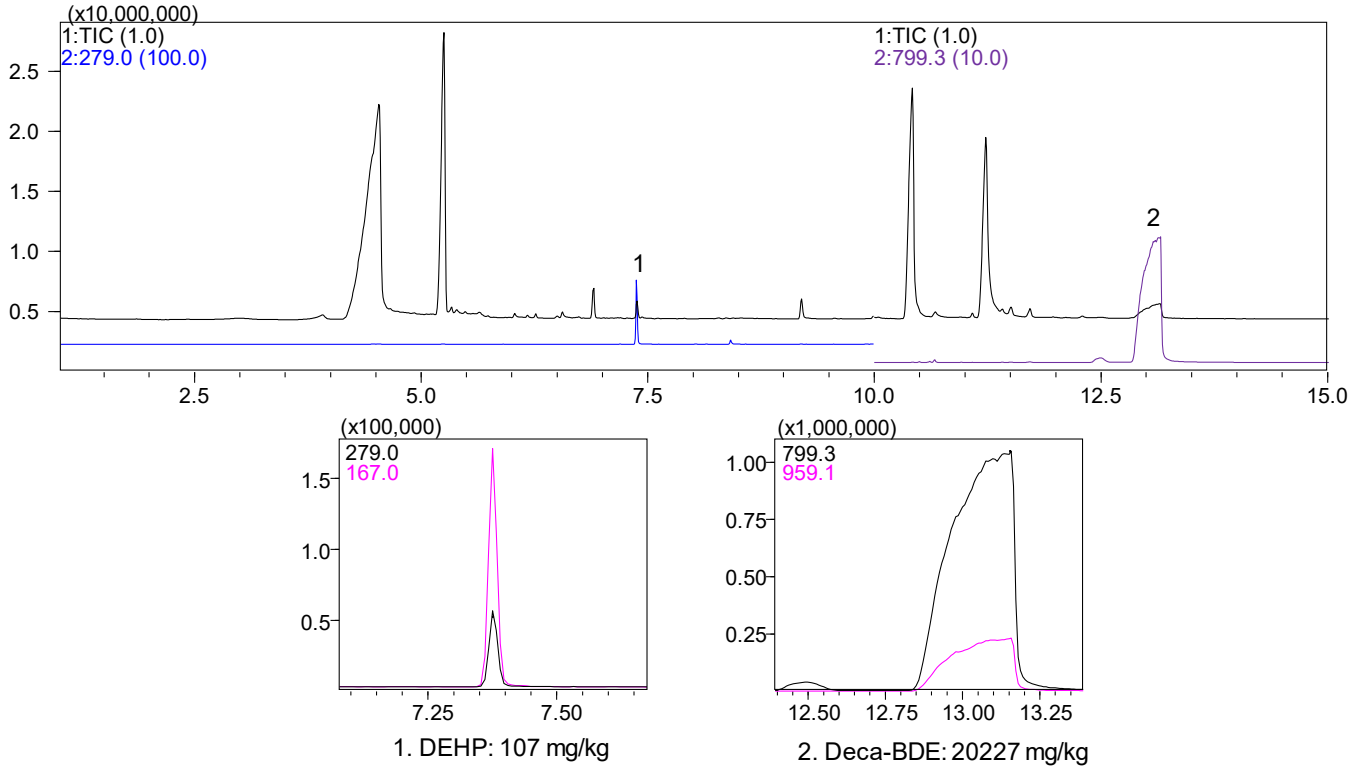

Fig. 3: Mass Chromatograms for Compounds Detected in a PBT Resin

First Edition: Apr, 2015

Shimadzu Corporation
www.shimadzu.com/an/

SHIMADZU
Excellence in Science

Application Data Sheet

No.135

GC-MS
Gas Chromatograph Mass Spectrometer

Screening Analysis of Phthalate Esters and Qualitative Analysis of Other Additives in Medical Supplies Using the Py-GC/MS Screening System

BACK TO CONTENTS

Although phthalate esters are used as plasticizing agents in plastics, there are concerns over their reproductive toxicity. This has led to regulatory restrictions on their use, including a Restriction of Hazardous Substances (RoHS) Directive that added phthalate esters to the list of restricted substances. The phthalate ester DEHP is used widely in blood transfusion bags, blood transfusion tubing, and other medical supplies, and the elution and transfer of DEHP into the contents of medical supplies is viewed as a problem. The use of medical supplies that are free of phthalate esters is recommended in notifications issued by various countries (Japan's Ministry of Health, Labour and Welfare in 2002, USA's FDA in 2002, Europe's EFSA in 2005, and Germany's BfR in 2013).
For some time, Soxhlet extraction-GC/MS and soaking extraction-GC/MS have been used to analyze phthalate esters in medical supplies, but these methods require a series of operations that can take several hours. Py-GC/MS is a new method of screening for phthalate esters that is adopted as part of International Standard IEC 62321-8 in 2017. The Py-GC/MS screening method requires no organic solvents and allows for rapid sample preparation. Shimadzu offers this analysis method in the form of the Py-Screener system.
This Application Data Sheet uses Py-Screener to analyze various medical supplies. A simultaneous Scan/SIM analysis method was paired with Py-Screener's high-speed scanning mode to perform a highly sensitive screening analysis for phthalate esters using SIM and, simultaneously, perform a qualitative analysis of other additives based on Scan information.

Analytical Conditions

Py-GC/MS was performed using the analytical conditions included with Py-Screener. Refer to GC/MS Application Data Sheet No. 110, "Analysis of Phthalate Ester Using the Py-Screener (1)“, for details on these analytical conditions.
Seven different medical supplies, including blood transfusion bags and blood transfusion tubing, were used as samples and data was gathered using simultaneous Scan/SIM analysis. SIM can perform highly sensitive analysis and was used to screen for phthalate esters. Simultaneously, other additives were identified by obtaining total ion current chromatograms (TICs) with Scan, then performing a similarity search for mass spectral data from unknown peaks with the NIST Mass Spectral Library (2014).
Calibration curves were prepared using a 1000 mg/kg standard sample of phthalate esters (P/N: 225-31003-91, Shimadzu) and used to quantify the phthalate esters content of medical supplies.

Analytical Results

SIM chromatograms of phthalate esters and TICs of Scan data obtained from analysis of each medical supply are shown in Figs. 1, 2 and 3. Results for each sample are shown in Table 1. A high concentration of DEHP (approx. 8%) was detected in the blood transfusion bag, blood transfusion tubing, and intravenous tubing 1. Additives detected other than phthalate esters were the phthalic acid alternative bis(2-ethylhexyl) adipate, the plasticizing agent tri(2-ethylhexyl) trimellitate (TOTM), the antioxidant agents tris(2,4-di-tert-butylphenyl) phosphate, and the lubricants palmitic acid, palmitic acid methyl ester, and stearic acid butyl ester.

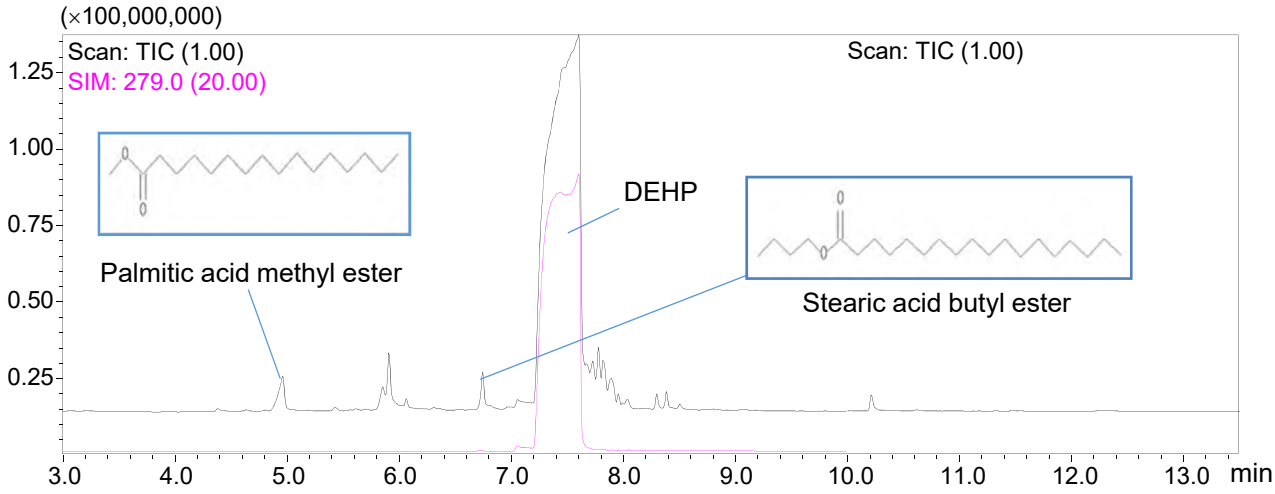

Fig. 1: SIM Chromatogram of Phthalate Ester and TIC of Scan Data Obtained by Analysis of a Blood Transfusion Bag

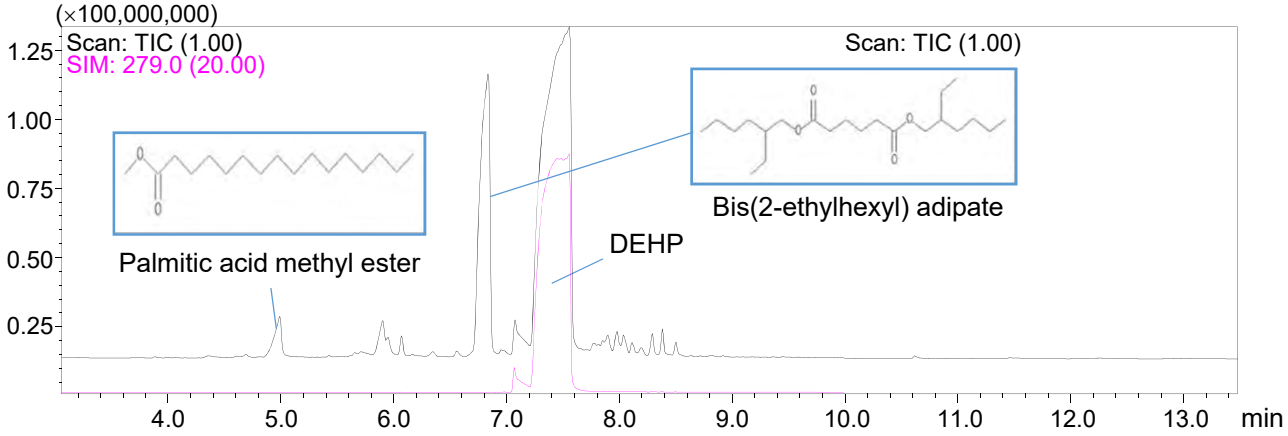

Fig. 2: SIM Chromatogram of Phthalate Ester and TIC of Scan Data Obtained by Analysis of Blood Transfusion Tubing

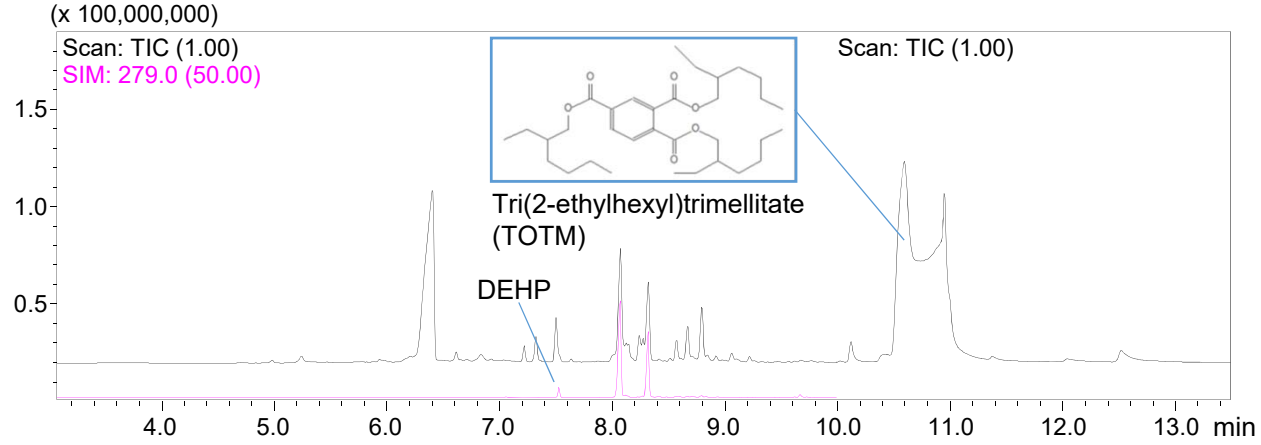

Fig. 3: SIM Chromatogram of Phthalate Ester and TIC of Scan Data Obtained by Analysis of Intravenous Tubing 2

Table 1: Phthalate Esters Screening Results and Qualitative Analysis Results for Other Additives by Medical Supply

Sample	Blood Transfusion Bag		Blood Transfusion Tubing		Intravenous Bag 1		Intravenous Bag 2		Intravenous Tubing 1		Intravenous Tubing 2		Syringe	
Compound	Concentration (mg/kg)	%RSD	Concentration (mg/kg)	%RSD	Concentration (mg/kg)	%RSD	Concentration (mg/kg)	%RSD	Concentration (mg/kg)	%RSD	Concentration (mg/kg)	%RSD	Concentration (mg/kg)	%RSD
DIBP	N.D.	-	N.D.	-	N.D.	-	N.D.	-	N.D.	-	N.D.	-	N.D.	-
DBP	N.D.	-	152	11.2	N.D.	-	144	7.1	N.D.	-	N.D.	-	N.D.	-
BBP	N.D.	-	N.D.	-	N.D.	-	N.D.	-	N.D.	-	N.D.	-	N.D.	-
DEHP	87,737	6.2	75,537	5.1	N.D.	-	107	9.3	81,199	3.4	206	2.4	N.D.	-
DNOP	N.D.	-	N.D.	-	N.D.	-	N.D.	-	N.D.	-	N.D.	-	N.D.	-
DINP	N.D.	-	N.D.	-	N.D.	-	N.D.	-	N.D.	-	N.D.	-	N.D.	-
DIDP	N.D.	-	N.D.	-	N.D.	-	N.D.	-	N.D.	-	N.D.	-	N.D.	-

Mean concentration and %RSD calculated from results of n = 3 consecutive analyses. N.D.: <30 mg/kg

Other Additives	Palmitic acid (lubricant)	Bis(2-ethylhexyl) adipate (plasticizer)	Tris(2,4-di-tert-butylphenyl) phosphate (antioxidant)	Palmitic acid (lubricant)	Palmitic acid (lubricant)	Tri(2-ethylhexyl) trimellitate (TOTM) (plasticizer)	Tris(2,4-di-tert-butylphenyl) phosphate (antioxidant)
	Stearic acid butyl ester (lubricant)	Palmitic acid methyl ester (lubricant)					

First Edition: May 2018

SHIMADZU

SHIMADZU
Excellence in Science

Application News

Gas Chromatograph Mass Spectrometer

No. GCMS-1504

A Pyrolysis-GC/MS Screening System for Analysis of Phthalate Esters and Brominated Flame Retardants

BACK TO CONTENTS

■ Introduction

The Restriction of Hazardous Substances (RoHS) Directive controls six hazardous substances commonly used in electronic and electrical equipment [(1)]. Two of the restricted substances are compound classes commonly used in flame retardants: polybrominated biphenyls (PBB) and polybrominated diphenyl ethers (PBDE), both known to cause serious health concerns due to their high halogen content. Beside brominated flame retardants, phthalate esters have also been controlled by a number of regulatory authorities. The United States congress has prohibited the use of six specified phthalate esters (DBP, DEHP, BBP, DINP, DIDP and DnOP) in children's toys at concentrations higher than 0.1% under the Consumer Product Safety Improvement Act of 2008 (CPSIA) [(2)]. The European commission has identified DBP, DEHP and BBP as reproductive toxicants under directive 2005/84/EC [(3)]. The Environmental Protection Agency (EPA) has proposed adding eight phthalates to the list of chemicals of concern under the Toxic Substances Control Act (TSCA), including DIBP, DBP, BBP, DEHP, DnOP, DINP, DnPP and DIDP [(4)]. The Food and Drug Administration (FDA) Center for Drug Evaluation and Research (CDER) recommends avoiding the use of DBP and DEHP as excipients in CDER-regulated drug and biologic products, including prescription and nonprescription products [(5)].

To quantitate these substances in a polymer matrix, the traditional approach involves solvent extraction of PBBs, PBDEs and phthalate esters from the sample matrix, followed by detection and quantitation by gas chromatography/mass spectrometry (GC/MS). This method is time consuming and poses the risk of exposure to multiple toxic solvents.

Pyrolysis followed by GC/MS has been well established for detection of volatile and semi-volatile compounds in both natural and synthetic polymers. Using the pyrolysis technique described here, a temperature programed micro-furnace provides thermal desorption processes at two temperature ranges, releasing the PBBs, PBDEs and phthalate esters from the polymer matrix for subsequent analysis by GC/MS.

In this application note, a PY-GC/MS method has been used to screen for seven phthalate esters and 11 brominated flame retardants. A commercially available method package was used, which includes phthalate ester and PBDE standards, pre-registered instrument methods with acquisition and data processing parameters, and calibration curves for semi-quantitative calculation of compound concentration. Quantitation results were generated with minimal sample preparation, requiring no organic solvents. A software program for efficient multi-analyte data confirmation and QAQC review is also discussed.

■ Experimental

Py-Screener Package

This study was conducted using the Shimadzu GCMS-QP2010 Ultra, Frontier Multi-Shot EGA/PY-3030D pyrolyzer, and AS-1020E Auto-Shot sampler, as shown in Figure 1.

Figure 1: Frontier Multi-Shot EGA/PY-3030D pyrolyzer and AS-1020E Auto-Shot sampler installed on the Shimadzu GCMS-QP2010 Ultra

BACK TO CONTENTS

The Frontier Multi-Shot EGA/PY-3030D pyrolyzer and AS-1020E Auto-Shot sampler were installed on the Shimadzu GCMS-QP2010 Ultra, with a UA-PBDE metal capillary column (15 m x 0.25 mm x 0.05 µm). A method package called Py-Screener has been developed and applied in this application. Py-Screener is a method package targeting seven phthalates and 11 brominated flame retardants. It contains pre-registered instrument acquisition methods for the Pyrolyzer and the GC/MS, as well as a data processing analysis method including quantitation parameters and calibration curves developed using phthalate and PBDE standards. Refer to Table 1 and Table 2 for experimental details and complete compound list.

Analytical standards used for this project were included with the Py-Screener package. The phthalate standards were comprised of three thin polymer films, which contain seven phthalates at 0, 100 ppm, and 1000 ppm, and one flame retardant standard containing 11 PBBs and PBDEs. All standards and samples were prepared by slicing off small pieces of the polymer using the knife from the sampling tool kit. Approximately 0.5 mg of standards and samples were weighed using an electronic balance with accuracy of 0.01 mg before loading into the sample cups. For ease of the application, the Py-Screener package also includes sample preparation videos, illustrated troubleshooting procedures and routine maintenance.

Table 1: Experimental conditions for the instrument acquisition method

Gas Chromatograph	**CG-2010 Plus**	
Column	UA-PBDE, 15 m x 0.25 mm x 0.05 µm (Shimadzu PN 220-94824-20)	
Oven Program	80 °C, no hold 20 °C/minute to 300 °C, hold 5 minutes	
Injector	Split mode, split ratio 50:1 300 °C Split Liner w/ wool (Shimadzu PN 220-90784-00)	
Carrier Gas Carrier Gas Flow	Helium Constant linear velocity mode, 52.1 cm/second Total Flow 54 mL/minute, Column Flow = 1.00 mL/minute Purge Flow 3.0 mL/minute	
Interface Temperature	320 °C	
Mass Spectrometer	**GCMS-QP2010 Ultra**	
Ion Source Temperature Solvent Cut Time Detector Voltage	230 °C 0.5 minutes Relative to tune + 0.1 kV	
MS Operating Mode	Acquisition mode: Scan/SIM Total loop time 0.45 second	
	Scan event time 0.15 second Mass range: 50-1000 amu	SIM event time 0.3 second SIM method details listed in table 2
Pyrolyzer	**PY-3030D (Frontier Labs)**	
Sample amount Furnace Temp PY-GC Interface Temperature	0.5 mg TD1 200 °C to 300 °C @ 20 °C/minute, total 5 minutes TD2 300 °C to 340 °C @ 5 °C/minute, total 9 minutes Furnace temperature plus 100 °C, up to 300 °C	
Analysis Time		
PY program GC/MS program Total Cycle Time per sample	14 minutes 16 minutes 30 minutes	

BACK TO CONTENTS

Table 2: Compound list and selected ions for the SIM method

Compound Name	Abbreviation / Congeners	Selected Ions for the SIM Mode		
		Quantitation	Reference #1	Reference #2
Diisobutyl phthalate	DIBP	223.0	205.0	149.0
Dibutyl phthalate	DBP	223.0	205.0	149.0
Butyl benzyl phthalate	BBP	206.0	91.0	149.0
Di(2-ethylhexyl) phthalate	DEHP	279.0	167.0	149.0
Di(*n*-octyl) phthalate	DnOP	279.0	167.0	149.0
Diisononyl phthalate	DINP	293.0	167.0	149.0
Diisodecyl phthalate	DIDP	307.0	167.0	149.0
Hexabromocyclododecane	HBCDD	238.9	560.6	
2,2',4,4'-tetrabromodiphenyl ether	BDE-47	325.8	483.6	
2,2',3,4,4'-pentabromodiphenyl ether	BDE-99	403.8	561.6	
2,2',4,4',6-pentabromodiphenyl ether	BDE-100	403.8	561.6	
2,2',4,4',5,5'-hexabromodiphenyl ether	BDE-153	483.6	643.5	
2,2',4,4',5,6'-hexabromodiphenyl ether	BDE-154	483.6	643.5	
2,2',3,4,4',5,6'-heptabromodiphenyl ether	BDE-183	561.6	721.4	
2,2',3,3',4,4',6,6'-Octabromodiphenyl ether + 2,2',3,4,4',5,6,6'-Octabromodiphenyl ether	BDE-197+204	641.5	643.5	
Nonabromodiphenyl ethers	BDE-206+207+208	719.4	879.2	
Decabromodiphenyl ether	BDE-209	799.3	959.1	
Decabrominated biphenyl	BB-209	783.3	785.3	

PY-GC/MS Method

In the micro-furnace of the pyrolyzer, the sample undergoes a two-step thermal desorption process, where the temperature increases from 200 °C to 300 °C at 20 °C per minute, followed by a second temperature ramp from 300 °C to 340 °C at 5 °C per minute. PBBs, PBDEs and phthalate esters are released in the temperature controlled micro-furnace and are transferred to GC/MS for chromatographic separation and analysis.

A simultaneous selected ion monitoring (SIM) and full scan acquisition method (Scan/SIM) was used on the GCMS-QP2010 Ultra. Using a Scan/SIM method provides enhanced sensitivity of the target compounds by monitoring their signature fragments, while simultaneously screening for the unknown analytes in the full mass range at the same time. Because analysis takes place by rapidly alternating between the two modes, a fast scan rate is essential to assure adequate sensitivity for both SIM and full scan modes.

The Py-Screener method package includes pre-registered retention indices for all the target compounds. Retention time for the target compounds are determined using the retention indices and the retention time for the homologous series of hydrocarbons under the same acquisition conditions using Automatic Adjust of Retention Time (AART) function. A mixture containing saturated hydrocarbon n-isomers from Octane (C8) to Tetracontane (C40) comes with the package and is used in the AART function. Retention time of all 18 target compounds is predicted and is used to adjust the acquisition and data processing retention time parameters in the method.

■ Results and Discussion

Calibration Standards

Four standards were analyzed using the Scan/SIM method, which include three standards with phthalates at 0 ppm, 100 ppm and 1000 ppm, and one with PBDEs at various concentration between 26 ppm and 780 ppm. Total ion chromatograms (TIC) for two standards are shown in Figure 2. Figure 3 shows the SIM chromatographic profiles for the individual target compounds. DIBP, DBP, BBP, DEHP, and DnOP present as narrow sharp chromatographic peaks, while the profiles for DINP and DIDP present as a broad cluster of chromatographic peaks due to their multiple isomeric components. The area count of mass chromatogram in SIM mode for each compound was determined, and applied to the calibration curve in the quantitation method.

BACK TO CONTENTS

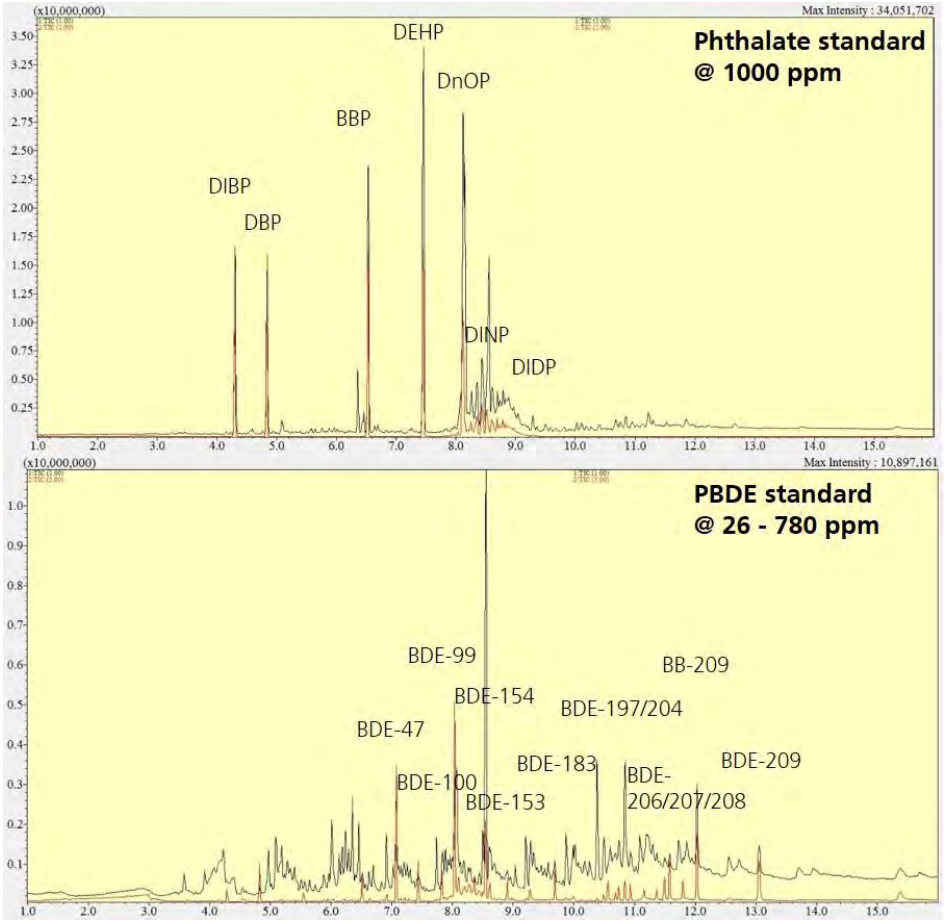

Figure 2: Total ion chromatograms (TIC) for the phthalate and PBDE standards, with full scan mode shown in black and SIM mode shown in red. Phthalate standard contains seven phthalates at 1000 ppm. The PBDE standard contains PBDEs and PBBs at various concentrations between 26 and 780 ppm.

Figure 3: Chromatographic profile of the target compounds extracted from SIM chromatogram of the phthalate and PBDE standards. The primary SIM ions are shown in black, and the secondary reference ions are shown in pink.

BACK TO CONTENTS

LabSolution Insight

LabSolution Insight is a software program designed for simultaneously analyzing data sets from multiple samples. With LabSolution Insight, quantitative results for a complete series of data files can be displayed side-by-side for comparison and QC review. All of the chromatograms from a selected target compound can be displayed simultaneously, making it easy to review the detected peaks and confirm the quantitative results. Color-coded QAQC flags quickly identify any outliers that require further examination. Results can be displayed in a variety of ways, allowing users to select the view that is best suited for their workflow, and when necessary, peaks can be re-integrated and re-quantified directly from LabSolution Insight.

For this project three polymer samples were analyzed using the PY-GC/MS method described above; they are labeled Blue Conveyor, White Conveyor, and Gasket. A blank sample cup was also analyzed using the same method for quality control purpose. Figure 4 shows the total ion chromatograms of the three polymer samples. The pre-registered calibration curve from the Py-Screener package was used for quantitation. The calibration is based on a one-point calibration from analysis of the highest phthalate standard at 1000 ppm, and the PBDE standard. The quantitation results are categorized into three groups to comply with multiple regulations: below 500 ppm, between 500 and 1500 ppm, and beyond 1500 ppm. All 7 target phthalate compounds from one standard and the three samples are displayed side-by-side in LabSolution Insight, and the outliers with concentration above 1500 ppm are labeled with flags, as shown in Figure 5.

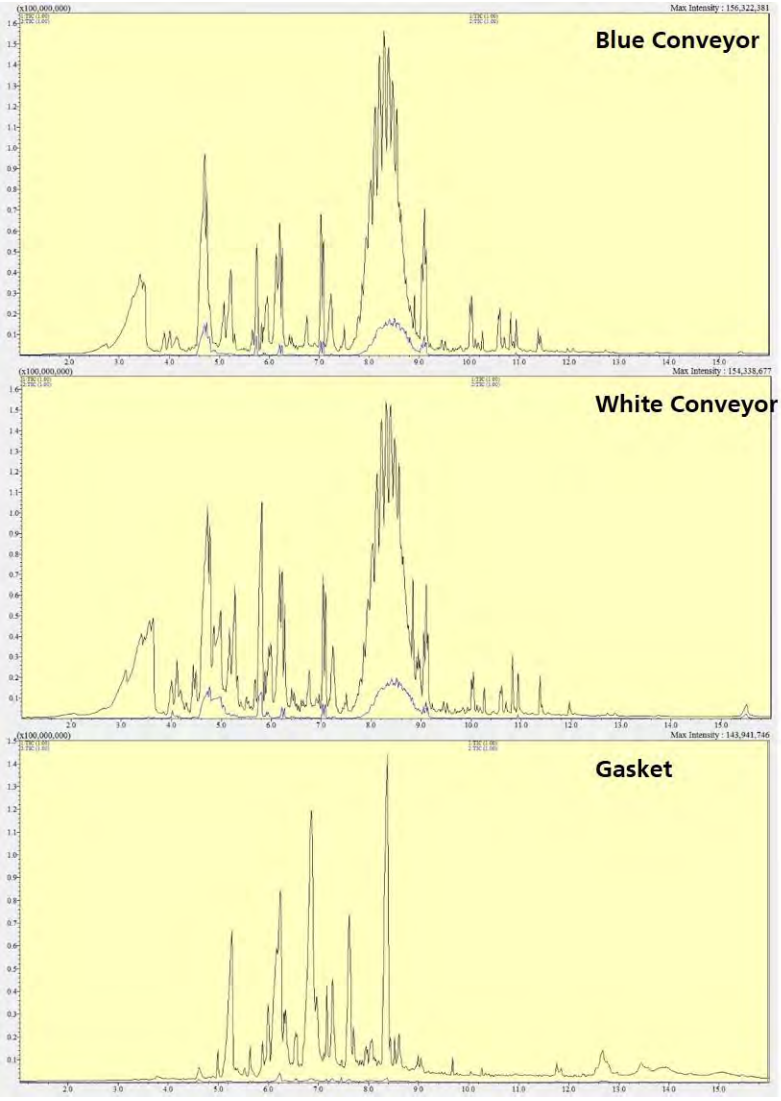

Figure 4: Total ion chromatogram from three samples - *Blue Conveyor*, *White Conveyor*, and *Gasket*, with full scan mode shown in black and selected ion monitoring (SIM) mode shown in blue. Note that the noise level in SIM mode is reduced significantly compared to full scan mode.

BACK TO CONTENTS

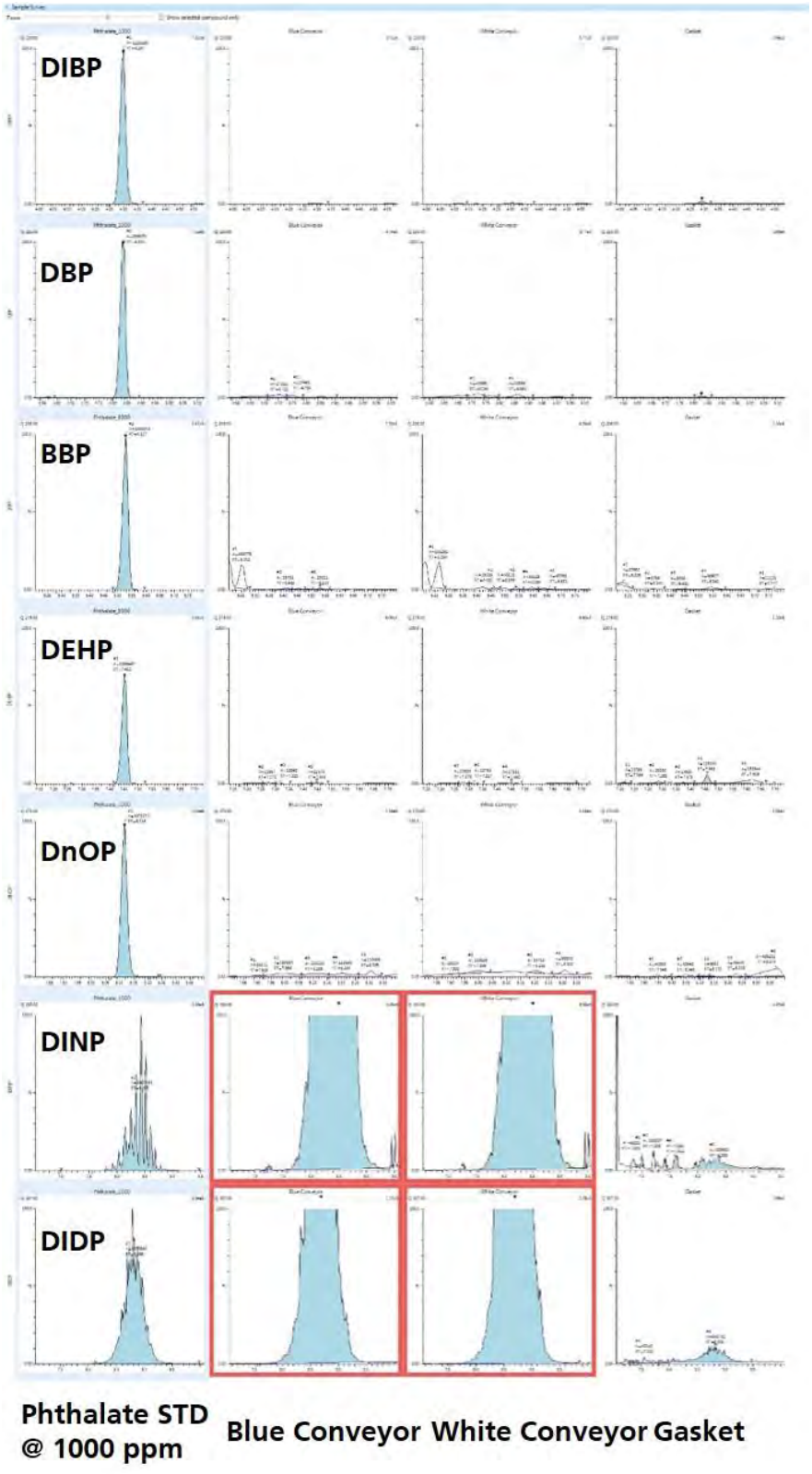

Figure 5: Quantitative analysis of the seven phthalate analytes in one standard and three polymer samples using the LabSolution Insight QAQC software. All the phthalate target compounds from three samples with unknown phthalate concentration are displayed with intensity scaled at the same level as phthalate standard at 1000 ppm. Phthalate content higher than 1500 ppm have been automatically flagged with a red box by the LabSolution Insight software.

BACK TO CONTENTS

The two samples labeled Blue Conveyor and White Conveyor have similar chromatographic profiles, which both show significant phthalate content compared to the Gasket sample. Quantitative analysis results on the blank and the three polymer samples are shown in table 3. DINP and DIDP were detected at around 3% and 0.7% in both Blue Conveyor and White Conveyor samples, which exceed the 0.1% limit in several regulations. The Gasket sample shows only low content of DINP and DIDP at about 0.03% and 0.02%. All the other types of phthalates and PBDEs are either negligible or non-detected in all the three samples.

Table 3: Quantitative analysis result of three polymer samples

Compound Name	Blank (ppm)	Blue Conveyor (ppm)	White Conveyor (ppm)	Gasket (ppm)
DIBP	ND	ND	ND	**23**
DBP	**1**	ND	ND	**11**
BBP	**< 1**	**9**	ND	ND
DEHP	**< 1**	**12**	**11**	**81**
DNOP	ND	ND	ND	ND
DINP	ND	**31489**	**31722**	**297**
DIDP	ND	**7149**	**7860**	**192**
HBCDD	ND	ND	ND	ND
Tetra-BDE (BDE-47)	ND	ND	ND	ND
Penta-BDE (BDE-100)	ND	ND	ND	ND
Penta-BDE (BDE-99)	ND	ND	ND	ND
Hexa-BDE (BDE-154)	ND	ND	ND	ND
Hexa-BDE (BDE-153)	ND	ND	ND	ND
Hepta-BDE (BDE-183)	ND	ND	ND	ND
Octa-BDE (BDE-197+204)	ND	ND	ND	ND
Nona-BDE	ND	ND	ND	ND
Deca-BDE (BDE-209)	ND	ND	ND	ND

QAQC

Phthalate standards at 0 ppm and 100 ppm were analyzed using the same method to support quality control. In LabSolution Insight, QAQC criteria were applied so that the data will be highlighted when either of the following two conditions was met: the concentration of any of the target compounds in 0 ppm standard exceeds 10 ppm, or the signal to noise ratio of 100 ppm standard falls below 30.

Since the Py-Screener package was developed for phthalate and PBDE screening for several regulations, the quantitation is only adequate enough to be categorized in those three groups. To achieve further accuracy, sohexlet extraction followed by liquid injection GC/MS will be required. Regular liquid injection with capillary column Rxi-1HT (15 m x 0.25 mm x 0.1 µm) is recommended instead of pyrolysis. In this case, the Twin Line MS kit can be used to save time on column switching

■ Summary and Conclusion

The Py-Screener method package was used to investigate the phthalates and PBDEs content in three polymer samples. Experimental conditions and data processing method are described in detail. The LabSolution Insight program was used to review multiple data and flag outliers based on defined QAQC parameters.

■ References

1. Directive 2002/95/EC, Official Journal of the European Union
2. Public law 110–314, Consumer Product Safety Improvement Act of 2008
3. Directive 2005/84/EC, Official Journal of the European Union
4. Phthalates action plan, U.S. Environmental Protection Agency
5. Guidance for industry limiting the use of certain phthalates as excipients in CDER-regulated products, U.S. Department of Health and Human Services Food and Drug Administration Center for Drug Evaluation and Research

First Edition: September 2015

SHIMADZU Corporation
www.shimadzu.com/an/

SHIMADZU SCIENTIFIC INSTRUMENTS
7102 Riverwood Drive, Columbia, MD 21046, USA
Phone: 800-477-1227/410-381-1227, Fax: 410-381-1222
URL: www.ssi.shimadzu.com

SHIMADZU
Excellence in Science

Application Data Sheet

No. 14

GC
Gas Chromatograph

Simultaneous Analysis of Lower Aldehydes That Do Not Require Derivatization

BACK TO CONTENTS

The conventional method used to simultaneously analyze lower aldehydes by gas chromatography (GC) involves reacting them with a derivatizing agent before analysis in order to increase stability and detection sensitivity. However, derivatization can be difficult for some sample compositions or coexisting components. Therefore, there has been demand for an alternate method that enables direct, high-sensitivity measurement of lower aldehydes. Barrier discharge ionization detectors (BID) uses a revolutionary plasma technology to detect all compounds except He and Ne. Because BID is able to detect lower aldehydes, including formaldehyde, without derivatizing the aldehydes, they are especially helpful for analyzing aldehydes in samples such as resins, chemical products, and water.
This Data Sheet introduces the analyzing lower aldehydes in water using a Shimadzu HS-20 headspace sampler and a Shimadzu Tracera High Sensitivity Gas Chromatograph System (GC-BID).

Analysis Results

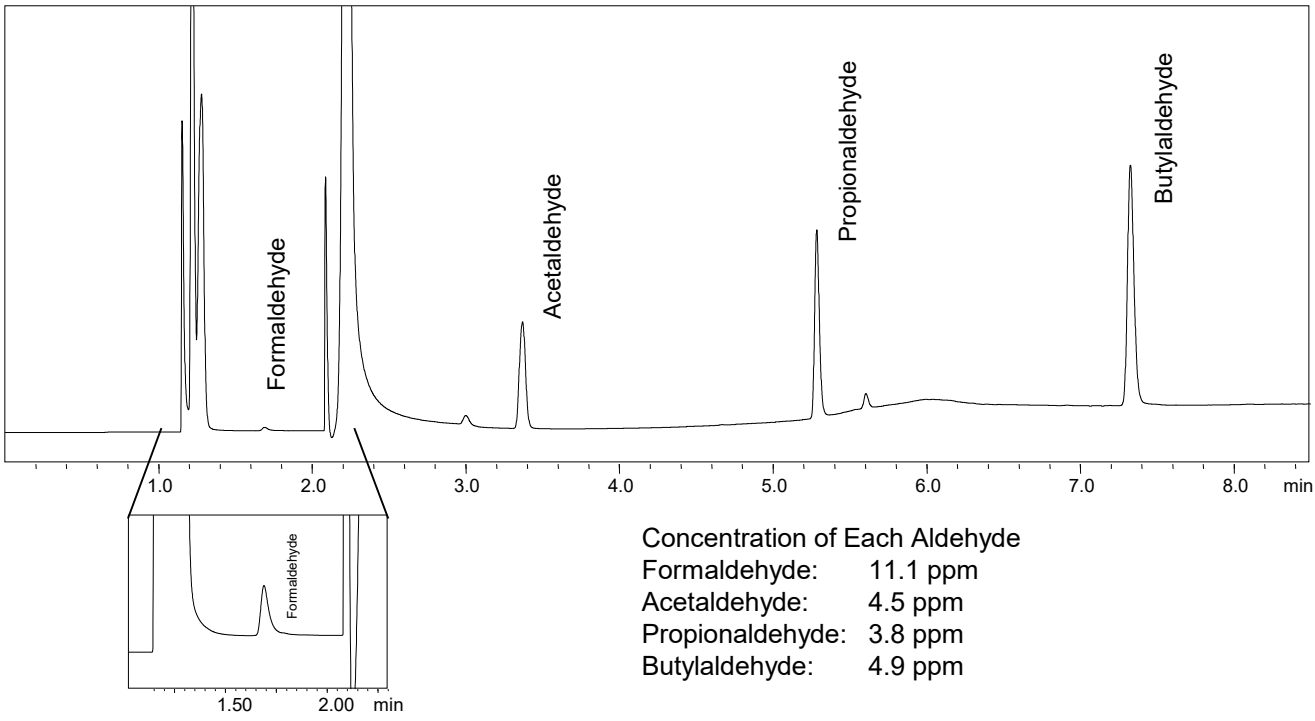

Concentration of Each Aldehyde
Formaldehyde: 11.1 ppm
Acetaldehyde: 4.5 ppm
Propionaldehyde: 3.8 ppm
Butylaldehyde: 4.9 ppm

Fig. 1: Chromatogram of Aldehydes in Water

Table 1: Repeatability of Area Values (μV × sec)

	1	2	3	4	5	Ave.	RSD %
Formaldehyde	24803	25291	25133	25219	25335	25156	0.84
Acetaldehyde	745944	736335	750353	760809	760429	750774	1.37
Propionaldehyde	1000860	975441	1005373	1026178	1027918	1007154	2.13
Butylaldehyde	1771850	1695015	1771917	1815825	1807684	1772458	2.69

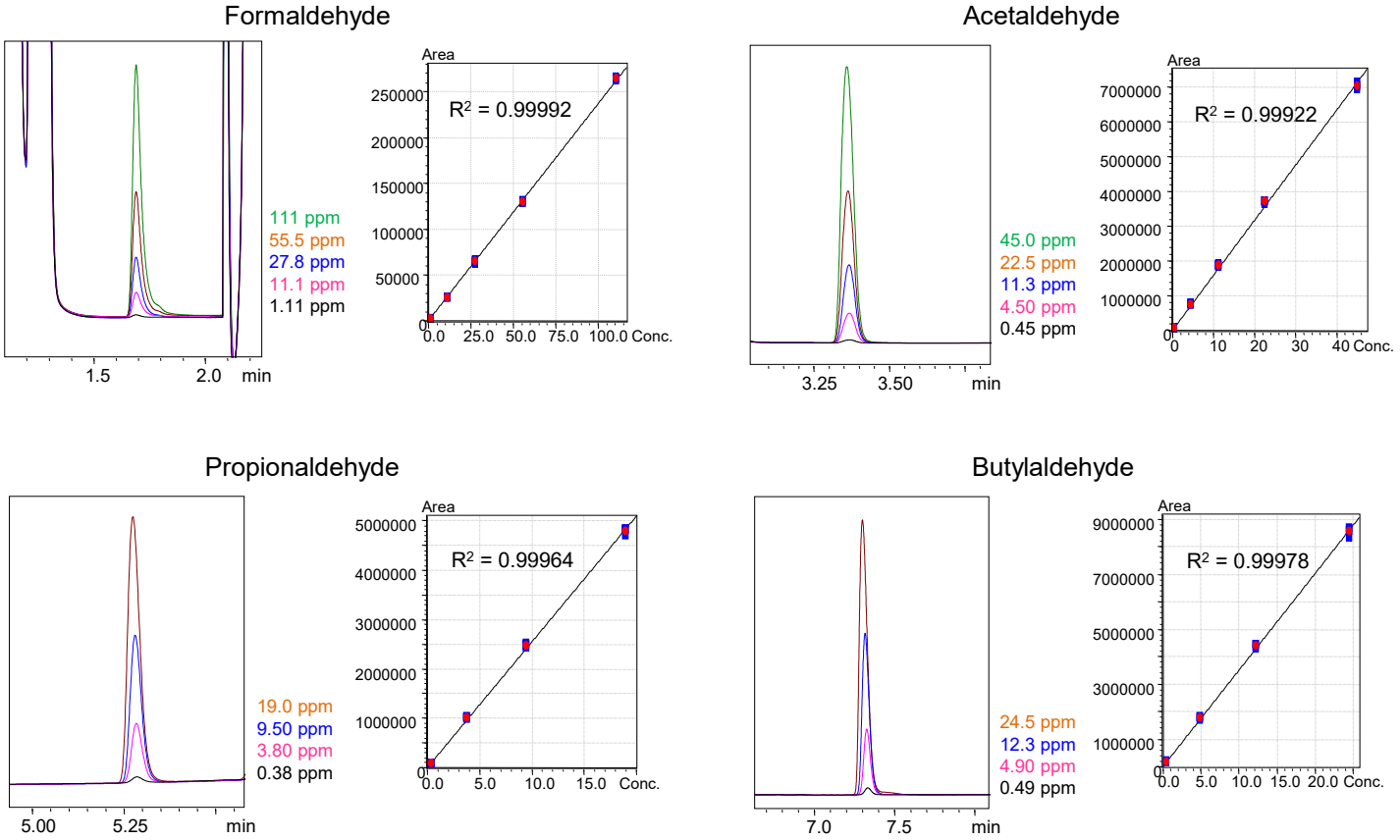

Fig. 2: Linearity of Respective Components

Instruments Used and Analysis Conditions

Gas Chromatograph: Tracera (GC-2010 Plus A + BID-2010 Plus)
Headspace Sampler: HS-20
Software: LabSolutions LC/GC

HS-20

Oven temp.:	80 °C	Vial agitation:	Off
Vial warming time:	30 min.	Vial pressurization pressure:	77 kPa
Vial pressurization time:	1 min.	Load time:	0.5 min.
Injection time:	1 min.	Needle flush time:	8 min.
Sample line temp.:	150 °C	Transfer line temp.	140 °C
Vial volume:	20 mL	Sample loop volume:	1 mL

Tracera

Column:	Rt®-U-BOND (0.53 mm I.D. × 30 m, d.f. 20 μm) Note: A 2.5 m × 0.53 mm RESTEK brand particle trap is connected via an SGE SilTite™ μ-Union.		
Column temp.:	100 °C – 5 °C/min – 110 °C – 20 °C/min – 180 °C (3 min), Total 8.5 min		
Carrier gas:	He (99.9999 %)		
Carrier gas control:	Constant linear velocity (55 cm/min)	Split ratio:	1:3
Detector temp.:	190 °C	Plasma gas:	Helium at 50 mL/min

Note: 3mL of sample solution and 1g of sodium chloride was sealed in a vial, and completely dissolved sodium chloride before analyzing the sample.

First Edition: January 2016

Shimadzu Corporation
www.shimadzu.com/an/

SHIMADZU
Excellence in Science

Application Data Sheet

No.118

GC-MS
Gas Chromatograph Mass Spectrometer

Analysis of Organic Solvents and Specified Chemical Substances in a Working Environment Using Two Different Columns (1)

BACK TO CONTENTS

Measurements of a working environment are mandated by Japan's Industrial Safety and Health Act for the purpose of preventing employee health problems caused by toxic factors in the workplace. These toxic factors include organic solvents and specified chemical substances. Many of these are measured using the solid sampling - gas chromatograph method.

This article investigates the analysis of 58 organic solvents (including some specified chemical substances) subject to the working environment measurement . A gas chromatograph mass spectrometer (GC-MS) was used, which effectively optimizes analysis and heightens analytical accuracy. This investigation used two analysis columns with different liquid phases.

From the results of this investigation, it was found that using two different columns made it possible to separate the 58 organic solvents with heightened identification accuracy.

Experiment

For 56 of the 58 organic solvents that are to be eluted with carbon disulfide, standard solvents were diluted with carbon disulfide to obtain twice the control concentration for each solvent and a standard mixture stock solution was prepared. (Preparation assumed that the amount of actual working environment sample collected was 1 L, and the amount of eluted solvent was 1 mL.) In the same way, methanol and isopropyl alcohol standards were diluted with purified water to obtain twice the control concentration for each solvent and a standard mixture stock solution was prepared. (Preparation assumed that the amount of actual working environment sample collected was 1 L, and the amount of eluted solvent was 1 mL.)
These standard stock solutions were then measured using the analysis conditions in Table 1.

Table 1: Analysis Conditions

Gas chromatograph mass spectrometer: GCMS-QP2020

GC		MS	
Column[*1, 3]:	Stabilwax (30 m × 0.25 mm I.D., 0.5 μm)[*4]	Ion source temp.:	200 °C
Column[*2]:	Rtx-624 (30 m × 0.25 mm I.D., 1.4 μm)[*5]	Interface temp.:	240 °C
Sample injection quantity:	1 μL[*1, 2], 0.5 μL[*3]	Ionization current:	20 mμA (high concentration)
Injection port temp.:	230 °C	Measurement mode:	Scan mode
Injection mode:	Split	Measurement mass range:	*m/z* 20 to 250
Split ratio:	20	Event time:	0.3 sec
Control mode[*1, 3]:	Constant linear velocity (47 cm/sec)		
Control mode[*2]:	Constant linear velocity (49 cm/sec)		
Oven temp.[*1]:	50 °C (1 min) → (5 °C /min) → 70 °C → (25 °C /min) → 240 °C (2.5 min)		
Oven temp.[*2]:	50 °C (1 min) → (10 °C /min) → 80 °C → (40 °C /min) → 200 °C → (25 °C /min) →230 °C (1.5 min)		
Oven temp.[*3]:	50 °C (1 min) → (10 °C /min) → 70 °C → (25 °C /min) → 240 °C (2 min)		

*1 Analysis conditions 1: 54 organic solvents
*2 Analysis conditions 2: Carbon tetrachloride and 1,2-dichloropropane
*3 Analysis conditions 3: Methanol and isopropyl alcohol
*4 Code No.: 10638 (Restek Corp., Shimadzu GLC)
*5 Code No.: 10968 (Restek Corp., Shimadzu GLC)

Analysis Results

Fig. 1 shows the total ion current chromatogram obtained by measuring the 56 organic solvents eluted with carbon disulfide using analysis conditions 1. Separation was impossible in terms of retention time or *m/z* between carbon tetrachloride and 1,1,1-trichloroethane, and between toluene and 1,2-dichloropropane, respectively. Accordingly, they were analyzed using analysis conditions 2. The results showed that it was possible to separate these components using the retention times (Fig. 2). Methanol and isopropyl alcohol were measured using analysis conditions 3 (Fig. 3).

The use of two different columns made it possible to separate all 58 organic solvents with improved identification accuracy.

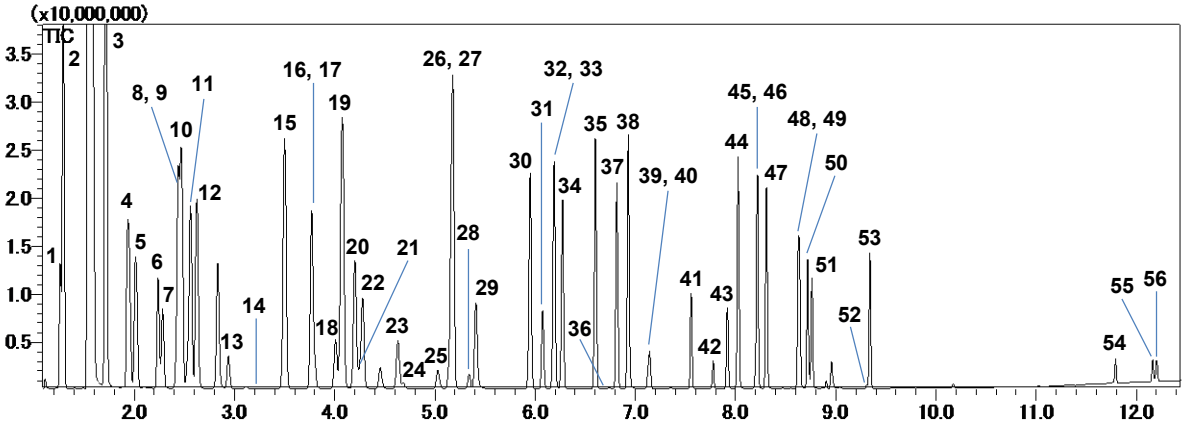

1. n-Hexane, 2. Ethyl ether, 3. Methylcyclohexane, 4. Acetone, 5. Methyl acetate, 6. trans-1,2-Dichloroethylene, 7. Tetrahydrofuran,
8. Carbon tetrachloride, 9. 1,1,1-Trichloroethane, 10. Ethyl Acetate, 11. Isopropyl acetate, 12. Methyl ethyl ketone, 13. Dichloromethane,
14. Benzene, 15. n-Propyl acetate, 16. cis-1,2-Dichloroethylene, 17. Trichloroethylene, 18. Methyl isobutyl ketone, 19. Isobutyl acetate,
20. 2-Butanol, 21. Chloroform, 22. Tetrachloroethylene, 23. Toluene, 24. 1,2-Dichloropropane, 25. 1,4-Dioxane, 26. 1,2-Dichloroethane,
27. n-Butyl acetate, 28. Methyl n-butyl ketone, 29. Isobutyl alcohol, 30. Isopentyl acetate, 31. Ethylbenzene, 32. p-Xylene, 33. 1-Butanol,
34. m-Xylene, 35. n-Pentyl acetate, 36. Methyl Cellosolve, 37. o-Xylene, 38. Isopentyl alcohol, 39. Cellosolve, 40. Chlorobenzene,
41. Styrene, 42. Cellosolve acetate, 43. Cyclohexanone, 44. 2-Methylcyclohexanone, 45. N,N-Dimethylformamide, 46. 3-Methylcyclohexanone,
47. 4-Methylcyclohexanone, 48. Butyl Cellosolve, 49. Cyclohexanol, 50. cis-2-Methylcyclohexanol, 51. trans-2-methyl-cyclohexanol,
52. 1,1,2,2-Tetrachloroethane, 53. ortho-Dichlorobenzene, 54. o-Cresol, 55. p-Cresol, 56. m-Cresol

Fig. 1: Total Ion Current Chromatogram for 56 Organic Solvents (Stabilwax)

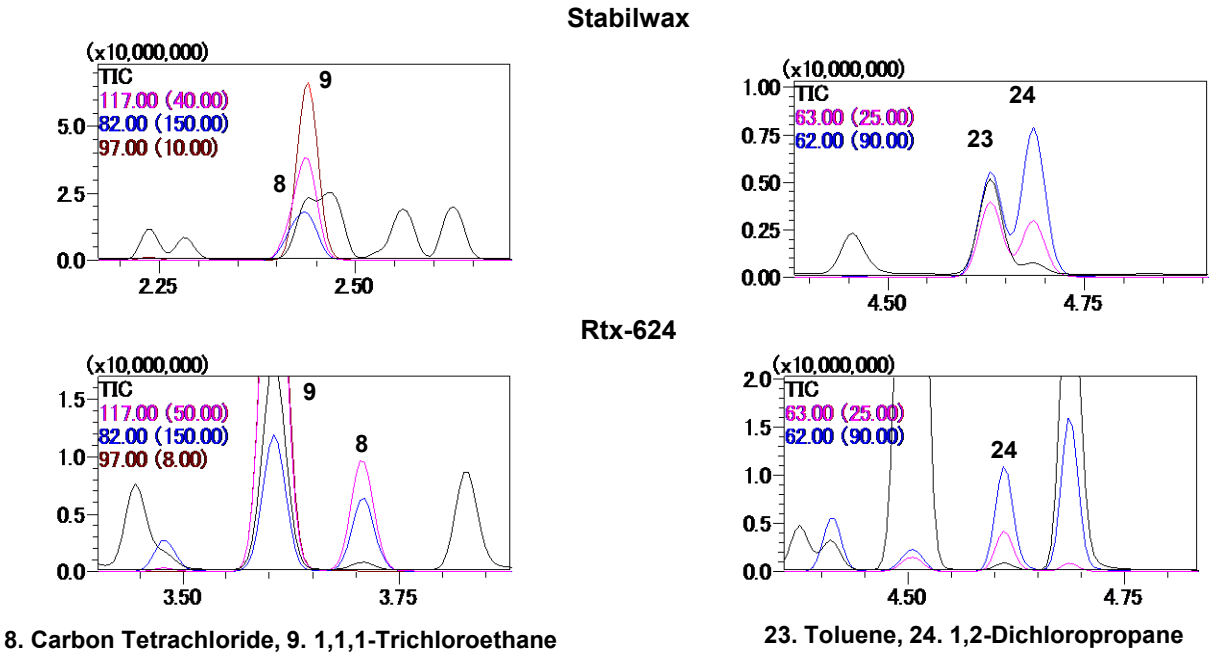

8. Carbon Tetrachloride, 9. 1,1,1-Trichloroethane

23. Toluene, 24. 1,2-Dichloropropane

Fig. 2: Separation Between Carbon Tetrachloride and 1,1,1-Trichloroethane, and Between Toluene and 1,2-Dichloropropane (Upper: Stabilwax; Lower: Rtx-624)

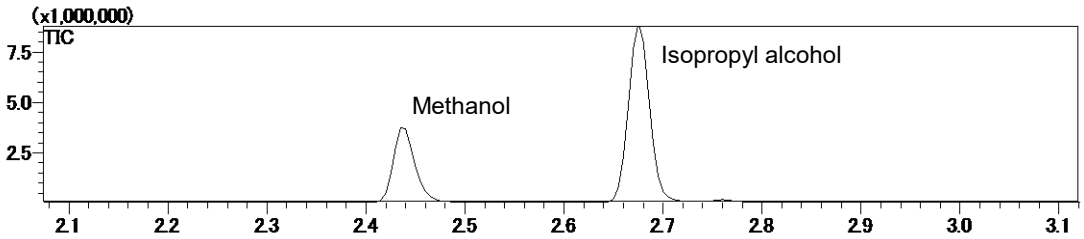

Fig. 3: Total Ion Current Chromatogram for Methanol and Isopropyl Alcohol (Stabilwax)

First Edition: March 2016

Shimadzu Corporation
www.shimadzu.com/an/

BACK TO CONTENTS

SHIMADZU
Excellence in Science

Application Data Sheet

No.119

GC-MS
Gas Chromatograph Mass Spectrometer

Analysis of Organic Solvents and Specified Chemical Substances in a Working Environment Using Two Different Columns (2)

BACK TO CONTENTS

Application Data Sheet No. 118 presented the successful separation of 58 organic solvents (including some specified chemical substances) subject to the working environment measurement, using two columns (Stabilwax and Rtx-624) with different liquid phases.
For the purpose of quantifying the 58 organic solvents automatically and continuously, analysis was performed using the Twin Line MS system, where the outlets from two different columns were connected to the MS unit simultaneously.
This Application Data Sheet introduces the results of investigating the quantitative analysis of 58 organic solvents using the Twin Line MS system.

Experiment

For the 56 solvents that are to be eluted with carbon disulfide, standard solvents were diluted with carbon disulfide to obtain twice the control concentration for each solvent and a standard mixture stock solution was prepared. (Preparation assumed that the amount of actual working environment sample collected was 1 L, and the amount of eluted solvent was 1 mL.) The mixed standard stock solution was further diluted with carbon disulfide to prepare standard solutions at concentrations of 1/1, 1/5, 1/10, 1/50 and 1/100 the control concentration, respectively. In the same way, methanol and isopropyl alcohol standards were diluted with purified water to prepare standard mixture solutions at concentrations of 2×, 1/1, 1/5, 1/10, 1/50 and 1/100 the control concentration, respectively.
These prepared standard solutions and standard stock solutions were measured using the analysis conditions in Table 1. High-sensitivity and high-accuracy analysis was possible by using the Smart SIM automatic method creation function.

Table 1: Analysis Conditions

Gas chromatograph mass spectrometer: GCMS-QP2020

GC		MS	
Column[*1, 3]:	Stabilwax (30 m × 0.25 mm I.D., 0.5 μm)[*4]	Ion source temp.:	200 °C
Column[*2]:	Rtx-624 (30 m × 0.25 mm I.D., 1.4 μm)[*5]	Interface temp.:	240 °C
Sample injection quantity:	1 μL[*1, 2], 0.5 μL[*3]	Ionization current:	20 mA (high concentration)
Injection port temp.:	230 °C	Measurement mode:	SIM mode
Injection mode:	Split	Measurement mass range:	See Table 2.
Split ratio:	20 Note 1)	Event time:	0.2 sec
Control mode[*1, 3]:	Constant linear velocity (47 cm/sec)		
Control mode[*2]:	Constant linear velocity (49 cm/sec)		
Oven temp.[*1]:	50 °C (1 min) → (5 °C/min) → 70 °C → (25 °C/min) → 240 °C (2.5 min)		
Oven temp.[*2]:	50 °C (1 min) → (10 °C /min) → 80 °C → (40 °C/min) → 200 °C → (25 °C/min) → 230 °C (1.5 min)		
Oven temp.[*3]:	50 °C (1 min) → (10 °C/min) → 70 °C → (25 °C/min) → 240 °C (2 min)		

*1 Analysis conditions 1: 54 organic solvents
*2 Analysis conditions 2: Carbon tetrachloride and 1,2-dichloropropane
*3 Analysis conditions 3: Methanol and isopropyl alcohol
*4 Code No.: 10638 (Restek Corp., Shimadzu GLC)
*5 Code No.: 10968 (Restek Corp., Shimadzu GLC)
Note 1: Change the value depending on the amount of sample collected and the concentration range of the calibration curve.

<Twin Line MS System>

The outlets for two different columns were connected simultaneously to the MS unit, so data could be acquired for the different columns without compromising the vacuum in the MS unit. (A small quantity of helium gas flowed through the column that was not used for analysis to prevent column degradation.)

・Features of the System
1) There is no connector from the injection port to the MS unit, so there are no concerns about adsorption or contamination.
2) Provides smaller retention time fluctuation than the flow line switching system.
3) The simple system construction provides little possibility of carrier gas leakage.
4) For column maintenance, only a Vespel ferrule and a nut need replacement.
5) Use of two different columns can widen the scope of the investigation of analysis conditions when adding target components.

Analysis Results

Of the 56 organic solvents eluted with carbon disulfide, Fig. 1 shows the SIM chromatograms for methyl cellosolve (control concentration: 0.1 ppm), measured with analysis conditions 1, and carbon tetrachloride and 1,2-dichloropropane, measured with analysis conditions 2. For methyl cellosolve, sufficient sensitivity was obtained at the control concentration (standard solution concentration: 0.3 mg/mL). Carbon tetrachloride and 1,2-dichloropropane were able to be selectively detected using the Rtx624.

For the 56 organic solvents, calibration curves were created with the concentrations ranging from 1/100 the control concentration (1/10 for methyl cellosolve) to twice the control concentration. The correlation coefficients (R) for the calibration curves were at least 0.998, which were favorable results. In addition, the standard solutions at 1/00 the control concentration (standard solution at the control concentration for methyl cellosolve) were measured five times to calculate the repeatabilities. Favorable results were obtained for all components, with a repeatability of 4% max. Favorable results were also obtained for methanol and isopropyl alcohol, with a correlation coefficient (R) for the calibration curve of 0.999 min. and a repeatability of 3% max. The results are shown in Table 2.

From the results of investigating analysis of 58 organic solvents using the Twin Line MS system, it was proved that automatic and continuous measurements were possible while maintaining quantitative accuracy.

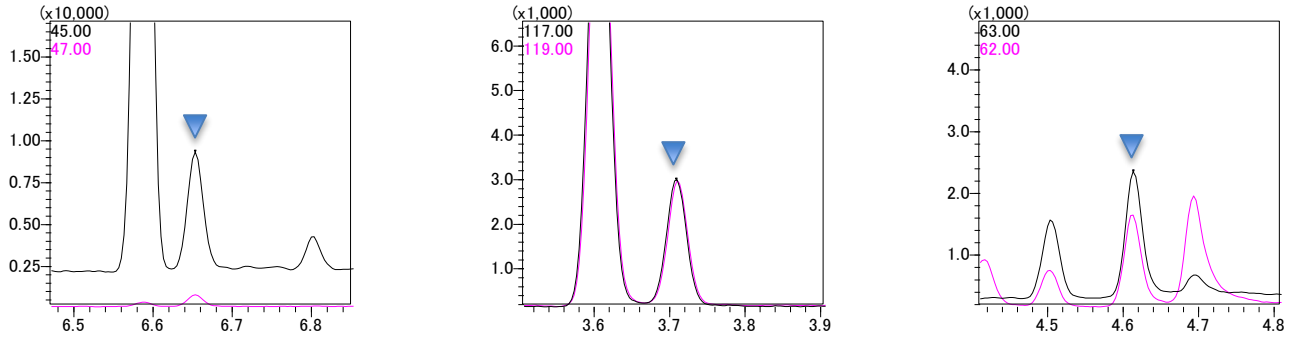

Fig. 2: SIM Chromatograms for Methyl Cellosolve, Carbon Tetrachloride, and 1,2-Dichloropropane
(Methyl cellosolve: 0.3 mg/mL, carbon tetrachloride: 0.3 mg/mL, 1,2-dichloropropane: 0.04 mg/mL)

Table 2: Calibration Curve Linearity and Repeatability
(1/100 the control concentration, except for methyl cellosolve, which was at the control concentration; n=5)

Name of Compound	Ions Monitored	%RSD	Correlation Coefficient: R	Name of Compound	Ions Monitored	%RSD	Correlation Coefficient: R
n-Hexane	86, 56	3.6	0.999	p-Xylene	106, 105	2.4	0.999
Ethyl ether	74, 45	3.3	0.999	1-Butanol	56, 43	1.8	0.999
Methylcyclohexane	82, 70	3.8	0.998	m-Xylene	106, 105	2.1	0.999
Acetone	58, 39	3.1	0.999	n-Pentyl acetate	70, 61	2.4	0.999
Methyl acetate	74, 59	2.6	0.999	Methyl Cellosolve	45, 47	3.4	0.999
trans-1,2-Dichloroethylene	96, 98	2.9	0.999	o-Xylene	106, 105	2.3	0.999
Tetrahydrofuran	72, 71	2.4	0.999	Isopentyl alcohol	70, 55	2.1	0.999
1,1,1-Trichloroethane	99, 97	2.8	0.999	Cellosolve	59, 72	2.3	0.999
Ethyl Acetate	70, 45	2.7	0.999	Chlorobenzene	112, 114	2.1	0.999
Isopropyl acetate	87, 59	3.0	0.999	Styrene	104, 78	2.3	0.999
Methyl ethyl ketone	72, 57	2.4	0.999	Cellosolve acetate	72, 59	2.1	0.999
Dichloromethane	84, 86	2.9	0.999	Cyclohexanone	98, 55	2.0	0.999
Benzene	78, 77	3.7	0.999	2-Methylcyclohexanone	112, 84	1.5	0.999
n-Propyl acetate	73, 42	3.5	0.999	N,N-Dimethylformamide	73, 30	2.7	0.999
cis-1,2-Dichloroethylene	96, 98	1.8	0.999	3-Methylcyclohexanone	112, 97	1.9	0.999
Trichloroethylene	130, 132	2.6	0.999	4-Methylcyclohexanone	112, 83	1.1	0.999
Methyl isobutyl ketone	100, 85	1.4	0.999	Butyl Cellosolve	87, 75	1.8	0.999
Isobutyl acetate	73, 56	2.1	0.999	Cyclohexanol	82, 67	2.3	0.999
2-Butanol	59, 41	1.8	0.999	cis-2-Methylcyclohexanol	96, 81	1.3	0.999
Chloroform	85, 83	1.4	0.999	trans-2-methyl-cyclohexanol	96, 81	0.7	0.999
Tetrachloroethylene	166, 164	2.4	0.999	1,1,2,2-Tetrachloroethane	83, 85	2.5	0.999
Toluene	91, 92	2.4	0.999	ortho-Dichlorobenzene	146, 148	2.2	0.999
1,4-Dioxane	88, 58	2.2	0.999	o-Cresol	107, 108	2.7	0.999
1,2-Dichloroethane	49, 64	3.2	0.999	p-Cresol	107, 108	1.3	0.999
n-Butyl acetate	73, 61	2.2	0.999	m-Cresol	107, 108	1.2	0.999
Methyl n-butyl ketone	58, 100	1.7	0.999	Carbon tetrachloride*1	117, 119	1.4	0.999
Isobutyl alcohol	43, 42	2.2	0.999	1,2-Dichloropropane*1	63, 62	1.9	0.999
Isopentyl acetate	70, 55	2.1	0.999	Methanol*2	31, 29	2.1	0.999
Ethylbenzene	106, 65	1.9	0.999	Isopropyl alcohol*2	45, 43	1.1	0.999

*1: Substances (two types) to be measured using carbon disulfide as the elution solvent and Rtx624 as the analysis column
*2: Substances (two types) to be measured using purified water as the elution solvent and Stabilwax as the analysis column
The other 54 substances are subject to measurement using carbon disulfide as the elution solvent and Stabilwax as the analysis column.

First Edition: March 2016

Shimadzu Corporation
www.shimadzu.com/an/

SHIMADZU
Excellence in Science

Application Data Sheet

No.121

GC-MS
Gas Chromatograph Mass Spectrometer

Test Methods for Certain Aromatic Amines Derived from Azo Colorants

BACK TO CONTENTS

Some azo colorants have been identified as hazardous in that they form carcinogens when degraded. Accordingly, Japan's Ministry of Health, Labour and Welfare will restrict the sale of textiles and leather goods using these azo colorants, starting from April 1, 2016.
Azo colorants have an azo group (A-N=N-B) and account for over 50% of organic pigments. The azo group double bond is degraded on the surface of the skin, by intestinal bacteria, and by the liver, forming amines (A-NH2 and B-NH2). Some of the amines formed (certain aromatic amines) are suspected to be carcinogenic.
Consequently, these azo colorants are already restricted in the EU, China, and South Korea. In Japan, they are currently subject to voluntary restriction, but will be legally restricted starting April 1, 2016.
The analysis methods specified in JIS L 1940 (based on EN 14362-1:2012[1)] and EN 14362-3:2012[2)] test methods) will be applied to test azo colorants.
In South Korea and China, there are a number of manufacturers manufacturing and exporting textiles and leather goods. At testing service laboratories, inspection tests are implemented based on EN 14362-1 and -3 methods.
This data sheet provides an overview of inspection methods for certain aromatic amines derived from azo colorants, as well as a description on separation of certain aromatic amines.

[1)] EN 14362-1:2012 Textiles. Methods for determination of certain aromatic amines derived from azo colorants. Detection of the use of certain azo colorants accessible with and without extracting the fibres
[2)] EN 14362-3:2012 Textiles. Methods for determination of certain aromatic amines derived from azo colorants. Detection of the use of certain azo colorants, which may release 4-aminoazobenzene

Experiment

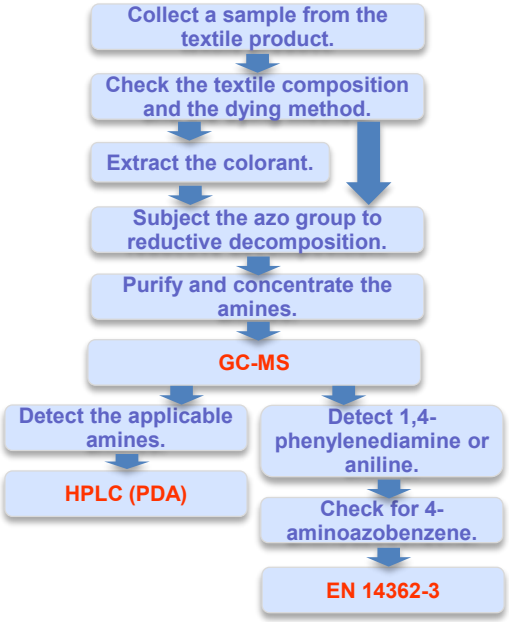

Fig. 1: An Example of Analysis Sequence Based on EN 14362-1

EN14362-1 explains the method for chromatographs, such as GC, GC/MS, HPLC, HPLC/MS and capillary electrophoresis (CE)/MS. Fig. 1 shows the example of analytical sequence when quantifying certain aromatic amines derived from azo colorants in textile products. Firstly, collect a sample from the textile product. Next, subject the azo group to reductive decomposition. Depending on the textile composition and dyeing methods, however, the colorants may need to be extracted in advance. Purify and concentrate the obtained amines, and measure them with GC-MS. If the applicable amines are detected, use another type of chromatography to confirm that the results are not a false positive. In this example, HPLC is used. The detection rate depends on the target substance, sometimes reaches up to several percent.

With the method specified in EN 14362-1, 4-aminoazobenzene is detected as aniline or 1,4-phenylenediamine. These are formed from azo colorants that are not restricted. If aniline or 1,4-phenylenediamine is detected, testing based on EN 14362-3, which can detect 4-aminoazobenzene, is required.

The GC-MS analysis conditions are shown in Table 1. A medium polarity column is utilized for the analysis, as already reported in Application Datasheet No. 29, "The Analysis of Certain Aromatic Amines Formed from Azo Colorants and Pigments".

Table 1: Analysis Conditions

GC-MS:	GCMS-QP2020
Column:	VB-35 (30 m L. × 0.25 mm I.D., df = 0.25 μm; (35%-Phenyl)-methylpolysiloxane; ValcoBond® Capillary Columns)
GC	
Injection Volume:	1 μL
Injection Unit Temp.:	240 °C
Column Temp.:	100 °C (1 min) → (20 °C /min) → 300 °C (3 min)
Carrier Gas Control:	Constant linear velocity (37.2 cm/sec)
Injection Mode:	Split (8:1)
Carrier Gas:	Helium
MS	
Interface Temp.:	280 °C
Ion Source Temp.:	250 °C
Measurement Mode:	Scan/SIM

BACK TO CONTENTS

Analysis Results

To show the analysis pattern for the applicable certain aromatic amines, a chromatogram obtained by measuring a standard sample is shown in Fig. 2. Table 2 shows the retention times of these compounds as well as the *m/z* values used for selected ion monitoring (SIM).

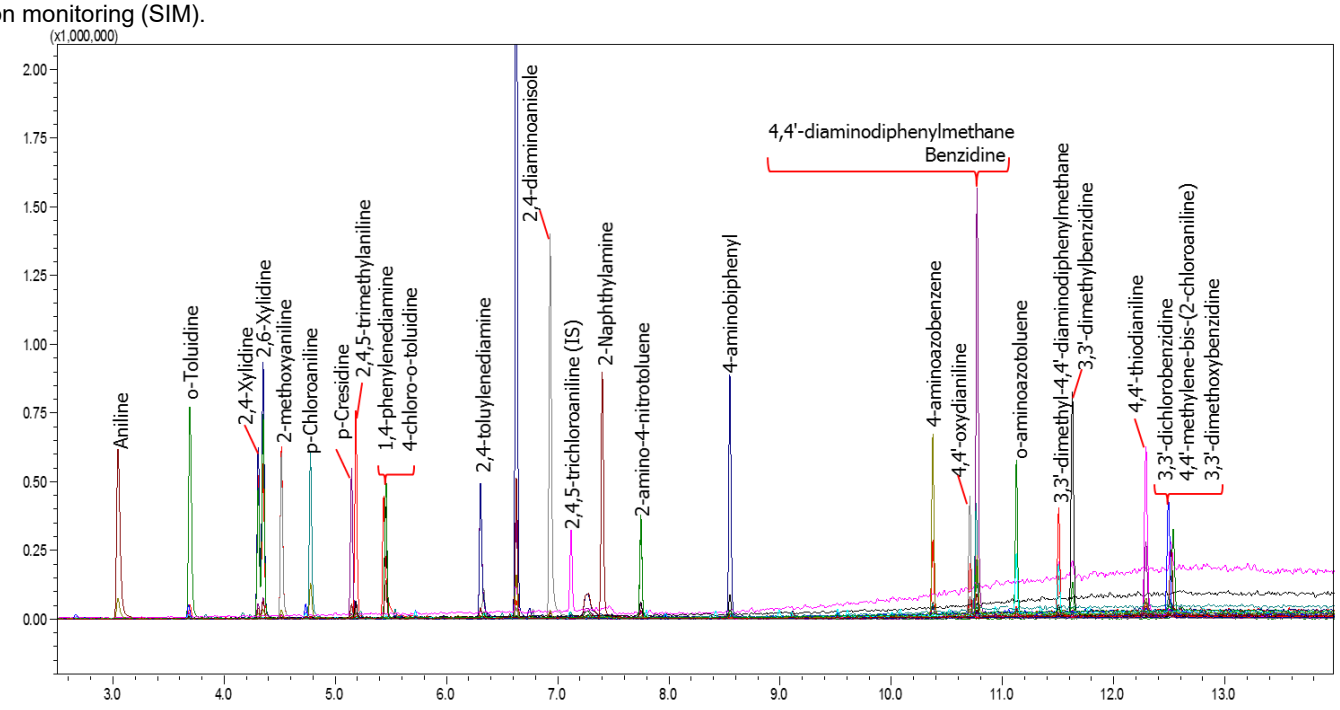

Fig. 2: Chromatogram Obtained by Measuring Certain Aromatic Amines

Table 2: Retention Times and SIM *m/z* Values

No.	Compound	RT (min)	Quantitative Ion (m/z)	No.	Compound	RT (min)	Quantitative Ion (m/z)
1	Aniline	3.04	93	15	2-amino-4-nitrotoluene	7.74	152
2	o-Toluidine	3.68	106	16	4-aminobiphenyl	8.54	169
3	2,4-Xylidine	4.30	121	17	4-aminoazobenzene	10.37	92
4	2,6-Xylidine	4.34	121	18	4,4'-oxydianiline	10.70	200
5	2-methoxyaniline	4.50	123	19	4,4'-diaminodiphenylmethane	10.76	198
6	p-Chloroaniline	4.77	127	20	Benzidine	10.76	184
7	p-Cresidine	5.13	122	21	o-aminoazotoluene	11.12	106
8	2,4,5-trimethylaniline	5.18	120	22	3,3'-dimethyl-4,4'-diaminodiphenylmethane	11.50	226
9	1,4-phenylenediamine	5.42	108				
10	4-chloro-o-toluidine	5.44	141	23	3,3'-dimethylbenzidine	11.62	212
11	2,4-toluylenediamine	6.29	121	24	4,4'-thiodianiline	12.28	216
12	2,4-diaminoanisole	6.92	123	25	3,3'-dichlorobenzidine	12.48	252
13	2,4,5-trichloroaniline (IS)	7.11	195	26	4,4'-methylene-bis-(2-chloroaniline)	12.51	231
14	2-Naphthylamine	7.39	143	27	3,3'-dimethoxybenzidine	12.53	244

Summary

GC-MS was used to quantify certain aromatic amines originating from azo colorants. Test methods such as EN 14362, ISO 24362, and JIS L1940 are used as analysis methods for textile products. ISO 17234-1:2015 and ISO 17234-2:2011 test methods are used for leather goods.

First Edition: July, 2016

Shimadzu Corporation
www.shimadzu.com/an/

SHIMADZU
Excellence in Science

Application Data Sheet

No.125

GC-MS
Gas Chromatograph Mass Spectrometer

Analysis of Naphthalene in a Working Environment

BACK TO CONTENTS

Working environment measurements are obligatory under the Japanese Industrial Safety and Health Act. The purpose is to prevent health problems in workers caused by toxic factors in the working environment. In November 2015, naphthalene was added to the list of specified chemical substances in an amendment to the Ordinance on Prevention of Hazards Due to Specified Chemical Substances, Working Environment Measurement Standards, etc.
In this article, an investigation was performed using a gas chromatograph mass spectrometer (GC-MS), in accordance with the naphthalene standard measurement analysis method. This method is outlined in appendix 4 of separate volume 06, naphthalene detailed risk assessment, of the report by the investigative commission on risk assessment for chemical substances (first report, 2014).
From the results of this investigation, it was evident that naphthalene in the working environment could be analyzed with high accuracy.

Experiment

The sampling conditions were indicated as follows: The sampling flow rate was 0.02 L/min or 0.1 L/min, and the sampling times were 10 minutes (fixed point) and 240 minutes (individual exposure). As a result, the air sampling quantities were 0.2 L or 1.0 L for the fixed point, and 4.8 L or 24 L for the individual exposure. When the air sampling quantity was 1.0 L (fixed point), the standard solution concentration, which is equivalent to a control concentration of 10 ppm, was 10.5 μg/mL. In addition, when the air sampling quantity was 4.8 L (individual exposure), the standard solution concentration, which is equivalent to a control concentration of 10 ppm, was 50.4 μg/mL.
Standard solutions at 0.1 μg/mL, 0.2 μg/mL, 1 μg/mL, 2 μg/mL, 10 μg/mL, 20 μg/mL, and 100 μg/mL were prepared by diluting the naphthalene standard product with dichloromethane, in order to enable measurements in a range from 1/100th of the control concentration to 2x the control concentration. In this case, the solutions were prepared in such a way that the naphthalene-d8 concentration in each of the standard solutions was 2 μg/mL. Each of these prepared standard solutions was measured using the analytical conditions in Table 1.

Table 1: Analytical Conditions

Gas Chromatograph Mass Spectrometer: GCMS-QP2020

GC		MS	
Column:	Stabilwax (30 m × 0.25 mm I.D., 0.5 μm)	Ion Source Temperature:	200 °C
		Interface Temperature:	240 °C
Sample Injection Volume:	1 μL	Ionization Current:	20 μA (High concentration)
Injection Port Temperature:	230 °C		
Injection Mode:	Split	Measurement Mode:	Scan
Split Ratio:	20	Measurement Mass Range:	*m/z* 50 - 250
Control Mode:	Constant linear velocity (47 cm/sec)	Event Time:	0.3 sec
Oven Temperature:	50 °C (1 min) → (20 °C/min) → 240 °C (3 min)	Measurement Mode:	SIM
		Monitor Ion:	
		Naphthalene:	128, 127, 129
		Naphthalene-d8:	136, 137, 134
		Event Time:	0.3 sec

Results

Fig. 1 shows the total ion current chromatograms obtained by measuring the 10 μg/mL naphthalene standard solution. For naphthalene, a calibration curve was created with a concentration range of 0.1 μg/mL to 100 μg/mL. The results for the correlation coefficient (R) for the calibration curve were a favorable 0.99994 or higher (Fig. 2). Fig. 3 shows the SIM chromatogram for the 0.1 μg/mL standard solution. In addition, the 0.1 μg/mL standard solution was measured five times, and the repeated analysis accuracy was calculated. The result for the repeated analysis accuracy was a favorable 2 % or less. The results are shown in Table 2.

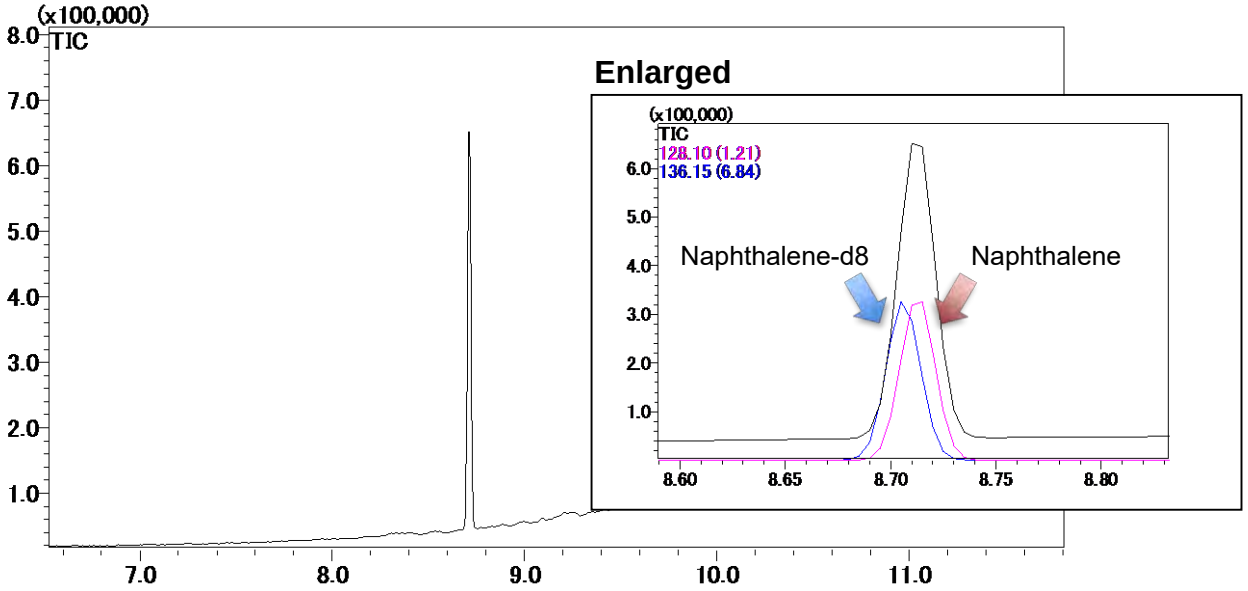

Fig. 1: Total Ion Current Chromatograms for Naphthalene and Naphthalene-d8

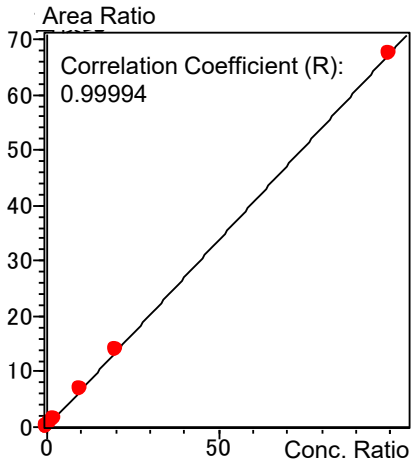

Fig. 2: Calibration Curve
(0.1 μg/mL to 100 μg/mL; Internal Standard Method)

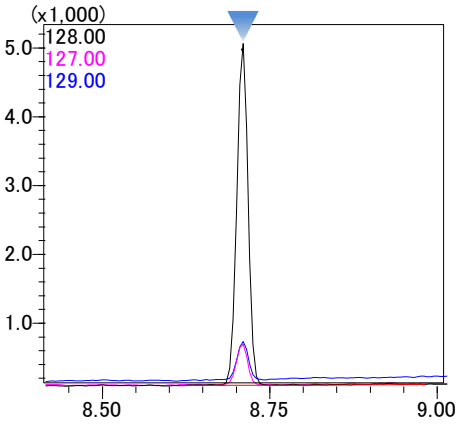

Fig. 3: SIM Chromatograms for the 0.1 μg/mL Standard Solution

Table 2: Repeated Analysis Accuracy (n=5)

Concentration units: μg/mL

ID	Compound Name	Data 1	Data 2	Data 3	Data 4	Data 5	Average	Standard Deviation	Coefficient of Variation (%)
1	Naphthalene	0.0925	0.0912	0.0902	0.0902	0.0911	0.0910	0.0009	1.04

Conclusions

Using the GCMS-QP2020, it was possible to analyze naphthalene in a working environment with good accuracy. Combining this with the Twin Line MS system would also enable the analysis of organic solvents in the working environment (including some of the specified chemical substances), reported in Application Data Sheets No. 118 and No. 119.

First Edition: March, 2017

Shimadzu Corporation

www.shimadzu.com/an/

SHIMADZU
Excellence in Science

Application Data Sheet

No.131

GC-MS
Gas Chromatograph Mass Spectrometer

Analysis of Leachate from Water Supply Equipment Using Purge and Trap GC/MS

BACK TO CONTENTS

Water supply equipment refers to materials or equipment used in water supply facilities. The quality of these materials is required to conform to the standards designated by ordinances from the Ministry of Health, Labour and Welfare, as per "tests related to the quality of materials in equipment" (notification no. 45 by the Ministry of Health, Labour and Welfare in 2000). This, in turn, was prescribed on the basis of "ministerial ordinance regarding the technical standards for water supply facilities" (ordinance no. 15 by the Ministry of Health and Welfare in 2000). The six components shown in Table 1 are configured in the purge and trap (PT) GC/MS method. They differ significantly in terms of boiling point and solubility in water, so the method for the PT system is divided into two parts. However, since the sample volumes and trap tubes are completely the same in the two PT methods, system switching is not required, which means that consecutive analyses can be performed efficiently.
This Data Sheet presents the results of an investigation regarding the ease of quantifying the components in the leachate from water supply equipment via a purge and trap GC/MS.

Table 1: Purge and Trap (PT) Measurement Methods and the Components Targeted for Measurement

PT Method 1	1,3-butadiene, 1,2-butadiene	**PT Method 2**	Vinyl acetate, epichlorohydrin, styrene, N,N-dimethylaniline

Experiment

A standard product containing 1,3-butadiene, 1,2-butadiene, vinyl acetate, epichlorohydrin, styrene, and N,N-dimethylaniline was diluted with methanol to prepare a series of six mixed standard solutions at 0.25 μg/mL, 1.25 μg/mL, 2.5 μg/mL, 12.5 μg/mL, and 25 μg/mL.
Standard samples with 0.1 μg/L, 0.5 μg/L, 1 μg/L, 5 μg/L, and 10 μg/L of each component were prepared by adding a 2 μL fraction of the mixed standard solution at each concentration to 5 mL of Volvic (mineral water).
The prepared standard samples were measured using the analytical conditions listed in Table 2.
Note that the fluorobenzene and 4-bromofluorobenzene (the internal standard substances) were diluted with methanol to prepare a 12.5 μg/mL internal standard solution. This was added utilizing the system's internal standard automatic addition function in order to reach a concentration in water of 5 μg/L.

Table 2: Analytical Conditions

Purge and Trap Gas Analyzer: AquaPT 6000
Gas Chromatograph Mass Spectrometer GCMS-QP2020

PT1	Trap Tube:	AQUA TRAP 1	PT2	Trap Tube:	AQUA TRAP 1
	Sample Volume:	5 mL		Sample Volume:	5 mL
	MCS*1:	Not used.		MCS*1:	Not used.
	Purge Time:	1.5 min		Purge Time:	18 min
	Purge Flowrate:	40 mL/min		Purge Flowrate:	60 mL/min
	Sample Heater:	ON (30 °C)		Sample Heater:	ON (30 °C)
	Dry Purge Time:	0.5 min		Dry Purge Time:	1 min
	Number of Rinse Cycles	3 cycles		Number of Rinse Cycles	9 cycles*2
	Desorption Temperature:	220 °C		Desorption Temperature:	220 °C
	Desorption Time:	2 min		Desorption Time:	2 min

GC			MS		
	Column:	InertCap AQUATIC (60 m × 0.25 mm I.D., 1.00 μm)		Ion Source Temperature:	200 °C
	Injection Port Temperature:	150 °C		Interface Temperature:	200 °C
	Injection Mode:	Split		Measurement Mode:	SIM mode
	Split Ratio:	3		Event Time:	0.3 sec
	Purge Flowrate:	3.5 mL/min			
	Control Mode:	Constant pressure (180 kPa)			
	Oven Temperature:	40 °C (1 min) → (3 °C/min) → 80 °C → (20 °C/min) → 200 °C (10 min)			

*1: Moisture Control System
*2: Up to nine cycles can be configured, and residue prone N,N-dimethylaniline can be analyzed with good accuracy.

Results

Fig. 1 shows the total ion current chromatogram obtained by measuring the 1 μg/mL standard sample in scan mode. Fig. 2 shows the SIM chromatograms for each component of the 0.1 μg/L standard sample. Sufficient sensitivity was obtained, even at concentrations of 1/10 or less of the reference level. In addition, Table 3 shows the results for the linearity (correlation coefficient: R) of the calibration curve (0.1 μg/L, 0.5 μg/L, 1 μg/L, 5 μg/L, and 10 μg/L) and the repeated analysis accuracy. A favorable result of 5 % or less was obtained for the repeated analysis accuracy.

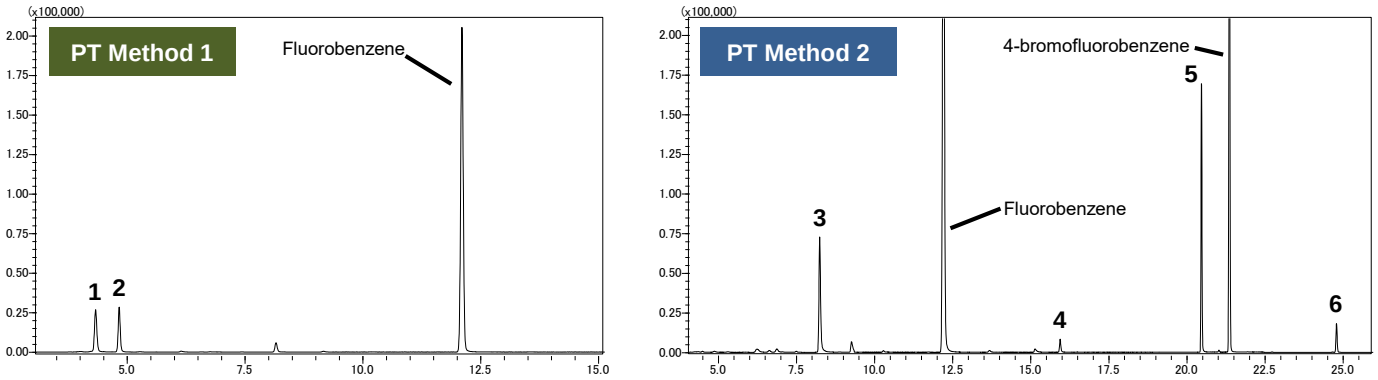

1. 1,3-butadiene; 2. 1,2-butadiene; 3. Vinyl acetate; 4. Epichlorohydrin; 5. Styrene; 6. N,N-dimethylaniline

Fig. 1: Total Ion Current Chromatogram for the Standard Sample (1 μg/L) (Left: PT Method 1; Right: PT Method 2)

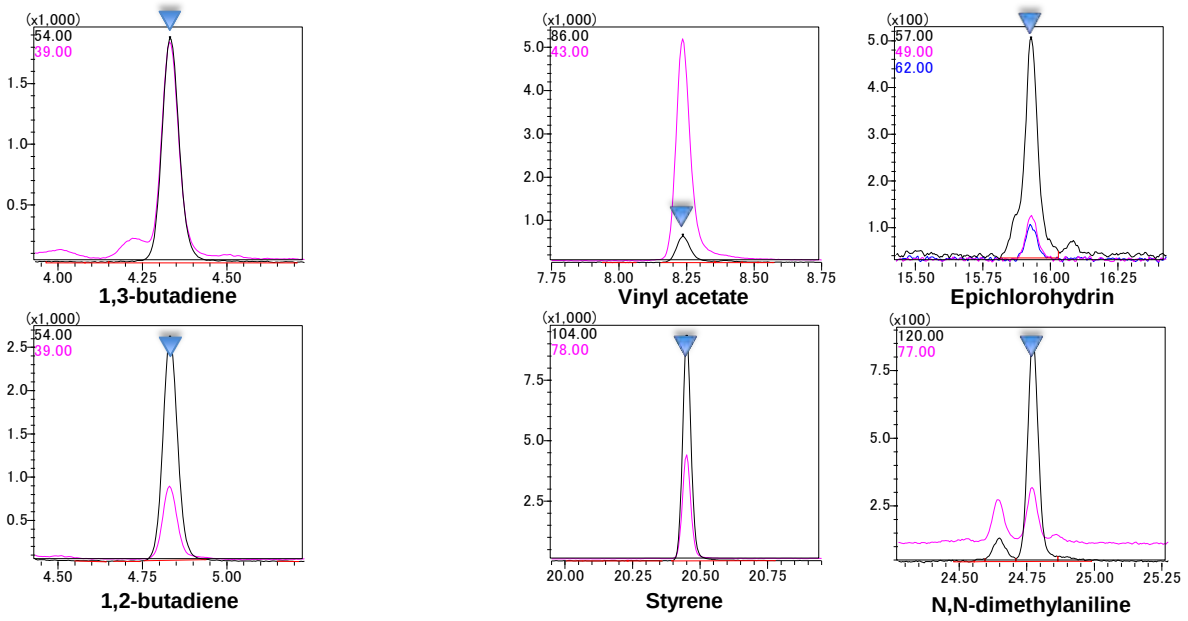

Fig. 2: SIM Chromatograms for the Standard Sample (0.1 μg/L) (Left: PT Method 1; Right: PT Method 2)

Table 2: Calibration Curve Linearity and Repeated Analysis Accuracy

ID	Compound Name	Correlation Coefficient: R	Coefficient of Variation (%)
1	1,3-butadiene	0.9988	2.3
2	1,2-butadiene	0.9991	1.5

* 0.5 μg/L, n=5

ID	Compound Name	Correlation Coefficient: R	Coefficient of Variation (%)
3	Vinyl acetate	0.9997	4.6
4	Epichlorohydrin	0.9999	3.4
5	Styrene	0.9998	2.8
6	N,N-dimethylaniline	0.9984	3.8

* 0.1 μg/L, n=5

Conclusions

From the results of an investigation of analytical conditions using the AquaPT 6000 as the purge and trap, and the GCMS-QP2020 as the GC/MS, it is evident that using this system enabled the measurement of components in the leachate from water supply equipment with high sensitivity and high accuracy.

First Edition: March, 2017

Shimadzu Corporation

www.shimadzu.com/an/

SHIMADZU
Excellence in Science

Application Data Sheet

No.136

GC-MS
Gas Chromatograph Mass Spectrometer

Off-Flavor Analysis in Chemical Material Using a Thermal Desorption Method

BACK TO CONTENTS

In recent years, there has been an increase in claims related to food and chemical products. Analysis via GC-MS(/MS) has been used as a method of specifying off-flavor causing substances. However, knowledge of the off-flavor causing substance (quality of the odor, offensive odor threshold value, and other information) is required; as a result, inexperienced analysts cannot perform such an analysis. In addition, off-flavor claims must be addressed quickly, so samples in a variety of forms must be preprocessed quickly and conveniently.
The thermal desorption (TD) method is a form of pretreatment in which an adsorbent or the sample itself is heated to a high temperature, and the gases produced are loaded into a GC-MS(/MS), enabling samples to be pretreated quickly and conveniently. In addition, in a GC/MS off-flavor analysis system, information on the parameters needed for off-flavor analysis and the main off-flavor causing substances is contained in a database, allowing analysts with no expertise or experience with off-flavor analysis to perform the analysis.
In this investigation, off-flavor samples were pretreated with the TD method, and chemical products were analyzed using a GC/MS off-flavor analysis system.

Experiment

A chemical product involved in an off-flavor claim (hereinafter the defective product) was sliced thinly, and a TD glass tube (SHIMADZU, P/N: S223-57119) was filled with approx. 40 mg of this sample. Both ends were fastened with 5 mg of quartz wool, it was heated at 250 °C for 30 minutes, and the gases produced were loaded into a GC-MS(/MS). In addition, a chemical product not involved in an off-flavor claim (hereinafter the normal product) was pretreated using the same procedures. The sample loaded was analyzed in GC-MS/MS Scan/MRM mode. The analysis conditions are shown in Table 1, and the analysis samples are shown in Fig. 1.

Table 1: Analysis Conditions

[Instrument Configuration]			
GC-MS/MS:	GCMS-TQ™ 8040		
Sample Loader:	TD-30		
Workstation (GCMS-TQ™8040):	GCMSsolution™ Ver.4.45		
Workstation (TD-30):	TD-30 Control Software		
Database Software:	GC/MS Off-Flavor Analysis System		
Column:	InertCap™ Pure-WAX (30 m x 0.25 mm I.D., df = 0.25 μm) (GL Sciences Inc.)		
[TD-30]		[MS]	
Tube Desorption Temperature:	250 °C	Ion Source Temperature:	200 °C
Tube Desorption Flowrate:	120 mL/min (5 min)	Interface Temperature:	250 °C
Trap Cooling Temperature:	-20 °C	Measurement Mode:	Scan/MRM Simultaneous Measurement
Trap Desorption Temperature:	250 °C	Scan Mass Range:	m/z 45 to 500
Joint Temperature:	250 °C	Scan Event Time:	0.1 sec.
Valve Temperature:	250 °C	Scan Speed:	5000 u/sec.
Transfer Line Temperature:	250 °C	MRM Event Time:	0.3 sec.
		MRM Transition:	Using GC/MS Off-Flavor Analysis System Transitions
[GC]			
Control Mode:	Pressure		
Pressure:	83.5 kPa		
Injection Mode:	Split 1:5 (Split Flowrate 7.2 mL/min)		
Column Oven Temperature:	50 °C (5 min) – (10 °C/min) – 250 °C (10 min)		

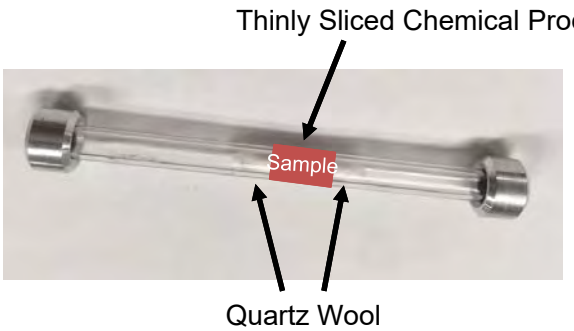

If the TD method is used, pretreatment can be performed simply by adding the sample to a glass tube. In addition, the gases produced by the sample can be loaded directly, so the loaded amount can be adjusted.

Fig. 1: Analysis Sample

4. Calibration curves
Curves were created in the same manner as Fig. 2 (figures omitted). The measurement amount (vertical axis) is an intensity ratio (internal standard correction)[*1 *2] which is the analytical line intensities of Pb, Bi, and Se divided by the RhKα scattered radiation intensity. Table 4 shows the accuracies and lower limits of detection. The values are approximately the same as those for the flat-surface samples.

Table 4 Calibration Curve Accuracy and Lower Limit of Detection [wt%]

	Pb	Bi	Se
Accuracy	0.0038	0.11	0.0057
Lower Limit of Detection	0.0018	--- (Due to high content)	0.00075

5. Quantitative analysis and repeatability test
The static repeatability testing was performed on four samples by repeating quantitative analysis 10 times. Table 5 shows the results for Pb.

Table 5 Quantitative Analysis and Repeatability Test Results for Pb [wt%]

Samples	①	②	③	④
Average	0.183	0.105	0.0375	0.242
Standard deviation	0.0020	0.0041	0.00073	0.0016
Coefficient of variation [%]	1.1	3.9	2.0	0.68

6. AA analysis
Chips were dissolved in acid and analyzed with AA.
(1) Preparation
Fig. 4 shows the acidic dissolution procedure.

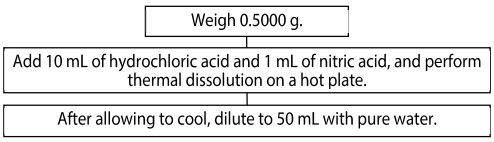

Fig. 4 Acidic Dissolution Procedure

(2) Measurement method
Frame measurement (calibration curve method)
(3) Calibration curve samples
Pb 5, 10, 20, 30 mg/L (HCl 20 %, HNO_3 2%)
(4) Measurement results

Table 6 Pb Measurement Results [wt%]

Samples	①	②	③	④
Concentration in solid	0.187	0.0995	0.0354	0.266

7. Comparison of EDX and AA
Table 7 shows the relative error of each instrument with respect to the certified values. Although the error of AA is about 5 %, the error of EDX is a little less than 10 % at the maximum, which is a slightly large value. However, since EDX is advantageous in that chip-form samples can be analyzed easily without disolving in acid, it can be used depending on the required precision for control reference judgment.
For example, if the standard for judging quantitative values with respect to management criteria of environmentally hazardous substances is set as 0.07 wt%, the sample ③ is less than the management criteria from the following formula (refer to Table 5).

Criterion formula (quantitative value + 3σ) $= 0.0375 + 3 \times 0.00073$
$= 0.040 < 0.07$ [wt%]

Table 7 Relative Error with Respect to Certified Values for EDX and AA [%]

Samples	①	②	③	④
EDX	-7.1	+1.0	+5.0	-9.7
AA	-5.1	-4.3	-0.8	-0.7

Measurement Conditions

EDX

Instrument	: EDX-8000/(7000)
Element - analytical line * *	: $PbL\beta_1$, BiLα, SeKα, RhKα
Analysis method/profile correction	: Calibration curve method/BG internal standard correction[*1 *2]
Detector/X-ray tube	: SDD/Rh target
Tube voltage - current	: 50 [kV] - Auto [μA]
Collimator/primary filter	: 10 [mmφ]/#4
Measurement atmosphere	: Air
Integral time/dead time	: 600 [sec]/max. 30 [%]

AA

Instrument	: AA-7000
Analytical wavelength	: 283.3 nm
Slit width	: 0.7 nm
Current value	: 10 mA
Ignition mode	: BGC-D2

* * Analytical line
Since Pb and Bi have neighboring atomic numbers, the X-ray fluorescence X-ray spectrum of each element overlaps. In addition, when As and Se are coexisting elements, the AsKα line overlaps the PbLα line and the SeKβ line overlaps the $PbL\beta_1$ line. Although the $PbL\beta_1$ line was selected as the analytical line, overlap correction was applied using Se and Bi since the SeKβ line and $BiL\beta_1$ line overlap. Fig. 5 shows the profiles neighboring the analytical line $PbL\beta_1$ and Table 8 lists the energy values for reference.

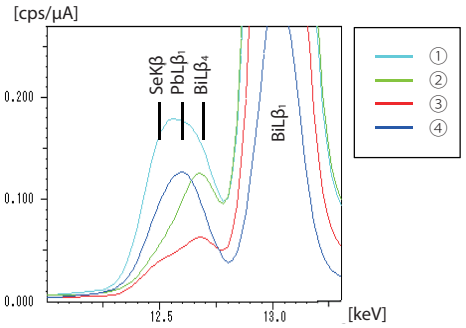

Fig. 5 Spectra of Analytical Lines

Table 8 Energy of Analytical Lines and Neighboring Lines (Reference)

Fluorescent X-Ray	Energy [keV]
AsKα	10.53
$PbL\alpha_{1,2}$	**10.55**
$BiL\alpha_{1,2}$	10.84
SeKβ	12.50
$PbL\beta_{1,2}$	**12.61**
$BiL\beta_4$	12.69
$BiL\beta_{1,2}$	13.02

Conclusion

The effectiveness of overlap correction was confirmed in regard to the quantitation of low contents of lead coexisting with bismuth. Since sufficient precision was obtained by using overlap correction in conjunction with profile correction even in the analysis of cutting chips, these methods are usable in the management of RoHS analysis that tends to involve many samples with irregular shapes. These methods can be utilized for application to other elements and materials according to purpose and use (precision, sample shape, time, preparation, etc.).

*1 Shimadzu Application News No. X246
*2 Hirotomo Ochi, Hideki Nakamura, Shinji Watanabe: Advances in X-Ray Chemical Analysis, Japan, Vol. 38, p191 (2007)

First Edition: Nov. 2017

SHIMADZU
Shimadzu Corporation
www.shimadzu.com/an/

SHIMADZU
Excellence in Science

Application Data Sheet

No.137

GC-MS
Gas Chromatograph Mass Spectrometer

Analysis of VOC and SVOC Emissions from Automotive Interior Materials in Accordance with VDA278 Using the Thermal Desorption Method

BACK TO CONTENTS

In recent years, measures to reduce the use of organic compounds in automotive interiors have progressed. In Germany, the VDA278 standards were created for the analysis of volatile organic compounds (VOC) and semi-volatile organic compounds (SVOC) produced from automotive interior materials. In the VDA278, measurement samples are added to a TD glass tube. The VOC (up to C20) and SVOC (up to C32) are heated at different temperatures, and the gases produced are loaded into a GC-MS. The VOC and SVOC from the automotive interior materials can be analyzed conveniently and quickly. However, since the gas is loaded directly, if the SVOC content is highly concentrated, caution is needed regarding carryover.
The TD-30 thermal desorption system features an inert sample line that is kept as short as possible, and samples are heated up to 300 °C, reducing SVOC carryover. In this investigation, an analysis of VOC and SVOC emissions from automotive interior materials was attempted in accordance with VDA278 using the TD-30.

Experiment

Automotive interior materials (rubber, plastic, and leather) were sliced thinly, and TD glass tubes (from Shimadzu) were filled with approximately 30 mg of these samples. Both ends were fastened with 5 mg of quartz wool. The VOC samples were heated at 60 °C for 30 minutes, the SVOC samples were heated at 90 °C for 60 minutes, and the gases produced were loaded into a GC-MS. The samples loaded were analyzed in GC-MS Scan mode. The analysis conditions are shown in Table 1, and the analysis samples are shown in Fig. 1.

Table 1: Analysis Conditions

[Instrument Configuration]	
GC-MS:	GCMS-QP™ 2020
Sample Loader:	TD-30R
Workstation (GCMS-QP™2020):	GCMSsolution™ Ver.4.45
Workstation (TD-30):	TD-30 Control Software
Column:	SH-Rxi™-5Sil MS (60 m x 0.25 mm I.D., df = 0.25 μm) (SHIMADZU)

[TD-30]	
Tube Desorption Temperature:	90 °C for 30 min (VOC) 120 °C for 60 min (SVOC)
Tube Desorption Flowrate:	60 mL/min
Trap Cooling Temperature:	-20 °C
Trap Desorption Temperature:	280 °C for 10 min
Joint Temperature:	280 °C
Valve Temperature:	250 °C
Transfer Line Temperature:	280 °C

[GC]	
Control Mode:	Pressure
Pressure:	200 kPa
Injection Mode:	Split 1:100 (Column Flowrate 1.99 mL/min)
Column Oven Temperature:	40 °C (3 min) – (10 °C/min) – 300 °C (13.5 min)

[MS]	
Ion Source Temperature:	200 °C
Interface Temperature:	250 °C
Measurement Mode:	Scan Measurement
Scan Mass Range:	*m/z* 35-400
Scan Event Time:	0.5 sec
Scan Speed:	769 u/sec

(1) Flat Sample Tray Capable of Heating the Sample Directly

When the sample is added directly in the glass tube, if the glass tube is not stored horizontally, contamination will occur due to dropping of the wool and the sample. With the TD-30 sample tray, the glass tubes can be stored horizontally, eliminating any concerns about contamination.

(2) Inert Sample Line as Short as Possible and Capable of Being Heated

The TD-30 sample line is designed to be as short as possible, and is not connected to the GC sample vaporization chamber or other unnecessary parts. In addition, all parts of the sample line can be heated to at least 300 °C, so carryover is not a concern, even for SVOC with high boiling points.

Fig. 1: Features of Analysis Samples and the TD-30 When Analyzing Automotive Interior Materials

Analysis Results

Evaluative Results for Calibration Curves and Recovery Rates

The standard samples for the calibration curves were prepared by diluting toluene and n-hexadecane with methanol to concentrations of 0.5 μg/μL. 4 uL of the sample was added to a Tenax® TA collection tube, and the response factor was calculated. The response factor was used in the calculation of the quantitative values of the compounds in the automotive interior materials. The formula is shown below.

In addition, in order to evaluate the recovery rate for the analysis system, a standard sample of typical VOCs (with a concentration of approximately 0.11 ug/uL) was prepared. 4 uL of this was added to a Tenax® TA collection tube and then analyzed. When the recovery rate was calculated from the response factor, values between 60 % and 140 % were obtained regardless of the compound, which is a favorable recovery rate.

$$R_f = \frac{\mu g \text{ Toluene (C16)}}{\text{Peak area}} \times 1000000$$

Formula 1: Formula for the Response Factor (Rf)

$$\text{Emission } [\mu g/g] = R_f \text{ (Toluene, C16)} \times \frac{\text{Peak area [count]}}{1000 \times \text{sample weight [mg]}}$$

Formula 2: Formula for the Quantitative Values (Emission[μg/g]) of Compounds Produced by Automotive Interior Materials

Table 2: Recovery Rate for Typical VOCs

Name of Compound	Recovery Ratio (%)
Benzene	106.53
Toluene	93.49
p-Xylene	99.91
o-Xylene	75.38
2-Ethyl-1-hexanol	101.26
2,6-Dimethylphenol	94.19
Dicyclohexylamine	89.15

Analysis Results for Automotive Interior Materials

The quantitative values (μg/g) for compounds produced by rubber, plastic, and leather samples are shown in Table 3. A high concentration of Bis(2-ethylhexyl) phthalate (at a concentration of 333.28 μg/g) was detected from the leather sample. When a blank sample was analyzed immediately after analyzing the leather sample, the carryover was less than 0.05 %, which is a favorable result.

Table 3: List of Quantitative Values of Compounds Produced by Automotive Interior Materials

Name of Compound	VOC			SVOC		
	Rubber	Plastic	Leather	Rubber	Plastic	Leather
C8	0.00	0.00	0.00	0.00	0.00	0.11
Toluene	0.35	0.54	0.53	0.31	0.44	0.24
C9	0.00	0.00	0.00	0.00	0.00	0.13
C11	0.00	0.00	0.00	0.00	0.00	0.31
Benzene, 1,3-dichloro-	0.00	0.00	0.00	0.00	0.00	0.08
2-Propyl-1-pentanol	0.36	0.52	0.73	0.11	0.18	0.78
C12	0.00	0.00	0.17	0.00	0.03	0.06
Nonanal	0.00	0.00	0.43	0.09	0.06	0.87
C13	0.20	0.14	0.26	0.09	0.13	0.13
C15	0.14	0.12	0.36	0.13	0.16	0.14
C16	0.31	0.00	0.60	0.42	0.16	0.86
C18	0.14	0.00	0.73	0.39	0.00	2.02
C19	0.00	0.00	0.30	0.39	0.00	1.37
Dibutyl phthalate	0.00	0.00	2.92	0.00	0.00	17.53
C20	0.00	0.00	0.18	0.14	0.00	1.28
C22	0.00	1.09	0.17	0.00	0.00	0.82
C23	0.00	0.00	0.15	0.00	0.00	0.82
C25	0.00	0.00	0.00	0.00	0.00	1.78
Bis(2-ethylhexyl) phthalate	0.41	1.60	33.67	0.00	0.00	333.28

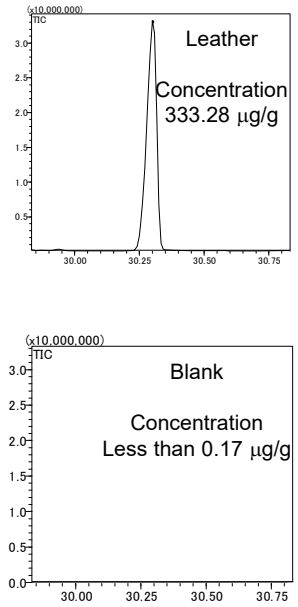

Fig. 2: Chromatograms for Bis(2-ethylhexyl) Phthalate in the Leather and Blank Samples

First Edition: December, 2017

Shimadzu Corporation
www.shimadzu.com/an/

SHIMADZU
Excellence in Science

Application News

No.X246A

X-ray Analysis

EDXRF Analysis of Arsenic and Lead in Dietary Supplement

BACK TO CONTENTS

In recent years, dietary supplements have become widely available in convenience stores and supermarkets. They are defined as food products that promote and maintain health and are used to improve disease prevention and enhance immunity. They are available in various types and forms, including tablet and powdered supplements, and processed herbal products, etc. Among these are products that are subject to safety standards that address the presence and concentrations of heavy metals, etc.[1)]

Analysis of toxic heavy metals such as As and Pb is typically conducted using an emission spectrophotometer (ICP) or atomic absorption spectrophotometer (AA), however, these require time-consuming preparation procedures. For analyte quantities ranging from a few to tens of ppm, measurement can be conducted using an X-ray fluorescence spectrometer, which permits very easy sample preparation.

Using an energy dispersive X-ray fluorescence spectrometer, we conducted quantitative analysis of As and Pb in a dietary supplement (herbal medicine), and evaluated their lower limit of detection and quantitation, respectively.

1) Example: Japan Health and Nutrition Food Association (JHNFA)

Standard Samples

Seven standard samples were prepared by mixing herbal powder with a standard solution used for atomic absorption analysis. The elements and standard values are shown in Table 1, and the preparation procedure is shown in Fig. 1.

Table 1 Standard Values

No.	As	Pb
(1)	50	0
(2)	30	5
(3)	20	10
(4)	10	20
(5)	5	30
(6)	0	50
(7)	0	0

Unit: ppm

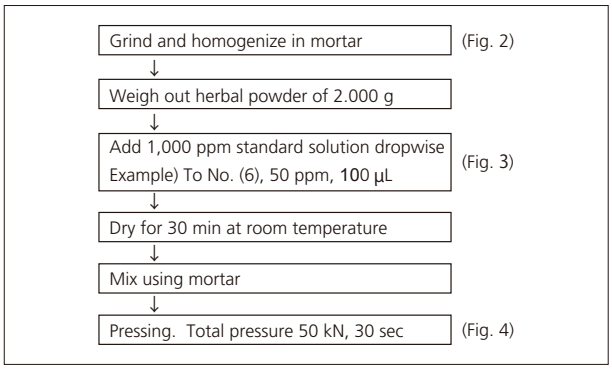

Fig. 1 Preparation Procedure

Fig. 2 Homogenization by Pulverizing

Fig. 3 Blend in Standard Solution

Fig. 4 Formed Briquette

Calibration Curves

The calibration curves for As (Kα line) and Pb (LΥ line) are shown in Fig. 5 and 6, respectively. Correction by the dj method was conducted for As, which is overlapped by Pb. We also generated those calibration curves with the internal standard which line is the RhKα C scattering (Compton) (figure not shown). Table 2 shows the accuracy of the respective calibration curves with and without internal standard correction. Accuracy refers to the variation of the calibration point using a numerical value indicated as 1 →

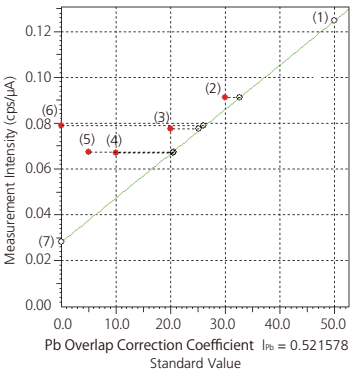

Fig. 5 Calibration Curve for As

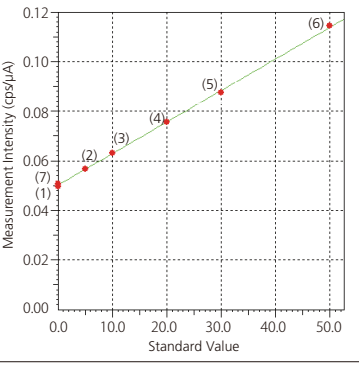

Fig. 6 Calibration Curve for Pb

BACK TO CONTENTS

Contaminant Analysis: ② Single Analysis (EDX)

An image of contaminant B is shown in Fig. 9. Based on its metallic luster, the contaminant was presumed to be inorganic, and analysis was performed using EDX. Fig. 10 shows the EDX profile, hit list, and library sample image, while Fig. 11 shows the EDX qualitative profiles for contaminant B and hit data. The biggest hit is a metal pad (stainless steel).
Hit data includes EDX data in the form of qualitative profiles and quantitative analysis results, as well as infrared spectra from FTIR data. No significant peaks appeared in the infrared spectrum obtained from hit data for contaminant B. This shows that highly accurate results can also be obtained with just a single analysis (EDX).

Fig. 9 Contaminant B

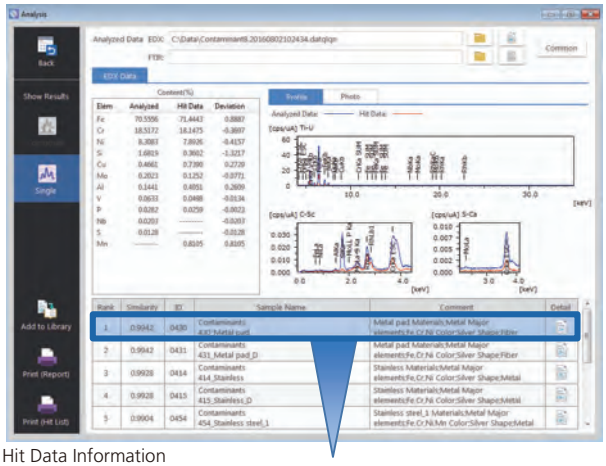

Hit Data Information
Metal pad Materials; Metal Major elements; Fe, Cr, Ni Color; Silver Shape; Fiber Hardness; Soft Metallic luster; Yes Technique; ATR (Ge)

Fig. 10 EDX Profiles, Hit List (top) and Library Sample Image (bottom)

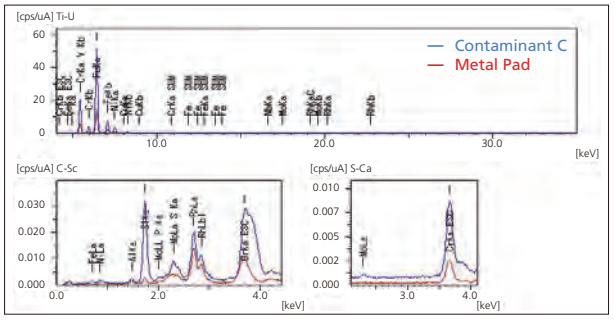

Fig. 11 EDX Profiles

Contaminant Analysis: ③ Single Analysis (FTIR)

An image of contaminant C is shown in Fig. 12. The contaminant was presumed to be organic based on its external appearance, and analysis was performed using FTIR. Fig. 13 shows the infrared spectra, hit list, and library sample image. The biggest hit was polypropylene. The major element is present at no more than 1 % according to the hit data for contaminant C. Thus, based on the hit data, it is possible to view infrared spectra from FTIR data as well as element information obtained by EDX.

Fig. 12 Contaminant C

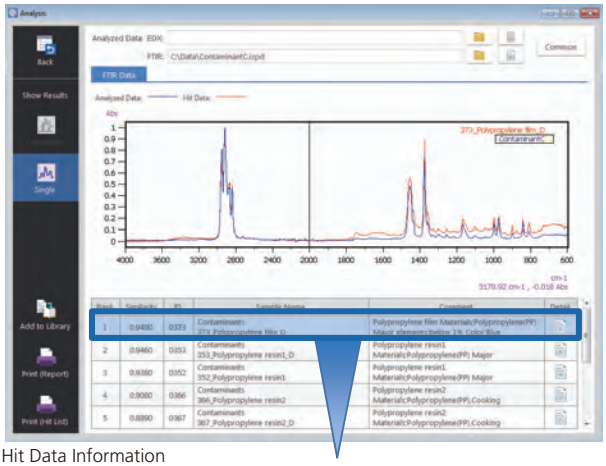

Hit Data Information
Polypropylene film Materials; Polypropylene (PP)
Major elements; below 1% Color; Blue Shape; Fragment Hardness; Soft Metallic luster; No Technique; ATR (Diamond)

Fig. 13 Infrared Spectra, Hit List (top) and Library Sample Image (bottom)

Conclusion

In this study, we could successfully perform a combined analysis of analytical data obtained by EDX and FTIR both quickly and simply by using EDXIR-Analysis. EDXIR-Analysis includes Shimadzu's own original database that contains a wealth of data that can also be easily added to by the user to create a user library. Reports can also be created to summarize analytical results, and electronic files can be grouped and stored for each data group.
EDXIR-Analysis, which incorporates the expertise of Shimadzu, provides more powerful support for contaminant analysis.

First Edition: Sep. 2016
(Second Edition: February 2017)

Shimadzu Corporation
www.shimadzu.com/an/

SHIMADZU
Excellence in Science

Application News

No. X264

X-Ray Analysis

Quantitative Analysis of Lead in Bismuth Bronze

- Matrix Elements/Profile Correction and Comparison with AA -

BACK TO CONTENTS

Some copper alloys are added with lead (Pb), but with the regulation of environmentally hazardous substances such as RoHS, it has been replaced by bismuth (Bi) in recent years. In X-ray fluorescence analysis, Bi interferes with Pb, that is, spectra overlap, so the quantitative accuracy of low content Pb may not be sufficient. In such cases, calibration curve method applying overlap correction by coexisting elements is effective.

Metal samples are generally measured in the plane of cutting and polishing, but there are cases in which the samples are irregular shapes such as chips and wiring. For irregularly shaped samples with coexisting elements, shape correction is required in addition to the overlap correction described above.

This article introduces an examination of the quantitative analysis precision when applying these corrections to a flat-surface sample and chip sample through a comparison with atomic absorption (AA) analysis.

K. Hori, S. Ueno

Samples

1. Four samples of bismuth bronze (MBH: 32X SEB 1, 2, 4, 5) and one sample of pure copper
2. Content (certified value)

Table 1 Pb, Bi, and Se Content [wt%]

Sample No.	SEB No.	Pb		Bi		Se	
		Certified Value	Uncertainty	Certified Value	Uncertainty	Certified Value	Uncertainty
①	1	0.197	0.003	4.25	0.05	0.812	0.012
②	2	0.104	0.002	4.57	0.05	0.044	0.002
③	4	0.0357	0.0008	2.48	0.04	0.119	0.003
④	5	0.268	0.007	1.056	0.016	0.471	0.006

3. Shape: 40 mmφ × 18 mmH ingot

Elements

Pb : Microdetermination
Bi, Se : Matrix element correction (overlap correction) *
* Due to Bi and Se spectra overlapping the Pb spectrum
Rh : Internal standard correction

Quantitative Analysis Using the Calibration Curve Method on Flat-Surface Samples

Quantitative analysis using the calibration curve method was performed.

1. Sample preparation
A flat surface was cut on the samples using a lathe. The samples were measured after ultrasonic cleaning with ethanol. Fig. 1 shows a sample.

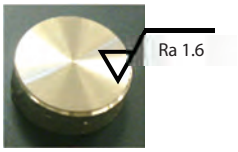

Fig. 1 Sample After Lathe Cutting

2. Calibration curves
Calibration curves were created using the five samples. Fig. 2 shows the calibration curves for Pb, Bi, and Se. Overlap correction (dj method) by coexisting elements of Bi and Se was applied to Pb. Table 2 shows the accuracies and the lower limits of detection calculated from the theoretical statistical changes in background intensity.
From the Pb calibration curve, it can be seen that the overlap of Bi is large. Accuracy is 0.0029 %, which is good in the calibration curve range 0 to 0.268 %.

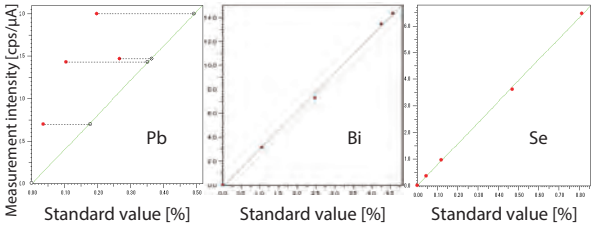

Fig. 2 Calibration Curves of Pb, Bi, and Se (Zero Point: Pure Copper)

Table 2 Calibration Curve Accuracy and Lower Limit of Detection [wt%]

	Pb	Bi	Se
Accuracy	0.0029	0.075	0.0079
Lower Limit of Detection	0.0015	--- (Due to high content)	0.00063

3. Quantitative analysis and repeatability test
The static repeatability testing was performed on sample ③ by repeating quantitative analysis 10 times using the calibration curves from section 2. Table 3 shows the results.

Table 3 Quantitative Analysis and Repeatability Test Results for Sample ③ [wt%]

	Pb	Bi	Se
Average	0.0368	2.35	0.122
Standard deviation	0.0012	0.043	0.0075
Coefficient of variation [%]	3.2	0.18	0.62

Quantitative Analysis with Profile Correction of Cutting Chips

In order to measure the samples in chip form, an internal standard correction effective for profile correction was applied to the calibration curves.[*1 *2] For the calibration curve sample, the flat-surface sample of the previous section was used.

1. Samples
Cutting chips of samples ① to ④ in Table 1
2. Preparation
Ultrasonic cleaning with ethanol
3. Setting
A sample container covered with 5 μm thick polypropylene film was used and the chips were evened out to cover an analysis diameter of 10 mmφ.

Fig. 3 Cutting Chips

BACK TO CONTENTS

Analysis of Elemental Content Differences in Plastic Materials

RoHS compliant ERM-EC680 and ERM-EC681 polyethylene reference materials were selected for data comparison as a genuine product and test product respectively. Qualitative and quantitative analysis was performed with EDX and a single reflection ATR attachment was used to measure their infrared spectra. The results are indicated in Fig. 3 and 4 and the instruments and analysis conditions are listed in Table 1.

By overlapping the EDX profiles and FTIR spectra respectively of the genuine product and test product, we can see that while there are content differences for S, Cl, Cr, Zn, Br, Cd, Sn, and Sb, there is no difference with respect to plastic (main component).

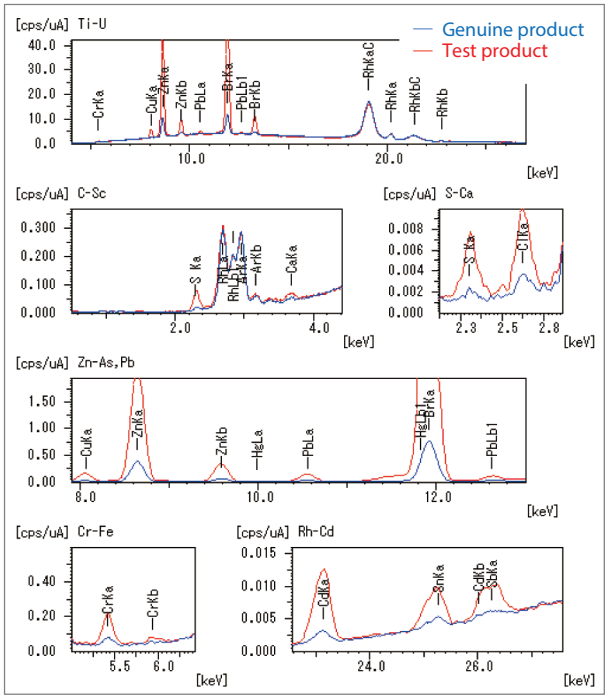

Fig. 3 Comparison of EDX Qualitative Profiles

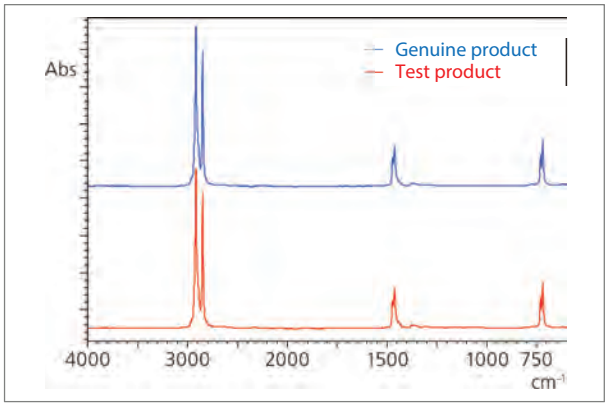

Fig. 4 Comparison of FTIR Spectra

The similarities determined using the data comparison function were 0.9616 with EDX data and 0.9830 with FTIR data, which resulted in a composite similarity of 0.9723 that suggests a difference in materials.

Table 2 indicates the result of determining whether there is a significant difference in similarity between genuine products and between a genuine product and test product, based on the repeatability accuracy observed through multiple comparisons. The EDX data results show a significant difference whereas the FTIR data results do not, which supports the assumption that the elemental content of the test product differs from the genuine product.

Table 1 Instruments and Analysis Conditions

[EDX]

Instrument	:	EDX-8000
X-ray Tube	:	Rh target
Voltage/Current	:	15 kV (C-Sc), 50 kV (Ti-U)/Auto
Atmosphere	:	Air
Measurement Diameter	:	10 mm ϕ
Primary Filter	:	Without (Ti-U, C-Sc), #1 (Rh-Cd), #2 (S-Ca), #3 (Cr-Fe), #4 (Zn-As, Pb)
Integration Time	:	30 sec (without Primary Filter) 60 sec (with Primary Filter)

[FTIR]

Instruments	:	IRAffinity-1S, MIRacle10 (Diamond prism)
Resolution	:	4 cm^{-1}
Accumulation	:	40
Apodization	:	Happ-Genzel
Detector	:	DLATGS

Table 2 Similarity Calculation Result

	EDX		FTIR	
n	Genuine product	Test product	Genuine product	Test product
1	0.9969	0.9616	0.9790	0.9830
2	0.9948	0.9613	0.9800	0.9800
3	0.9962	0.9613	0.9830	0.9810
4	0.9966	0.9612	0.9820	0.9830
5	0.9960	0.9613	0.9860	0.9790
Average	0.9961	0.9613	0.9820	0.9812
Standard deviation	0.0008	0.0002	0.0027	0.0018
Significant difference *	Yes		No	

* According to t-test (significant level: 5%)
Using commercially-available spreadsheet software

Summary

This time we introduced an example in which genuine products and test products were analyzed by utilizing the data comparison function of the EDXIR-Analysis software. By not only checking data visually but also quantifying them, differences between samples were easily distinguished.

Use of both EDX and FTIR instruments allows a multifaceted approach by enabling analysis of both organic and inorganic substances and assists in the risk management of raw materials in relation to safety. This software enables linkage and storage of various data as electronic files and provides powerful support in developing measures against silent change.

First Edition: Feb. 2017

SHIMADZU

Shimadzu Corporation
www.shimadzu.com/an/

SHIMADZU
Excellence in Science

Application News

No. A527

Spectrophotometric Analysis

Quantifying "Silent Change" Using EDXIR-Analysis Software: EDX-FTIR Contaminant Finder/Material Inspector

BACK TO CONTENTS

The act of changing raw materials without notifying business partners for the purpose of reducing costs is known as "silent change."
Since products manufactured with non-standard raw materials cannot be guaranteed in terms of quality and usage of such materials can lead to incidents, this has become a social issue. The management of safe and good quality raw materials is indispensable in the manufacture of high quality products.

The EDXIR-Analysis software features a data comparison function. EDX data or FTIR data, or both, can be used to quantify the differences between genuine products and test products in terms of similarity. This function facilitates verification of raw materials as standard materials and proves effective in acceptance inspections, sampling inspections, and primary screening.

In this article, we introduce an example analysis that utilizes the data comparison function.

S. Iwasaki

Analysis of Plastic Contaminated with Toxic Elements

In order to use the data comparison function, genuine product data is registered into the library first. Next, after a comparison is performed between the genuine product data and test product data, the similarity and comparisons of the respective element contents, profiles, and EDX images of the EDX analysis data and the similarity of FTIR spectra of the FTIR analysis data are displayed.

The following data comparison was performed for a genuine product and test product of polyvinyl chloride (PVC) plastic. The results are indicated in Fig. 1 and 2.

The similarities determined using the data comparison function were 0.8332 with EDX data and 0.8680 with FTIR data, which resulted in a composite similarity of 0.8506. Similarity is displayed in a 0 to 1 range and higher values indicate greater similarity between data. In other words, a value close to 1 is obtained when the components in the samples for comparison are equivalent. However, we can conclude that the sample tested here may include different raw materials due to the resulting composite similarity of 0.8506.

The EDX profile and FTIR spectrum of the test product also indicate that it contains lead (Pb) and components derived from acrylic (indicated with stars), which are not detected in the genuine product.

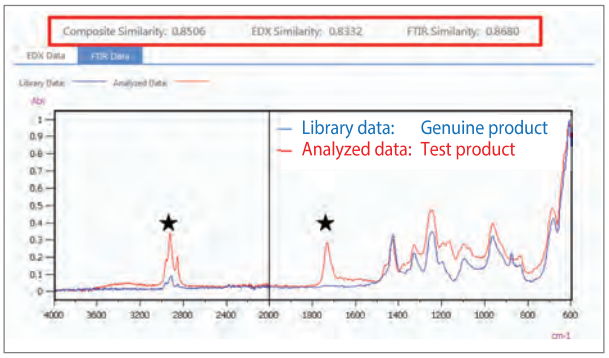

Fig. 2 Comparison of FTIR Spectra

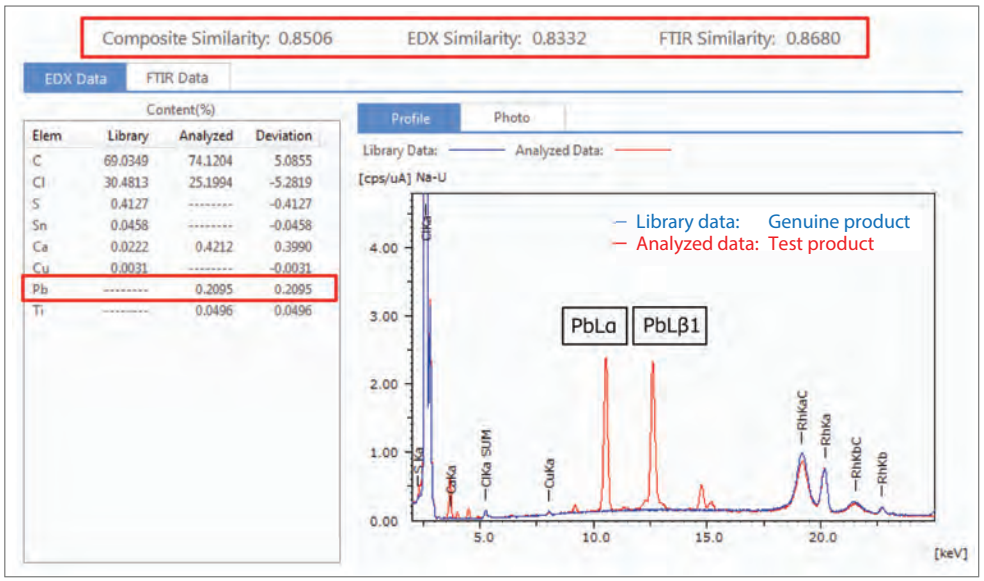

Fig. 1 Data Comparison Result and EDX Profiles

BACK TO CONTENTS

Analysis of Elemental Content Differences in Plastic Materials

RoHS compliant ERM-EC680 and ERM-EC681 polyethylene reference materials were selected for data comparison as a genuine product and test product respectively. Qualitative and quantitative analysis was performed with EDX and a single reflection ATR attachment was used to measure their infrared spectra. The results are indicated in Fig. 3 and 4 and the instruments and analysis conditions are listed in Table 1.

By overlapping the EDX profiles and FTIR spectra respectively of the genuine product and test product, we can see that while there are content differences for S, Cl, Cr, Zn, Br, Cd, Sn, and Sb, there is no difference with respect to plastic (main component).

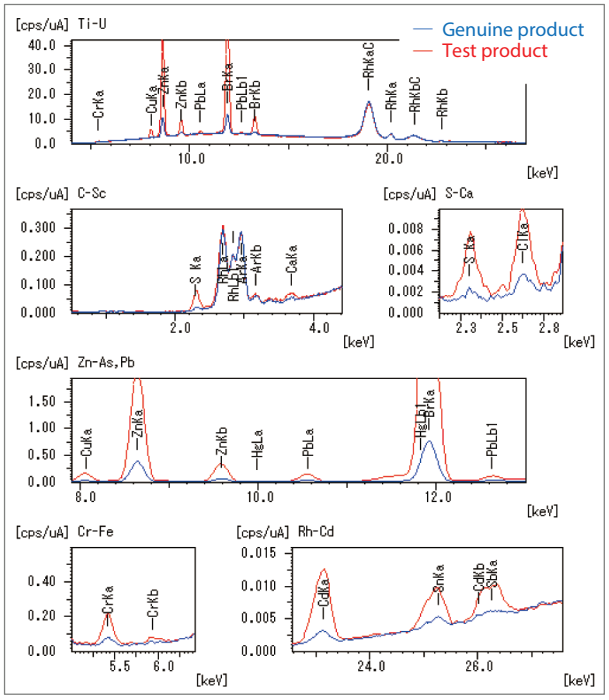

Fig. 3 Comparison of EDX Qualitative Profiles

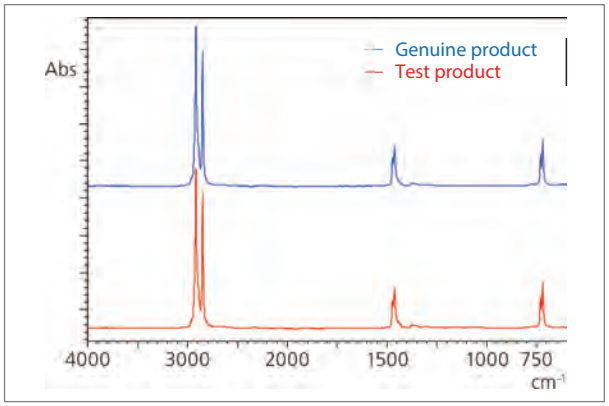

Fig. 4 Comparison of FTIR Spectra

The similarities determined using the data comparison function were 0.9616 with EDX data and 0.9830 with FTIR data, which resulted in a composite similarity of 0.9723 that suggests a difference in materials.

Table 2 indicates the result of determining whether there is a significant difference in similarity between genuine products and between a genuine product and test product, based on the repeatability accuracy observed through multiple comparisons. The EDX data results show a significant difference whereas the FTIR data results do not, which supports the assumption that the elemental content of the test product differs from the genuine product.

Table 1 Instruments and Analysis Conditions

[EDX]

Instrument	:	EDX-8000
X-ray Tube	:	Rh target
Voltage/Current	:	15 kV (C-Sc), 50 kV (Ti-U)/Auto
Atmosphere	:	Air
Measurement Diameter	:	10 mm ϕ
Primary Filter	:	Without (Ti-U, C-Sc), #1 (Rh-Cd), #2 (S-Ca), #3 (Cr-Fe), #4 (Zn-As, Pb)
Integration Time	:	30 sec (without Primary Filter) 60 sec (with Primary Filter)

[FTIR]

Instruments	:	IRAffinity-1S, MIRacle10 (Diamond prism)
Resolution	:	4 cm^{-1}
Accumulation	:	40
Apodization	:	Happ-Genzel
Detector	:	DLATGS

Table 2 Similarity Calculation Result

	EDX		FTIR	
n	Genuine product	Test product	Genuine product	Test product
1	0.9969	0.9616	0.9790	0.9830
2	0.9948	0.9613	0.9800	0.9800
3	0.9962	0.9613	0.9830	0.9810
4	0.9966	0.9612	0.9820	0.9830
5	0.9960	0.9613	0.9860	0.9790
Average	0.9961	0.9613	0.9820	0.9812
Standard deviation	0.0008	0.0002	0.0027	0.0018
Significant difference *	Yes		No	

* According to t-test (significant level: 5%)
Using commercially-available spreadsheet software

Summary

This time we introduced an example in which genuine products and test products were analyzed by utilizing the data comparison function of the EDXIR-Analysis software. By not only checking data visually but also quantifying them, differences between samples were easily distinguished.

Use of both EDX and FTIR instruments allows a multifaceted approach by enabling analysis of both organic and inorganic substances and assists in the risk management of raw materials in relation to safety. This software enables linkage and storage of various data as electronic files and provides powerful support in developing measures against silent change.

First Edition: Feb. 2017

SHIMADZU

Shimadzu Corporation
www.shimadzu.com/an/

SHIMADZU
Excellence in Science

Application News

No. A567

Spectrophotometric Analysis

Combined Analysis of a Contaminant Using a Compact FTIR and EDX

BACK TO CONTENTS

Demands regarding the analysis of contaminants that are mixed in or adhered to products are increasing for food and chemical manufacturers and inspection agencies which are consigned inspections.

This increase in demands has drawn attention to energy dispersive X-ray fluorescence spectrometers (EDX) which are suited to analyzing inorganic elements such as metals and to Fourier transform infrared spectrophotometers (FTIR) which are optimal for the analysis of organic substances such as polymeric compounds. Cases where one sample is analyzed using both instruments are increasing as well. However, data obtained with each instrument requires respective analysis procedures and results are sometimes influenced by the operator's knowledge and experience. It is in light of such situations that Shimadzu developed the EDX-FTIR contaminant finder/material inspector, EDXIR-Analysis™ software. The first in the industry, this software is capable of combining and analyzing data acquired from a Shimadzu EDX and FTIR. Details of the software are introduced in Application News Nos. A522A [1] and A527 [2]. This article introduces an example analysis of a contaminant using the EDX-FTIR combined analysis system shown in Fig. 1.

R. Fuji, T. Nakao

Fig. 1 EDX-FTIR Combined Analysis System

Measurement Sample

A contaminant found in a food production process (Fig. 2) was used as the measurement sample. About 4 mm in size and white on the surface, the sample is hard when handled with tweezers. The sample was measured by fixing it in place using the EDXIR-Holder™ shown in Fig. 3, which is a sample holder/stocker for contaminant measurement and effective for streamlining analysis processes for EDX and FTIR. Details of the EDXIR-Holder are introduced in Application News No. A537 [3].

Fig. 2 Photograph of Contaminant Found in a Food Production Process

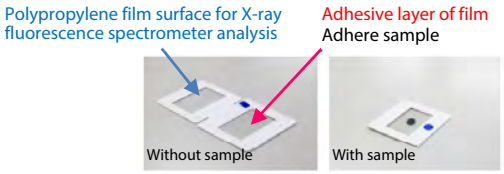

Fig. 3 EDXIR-Holder: Sample Holder/Stocker for Contaminant Measurement

Measurement Using FTIR

IRSpirit™, a compact FTIR, was used for measurement with the QATR™-S single-reflection ATR accessory, which is designed especially for the IRSpirit series, with a diamond prism installed (Fig. 4). Fig. 5 shows the sample set on the instrument and Table 1 lists the measurement conditions that were used. In using the IRSpirit, the dedicated IR Pilot program was used to facilitate measurement. IR Pilot allows operators with minimal FTIR experience to analyze samples by simply selecting the analysis purpose and the accessory. The measured spectrum and the search result from the standards library with the highest similarity are drawn superimposed in Fig. 6. In this case, protein was identified as the best match.

Fig. 4 IRSpirit with QATR-S Single-Reflection ATR Accessory (Diamond prism)

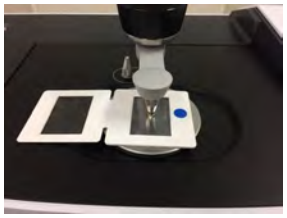

Fig. 5 Sample Set on Instrument

Table 1 Measurement Conditions

Instrument	: IRSpirit-T (KRS-5 window) QATR-S
Resolution	: 4 cm^{-1}
Accumulation Times	: 20
Apodization Function	: SqrTriangle
Detector	: DLATGS

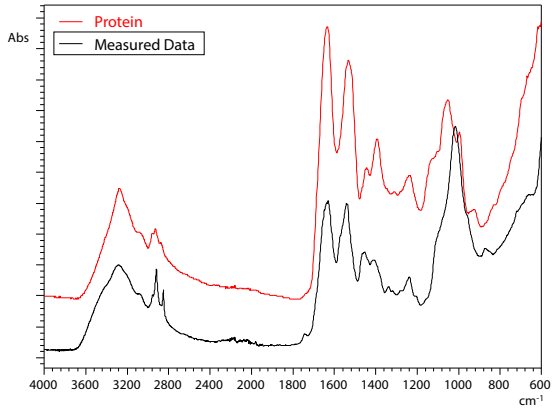

Fig. 6 Infrared Spectra of Measured Data and the Search Result

BACK TO CONTENTS

Measurement Using EDX

Measurement was done using the EDX-7000 energy dispersive X-ray fluorescence spectrometer (Fig. 7) according to the measurement conditions listed in Table 2. The sample was set on the instrument as shown in Fig. 8. For measurement using EDX, the EDXIR-Holder is closed and placed so that the side with polypropylene film is facing the X-ray beam source (bottom). The EDXIR-Holder enables easy setting of samples between EDX and FTIR instruments and contributes to alleviating and improving the efficiency of analysis tasks.

Fig. 7 EDX-7000 Energy Dispersive X-Ray Fluorescence Spectrometer

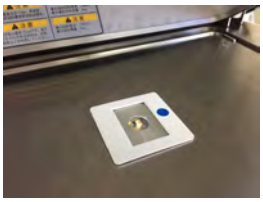

Fig. 8 Sample Set on Instrument

Table 2 Measurement Conditions

Instrument	: EDX-7000
X-Ray Tube Target	: Rh
Voltage / Current	: 50 kV (Al-U) / Auto
Atmosphere	: Vacuum
Analysis Diameter	: 1 mmϕ
Filter	: None
Integration Time	: 100 s

Fig. 9 shows the qualitative and quantitative analysis results which indicate that $_{20}$Ca and $_{15}$P are the primary elements of the contaminant. Conventionally, the identification of a contaminant requires the analysis of each of the EDX and FTIR measurement results. In this instance however, the EDXIR-Analysis software was used to read and analyze the data acquired from the instruments.

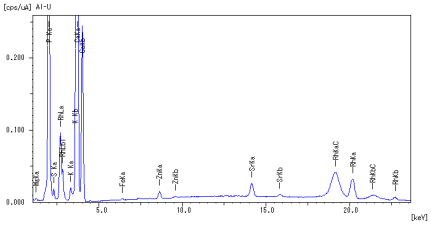

Elements	Ca	P	Mg	K	S	Sr	Zn	Fe
Quantitative Value [wt%]	68.1	28.3	1.8	0.95	0.66	0.09	0.09	0.04

Fig. 9 Qualitative and Quantitative Analysis Results

EDXIR-Analysis, IRTracer, IRAffinity, EDXIR-Holder, IRSpirit and QATR are trademarks of Shimadzu Corporation.

Analysis Using EDXIR-Analysis Software

Analysis was done using the EDXIR-Analysis software. The contaminant library used in analysis was developed by measuring and accumulating data of contaminants provided by water supply organizations and food manufacturers using Shimadzu's EDX and FTIR. Comprising a total of 485 entries, various contaminants such as tap water contaminants and food contaminants are registered.

The hit list shown in Fig. 10 indicates that with a similarity of 0.9160, the most probable match is white bone particle (a mixture of calcium phosphate and protein). Similarity values are within the range from 0 to 1 and larger values indicate that the analyzed data (acquired data) and the hit data (data in the library) are more similar. By comparing the element content and X-ray fluorescence profile of the analyzed data and hit data in Fig. 11 and the infrared spectra in Fig. 12, we can see that the two are highly similar. In addition, images of the sample can be compared as shown in Fig. 13, allowing evaluation of similarity with candidate substances in terms of color, shape, and texture. Based on these various aspects it was concluded that the contaminant is bone.

Fig. 10 Hit List

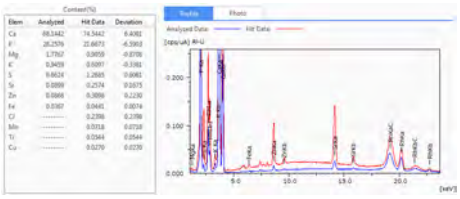

Fig. 11 Element Content and X-Ray Fluorescence Profiles of Analyzed Data and Hit Data

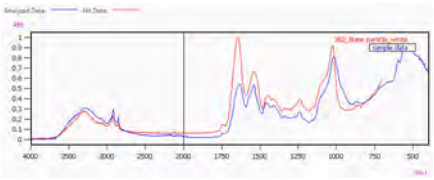

Fig. 12 Infrared Spectra of Analyzed Data and Hit Data

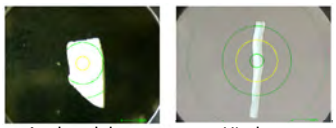

Analyzed data Hit data

Fig. 13 Sample Images of Analyzed Data and Hit Data

The EDXIR-Analysis software enabled easy and swift obtaining of analysis results that combine the inorganic element information acquired using EDX and the organic compound information acquired using FTIR.

References

(1) Application News No. A522A "Contaminant Analysis Using EDXIR-Analysis Software for Combined EDX-FTIR Analysis"
(2) Application News No. A527 "Quantifying "Silent Change" Using EDXIR-Analysis Software: EDX-FTIR Contaminant Finder/Material Inspector"
(3) Application News No. A537 "Introducing the EDXIR-Holder: Sample Holder/Stocker for Contaminant Measurement"

First Edition: Apr. 2018

Shimadzu Corporation
www.shimadzu.com/an/

SHIMADZU
Excellence in Science

Application News

No. A587

Spectrophotometric Analysis

Analysis of a Filter Paper Surface Contaminant with the GladiATR™ Vision Observation-Type ATR

BACK TO CONTENTS

ATR (attenuated total reflection) is a powerful type of reflectance method that enables measurement of minute or thick samples which are difficult to measure using the transmission method. The ATR method acquires an absorbance spectrum of a sample surface by measuring the total reflection of light from the sample surface. Characteristics of this method include simplicity compared to other surface analysis methods, absorbance intensity that depends on wavelength, and the ability to adjust the penetration depth of light into the sample by changing the incident angle and crystal refractive index.

Shimadzu offers an extensive variety of ATR accessories, including those that enable observation and others equipped with a pressure sensor. This article introduces an example of analyzing a contaminant using one of these ATR accessories, the GladiATR Vision (Fig. 1) manufactured by PIKE Technologies.

R. Fuji

Fig. 1 GladiATR Vision

GladiATR Vision Features

The GladiATR is an ATR accessory that features high throughput, a high clamping pressure, a wide measurement wavenumber range, and optional crystal plates that support heating to high temperatures.

In addition to the above, the GladiATR Vision also includes a function for observing minute samples. The diamond crystal has a monolithic structure that is difficult to damage by pressure.

Observation on the GladiATR Vision is performed through the diamond crystal. Locating the correct measurement position is easy since the position for measurement can be observed in real-time on the LCD screen. Observation is also possible through the diamond crystal for thick opaque samples.

The GladiATR Vision, as illustrated in Fig. 2, employs an innovative optical design that enables infrared measurement and visual observation to be performed simultaneously. The measurement position on the sample can be observed at 110 times magnification. The ability to optimally place and analyze samples at the center of the diamond crystal allows measurement at sizes down to 50 µm.

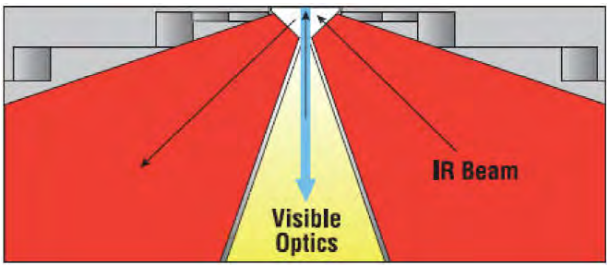

Fig. 2 Optical Method Employed by the GladiATR Vision

Analysis of a Filter Paper Surface Contaminant

The ATR method involves irradiating an infrared beam onto the sample from below, as illustrated in Fig. 3. This means that the actual measurement position may be incorrect if the position of the target contaminant cannot be determined from the other side such as on a piece of paper or resin.

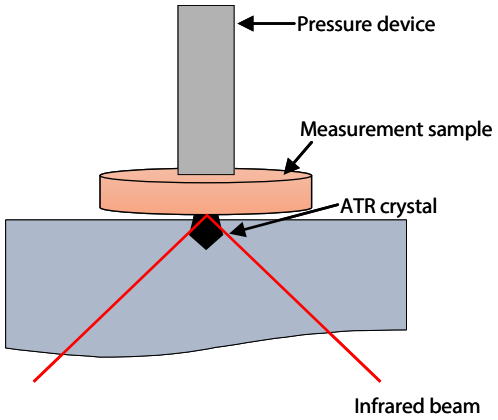

Fig. 3 ATR Method Principle

Fig. 4 (a) and (b) show the sample for measurement. Since the location of the contaminant cannot be confirmed from the other side, the observation-type ATR GladiATR Vision was used to perform measurement.

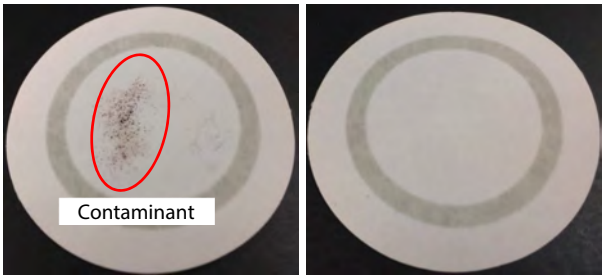

(a) Measurement side (b) Other side

Fig. 4 Optical Method Employed by the GladiATR Vision

Table 1 lists the measurement conditions, Fig. 5 shows the observation image, and Fig. 6 shows the measurement results. The filter paper sample was placed directly onto the GladiATR Vision and the contaminant on the surface of the filter paper was measured. Since influence from the filter paper component was expected, the other side without the contaminant was also measured for comparison.

Table 1 Measurement Conditions

Instrument	: IRTracer™-100, GladiATR Vision
Resolution	: 4 cm^{-1}
Accumulation	: 40
Apodization function	: Sqr-Triangle
Detector	: DLATGS

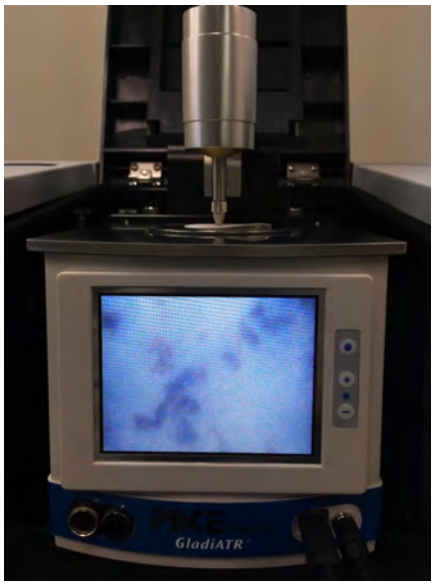

Fig. 5 Observation Image of Contaminant

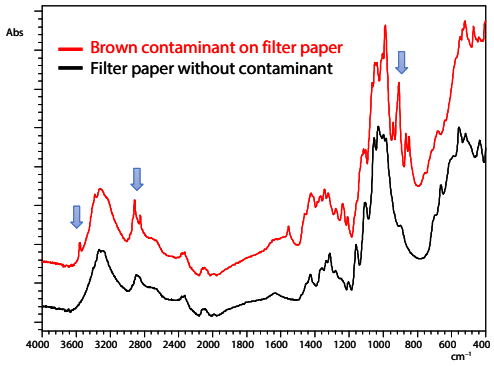

Fig. 6 Measurement Results

In Fig. 6, a difference in peaks in the vicinities of 3600 cm^{-1}, 2800 cm^{-1}, and 900 cm^{-1} can be observed (blue arrows in the figure). By performing analysis using the library provided as standard on the FTIR, the contaminant appears to be sucrose, as shown in Fig. 7 (a) and (b). (The filter paper component is cellulose.)

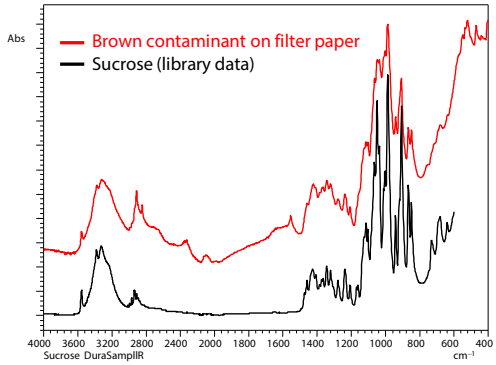

Fig. 7 (a) Analysis Result of Contaminant

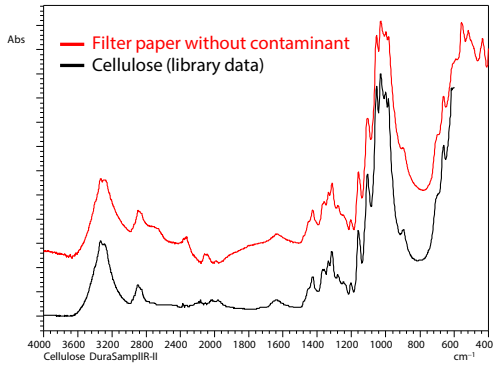

Fig. 7 (b) Analysis Result of Filter Paper

Conclusion

An observation-type ATR accessory is helpful for samples on which the position of a contaminant cannot be determined from the other side. By using the GladiATR Vision, fine adjustment of the sample position is made easy by checking the image on an LCD screen.
The GladiATR Vision can be attached to the Shimadzu IRTracer-100 and IRAffinity™-1S.

First Edition: Dec. 2018

Shimadzu Corporation
www.shimadzu.com/an/

SHIMADZU
Excellence in Science

Application News

No. X265

X-Ray Analysis

X-Ray Fluorescence Analysis of Residual Catalysts

BACK TO CONTENTS

Many familiar industrial products are made of organic compounds and their manufacturing processes involve various synthesis reactions and metal catalysts. Catalysts are mainly divided into two categories: homogeneous catalysts and heterogeneous catalysts. In general, homogeneous catalysts are used for manufacturing pharmaceuticals and chemicals. While the reactions of homogeneous catalysts can be controlled rigorously, separation of reaction products is difficult.
Meanwhile, there is a need to control the amount of residual catalysts in terms of the safety of the products and the re-use of expensive catalysts. For example, the Guideline for Elemental Impurities (ICH Q3D) enforced in April 2017 requires a risk assessment for substances, such as catalysts, that are purposely added during the manufacturing process.
This article introduces an example analysis of the amount of residual homogeneous catalyst following a synthesis reaction using the Pharmaceuticals Impurities Screening Method Package; in this example we used palladium (Pd), a substance widely used as a catalyst, for a cross-coupling reaction which is widely used for the synthesis of organic compounds.

S. Ueno

Sample

(1) Measurement Samples

1. Suzuki-Miyaura Cross Coupling Reaction Experiment Kit 2: sold by Wako Pure Chemical Industries
2. Silia*MetS*™ DMT metal scavenger: made by SiliCycle

We used a scientific experiment kit consisting of reagents and a catalyst, palladium acetate, for synthesizing two types of fluorophores (fluorophore 1 and 2) by employing the Suzuki-Miyaura cross-coupling reaction. A metal scavenger for palladium (Pd) was used to remove the catalyst.

(2) Calibration curve standard solution

USP-TXM 4 (standard solution made by SPEX, U.S.A.)

Solutions with six different concentration levels were prepared: blank (pure water), 1 mg/kg, 10 mg/kg, 20 mg/kg, 50 mg/kg, and 100 mg/kg.

Elements

Pd

Pretreatment and Sample Setting

Without any pretreatment, each solution was poured into a sample container, which was covered with 5 µm thick polypropylene film, until the liquid depth was 5 mm or more. The container was then directly set on the instrument stage as shown in Fig. 1.

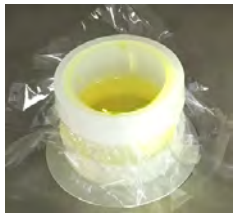

Fig. 1 Sample Set in Instrument

Calibration Curve

The calibration curve is shown in Fig. 2 and the correlation coefficient and accuracy are shown in Table 1.

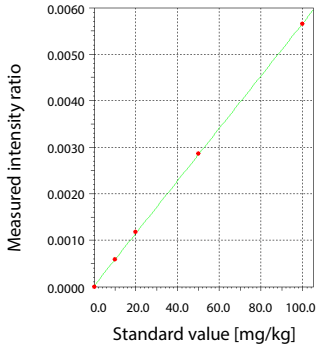

Fig. 2 Calibration Curve

Table 1 Calibration Curve Data

Correlation coefficient	0.9996
Accuracy [mg/kg]	0.36

Quantitative Analysis Results

The amount of Pd was quantitatively analyzed by the calibration curve method at three stages: ① prior to adding the catalyst, ② after adding the catalyst (adjusted value: 60 mg/kg), and ③ after separating and removing the catalyst. The results are shown in Table 2. It was found that by using the pharmaceuticals impurities screening method package, it is possible to perform an analysis in the order of mg/kg even when the integration time is substantially shortened to 300 s from the standard condition of 1,800 s.

Table 2 Quantitative Analysis Results [mg/kg]

Sample	Fluorophore 1	Fluorophore 2
①	Below the lower quantitation limit	Below the lower quantitation limit
②	64.4	70.0
③	Below the lower quantitation limit	Below the lower quantitation limit
Post-filtration powder (for reference)	(426)	(430)
Lower quantitation limit	2.3*1	

*1 Calculated from the repeatability from six measurements of the mg/kg solutions.

Measurement Conditions

Table 3 Measurement Conditions

Instrument	:	EDX-7000
Analysis Method	:	Calibration curve method
Detector/X-Ray Tube	:	SDD/Rh target
Tube Voltage - Current	:	50 [kV] - Auto [µA]
Collimator/Primary Filter	:	10 [mmϕ] / #1, #2
Measurement Atmosphere	:	Air
Integration Time/Dead Time	:	300 [sec.]/Max. 30[%] (sample)
Integration Time/Dead Time	:	1,800 [sec.]/Max. 30[%] (calibration curve)

Analysis Flow

The analysis process flow, images of the samples at each stage in analysis, and the X-ray fluorescence (XRF) spectra are shown in Fig. 3.

① Reagents other than the catalyst of sample 1 is mixed for eacohf Fluorophore 1 and 2.

Fluorophore 1 2

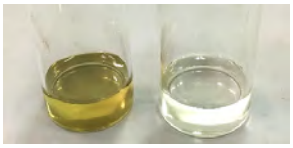

② The catalyst (palladium acetate) was added to each solution.

Fluorophore 1 2

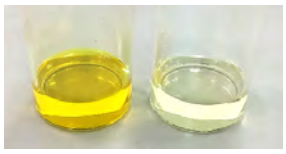

③ After adding sample 2 (metal scavenger) to each solutions, the solutions were left for a certain amount of time and then filtered.

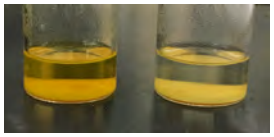

Pre-filtration

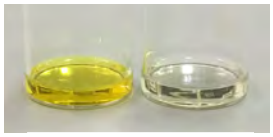

Post-filtration

④ The separated powder after filtration

Fluorophore 1 2

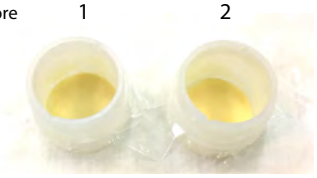

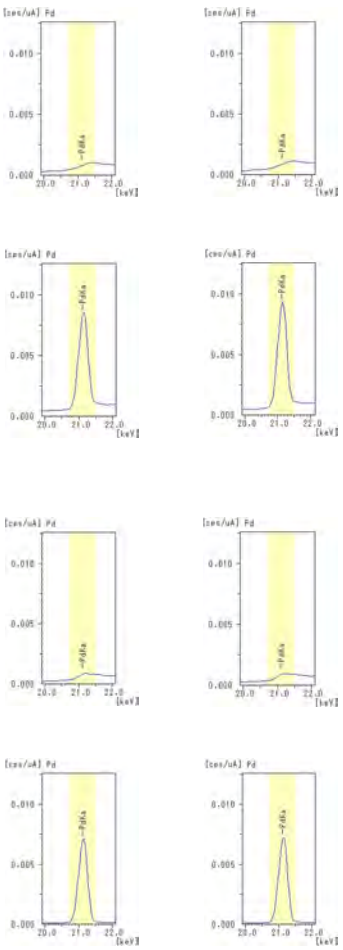

Fig. 3 Analysis Flow, Sample Images, and Analysis Results

Pharmaceuticals Impurities Screening Method Package

Elements that can be analyzed with the pharmaceuticals impurities screening method package for XRF spectrometry are shown in Table 4. Among the 24 elements listed in the ICH Q3D, a total of 12 elements can be analyzed.

Table 4 Elements That Can Be Analyzed with the Method Package

Classification	Elements
Class 1	: Cd, Pb, As, Hg
Class 2A	: V, Co, Ni
Class 2B	: Ir, Pt, Ru, Rh, Pd

Conclusion

Methods commonly used for analyzing inorganic impurities such as atomic absorption spectrophotometry, inductively coupled plasma (ICP) atomic emission spectroscopy, and ICP mass spectrometry require the wet digestion of solid and powder samples as pretreatment. However, by using XRF spectrometry, samples of all forms can be analyzed in their original form, such as a solution or powder, without pretreatment as long as the element to be analyzed is evenly dispersed in the sample.

This study shows that by using the pharmaceuticals impurities screening method package, an analysis in the order of mg/kg can be performed even when the integration time is substantially shortened to 300 s from the standard condition of 1,800 s. The package is effective in controlling the residual amount of catalysts in accordance with control standards and target accuracy levels.

First Edition: Jun. 2018

Shimadzu Corporation
www.shimadzu.com/an/

SHIMADZU
Excellence in Science

Application Data Sheet

No.116

GC-MS
Gas Chromatograph Mass Spectrometer

Compound Identification Procedures Combined with Quick-CI

BACK TO CONTENTS

The Quick-CI function is enable easy and simple use of the EI and PCI (Positive ion chemical ionization) mode using an NCI ion source without venting the MS. PCI can be obtained as a simple method of confirming molecular weight by molecule protonation and the combination of EI and PCI is a powerful identification technique when a compound cannot be identified based on its EI mass spectrum alone. Also, since the selected ionization mode is saved in a method file, the user can switch between EI and PCI for consecutive analyses.
This Application Data Sheet presents a compound identification performed by combining the mass spectrum information obtained by the EI and the PCI using an NCI ion source.

Similarity Search Results Obtained Using Only EI

GC/MS with the EI can be used for compound identification since it produces many fragment ions, and a rich mass spectral library is available. However, the EI cannot detect molecular ions of some compounds such as those with functional groups that include amino groups, carbonyl groups, and carboxyl groups, and those with ether linkages. Therefore, performing a similarity search of a library will produce results that include compounds of similar structure and structural isomers. This makes it difficult to identify the target compound. In these cases, compounds can be identified easily by combining the information from the EI with molecular weight information obtained from protonated molecules by the PCI.
Fig.1 shows an example of a similarity search performed after the EI (Table 1) is used to measure a type of cathinone, which is a dangerous drug. Because the molecule ion is not detected and there is little mass spectral pattern to analyze, the similarity search shows other structurally similar cathinones and phenethylamines that have a similarity score close to the target molecule.

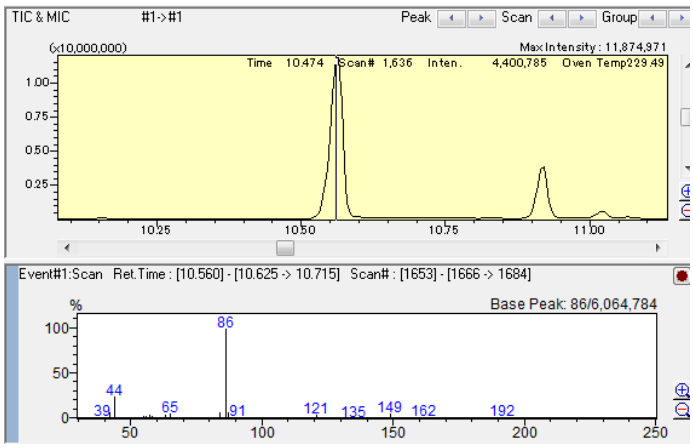

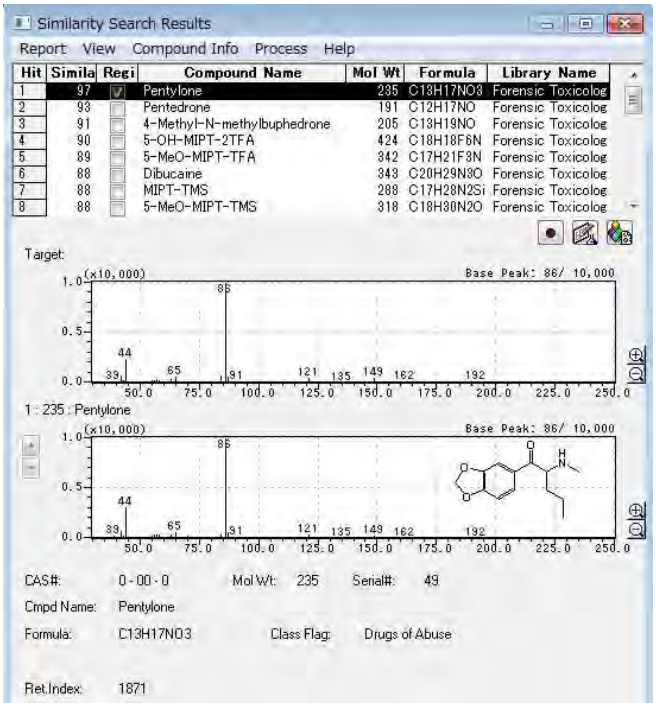

Fig. 1 Total Ion Current Chromatogram and Library Search Results for Pentylone Obtained Using the EI

Table 1 Analytical Conditions

GC-MS:	GCMS-QP2020
Column:	Rxi®-5Sil MS (length: 30 m; 0.25 mm I.D.; df = 0.25 μm)
Glass Insert:	Splitless insert with wool (P/N: 221-48876-03)
[GC]	
Injection Unit Temp.:	260 °C
Column Oven Temp.:	60 °C (5 min) → (10 °C /min) → 320 °C (15 min)
Injection Mode:	Splitless
Carrier Gas Control:	Linear velocity (45.6 cm/sec)

[[MS]			
Interface Temp.:	280 °C		
Ion Source Temp.:	200 °C		
Measurement Mode:	Scan		
Scan Event Time:	0.3 sec		
EI		CI	
Scan Range:	*m/z* 40 – 600	Scan Range:	*m/z* 60 – 600
		Reagent Gas:	Isobutane (240 kPa)

Similarity Search Results Combined Molecular Weight Information

Fig. 2 shows the total ion current chromatogram (TICC) and mass spectra obtained after measuring pentylone by both the EI and the PCI using the Quick-CI function. The results obtained from the EI and the PCI can be used in tandem by utilizing a data comparison feature of GCMSsolution. The PCI mass spectrum shows that the protonated molecule is measured at *m/z* 236, which leads to an estimate that the molecular weight is 235. After the initial similarity search, search results can be narrowed down using the molecular weight data (Fig. 3). Inputting the estimated molecular weight before performing a similarity search of the EI mass spectrum reduces the number of results to that of just pentylone (Fig. 4).
When compound identification is difficult using only the mass spectrum obtained from the EI, combining the mass spectrum information from the EI with molecular weight information obtained from the PCI allows for easy compound identification.

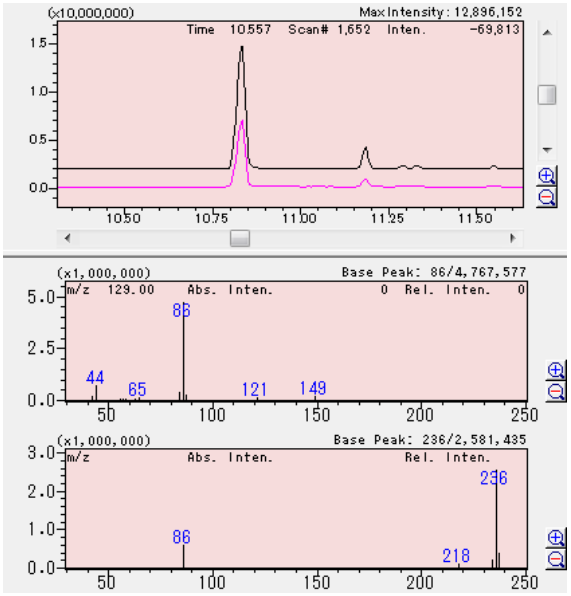

Black: TICC obtained by EI
Pink: TICC obtained by PCI

EI mass spectrum

PCI mass spectrum

A molecular weight of 235 can be estimated based on *m/z* 236 detected for the protonated molecular ion.

Fig. 2 TICC and Mass Spectra Obtained by the EI and PCI Using an NCI Ion Source

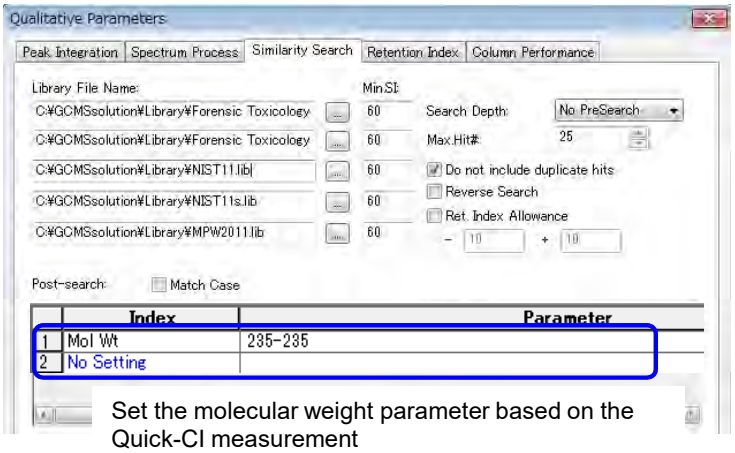

Set the molecular weight parameter based on the Quick-CI measurement

Fig. 3 Qualitative Analysis Parameter Window

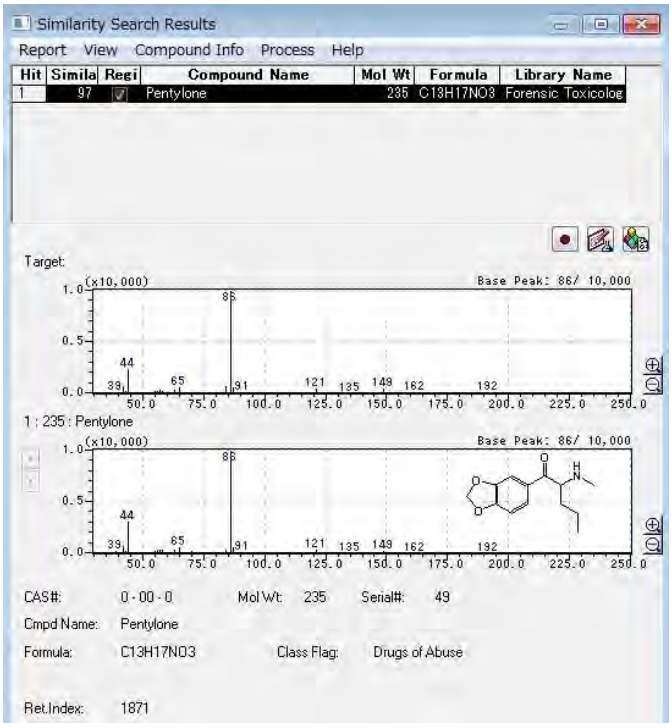

Fig. 4 Narrowing Down EI Mass Spectrum Similarity Search Results Using the Molecular Weight Information

First Edition: Nov, 2015

Shimadzu Corporation
www.shimadzu.com/an/

SHIMADZU
Excellence in Science

Application Data Sheet

No. 123

GC–MS
Gas Chromatograph Mass Spectrometer

Py-GC/MS Analysis of Electronic Circuit Board Parts Using Nitrogen Carrier Gas

BACK TO CONTENTS

Helium, which is used as a carrier gas for GC-MS, has in recent years been subject to dramatic price increases and delivery delays. This can, in some cases, make it difficult to obtain Helium. Equipped with a newly developed turbomolecular pump, the GCMS-QP2020 can be operated using replacement carrier gases, such as hydrogen and nitrogen. The measurement range guidelines for each carrier gas is shown in Fig. 1. Although nitrogen provides less sensitivity than helium, its price is ten times lower and it is easily available.

This application data sheet introduces an analysis of the instantaneous pyrolysis of an electronic circuit board using Py-GC/MS, while comparing the usage of nitrogen versus helium as the carrier gas.

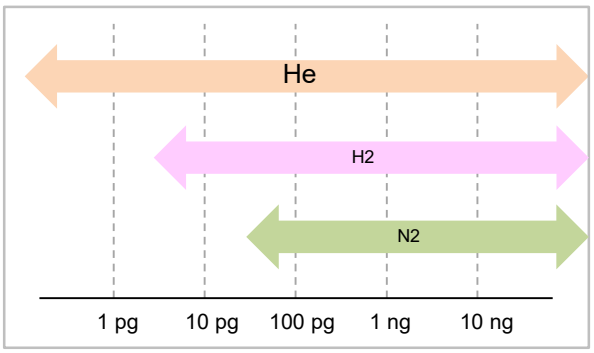

Fig. 1: Measurement Range Guidelines for Each Carrier Gas* (On-Column Amount)

* These measurement ranges are at best only guidelines, and may be unsuitable depending on the target compound's sensitivities and characteristics.

Conversion of Analysis Methods

In changing the carrier gas from helium to nitrogen, the length of the column was changed from 30 m to 20 m and the inner diameter was changed from 0.25 mm to 0.18 mm. The analysis conditions were converted using the web-based "EZGC™ Method Translator*1" provided by Restek Corporation (http://www.restek.com/ezgc-mtfc). For more information regarding the "EZGC™ Method Translator," refer to Application Data Sheet No. 120. The analysis conditions for analyses using helium and nitrogen as the carrier gas are shown in Table 1.

Table 1: Analytical Conditions

Pyrolyzer	: Multi-Shot Pyrolyzer EDA/PY-3030D
GC-MS	: GCMS-QP2020
Glass insert	: Deactivated split glass insert with wool (P/N: 225-20803-01)
[PY]	
Analysis mode	: Single shot
Furnace temp.	: 600 ˚C (1 min)
Interface temp.	: 300 ˚C

- Helium carrier gas -

Purity	: 99.99 %
Gas purification filter	: Click-ON triple trap (Helium Specific) SGT P/N: SGT-CO1051
[GC]	
Column	: SH-Rxi™-5Sil MS (length 30 m, 0.25 mm I.D., df=0.25 μm)
Injection temp.	: 300 ˚C
Column oven temp.	: 40 ˚C (2 min)→(15 ˚C/min)→320 ˚C (10 min)
Injection mode	: Split
Split ratio	: 50
Flow control mode	: Linear velocity (39.5 cm/sec)
Initial column flow	: 1.2 mL/min
[MS]	
Ionization mode	: EI
Interface temp.	: 300 ˚C
Ion source temp.	: 230 ˚C
Acquisition mode	: Scan
Scan event time	: 0.3 sec
Scan range	: *m/z* 60 to 600

- Nitrogen Carrier Gas -

Purity	: 99.99 %
Gas purification filter	: Click-ON triple trap SGT P/N: SGT-CO1005
[GC]	
Column	: SH-Rxi™-5Sil MS (length 20 m, 0.18 mm I.D., df=0.18 μm)
Injection temp.	: 300 ˚C
Column oven temp.	: 40 ˚C (2 min)→(14.8 ˚C/min)→320 ˚C (10.15 min)
Injection mode	: Split
Split ratio	: 50
Flow control mode	: Linear velocity (26.2 cm/sec)
Initial column temp.	: 0.32 mL/min
[MS]	
Ionization mode	: EI
Interface temp.	: 300 ˚C
Ion source temp.	: 230 ˚C
Acquisition mode	: Scan
Scan event time	: 0.3 sec
Scan range	: *m/z* 60 to 600

*1: EZGC™ Method Translator is a trademark of Restek Corporation.

Analysis Results

The total ion current chromatograms (TICC) measured for the instantaneous pyrolysis of electronic circuit boards using helium and nitrogen as the carrier gases are shown in Fig. 2. By using the EZGC™ Method Translator, a nearly identical chromatogram pattern could be obtained. Table 2 shows the results of a library search of typical detected peaks using the NIST 14 mass spectral library, and Fig. 3 shows the mass spectrum for the Bisphenol A detected. Even when nitrogen is used as the carrier gas, the mass spectrum is virtually the same as that when helium is used as the carrier gas. This means that existing mass spectral libraries can be used as is. For qualitative applications or quantitative analysis at a μg/mL (ppm) level, it is possible that a transition to nitrogen carrier gas can be made.

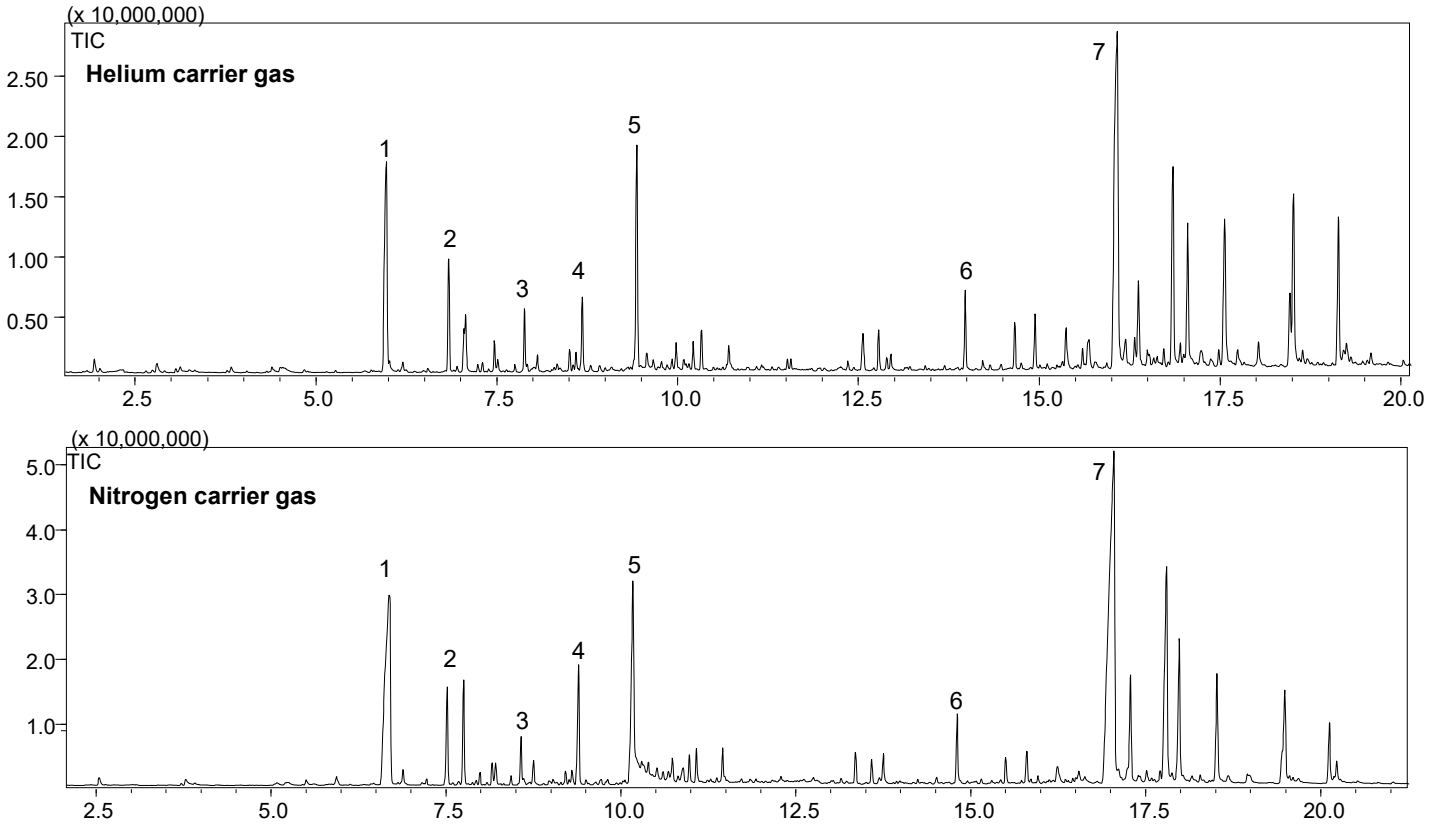

Fig. 2: Total Ion Current Chromatogram (TICC) Measured for the Instantaneous Pyrolysis of Electronic Circuit Board
Top: Helium Carrier Gas, Bottom: Nitrogen Carrier Gas

Table 2: Results of Library Search for Typical Compounds Detected

No.	Identified Compound	Similarity (SI)	
		He Carrier Gas	N2 Carrier Gas
1	Phenol	99	98
2	Methylphenol	98	98
3	Xylenol	97	98
4	Isopropylphenol	96	97
5	Isopropenylphenol	94	92
6	Cumylphenol	94	93
7	Bisphenol A	95	98

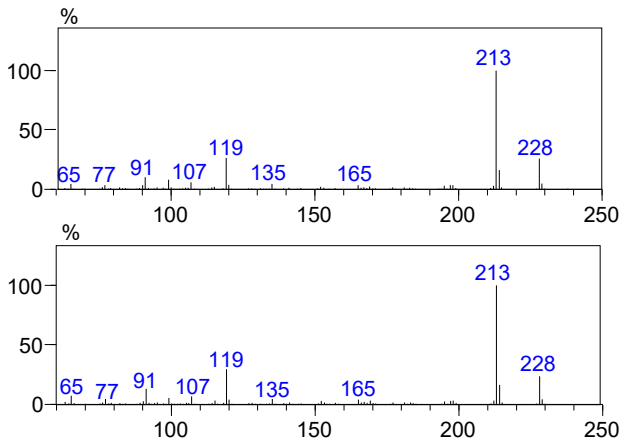

Fig. 3: Mass Spectrum for Bisphenol A Detected
Top: Helium Carrier Gas, Bottom: Nitrogen Carrier Gas

First Edition: April, 2016

Shimadzu Corporation
www.shimadzu.com/an/

SHIMADZU
Excellence in Science

Application Note

No. 14

UV Degradation Analysis of Material for Solar Cell Modules Using GC/MS and FTIR

Y. Katayama, S. Takeuchi

1. Introduction

Materials for solar cell modules are expected to maintain their performance for over a decade despite the harsh environmental conditions such as high temperatures and ultraviolet irradiation to which they are subjected outdoors. However, there is concern that UV-induced degradation may occur in materials used in modules such as ethylene-vinyl acetate (EVA) which is a copolymer used as a clear encapsulation film.

This article introduces three example analyses: analysis of EVA film subjected to intense UV irradiation using a UV (ultraviolet) -Py (double-shot pyrolyzer) / GC-MS (gas chromatograph mass spectrometer) system, evolved gas analysis by mass spectrometry (EGA-MS) of EVA film which was degraded by UV irradiation in the same way as with the above, and analysis of the same using a Fourier transform infrared spectrophotometer (FTIR).

EVA: ethylene-vinyl acetate copolymer

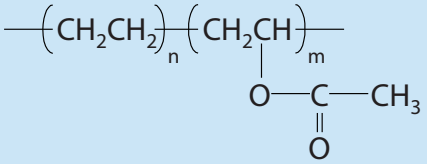

Fig. 1 Structural formula of ethylene-vinyl acetate (EVA) copolymer

Analytical Applications Department,
Analytical & Measuring Instruments Division

2. UV degradation of EVA film using a UV-Py/GC-MS system

The UV-Py/GC-MS system shown in Fig. 2 was made by combining a micro-UV irradiator (UV-1047 Xe) manufactured by Frontier Laboratories Ltd., and the GCMS-QP2020 gas chromatograph mass spectrometer manufactured by Shimadzu Corporation. Compared to conventional weather testing methods such as outdoor exposure testing and weatherometer testing, this system enables rapid UV degradation of EVA film.

In addition, this UV-Py/GC-MS system is capable of performing GC/MS analysis of volatile degradation products which are generated due to UV irradiation.

Degradation samples can be analyzed employing evolved gas analysis by mass spectrometry (EGA-MS), a method available with the Py/GC-MS, and by using a Fourier transform infrared spectrophotometer (FTIR) to elucidate the changes in the resin structure that are induced by UV irradiation.

Fig. 3 shows the procedure for UV degradation of EVA film using the UV-Py/GC-MS system.

Fig. 2 UV-Py/GC-MS system (UV-1047Xe+PY-3030D+GCMS-QP2020)

(1) Weighing
Weigh out approx. 2 mg of the sample and place the sample in the dedicated Eco-cup.

(2) Setting the cup in the instrument
Set the dedicated Eco-cup in the UV sampler. Fill the furnace with air.

(3) UV irradiation
Immerse the column in liquid nitrogen and perform UV irradiation.
This research was done using irradiation times of 0, 1, 2, and 5 hours.

(4) Purging with helium
In order to purge the air inside the column with helium, wait for 15 minutes after switching to helium.

(5) GC/MS analysis
After connecting the column to the mass spectrometer, take the column out from the liquid nitrogen and perform analysis.

(6) Collection of degradation sample
After analysis, take the degradation sample out from the UV sampler.

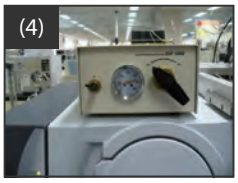

EGA-MS analysis
Analysis of changes in material properties before and after UV irradiation through evolved gas analysis by mass spectrometry (EGA-MS)

Py/GC-MS system
(PY-3030D+GCMS-QP2020)

FTIR analysis
Molecular structure analysis of EVA in the vicinity of the film surface by total reflectance spectroscopy (ATR method)

IRAffinity-1S
Fourier transform infrared spectrophotometer

Fig. 3 Measurement flow for UV-Py/GC-MS analysis

3. Analysis of volatile degradation products using the UV-Py/GC-MS system

3-1 Overview

Volatile degradation products generated through UV irradiation were analyzed using the UV-Py/GC-MS system.

Whereas evaluation of gas generated during degradation is not possible if employing methods such as outdoor exposure testing or weatherometer testing, evaluation of such gas is possible if using a UV-Py/GC-MS system.

Fig. 4 shows the schematic of the UV-Py/GC-MS system.

Analysis is done with this system by first setting the sample inside the furnace that is filled with air and then cooling the inlet of the column using liquid nitrogen. After performing UV irradiation for the set time, the evolved gas generated during the light-induced degradation of the sample is collected.

Subsequently, the air in the instrument is purged with helium and the column is connected to the mass spectrometer. After taking the column out from the liquid nitrogen, the evolved gas collected in the cooled section of the column is analyzed.

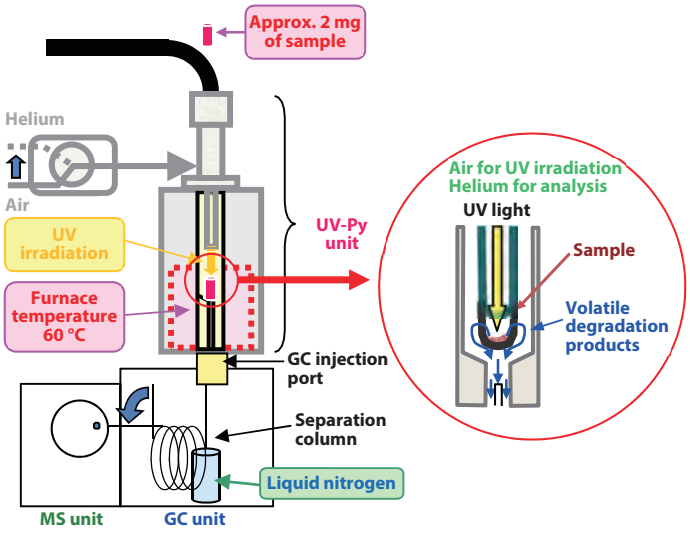

Fig. 4 Schematic of the UV-Py/GC-MS system

3-2 Analysis conditions

Table 1 lists the analysis conditions for volatile degradation products using the UV-Py/GC-MS system.

Table 1 Analysis conditions for volatile degradation products using the UV-Py/GC-MS system

Instrument	
<Conditions for the UV-Py>	
Irradiation time	0 hr, 1 hr, 2 hr, 5 hr
Helium purging time	15 min
Pyrolyzer furnace temperature	60 °C
Atmospheric gas	Air
<Conditions for the GC>	
Column	Ultra ALLOY-1 (30 m L. × 0.25 mm I.D. df=0.5 μm) manufactured by Frontier Laboratories
Injection port temperature	300 °C
Column temperature	40.0 °C → 20.0 °C /min → 300.0 °C (5.00 min)
Injection mode	Split mode
Carrier gas	Helium
Carrier gas pressure	50 kPa
Split ratio	40:1
<Conditions for the MS>	
Ion source temperature	200 °C
Interface temperature	300 °C
Measurement mode	SCAN
Measurement range	*m/z* 29-1090
Event time	0.5 sec

3-3 Analysis results

The result of analyzing the volatile degradation products generated through UV irradiation (0, 1, 2, 5 hours) using the UV-Py/GC-MS system is shown in Figs. 5 to 8.

Underlined compounds in the figures are compounds which are considered to be volatile degradation products of EVA.

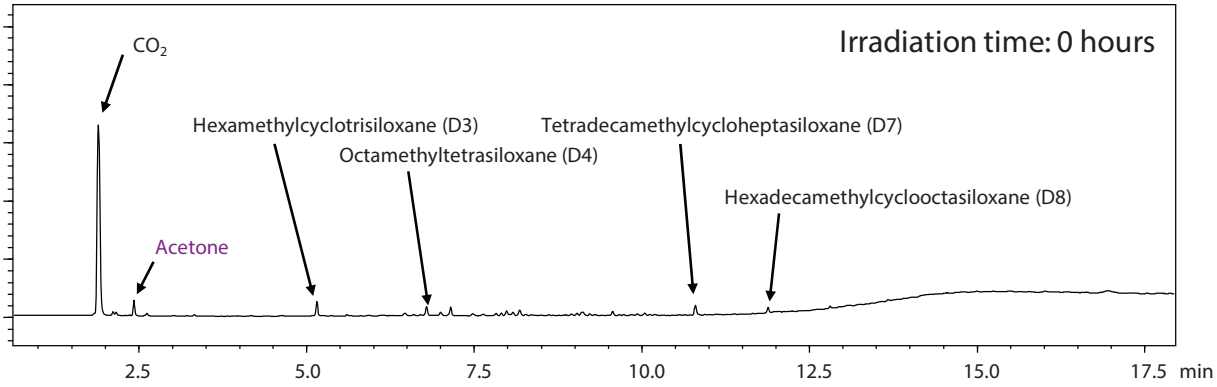

Fig. 5 UV-Py/GC-MS analysis results of volatile degradation compounds generated through UV irradiation (0 hours)

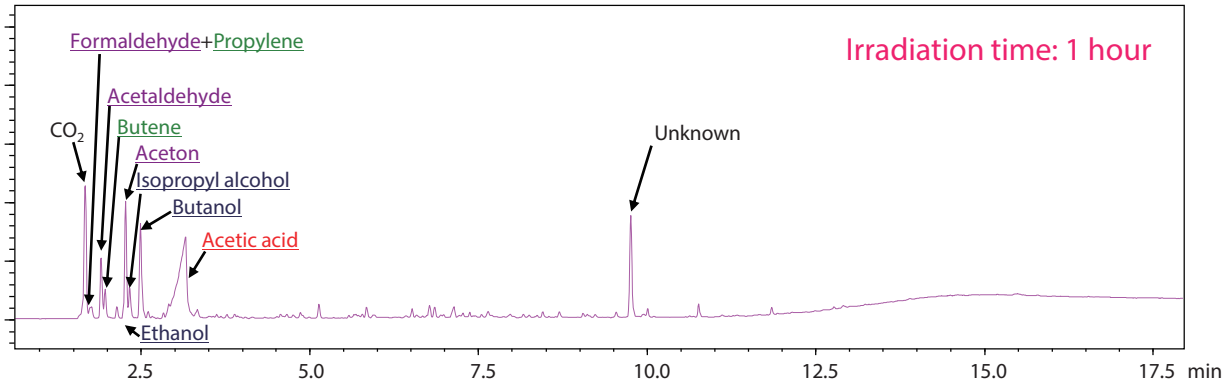

Fig. 6 UV-Py/GC-MS analysis results of volatile degradation compounds generated through UV irradiation (1 hour)

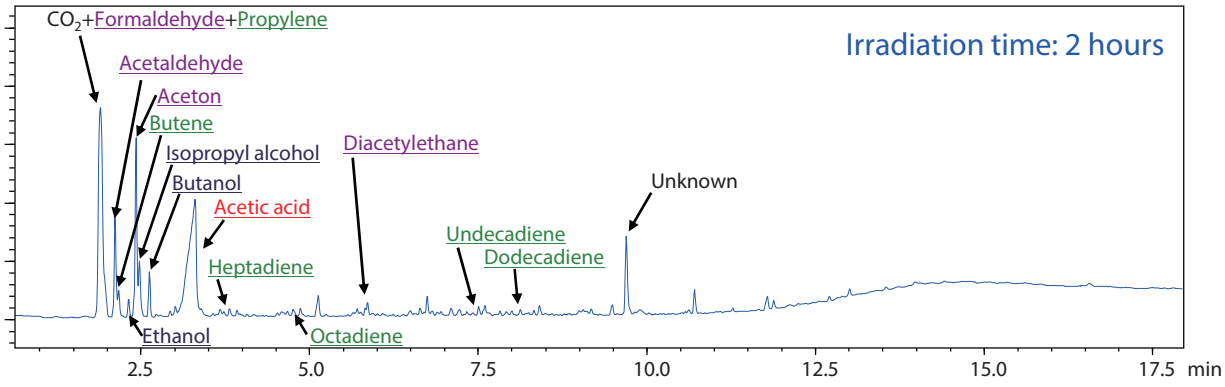

Fig. 7 UV-Py/GC-MS analysis results of volatile degradation compounds generated through UV irradiation (2 hours)

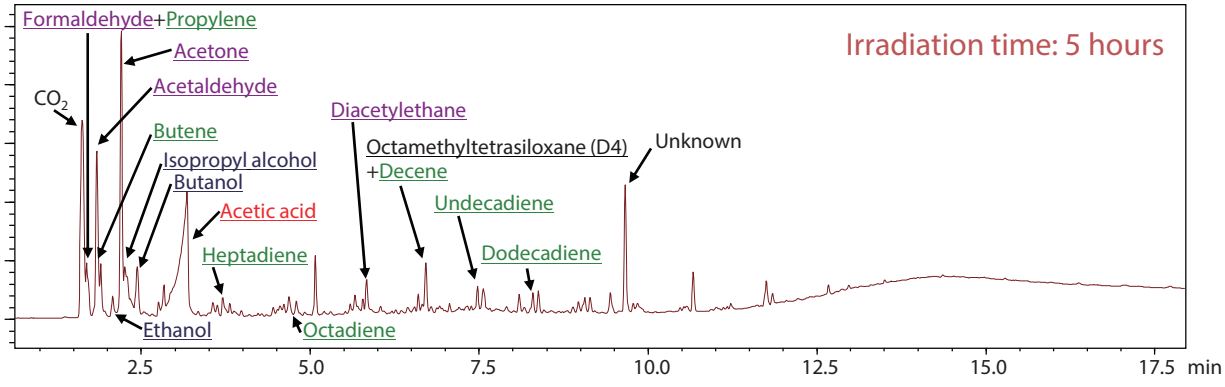

Fig. 8 UV-Py/GC-MS analysis results of volatile degradation compounds generated through UV irradiation (5 hours)

BACK TO CONTENTS

3-4 Expected light decomposition reaction of EVA

Based on Figs. 5 to 8, we can assume that compounds that have a greater peak area under a longer UV irradiation time are a product of light decomposition.

Since the EVA film used for analysis hardly contained any additives, we were able to observe the light decomposition of the EVA film itself and therefore infer the light decomposition reaction as shown in Fig. 9.

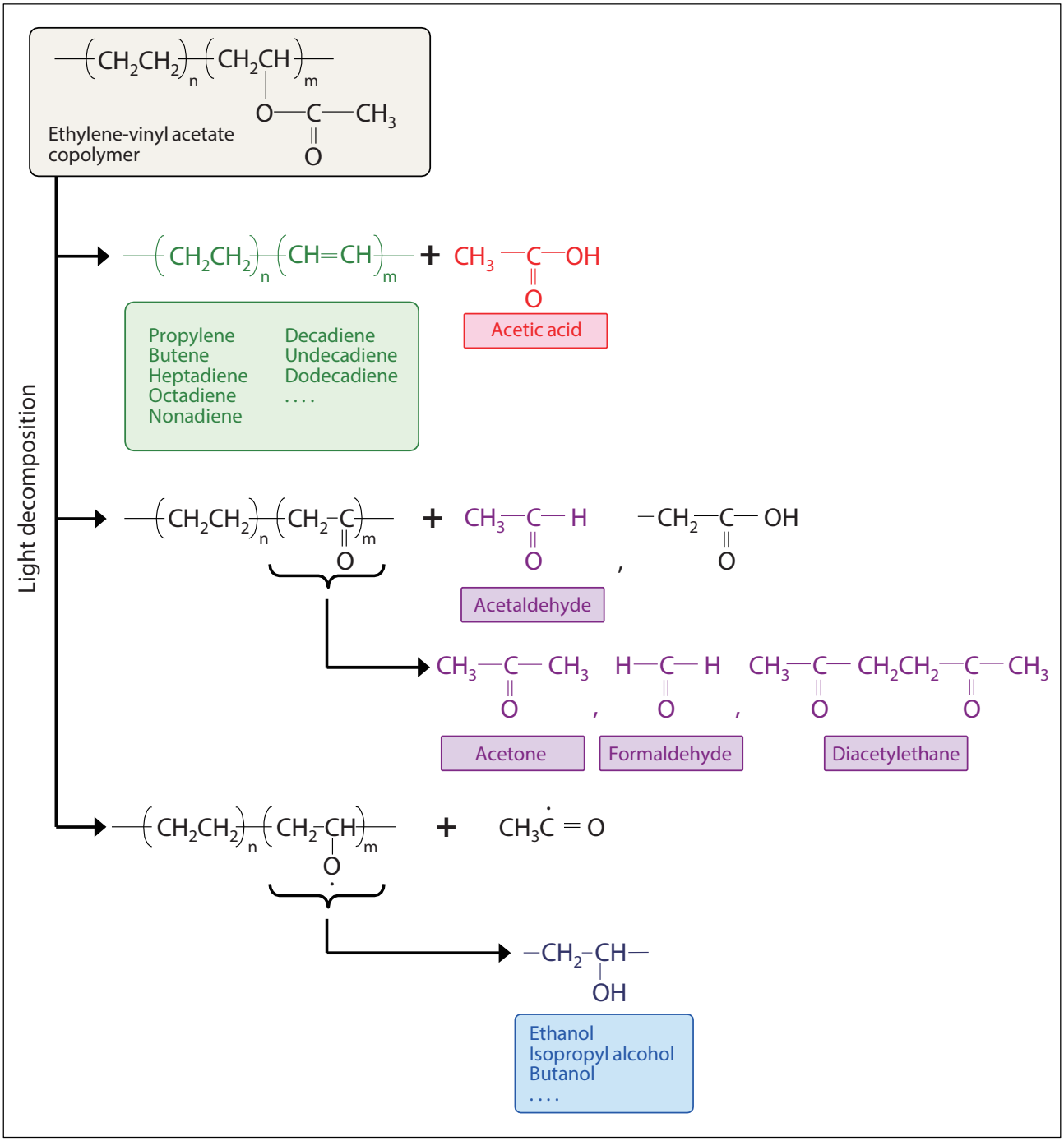

Fig. 9 The light decomposition reaction of EVA inferred based on measurement results

4. Analysis of UV-irradiated EVA through evolved gas analysis by mass spectrometry (EGA-MS)

4-1 Overview

Changes in the properties of EVA film from before and after UV irradiation were analyzed through evolved gas analysis by mass spectrometry (EGA-MS), which is a method that is available with a Py/GC-MS configuration.

Fig. 10 shows the schematic of the EGA-MS system.

Analysis by the EGA-MS method is done by connecting the outlet of the pyrolyzer with the GC detector using the inactivated tube (Ultra ALLOY, 2.5 m L. × 0.15 mm I.D.) installed inside the GC oven and then detecting, in real time, the various substances that are generated from the sample through heating.

By comparing the thermal decomposition temperatures of the degraded EVA film, it is possible to reveal the degree of cleavage reactions on the main chain that are caused by UV irradiation.

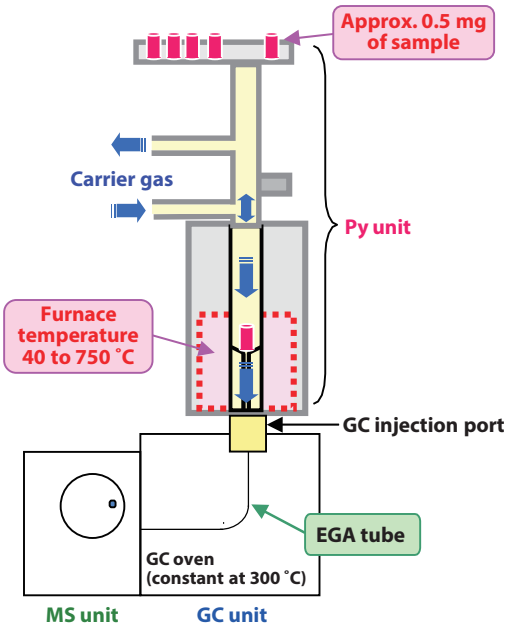

Fig. 10 Schematic of the EGA-MS system

4-2 Analysis conditions

The conditions for analyzing UV-irradiated EVA by EGA-MS are listed in Table 2.

Table 2 Analysis conditions for EGA-MS

Instrument	
<Conditions for the Py>	
Pyrolyzer furnace temperature	40.0 °C (2.00 min) → 20 °C /min → 750.0 °C (2.50 min)
Interface temperature	Auto (Upper Temp. 320 °C)
<Conditions for the GC>	
Column	Ultra ALLOY-DTM (2.5 m L. × 0.15 mm I.D., no liquid phase) manufactured by Frontier Laboratories
Injection port temperature	320 °C
Column temperature	Constant at 300 °C
Injection mode	Split mode
Carrier gas	Helium
Carrier gas pressure	120 kPa
Split ratio	40:1
<Conditions for the MS>	
Ion source temperature	250 °C
Interface temperature	320 °C
Measurement mode	SCAN
Measurement range	*m/z* 29-1090
Event time	0.5 sec

BACK TO CONTENTS

4-3 Analysis results

The EGA-MS analysis results of EVA film degraded by UV irradiation per each irradiation time are shown in Fig. 11.

The thermal decomposition temperature for each of the UV irradiation times is listed in Table 3.

We can see that a longer UV irradiation time results in a slightly lower thermal decomposition temperature for peak (2), meaning that the molecular weight is decreasing. This indicates that light decomposition is occurring on the main chain of the EVA film due to UV irradiation.

In addition, the difference in the absolute intensity of the thermal decomposition of the main chain (peak (2)) between each UV irradiation time was subtle. From this, we can assume that light decomposition is occurring only on the surface of the EVA film and not the entirety of the film.

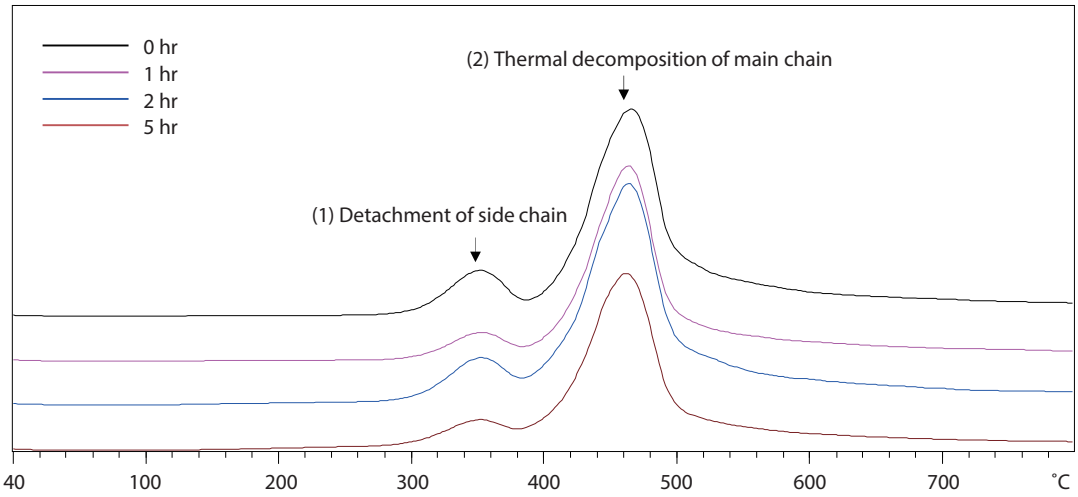

Fig. 11 EGA-MS analysis results of EVA film degraded under different UV irradiation times

Table 3 Thermal decomposition temperature of main chain under different UV irradiation times

UV irradiation time	0 hr	1 hr	2 hr	5 hr
Thermal decomposition temperature (°C)	465.5	463.7	463.9	461.9

5. Analysis of UV-irradiated EVA using a Fourier transform infrared spectrophotometer (FTIR)

5-1 Overview

Structural changes that occur in compounds through degradation can be analyzed using a Fourier transform infrared spectrophotometer (FTIR). Although the samples used in this research were only about 2 mm square in size, the surface spectrum of these samples can be measured easily by using the single reflection ATR accessory.

This section introduces the results obtained by installing the DuraSamplIR II, which is a single reflection ATR accessory, on Shimadzu's IRAffinity-1S Fourier transform infrared spectrophotometer and measuring samples which were UV-irradiated for 0, 2, and 5 hours respectively.

Fig. 12 IRAffinity-1S

Fig. 13 DuraSamplIR II

BACK TO CONTENTS

5-2 Analysis results

The spectra obtained by measuring the samples which were UV-irradiated for 0, 2, and 5 hours respectively are superimposed in Fig. 14. Changes with regard to functional groups can be observed: a decrease of the >C=O group originating from acetate in the vicinity of 1735 cm^{-1}, an increase of the >C=O group originating from ketone and aldehyde in the vicinity of 1716 cm^{-1}, and an increase in the peak intensity of the -OH group in the vicinity of 3300 cm^{-1}. Fig. 15 (a), (b), and (c) depict these peak changes by plotting them against the UV irradiation time. Each graph is based on the peak at 1465 cm^{-1} (CH2 and CH3 bending), with graphs (a) and (b) plotting the peak intensity ratio and graph (c) plotting the peak area ratio. For each sample, both the front and back sides are measured and plotted respectively.

These results indicate that the side chain structure of EVA changed at the sample surface due to UV irradiation, thereby generating compounds containing the -OH group or the >C=O group originating from aldehyde or ketone.

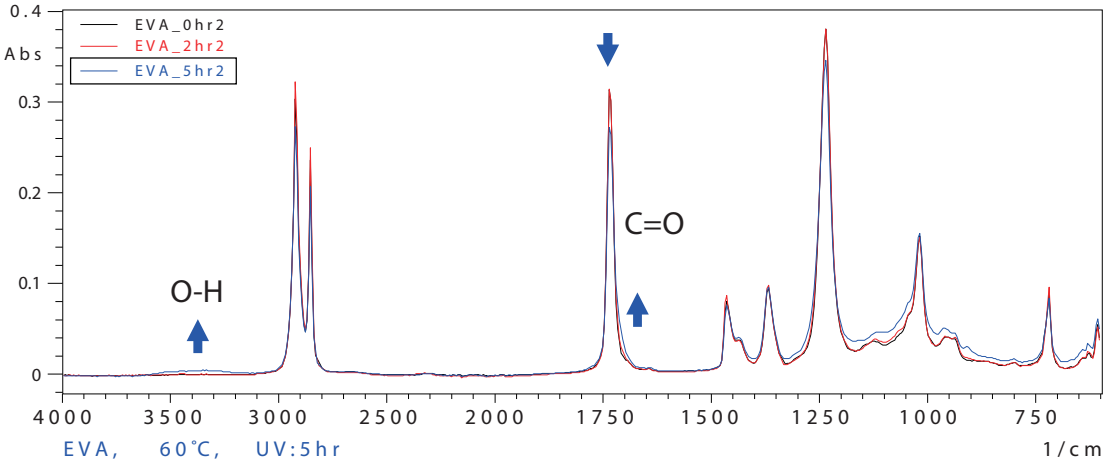

Fig. 14 IR absorbance spectra of EVA film before and after UV irradiation

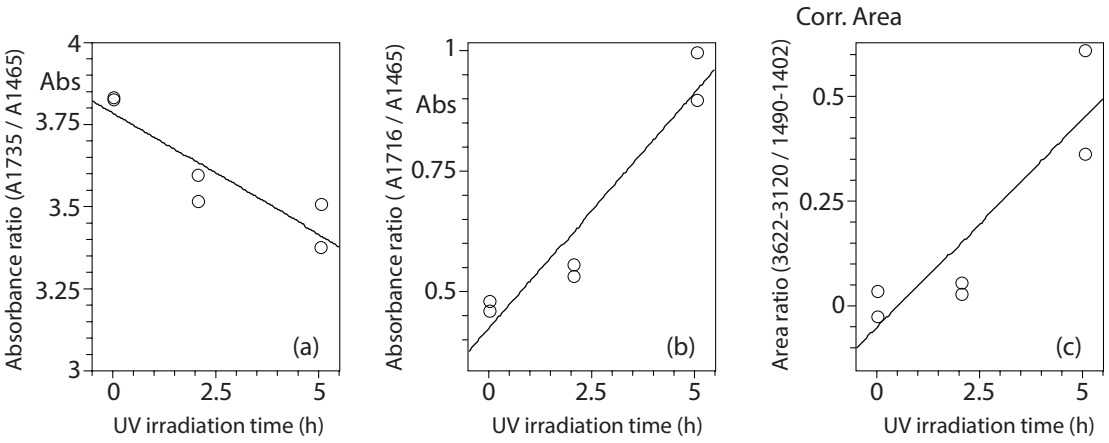

Fig. 15 Changes in functional groups (a) acetate, (b) ketone and aldehyde, and (c) O-H due to UV irradiation

6. Summary

We clarified the volatile degradation products which result from EVA film due to UV irradiation by measuring EVA film using a UV-Py/GC-MS system. We also were able to estimate the decomposition behavior of the main and sub chains through evolved gas analysis by mass spectrometry (EGA-MS) according to changes in the UV irradiation time and evaluate changes in functional groups based on the results obtained through FTIR. Both of these methods are effective in investigating the decomposition behavior of resin structures induced by UV irradiation.

* This publication is based upon the information available to Shimadzu on or before the date of publication, and subject to change without notice.

First Edition: Jan. 2018

SHIMADZU

Shimadzu Corporation

www.shimadzu.com/an/

SHIMADZU
Excellence in Science

Application News

No.A489

Spectrophotometric Analysis

High Speed Monitoring of Pyridine Adsorbing on Surface of TiO_2 Powder by Rapid Scan

BACK TO CONTENTS

Catalysts play an important role in promoting reactions in a wide range of industrial fields, including petroleum refining, petrochemical, gas purification, foods, fine chemicals, biochemicals, etc., and research and development of new catalysts is becoming increasingly important. Titanium oxide (TiO_2), which exists in forms that display a variety of crystalline structures, is well known as a photocatalytic substance. Here, using the rapid scan feature of the IRTracer-100 FTIR, we evaluated two types of TiO_2 powder having different crystalline structures.

Catalytic Characterization by Pyridine Adsorption Measurement

Solid oxides such as TiO_2 are widely used as catalysts. On the TiO_2 surface, there exist both Brønsted acid sites (B acid sites) that donate a proton to a companion molecule, and Lewis acid sites (L acid sites) that receive a pair of electrons from a companion molecule. Identification of these acid sites is possible using a basic molecule, such as pyridine, which is adsorbed on a solid oxide surface, thereby permitting measurement of the infrared spectrum. At the Lewis acid sites, the pyridine molecule bonds to the solid oxide. The presence of pyridine can be monitored by a pyridine characteristic absorption peak in the vicinity of 1440 cm^{-1}. At the Brønsted acid sites, the pyridine molecule becomes a pyridinium ion when the proton is donated. The pyridinium ion can be observed as a characteristic peak in the vicinity of 1540 cm^{-1}. In addition pyridine can bond to the substrate through physical adsorption and an H-bond. These alternative bonds give rise to IR absorption bands in the vicinities of 1585 cm^{-1} and 1435 cm^{-1}, and their intensities are dependent on the surface properties of the catalyst. When the catalyst possesses a hydroxyl group, a characteristic peak is observed in the vicinity of 1600 cm^{-1}.[1)] A schematic view of these bond states are shown in Fig. 1.

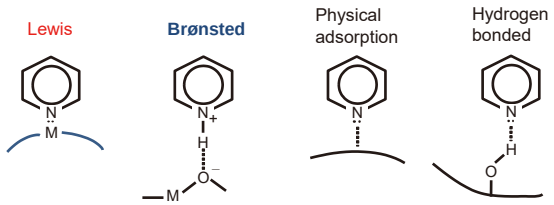

Brønsted acid (B acid): Gives proton (H^+) to companion molecule.
Lewis acid: Receives a pair of electrons from another molecule.

Fig. 1 Configuration of Pyridine Adsorbed on Metal Oxide

Measurement

Approximately 15 mg each of TiO_2 powder samples consisting of spindle-type and cubic-type crystalline structures, respectively, were formed into tablets. The tablets were then subjected to reduced pressure using a heat-vacuum resistant transmission cell, and heated at 200 °C for one hour. The sample tablets were allowed to cool to room temperature, and were then subjected to background measurement.
After acquisition of the background, the rapid scan measurement sequence was started, and pyridine vapor was immediately introduced. Table 1 shows the FTIR measurement conditions, and Table 2 shows the particle size and specific surface area of sample powder. In addition, the FTIR with the mounted chamber and the sample mounted in the cell are shown in the photographs of Fig. 2.

Table 1 FTIR Measurement Conditions

Instrument	: IRTracer-100
Resolution	: 4 cm^{-1}
Accumulation	: 1
Apodization	: Happ-Genzel
Detector	: MCT
Measurement Interval	: 0.19 second
Measurement Time	: 60 seconds

Table 2 Particle Size and Specific Surface Area of Sample Powder

	Particle Size	Specific Surface Area
Spindle	205 ± 75 nm	49 m^2/g
Cubic	18 ± 5 nm	52 m^2/g

Fig. 2 Photograph of IRTracer-100 with Mounted Environmental Chamber (left) and TiO_2 Tablet in Environmental Chamber (right)

Fig. 3 shows the spectral changes that occur following introduction of the pyridine. In the case of the spindle-type TiO_2, initially, L acid type pyridine bonding increases soon after the introduction of pyridine vapor as is evident by the adsorption band at 1444 cm^{-1}. As time elapses, a peak in the physical adsorption band at 1438 cm^{-1} increases in size.
As for the cubic type TiO_2, however, the initial period of pyridine adsorption shows only minor growth of the L acid peak at 1444 cm^{-1}. As time elapses, however, a peak in the physical adsorption band at 1438 cm^{-1} gradually exhibits increased intensity.

BACK TO CONTENTS

Although the specific surface area of both the specimens is more or less equivalent, the peak area of the L acid is greater for the spindle type than for the cubic type, indicating that there are more functional coordination deficit sites that function as an L acid. Fig. 4 shows the peak changes that occur when pyridine is introduced, in addition to electron microscope images. A comparison of the changes that occur in the peaks at 1444 cm^{-1} and 1438 cm^{-1} suggests that adsorption occurs more quickly in the spindle type than in the cubic type. Further, the results suggest that the spindle type possesses greater catalytic activity.

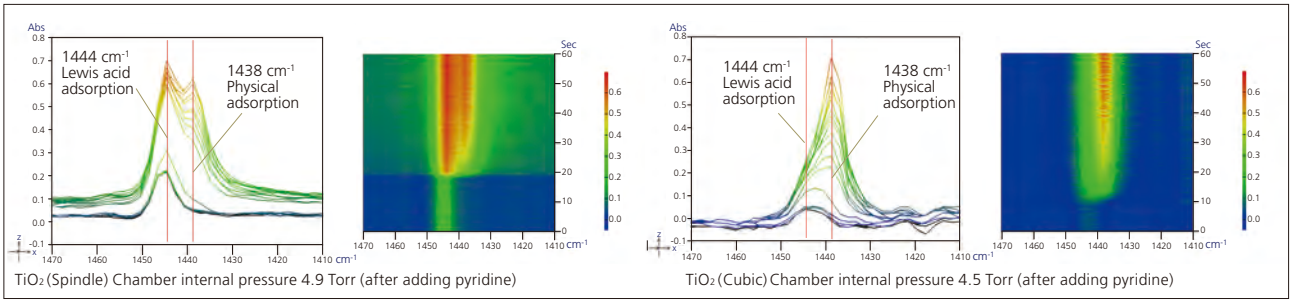

Fig. 3 Infrared Spectra (Left) and 2D Plot (Right) of Pyridine Adsorbing on Surface of TiO_2 Powder

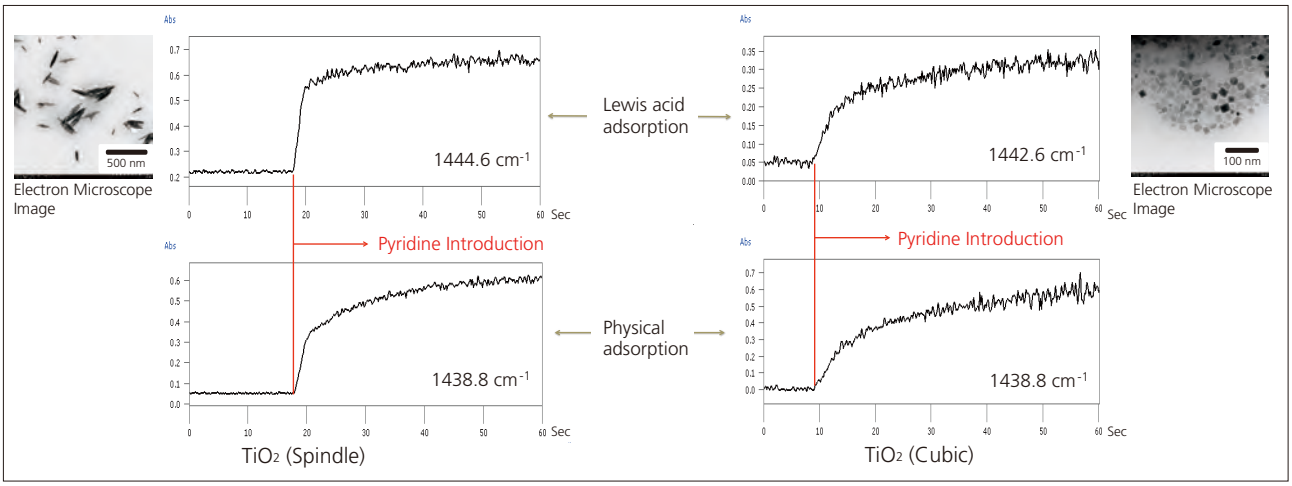

Fig. 4 Time-Course Graphs of Peak Intensity for Lewis Acid Position and Physical Adsorption and Micrographs of TiO_2 Powder

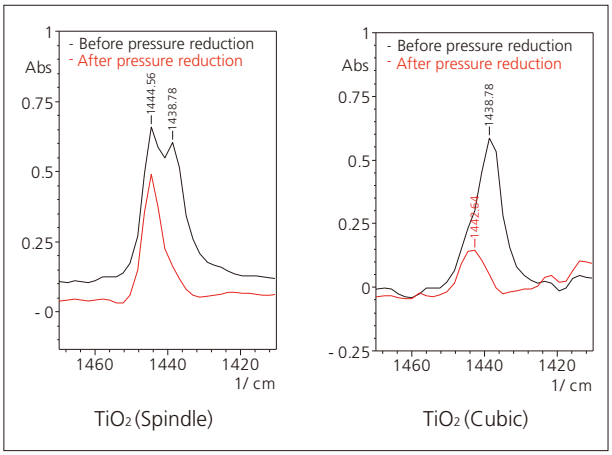

Fig. 5 Spectra Before and After Pyridine Pressure Reduction

Additionally, after permitting the pyridine to stabilize at about 5 Torr following its introduction, evacuation of the system was conducted until the system pyridine pressure was lowered to about 0.3 Torr, after which spectral measurement of the pyridine was conducted. Those results are shown in Fig. 5. The physical adsorption peak in the vicinity of 1438 cm^{-1} almost completely disappeared in both specimens.

Conclusion

Rapid scan FTIR measurement permitted quick (tens of seconds) and detailed observation of the process in which pyridine is adsorbed to a solid oxide surface.

The sample used for this measurement was generously provided by Professor Atsushi Muramatsu of the Institute of Multidisciplinary Research for Advanced Materials, Tohoku University, and guidance regarding the experimental method was kindly provided by Assistant Professor Kiyotaka Nakajima of the Hara Laboratory, Materials & Structures Laboratory, Tokyo Institute of Technology.

1) (M.I. 262 Zaki et al. / Colloids and Surfaces A: Physicochem. Eng. Aspects 190 (2001) 261–274)

First Edition: Aug. 2015

Shimadzu Corporation
www.shimadzu.com/an/

SHIMADZU
Excellence in Science

Application News

No. A563

Spectrophotometric Analysis

Analysis of Minute Objects Using a Sample Compartment Type Infrared Microscopy System

BACK TO CONTENTS

The sample compartment type infrared microscopy system is a combination of an FTIR instrument and the microspectroscopy accessory SurveyIR™ is a product manufactured by Czitek, LLC., which is designed to fit in the FTIR's sample compartment. The sample compartment type infrared microscopy system is capable of measurements on minute objects down to about 100 µm. Infrared spectra are detected using the FTIR's standard detector. SurveyIR is capable of transmission, reflectance, and ATR measurement (diamond or Ge prism), and an aperture can be selected from six sizes (2000, 250, 200, 160, 100, 60 µm). Therefore, measurement of minute areas is possible using SurveyIR if the sample is about 100 µm in size. In cases where the sample size is a few dozen µm, analysis using an infrared microscope equipped with an MCT detector is effective.

Fig. 1 shows an example system which combines Shimadzu's FTIR spectrophotometer IRSpirit™ (referred to as IRSpirit hereafter) with the SurveyIR.

IRSpirit features the highest signal to noise ratio and maximum resolution in its class. A highly compact FTIR, the instrument has a footprint smaller than an A3 sheet of paper with dimensions being a mere 390 (W) × 250 (D) × 210 (H) mm. In addition, the sample compartment of IRSpirit is easily accessible whether installed in "landscape" or "portrait" orientation, so that even a narrow opening on a lab bench can accommodate it. IRSpirit is also designed to accommodate transmission accessories such as a KBr pellet holder and demountable cells as well as existing Shimadzu and third party accessories such as single reflectance ATR attachments and diffuse reflectance attachments.

There are two models to IRSpirit which differ by the infrared detector that is used. One is the IRSpirit-T which is equipped with a DLATGS detector and the other is the IRSpirit-L which is equipped with a $LiTaO_3$ detector. The DLATGS detector is a high performance model featuring a temperature control function which can minimize the influence of ambient temperature changes on measurement results.

This article introduces example analyses of minute objects using a sample compartment type infrared microscopy system employing IRSpirit-T.

R. Fuji

Fig. 1 Sample Compartment Type Infrared Microscopy System (IRSpirit-T and SurveyIR)

Analysis of Fiber Using the ATR Method

The fiber shown in Fig. 2 with a diameter of about 80 µm was measured using the ATR method. Visible light observation of the area for measurement is possible through the diamond crystal, allowing for accurate centering and measurement while observing the sample. Table 1 lists the measurement conditions.

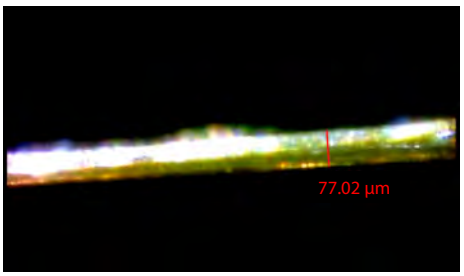

Fig. 2 Fiber

Table 1 Measurement Conditions

Instrument	: IRSpirit-T (KRS-5 window) SurveyIR
Resolution	: 8 cm^{-1}
Accumulation Times	: 128
Apodization Function	: SqrTriangle
Aperture Size	: 100 µm
Detector	: DLATGS
ATR Prism	: Diamond

Fig. 3 shows the search result from the Shimadzu Standard Library based on the obtained infrared spectrum. The results indicate that the fiber is a material that is similar to polyester.

Use of SurveyIR facilitated the specification of the measurement position thanks to the clarity of the sample observation image. In addition, a favorable infrared spectrum was obtained because unlike the conventional single reflectance ATR attachment, an aperture size appropriate for the sample size can be selected.

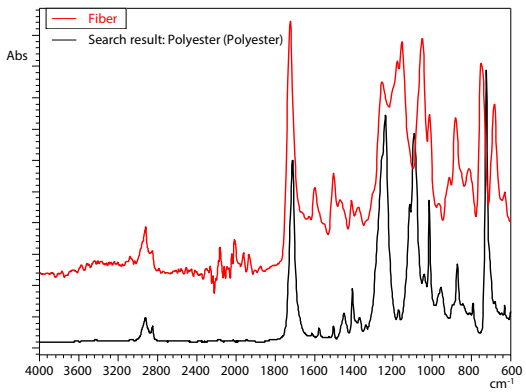

Fig. 3 Infrared Spectrum Obtained from Fiber and Search Result

BACK TO CONTENTS

Analysis of a White Minute Object Using the ATR Method

The white minute object shown in Fig. 4 with a length of about 130 µm was measured using the ATR method. Even in cases where minute objects for measurement are dispersed in multiple points, SurveyIR enables accurate centering of each point since the X, Y stage can be moved freely by manual operation. Also, samples with an uneven surface can be focused on fairly easily using the fine adjustment function of the Z axis.

Fig. 5 shows the obtained spectrum and the search result. Measurement conditions are the same as those listed in Table 1. The results indicate that the white minute object is calcium carbonate.

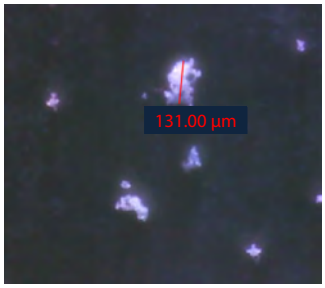

Fig. 4 White Minute Object

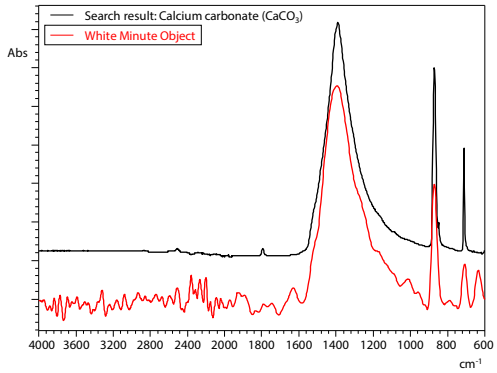

Fig. 5 Infrared Spectrum Obtained from White Minute Object and Search Result

Analysis of Transparent Film Using the Transmission Mode

The fairly large-sized transparent film shown in Fig. 6 was compressed in a diamond cell and measured using the transmission mode. Since the sample stage of SurveyIR can accommodate a diamond cell likewise general infrared microscopes, the process from pretreatment to measurement can be done smoothly. Fig. 7 shows the cell set on the sample stage.

LabSolutions™ IR is a control software for Shimadzu FTIR instruments that allows measurement of spectra while monitoring. Since both an image and the infrared spectra can be observed while adjusting the stage position, it is possible to find a measurement position that can yield the optimum peak intensity.

This measurement was done by setting the aperture size to 160 µm. Other conditions are the same as those listed in Table 1. Fig. 8 shows the obtained spectrum and the search result which indicate that the film material is polyethylene.

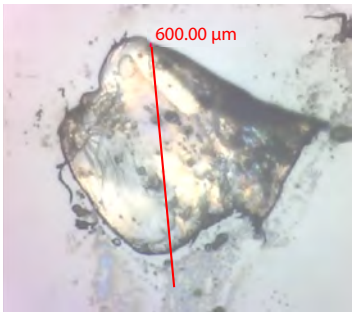

Fig. 6 Transparent Film

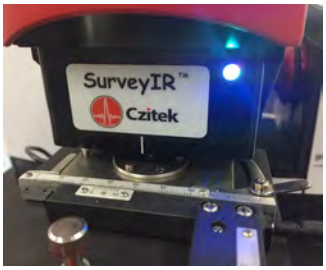

Fig. 7 Sample Stage with a Diamond Cell Set in Place

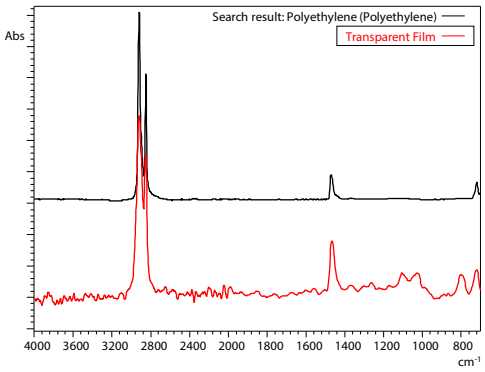

Fig. 8 Infrared Spectrum Obtained from Transparent Film and Search Result

Conclusion

Analysis of minute objects about 100 µm in size was done with good sensitivity using a sample compartment type infrared microscopy system. The system also has an outstanding observation function which allowed smooth acquisition of clear images using the fine adjustment function of the Z axis. The function also enabled measurement of sample dimensions. Switching between transmittance, reflectance, and ATR measurement is easy on the SurveyIR, making it possible to select the measurement method that is most appropriate for each sample. SurveyIR also features six aperture sizes which enable measurement according to the size of the sample.

In cases where the sample size is a few dozen µm, use of an infrared microscope equipped with an MCT detector is recommended.

SurveyIR is a product purchased from Czitek, LLC.

First Edition: Mar. 2018

Shimadzu Corporation
www.shimadzu.com/an/

SHIMADZU
Excellence in Science

Application News

No.A523

Spectrophotometric Analysis

Simultaneous Measurement and Visual Observation: Transmittance Measurement of Multilayer Film

BACK TO CONTENTS

By using the AIM-9000 infrared microscope together with AIMsolution Analysis software, measurement points can be visually observed at the same time as a spectrum is measured for the corresponding point.
In this example, a multilayer film sample is analyzed using simultaneous visual observation and spectral measurement.

Measurement of Multilayer Film

A microscope image of a 20 µm thick cross-section of multilayer film, sliced using a microtome, is shown in Fig. 1. Fig. 1 shows that the film consists of at least four layers.
The spectrum was measured by the transmission method, with the sliced multilayer film held horizontally. First, the sample and background (BKG) measurement points were specified, as shown in Fig. 2. In this case, a location where there is no film (air) was specified as the BKG position. The aperture sizes were set to 50 × 50 µm for measurement points 1 and 4, and 20 × 50 µm for measurement points 2 and 3.
The aperture size of the BKG point needs to be the same as that of the measurement point. If multiple measurement points with different sizes are selected, BKG is measured with the aperture automatically matched to the respective measurement point size. Measurement conditions are indicated in Table 1.

Results

An image of the microscope area and the spectrum from each point are shown in Fig. 3.
After the measurements were finished, the AIMsolution Analysis software launched automatically to make it easy to perform data processing and spectrum searches. A screenshot from the AIMsolution Analysis software is shown in Fig. 4. Measurement points and spectra are color-coded to make them easier to correlate. Furthermore, search results show the acquired spectrum at the top, a spectral hit in the middle, and the hit list at the bottom, as shown in Fig. 5.
That provides powerful support to analysts by providing a smooth process flow from confirming the measurement points, measurements, to analyzing the resulting data.

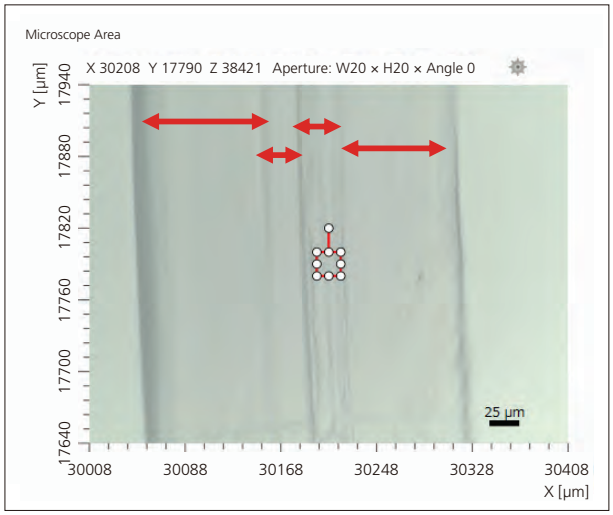

Fig. 1 Microscope Image of Multilayer Film Cross-Section

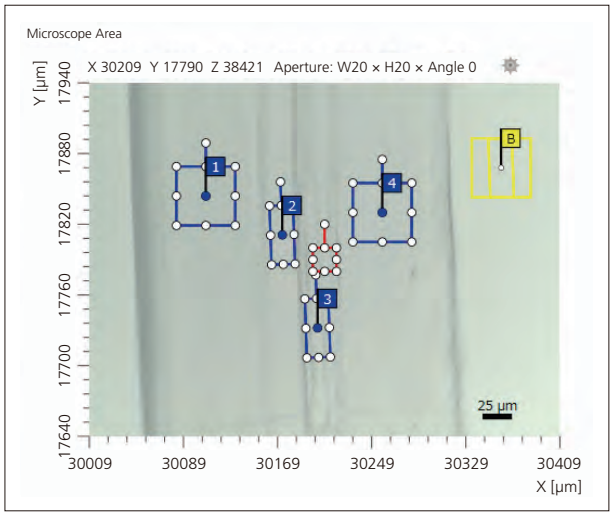

Fig. 2 Image Showing Measurement Points

Table 1 FTIR Measurement Conditions

Instrument	: IRTracer-100 AIM-9000
Resolution	: 8 cm^{-1}
Accumulation	: 10
Apodization	: SqrTriangle
Detector	: MCT
Aperture	: 20 × 50 µm, 50 × 50 µm

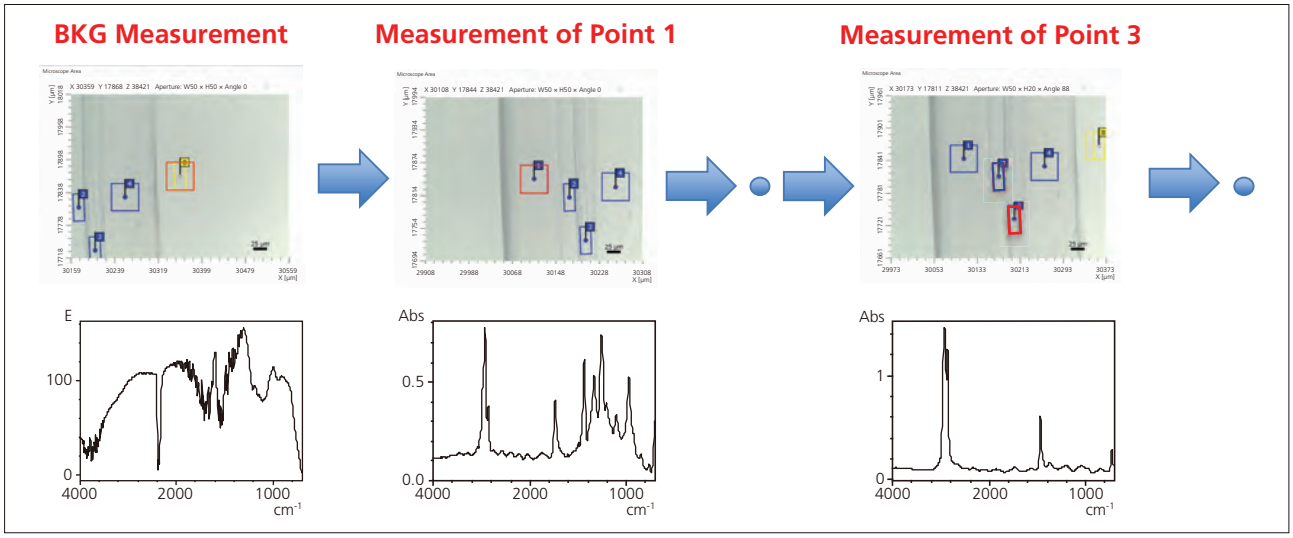

Fig. 3 Microscopic Images During Measurements and Measured Spectra

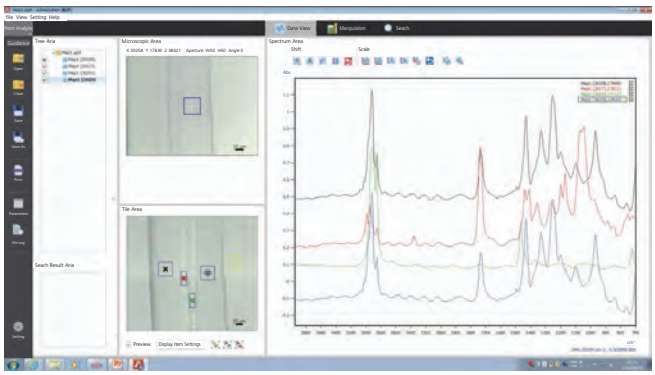

Fig. 4 Screenshot of AIMsolution Analysis Software

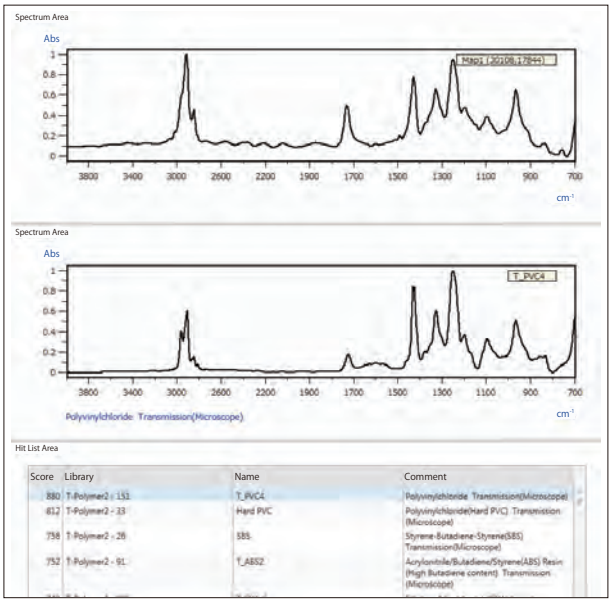

Fig. 5 Search Results

Conclusion

This simultaneous visual observation and measurement example showed how both images and spectra from measurement points can be viewed simultaneously in real time.
AIMsolution Analysis software displays each measurement point color-coded with the same color as the corresponding spectrum, which makes it visually easier to understand. The software also makes it easy to perform data processing, such as atmospheric correction and searches.
In this way, by using the AIM-9000 microscope with AIMsolution Measurement software for sample analysis and AIMsolution Analysis for data analysis, the system is able to immediately, during any step, provide more reliable information and a stress-free sample analysis workflow.

First Edition: Nov. 2016

Shimadzu Corporation
www.shimadzu.com/an/

SHIMADZU
Excellence in Science

Application News

No. A584

Spectrophotometric Analysis

Human Hair Cross-Section Analysis Using the AIM-9000 Infrared Microscope

BACK TO CONTENTS

In order to control the permeability of the product components of hair-treatment and hair-coloring products into human hair, measurement methods that allow direct and straightforward analysis of human hair need to be established.[1)]

The AIM-9000 infrared microscope enables visualization of component distributions in minute areas. This article introduces an example of analyzing cross sections of human hair using the AIM-9000. The cross sections of human hair were prepared using a microtome manufactured by Leica Biosystems.

S. Iwasaki

AIM-9000 Infrared Microscope with Mapping Program

Minute areas of samples can be analyzed in detail by combining the AIM-9000 infrared microscope with the optional mapping program. Fig. 1 shows the instruments used for analysis. The mapping program is capable of both area mapping measurement for analyzing the in-plane distribution of sample components, and line mapping measurement which is effective for analysis at regular intervals along straight lines. In addition to mapping measurement in the standard transmission and reflectance modes, ATR mapping measurement that uses the optional ATR objective mirror and pressure sensor is also available.

Fig. 1 **IRTracer^{TM}-100 Fourier Transform Infrared Spectrophotometer (Left) and AIM-9000 Infrared Microscope (Right)**

Preparation of Human Hair Sections

Untreated black hair and permed/bleached hair were prepared as samples of human hair.

A Leica Biosystems fully automatic rotary microtome was used to prepare the sample sections. Fig. 2 shows the HistoCore NANOCUT R which is the latest model. The cutting method on the HistoCore NANOCUT R can be switched between automatic and manual modes and the cutting thickness can be set from 0.25 to 300 µm. In this example, 3 µm thick sections were created through vitreous ice-embedding using the EF-13 electronic sample freezing device.

Fig. 2 **Leica Biosystems HistoCore NANOCUT R Fully Automatic Rotary Microtome**

Analysis of Human Hair Cross Sections

Mapping measurement was performed using the infrared microscope. The human hair sections were placed on a diamond cell and measured using transmission microspectroscopy. The aperture was set to 10 µm × 10 µm and the measurement interval was set to 5 µm. Table 1 lists the measurement conditions and Fig. 3 shows the representative infrared spectra of untreated black hair and permed/bleached hair.

The spectra show an amide I peak (C=O stretching vibrations) in the vicinity of 1650 cm^{-1} and a peak originating from cysteic acid (S-O stretching vibrations), which is an indicator of hair damage, in the vicinity of 1040 cm^{-1}. The cysteic acid peak only appears for the permed/bleached hair.

Table 1 **Measurement Conditions**

Instrument	: IRTracer-100, AIM-9000
Resolution	: 8 cm^{-1}
Accumulation	: 10
Apodization function	: Sqr-Triangle
Aperture size	: 10 µm × 10 µm
Measurement interval	: 5 µm
Detector	: MCT

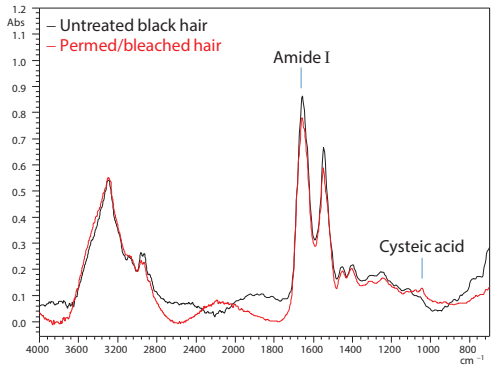

Fig. 3 **Representative Infrared Spectra of Untreated Black Hair and Permed/Bleached Hair**

Chemical Images of Hair Cross Sections

Observation images of untreated black hair and permed/bleached hair were acquired and chemical images were created from the mapping measurement results.
Chemical images were created from the results of mapping measurement using peak height and area, multivariate analysis (PCR/MCR), and the degree of similarity with target spectra. By this, component distributions that cannot be confirmed visually were successfully visualized. Mapping measurement is widely used for defect analyses as well as analysis of industrial materials and biological samples.
Fig. 4 (a) shows chemical images derived from amide I (peak correction area values near 1650 cm^{-1}). Amide I is widely distributed from the surface to the interior of the hair for both the untreated black hair and permed/bleached hair, and both favorably agree with their observation image counterparts.
Fig. 4 (b) shows chemical images derived from cysteic acid (peak correction area values near 1040 cm^{-1}). Compared to the untreated black hair, cysteic acid is distributed throughout the permed/bleached hair, which is assumed to be the result of hair damage.

Conclusion

This article introduced an analysis of human hair cross sections using the AIM-9000 infrared microscope. We were able to demonstrate the changes in composition of internal proteins resulting from hair damage. FTIR is an effective method for observing the components inside human hair and the changes that occur due to hair damage.

Acknowledgments:
We would like to thank Leica Microsystems GmbH for their cooperation in the cutting of samples.

References:
1) Satoshi Inamasu et al., "Analysis of Human Hair Cross Section Using Infrared Microspectroscopy"
J. Soc. Cosmet. Chem. Jpn. Vol.50, No.3 2016 P.209-217

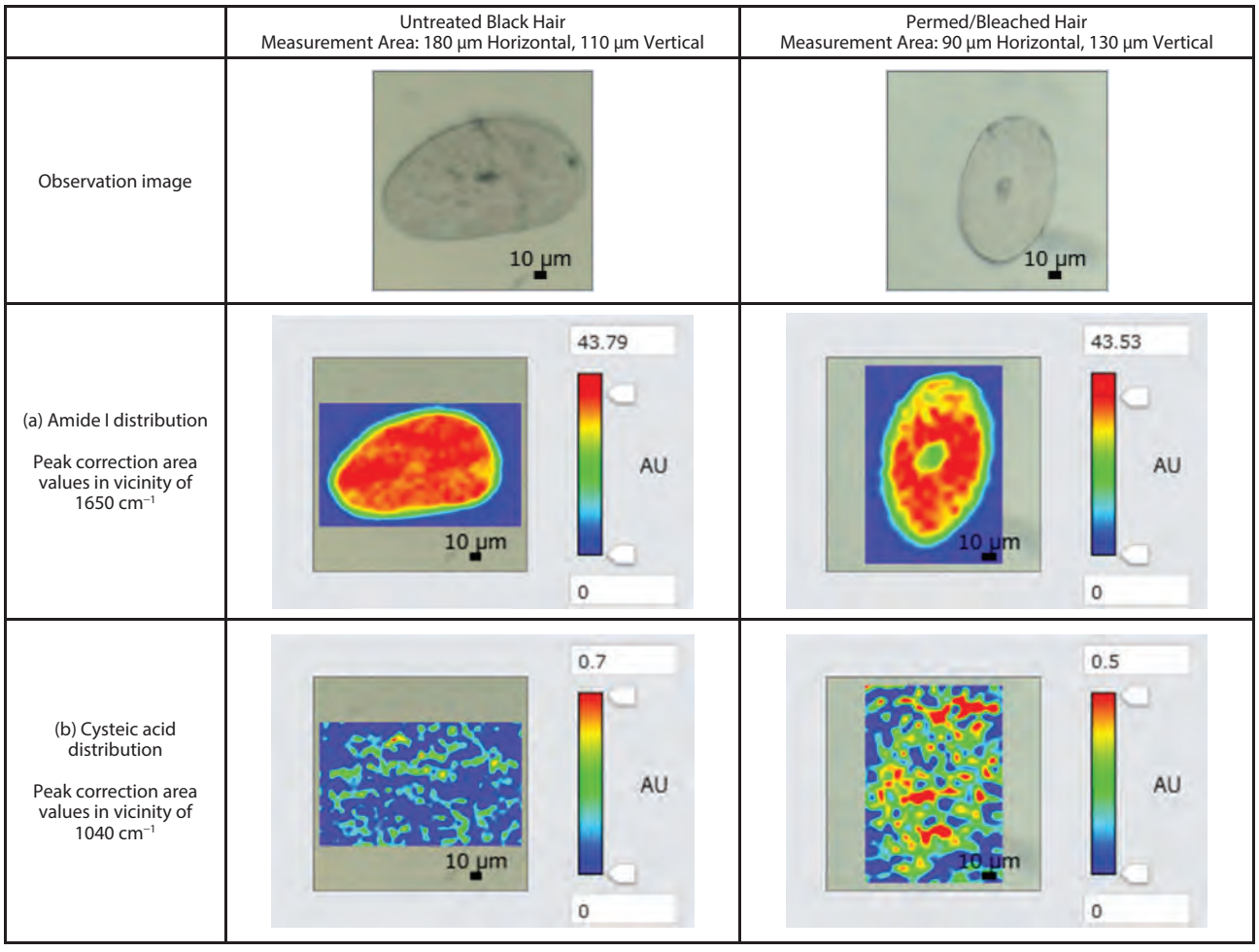

Fig. 4 **Chemical Images of Hair Cross Sections (Untreated Black Hair, Permed/Bleached Hair)**

First Edition: Dec. 2018

Shimadzu Corporation
www.shimadzu.com/an/

SHIMADZU
Excellence in Science

Application News

No. A555

Spectrophotometric Analysis

Measurement Examples of Small Samples and Small Areas

- Utilizing a Micro Sample Holder and Micro Beam Lens Unit -

BACK TO CONTENTS

Daily technical progress makes it possible to process small objects and small areas. Therefore, there are increasing needs for measuring the characteristics of such small samples and small areas.

Here, we describe an example of utilizing a UV-VIS spectrophotometer with a micro sample holder and a micro beam lens unit to meet the above needs.

K. Sobue

Sample Measurement with a Micro Sample Holder

Fig. 1 shows a micro sample holder which can hold a solid sample of about 5 to 10 mm in diameter or squared and about 1 to 5 mm thick. Three commercial band-pass filters of about 10 mm in diameter were set as shown in Fig. 2 and measured. Table 1 shows the analytical conditions and Fig. 3 shows the obtained transmittance spectra. The specified center wavelength of each filter is 500 nm, 730 nm, and 905 nm (tolerance 2 nm) respectively. The peak wavelength in their measured spectra is observed at almost the same wavelengths as written above.

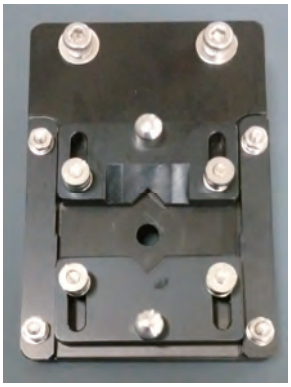

Fig. 1 Micro Sample Holder

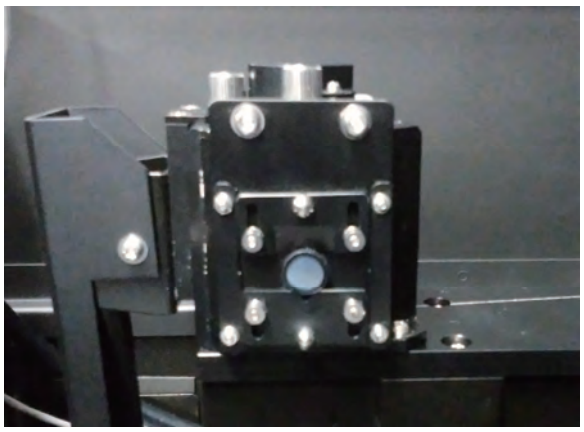

Fig. 2 Micro Sample Holder with a Sample Set on an Integrating Sphere

Table 1 Analytical Conditions

Instrument Used	: UV-2600, MPC-2600A Micro Sample Holder
Measurement Wavelength Range	: 350 to 800 nm/850 to 1050 nm
Scanning Speed	: Low speed
Sampling Pitch	: 1.0 nm
Slit Width	: 2.0 nm (Using mask provided with MPC)

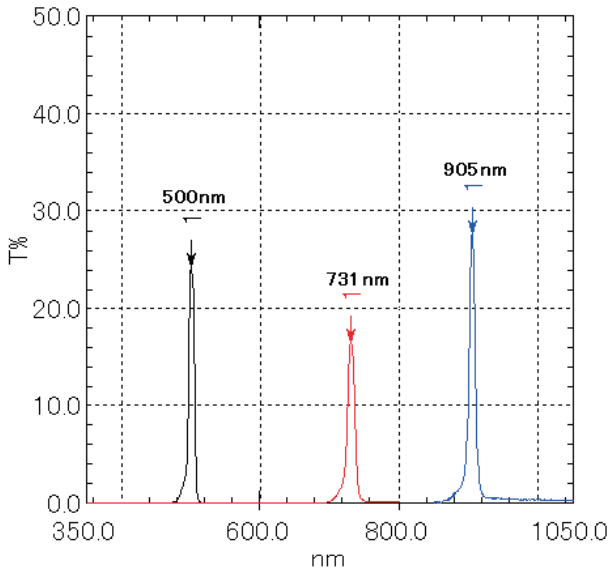

Fig. 3 Transmittance Spectra of Band-Pass Filters
Black: Center WL of 500 nm, Red: Center WL of 730 nm, Blue: Center WL of 905 nm

BACK TO CONTENTS

Measurement of Small Areas Using a Micro Beam Lens Unit

Fig. 4 shows a micro beam lens unit, which is capable of focusing light down to approximately ϕ1 mm. In addition, it can focus light at the center of the integrating sphere window or on the sample surface when it is used with a micro sample holder. In this example, small areas (2-mm square area) on a patterned film as shown in Fig. 5 were measured. Table 2 shows the analytical conditions and Fig. 6 shows the obtained transmittance spectra. Since each area had a different color, the measured transmittance spectra showed absorptions in the wavelength range corresponding to the color. Table 3 shows the color values calculated with the transmittance spectra. Fig. 7 and Fig. 8 show the color space of each area and the L*a*b* color space, respectively. The L*a*b* color coordinate system is used to represent the color of a body, where L* represents lightness, and a pair of a* and b* represents hue and chroma (saturation). It was confirmed that there was a correlation between visual color and the measurement results.

Table 2 Analytical Conditions

Instrument Used	: UV-2600, MPC-2600A Micro Beam Lens Unit
Measurement Wavelength Range	: 350 to 800 nm
Scanning Speed	: Medium speed
Sampling Pitch	: 1.0 nm
Slit Width	: 5.0 nm (Using mask provided with MPC)

Fig. 4 Micro Beam Lens Unit

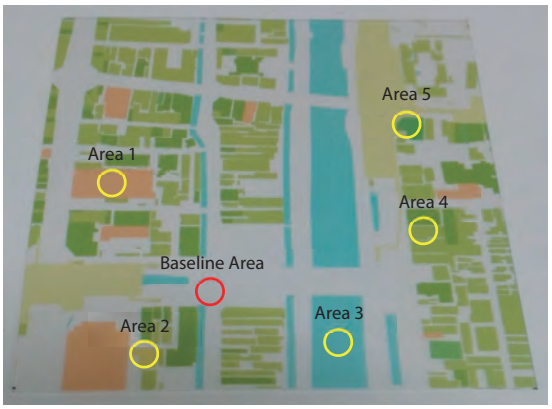

Fig. 5 Patterned Film and Measurement Area

Table 3 Color Values (D65, Viewing Angle of 2 Degrees)

Area	Visual Color	L*	a*	b*
1	Orange	92.68	2.74	13.32
2	Yellow green	96.41	-8.08	20.89
3	Light blue	92.38	-11.65	-5.55
4	Light green	92.04	-13.97	19.32
5	Green	86.76	-21.38	10.09

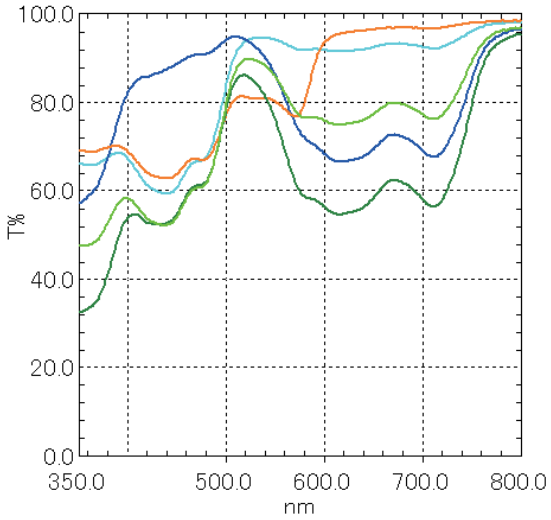

Fig. 6 Transmittance Spectra of Colored Areas in Patterned Film Orange: Area 1, Light Blue: Area 2, Blue: Area 3, Yellow Green: Area4, Green: Area 5

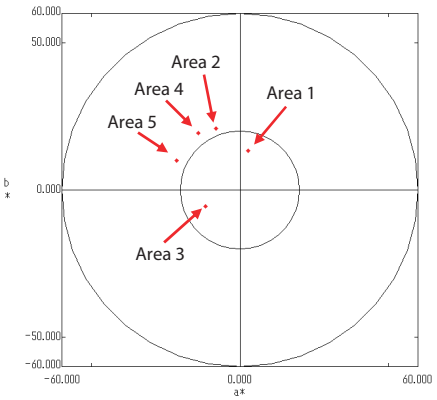

Fig. 7 Color Space of Each Area

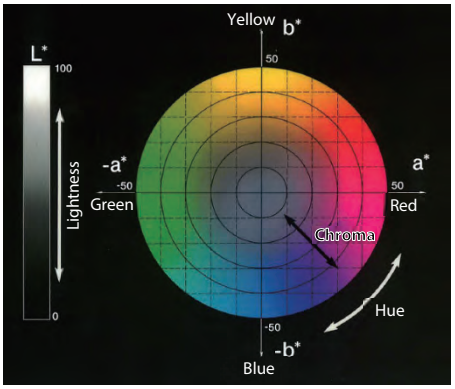

Fig. 8 L*a*b* Color Space

Conclusions

Small band-pass filters were held easily and measured with a micro sample holder. Small areas on a patterned film were measured with a micro beam lens unit. Various types of samples and a small area can be measured with accessories suitable for them.

First Edition: Oct. 2017

SHIMADZU

Shimadzu Corporation

www.shimadzu.com/an/

SHIMADZU
Excellence in Science

Application News

No. A556

Spectrophotometric Analysis

Evaluation of Transmittance/Reflectance Spectra of Dielectric Multilayer Films - Utilizing a Variable Angle Measurement Unit -

BACK TO CONTENTS

Dielectric multilayer films are coated on various optical elements such as lenses, mirrors and filters. They are also applied to items familiar to us such as cameras and binoculars. In addition, they are often utilized in photometers and are a very important optical element.

Here, we describe using a UV-VIS spectrophotometer with a variable angle measurement unit to measure the transmittance and reflectance spectra of filters coated with dielectric multilayer films.

K. Sobue

Sample Measurement Using a Variable Angle Measurement Unit

Fig. 1 shows the sample compartment of the MPC-2600A multi-purpose large sample compartment with a variable angle measurement unit mounted. Fig. 2 shows the structure of the variable angle measurement unit which employs a goniometer system that rotates the sample mounting stage and the detector (integrating sphere) coaxially. An arbitrary incident angle of light to a sample can be set. Transmittance measurement of a sample at an arbitrary incident angle is performed by rotating the sample mounting stage while keeping the integrating sphere position set at 180 degrees. In addition, the absolute specular reflectance can be measured by setting the incident angle of light to the sample (5 to 70 degrees) by rotating the sample mounting stage while also changing the detector position (10 to 140 degrees).

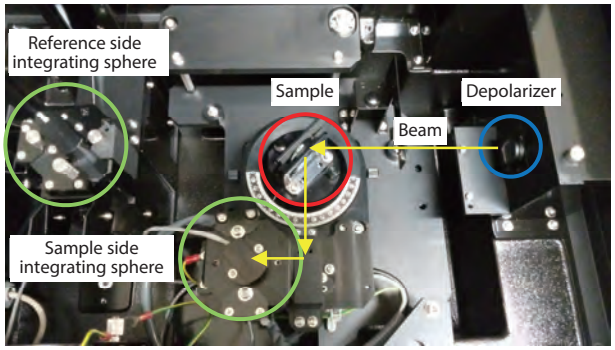

Fig. 1 Sample Compartment of MPC-2600A with Variable Angle Measurement Unit Mounted

Table 1 Analytical Conditions

Instrument Used	: UV-2600, MPC-2600A, Variable angle measurement unit, Quartz depolarizer*1
Measurement Wavelength Range	: 350 to 800 nm
Scanning Speed	: Medium speed
Sampling Pitch	: 1.0 nm
Slit Width	: 5.0 nm

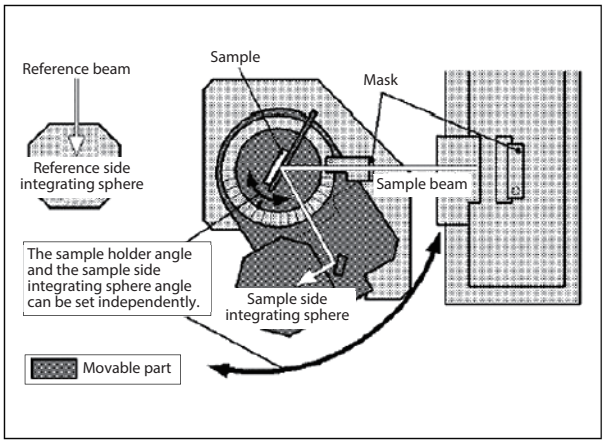

Fig. 2 Structure of Variable Angle Measurement Unit

Transmittance Spectra Measurement of Dielectric Multilayer Films

Two commercial band-pass filters which can selectively transmit light of a specific wavelength range by means of dielectric multilayer films were measured. The center wavelength of these filters was 500 nm and 730 nm respectively. Fig. 3 and 4 show the transmittance spectra measured by changing the incident angle of light to the band-pass filters. Table 1 shows the analytical conditions. A quartz depolarizer was used to depolarize any polarized light during measurement.

When the incident angle of light was 0 degrees, it was confirmed that light was transmitted at the center wavelength. In addition, when the incident angle increased, the transmitted wavelength region shifted to the blue and transmittance also decreased. It is assumed that light is not transmitted in regions other than the center wavelength because it is either absorbed or reflected. We therefore then measured the reflectance spectra with both filters.

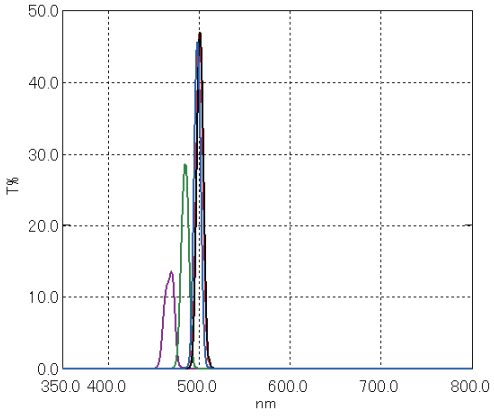

Fig. 3 Transmittance Spectra (Center Wavelength: 500 nm) Incident Angle of 0 ° (black), 5 ° (red), 12 ° (blue), 30 ° (green), 45 ° (purple)

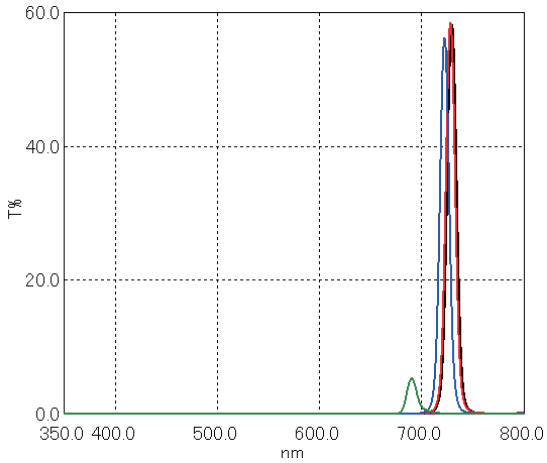

Fig. 4 Transmittance Spectra (Center Wavelength: 730 nm) Incident Angle of 0 ° (black), 5 ° (red), 12 ° (blue), 30 ° (green), 45 ° (purple)

Reflectance Spectra Measurement of Dielectric Multilayer Films

Reflectance spectra were measured with the same samples using the conditions shown in Table 2. Fig. 5 and 6 show the obtained absolute specular reflectance spectra for which the reflection angle of light was the same as the incident angle. A quartz depolarizer was used to depolarize any polarized light during measurement. For details on S/P polarization in reflectance measurement, please refer to Application News No. A394.

Table 2 Analytical Conditions

Instrument Used	: UV-2600, MPC-2600A, Variable angle measurement unit, Quartz depolarizer*1
Measurement Wavelength Range	: 350 to 800 nm
Scanning Speed	: Medium speed
Sampling Pitch	: 1.0 nm
Slit Width	: 5.0 nm

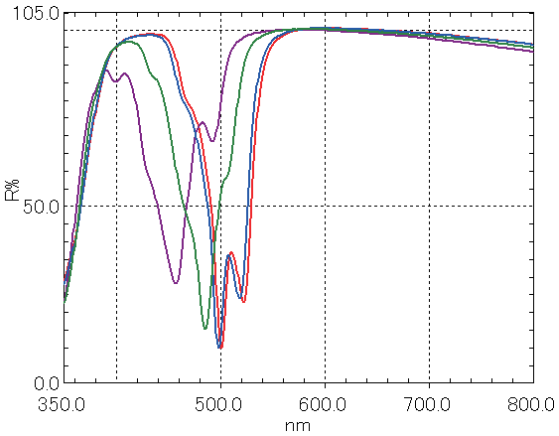

Fig. 5 Absolute Specular Reflectance Spectra (Center Wavelength: 500 nm) Incident Angle of 0 ° (black), 5 ° (red), 12 ° (blue), 30 ° (green), 45 ° (purple)

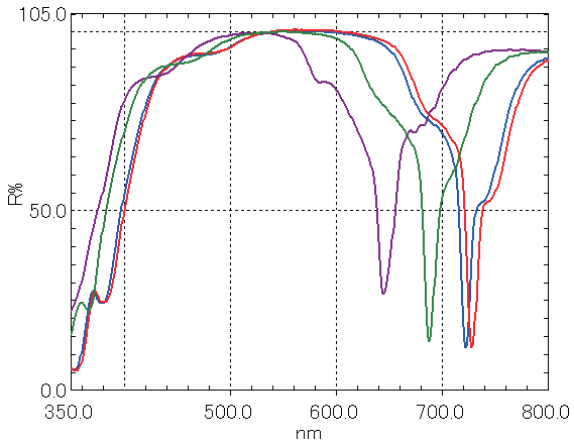

Fig. 6 Absolute Specular Reflectance Spectra (Center Wavelength: 730 nm) Incident Angle of 0 ° (black), 5 ° (red), 12 ° (blue), 30 ° (green), 45 ° (purple)

It was confirmed that the lowest reflectance is observed at the center wavelength with both band-pass filters. In addition, likewise with the transmittance spectra, it was confirmed that the wavelength at which reflectance decreases shifted to the blue as the incident angle increased. The transmittance spectra showed that the filters do not transmit light except at the center wavelength. With the reflectance spectra, however, low reflectance is observed in the ultraviolet region (less than 400 nm) and high reflectance is observed in other wavelength regions, except at the center wavelength. These results indicate that there are regions that do not transmit light by absorbing light and regions that do not transmit light by reflecting light.

Summary

The transmittance and reflectance spectra of dielectric multilayer films were measured at several incident angles using the UV-2600 and the MPC-2600A with a variable angle measurement unit mounted.

From the transmittance spectra of when the incident angle of light was 0 degrees, it was confirmed that light was transmitted at the center wavelength. In addition, when the incident angle increased, the center wavelength shifted to the blue. It was also confirmed from the reflectance spectra that the lowest reflectance is observed at the center wavelength. Also, likewise with the transmittance spectra, it was confirmed that the center wavelength shifts to the blue when the incident angle is increased. The obtained transmittance and reflectance spectra indicate that the wavelength regions where light is not transmitted are generated by the reflection and absorption of light.

*1: DEQ-2OP manufactured by Sigma Koki. Creates pseudo depolarized light.

First Edition: Oct. 2017

Shimadzu Corporation
www.shimadzu.com/an/

SHIMADZU
Excellence in Science

Application News

No. A579

Spectrophotometric Analysis

An Evaluation of the Dispersibility and Functional Group Information of Networked CNFs and the Optical Properties of CNF Film

BACK TO CONTENTS

Cellulose is a polysaccharide that is the primary component of plant cell walls. Cellulose that is fibrillated down to the order of nanometers is called nanocellulose and of such nanocelluloses, those that have a high aspect ratio (100 or higher) with a width of 4 to 100 nm and a length of a few µm are called cellulose nanofibers (CNFs). CNFs are gaining attention as state-of-the-art biomass material.

There are generally two types of CNFs: monodisperse CNFs and networked CNFs. Monodisperse CNFs have a width of approx. 3 to 5 nm and each fiber is dispersed. They are therefore transparent and can easily be added functions such as water-resistance and enzymatic barriers. Networked CNFs on the other hand are larger with a width of approx. 20 to 100 nm and only require mechanical fibrillation to make. They feature easy adhesion with resins and also easy processing. Regarding monodisperse CNFs, an evaluation of dispersibility is introduced in Application News No. S31.

This article studies the dispersibility and function group information of networked CNFs. The measurement samples are CNFs (wood-derived etc.) purchased from Sugino Machine Ltd., and fermented nanocellulose (product name: Fibnano) provided by Kusano Sakko Inc., and Prof. Kenji Tajima of Hokkaido University. We also evaluated the optical properties of CNF film purchased from Sugino Machine Ltd., the results of which are also introduced in this article.

K. Sobue

Dispersibility Evaluation of a Networked CNF Solution

Four types of samples were prepared for measurement as shown in Table 1: wood-derived CNF, cellulose made from carboxymethyl cellulose and powdered chitin respectively, and fermented nanocellulose (materials: glucose, fructose). After diluting each sample to a concentration of 0.1 wt%, the linear transmission and total light transmission were measured using the conditions listed in Table 2.

According to the linear transmission spectra shown in Fig. 1, wood-derived CNF indicates low transmission under 20 %T including the visible range. CMC exhibits high transmission exceeding 90 %T in the visible range, but drops steeply in the ultraviolet range at about 200 to 240 nm. Both chitin and fermented nanocellulose show a gradual decline in transmission from the long-wavelength range through to the short-wavelength range. All samples show a lower transmission in the linear transmission spectra compared to the total light transmission spectra (Fig. 2), suggesting that the samples are cloudy with a concentration of 0.1 wt%.

Table 1 List of Measurement Samples

Sample Name	Material
Wood-derived CNF	Cellulose
CMC	Carboxymethyl cellulose
Chitin	Powdered chitin
Fermented nanocellulose	Glucose, fructose

Table 2 Measurement Conditions

Instrument Used	:	UV-2600, ISR-2600 Plus
Measuring Wavelength Range	:	200 nm - 800 nm
Scan Speed	:	Medium speed
Sampling Interval	:	1.0 nm
Slit Width	:	2 nm (UV-2600) 5 nm (UV-2600+ISR-2600 Plus)
Light Source Changing Wavelength	:	323 nm

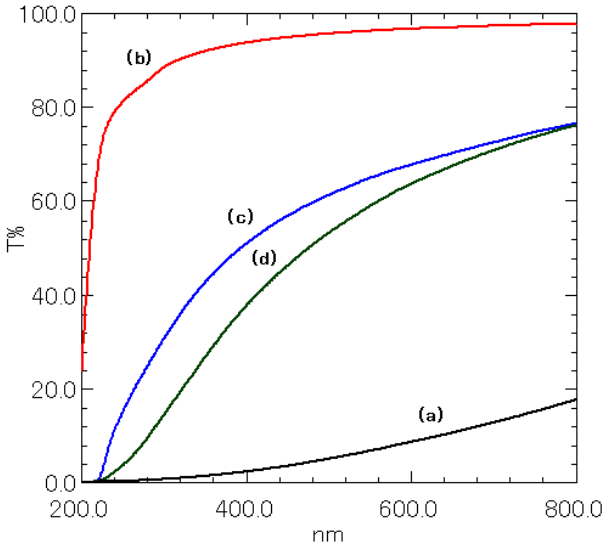

Fig. 1 Linear Transmission Spectra
(a) Wood-Derived CNF, (b) CMC, (c) Chitin, (d) Fermented Nanocellulose

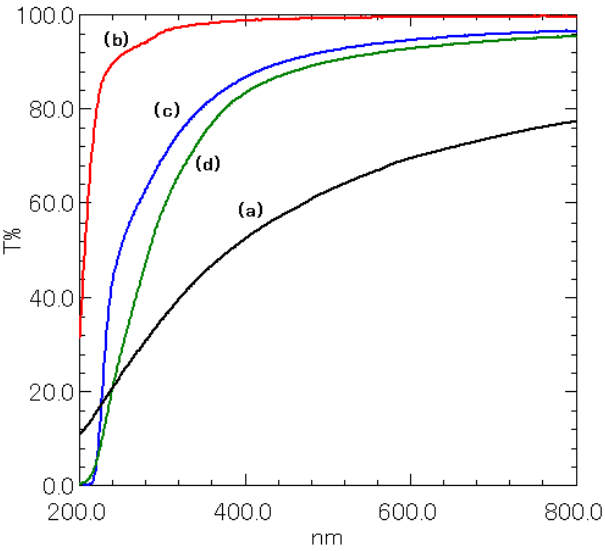

Fig. 2 Total Light Transmission Spectra
(a) Wood-Derived CNF, (b) CMC, (c) Chitin, (d) Fermented Nanocellulose

Functional Groups of Networked CNFs

Each sample in Table 1 was applied to and dried on aluminum foil as shown in Fig. 3 and then measured using the ATR method on an FTIR instrument. Table 3 lists the measurement conditions and Fig. 4 shows the measured infrared spectra.

Fig. 3 Wood-Derived CNF Applied to and Dried on Aluminum Foil

Table 3 Measurement Conditions

Instrument Used	:	IRSpirit™-T (KBr window), QATR™-S (wide-band diamond prism)
Resolution	:	4 cm^{-1}
Accumulation	:	32 times
Apodization Function	:	Happ-Genzel
Detector	:	DLATGS

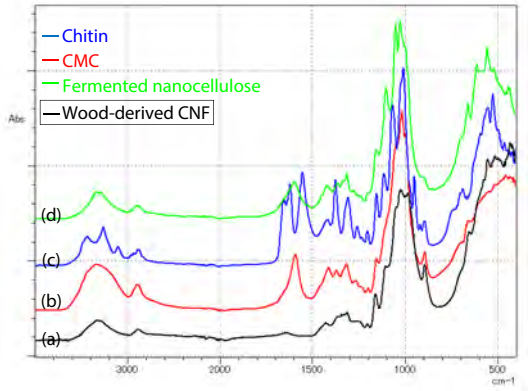

Fig. 4 Infrared Spectra
(a) Wood-Derived CNF, (b) CMC, (c) Chitin, (d) Fermented Nanocellulose

For wood-derived CNF, we can see a peak at 3600 to 3200 cm^{-1} caused by O-H stretching vibrations and a peak at 1100 to 900 cm^{-1} caused by C-O stretching vibrations. This matches with the cellulose included in the ATR and food additive libraries of LabSolutions™ IR. For CMC, in addition to the peaks observed for wood-derived CNF, there is a peak near 1600 cm^{-1} caused by COO^- asymmetrical stretching vibrations. Overall, the spectrum is similar to that of fermented nanocellulose. Regarding chitin, there is a peak near 3300 cm^{-1} caused by NH stretching vibrations from amide bonds, a peak near 1650 cm^{-1} caused by C=O stretching vibrations, and a peak near 1550 cm^{-1} caused by NH bending vibrations and CN stretching vibrations. As described, functional groups can be determined by using FTIR.

Optical Properties of CNF Film

The optical properties of CNF film were measured using the conditions listed in Table 2. For comparison reasons, commercially available polypropylene (PP) film and polyethylene (PE) film shown in Fig. 5 were measured as well. The measurement results are shown in Fig. 6

The linear transmission spectra show that the transmission of CNF film is low compared to that of PP film and PE film, and that there is only about 10 % of linear light transmission in the entire visible range. From the total light transmission spectra, we can see that if scattered light is included, CNF film transmits the same level of light as PP film and PE film in the visible range. Whereas PP film and PE film show a sharp drop in transmission due to the absorbance by additives in the ultraviolet range for wavelengths shorter than 250 nm, CNF film shows a gradual drop.

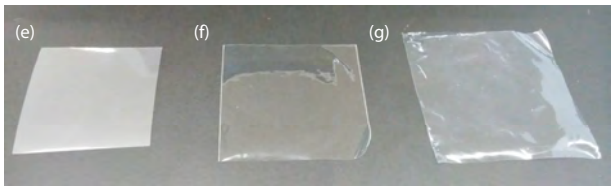

Fig. 5 (e) CNF Film, (f) PP Film, (g) PE Film

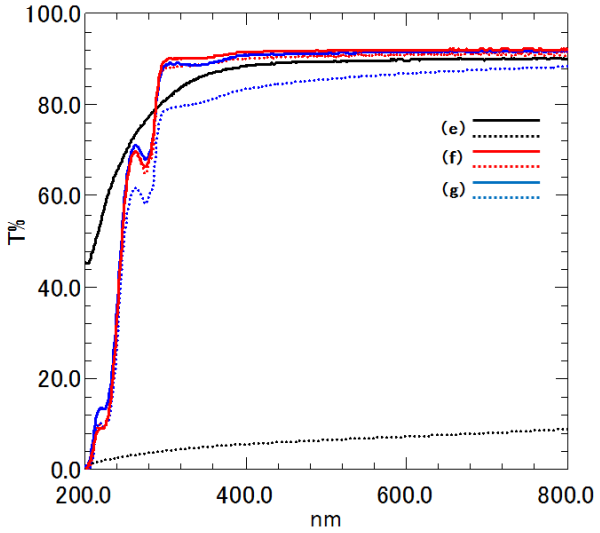

Fig. 6 Transmission Spectra
(Solid line: Total light, Dotted line: Linear)
(e) CNF Film, (f) PP Film, (g) PE Film

Conclusion

In this research, we studied the dispersibility and functional group information of networked CNF samples made of differing materials. By evaluating the dispersiblity of networked CNF solutions diluted to a concentration of 0.1 wt%, we determined that the CNFs are cloudy. It was also found that the transmission of each sample declines differently in the visible range and the ultraviolet range.

The functional groups of each sample were easily determined by measuring dried samples using the ATR method on an FTIR. Measurements suggested that CMC and fermented nanocellulose have a similar structure.

Evaluation of the optical properties of samples in film form was possible by comparing linear transmission and total light transmission. The CNF film we measured had a low linear transmission compared to PP film and PE film, but the total light transmission was at about the same level in the visible range.

Acknowledgments
We would like to thank Tokuo Matsushima of Kusano Sakko Inc, and Prof. Kenji Tajima of Hokkaido University for providing the samples used in these measurements and their knowledge regarding CNFs.

First Edition: Oct. 2018

SHIMADZU
Shimadzu Corporation
www.shimadzu.com/an/

BACK TO CONTENTS

SHIMADZU
Excellence in Science

Application News

No.A498A

Spectrophotometric Analysis

Measurement of Transmittance of Solar Battery Glass -Measurement of Transmittance of a Light Scattering Solid Sample-

BACK TO CONTENTS

Introduction

When measuring a solid sample with strong light scattering properties, using a 60 mm diameter integrating sphere can result in a change in photometric values at wavelengths where the detector is changed.
We have recently developed a 150 mm diameter integrating sphere. Using this integrating sphere increases the number of times light reflects inside the integrating sphere so when light reaches the detector it is more uniform, and also results in a more optimized detector arrangement, reducing the change in photometric values that occurs at detector switching wavelengths.
We introduce an example measurement of the transmittance of solar battery glass that is strongly light scattering, where the above described change in photometric values is prone to occur.

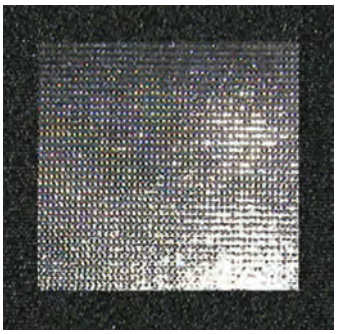

Fig. 1 Solar Battery Glass

Analysis of Solar Battery Glass

As shown in Fig. 1, solar battery glass has an uneven surface, and when light incidents on this surface it scatters unevenly.
When a sample of this type is analyzed, the incident light is reflected irregularly so there is a substantial difference in light behavior inside the integrating sphere between when a sample is measured and during baseline correction. This phenomenon sometimes gives rise to a change in photometric values at detector switching wavelengths.
We performed measurements of solar battery glass under the analytical conditions shown in Table 1, using the UV-3600 Plus and ISR-1503 (150 mm diameter integrating sphere with three detectors). Fig. 2 shows the UV-3600 Plus with ISR-1503 attached, and Fig. 3 shows the inside of the ISR-1503 on the left, and the sample installed on the right.

Fig. 2 UV-3600 Plus with ISR-1503 Attached

Table 1 Instrument and Analytical Conditions

Instrument used	: UV-3600 Plus UV-VIS-NIR spectrophotometer
Attachment	: ISR-1503 150 mm diameter integrating sphere (Internal wall: Barium sulfate)
Measurement wavelength range	: 250 to 2500 nm
Scanning speed	: Low speed
Sampling interval	: 1.0 nm
Photometric value	: Transmittance
Slit width	: (32)

Fig. 3 Inside the ISR-1503 (left) and with Sample Installed (right)

Analytical Results

Fig. 4 shows the spectrum obtained using the ISR-1503 to measure the transmittance of solar battery glass.
When analyzing a strongly light scattering solid sample with a 60 mm diameter integrating sphere, a change in photometric values tends to occur around the detector switching wavelengths of 870 nm and 1650 nm. Fig. 4 shows that this change is hardly visible in the measured spectrum.

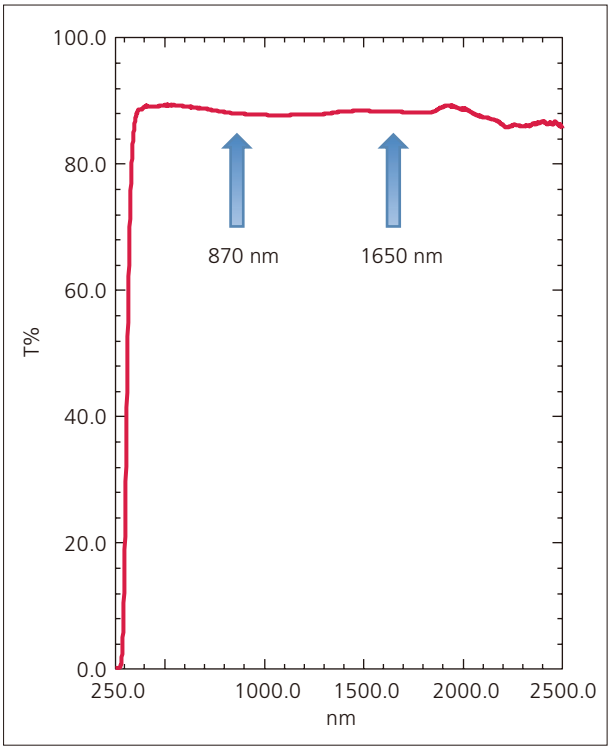

Fig. 4 Spectrum of Solar Battery Glass Measured with the ISR-1503

Advantages of the ISR-1503 Integrating Sphere

The advantages of the ISR-1503 are summarized in Table 2.
The ISR-1503 includes three detectors, PMT (photo-multiplier tube), InGaAs, and PbS detectors. This allows for high sensitivity measurements across the all measured wavelengths (200 to 2500 nm).
Samples can also be installed horizontally when measuring transmittance. This feature makes the ISR-1503 convenient for analyzing samples that require extra caution if installed vertically, such as powders that tend to spill, films that need to be fixed in place with tape, conical samples that are difficult to fix in place, and heavy samples that are at risk of falling.
Furthermore, the I R-1503 is designed with a small aperture ratio, which is the proportion of the internal surface area of the integrating sphere taken up by the inlet aperture. The aperture ratio used for reflectance measurements is 3.9 %, and for transmittance measurements is 2.8 %. The I R-1503 is compatible with the low aperture ratios prescribed in official analytical methods*1).
While a barium sulfate internal wall integrating sphere was used in this analysis, a Spectralon® fluorine-based resin*2) internal wall integrating sphere is also available. A Spectralon® specification integrating sphere results in no hydroxyl radical absorption around 1450 nm and 1950 nm, maintaining high reflectance across a wide wavelength range and so allowing for low-noise measurements.

Table 2 Advantages of the ISR-1503

(1)	High-sensitivity measurements with three detectors (PM , InGaAs and PbS) PM : 200 to 870 nm InGaAs : 870 to 1650 nm PbS : 1650 to 2500 nm
(2)	Samples can be placed horizontally.
(3)	Compatible with measurements that require low aperture ratios.

Conclusion

Using the UV-3600 Plus and ISR-1503 allowed for the collection of spectra with almost no change in photometric values at detector switching wavelengths, even when analyzing strongly light scattering solar battery glass.

*1) ISO 13468-2: 1999, DIN 14500: 2008, ASTM D 1003-92, ASTM E9003-96, JIS K5600-4-4, JIS K7136, JIS K7361-1, JIS K7375, JIS Z8722
*2) Spectralon® is a registered trademark of Labsphere, Inc.

BACK TO CONTENTS

First Edition: Dec. 2015

SHIMADZU
Shimadzu Corporation
www.shimadzu.com/an/

SHIMADZU
Excellence in Science

Application News

No.A507

Spectrophotometric Analysis

Evaluation of Functional Properties (Thermal Insulation and Lighting) of Fabric, Paper, Film, and Other Materials – Measuring Solar Transmittance/Reflectance Using ISR-1503 Integrating Sphere Attachment –

BACK TO CONTENTS

Interest in private power generation, energy-saving strategies, and other methods of caring for the environment is increasing alongside the global warming, energy disputes, and other environmental problems. A variety of functional materials and products are being developed with energy-saving characteristics not only in the electronics industry, but also in the construction and chemicals industry. These materials and products are often used in our immediate surroundings. Window glass and insulating film that transmits visible light but prevents transmission of near-infrared light are used to increase cooling and heating efficiencies in buildings. Items such as curtains and Japanese paper screen doors (shoji) have a variety of functions, such as thermal insulation and natural illumination. Parameters such as solar transmittance/reflectance are used to represent the optical properties of these materials and products and are described in Japanese Industrial Standards (JIS).
This article describes measuring the transmission and reflection spectra of four commercially available and common solar shields: curtains, shoji, roller blinds, and thermal insulation films. Measurements were made using a UV-3600 Plus UV-VIS-NIR spectrophotometer with ISR-1503 integrating sphere attachment, and solar transmittance software was used to calculate solar transmittance/reflectance.

Spectra Measurement

The UV-3600 Plus and ISR-1503 instruments are shown in Fig. 1. When using the ISR-1503 to take transmittance/zero-degree reflectance measurements, film samples, tapered samples, and powder samples can be analyzed without spillage by placing them in a horizontal orientation in the optical system as shown in Fig. 2.
Square, 5-cm samples of curtain, shoji (the paper that is normally mounted on a wooden frame), roller blind (a cloth curtain that is open and shut vertically), and thermal insulation film (applied to windows for a variety of functions) were cut out as shown in Fig. 3, and measurements were taken using the conditions shown in Table 1.

Fig. 1 UV-3600 Plus with ISR-1503 Attachment

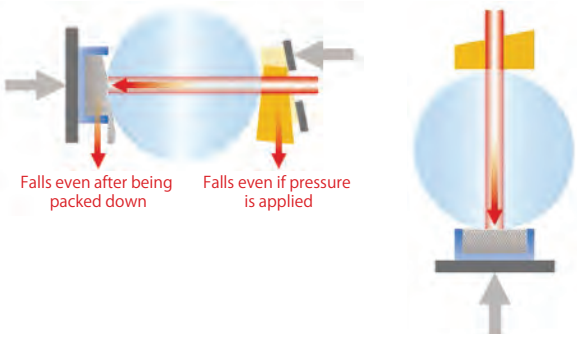

Fig. 2 Samples in Vertical and Horizontal Positions (Lateral View of Integrating Sphere)

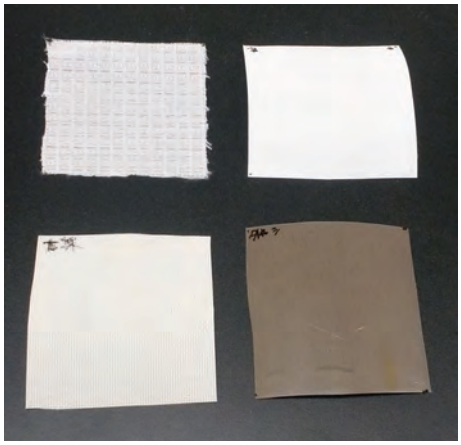

Fig. 3 Samples of Curtain, Shoji, Roller Blind, and Thermal Insulation Film

Table 1 Measurement Conditions

Instruments Used	: UV-3600 Plus, ISR-1503
Measured Wavelength Range	: 200 nm to 2500 nm
Scanning Speed	: Low speed
Sampling Interval	: 5.0 nm
Photometric Value	: Transmittance/Reflectance
Slit Width	: (32) nm
Light Source Switching Wavelength	: 310 nm
Detector Unit	: External (3 detectors)
Detector Switching Wavelength (s)	: 870 nm / 1650 nm
Grating Switching Wavelength	: 780 nm
S-beam/R-beam Switching	: Inversion
Step Correction	: Effective

BACK TO CONTENTS

The transmittance spectra of curtain materials are shown in Fig. 4, and the reflectance spectra are shown in Fig. 5. The curtain materials tested were normal curtain, curtain designed for natural illumination, and curtain designed for thermal insulation. The curtain designed for natural illumination generally has a higher transmittance but lower reflectance over the entire wavelength range compared to normal curtain. The curtain designed for thermal insulation generally has a lower transmittance but higher reflectance over the entire wavelength range compared to normal curtain. It can be presumed that increasing transmittance and lowering reflectance produce illuminating properties, while lowering transmittance and increasing reflectance produce thermal insulation properties.

The transmittance spectra of shoji materials are shown in Fig. 6, and the reflectance spectra are shown in Fig. 7. The shoji materials tested were plastic shoji, shoji designed for natural illumination, and shoji designed for thermal insulation. The shoji designed for natural illumination had a transmittance of around 45 % and reflectance of around 55 % over the entire wavelength range. The shoji designed for thermal insulation had a transmittance of around 20 % and reflectance of around 75 % over the entire wavelength range. The plastic shoji produced spectral shapes, transmittance results, and reflectance results similar to those obtained from the shoji designed for natural illumination.

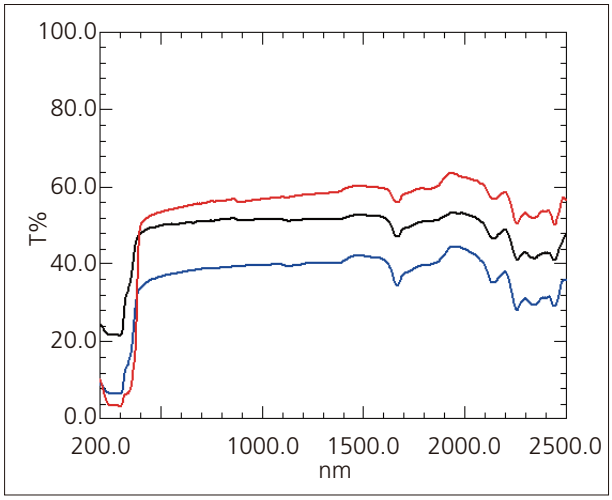

Fig. 4 Transmittance Spectra of Curtain Materials
Black: Normal, Red: Designed for Natural Illumination, Blue: Designed for Thermal Insulation

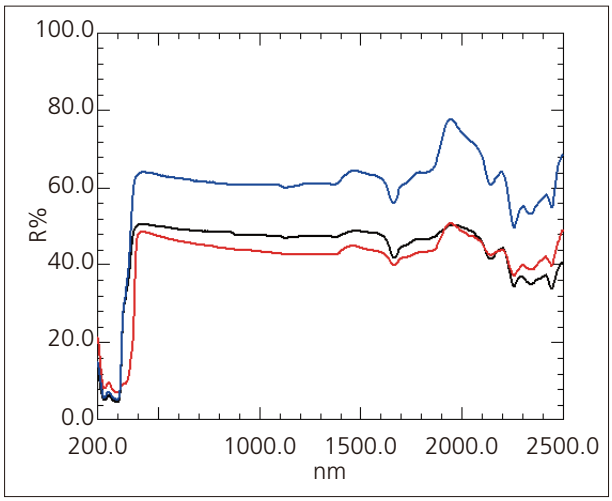

Fig. 5 Reflectance Spectra of Curtain Materials
Black: Normal, Red: Designed for Natural Illumination, Blue: Designed for Thermal Insulation

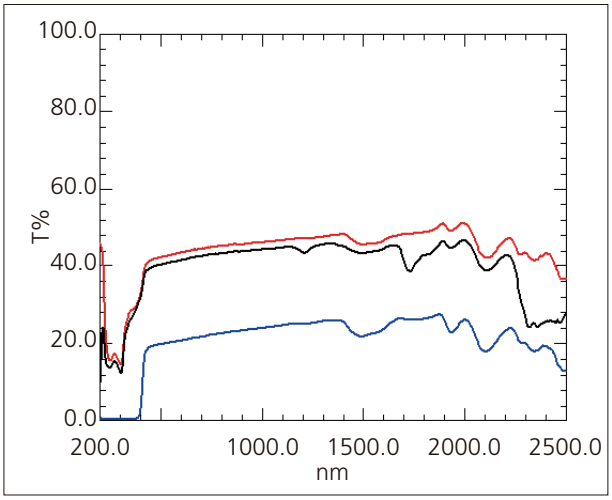

Fig. 6 Transmittance Spectra of Shoji Materials
Black: Plastic, Red: Designed for Natural Illumination, Blue: Designed for Thermal Insulation

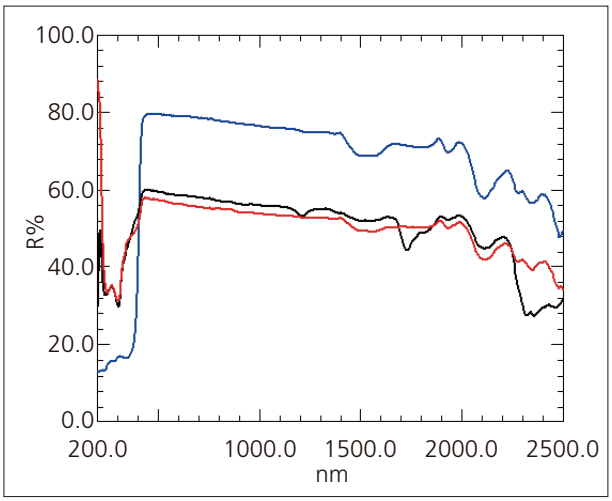

Fig. 7 Reflectance Spectra of Shoji Materials
Black: Plastic, Red: Designed for Natural Illumination, Blue: Designed for Thermal Insulation

BACK TO CONTENTS

The transmittance spectra of roller blind materials are shown in Fig. 8, and the reflectance spectra are shown in Fig. 9. The materials tested were roller blind designed for natural illumination, and roller blind designed for light shielding. The roller blind designed for natural illumination had a transmittance of around 35 % and reflectance of around 65 % over the entire wavelength range. The roller blind designed for light shielding had a transmittance of almost zero over the entire wavelength range, and a high reflectance in the visible region but low reflectance in the near-infrared region. It can be presumed that light shielding is produced by reflecting sunlight in the visible region while light in the near-infrared region is absorbed.

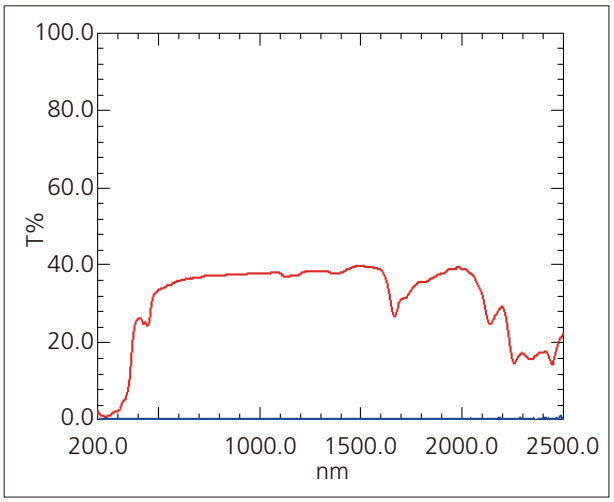

Fig. 8 Transmittance Spectra of Roller Blind Materials
Red: Designed for Natural Illumination,
Blue: Designed for Light Shielding

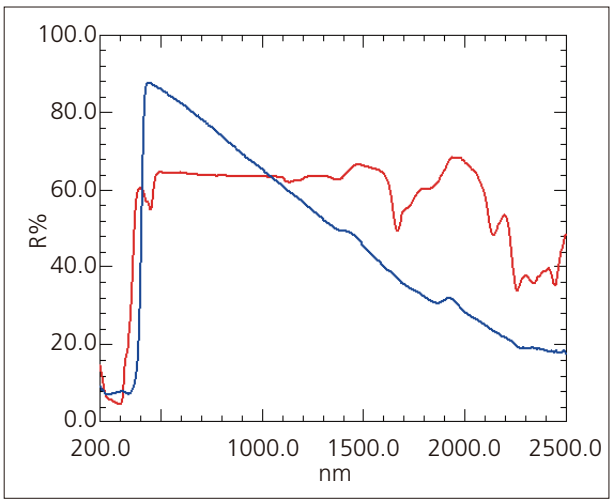

Fig. 9 Reflectance Spectra of Roller Blind Materials
Red: Designed for Natural Illumination,
Blue: Designed for Light Shielding

The transmittance spectra of thermal insulation films are shown in Fig. 10, and the reflectance spectra are shown in Fig. 11. The thermal insulation films tested were designed for 30 % and 80 % thermal insulation. The 30 % thermal insulation film had a lower transmittance in the near-infrared region compared to the visible region. Similarly, the 80 % thermal insulation film had a reduced transmittance in the near-infrared region, but allowed more transmission of 800 nm to 1000 nm light compared to near-infrared region light. It can be presumed the thermal insulation films tested produce a thermal insulation effect by absorbing sunlight, and not by reflecting sunlight.

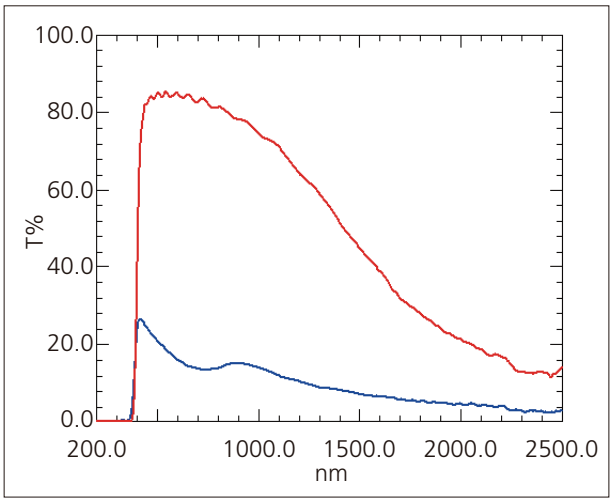

Fig. 10 Transmittance Spectra of Thermal Insulation Films
Red: 30 % Thermal Insulation,
Blue: 80 % Thermal Insulation

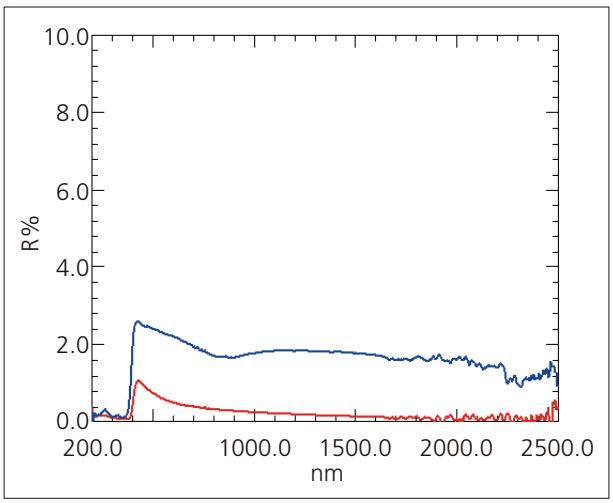

Fig. 11 Reflectance Spectra of Thermal Insulation Films
Red: 30 % Thermal Insulation,
Blue: 80 % Thermal Insulation

Table 2 Solar Transmittance/Reflectance and Visible Light Transmittance/Reflectance

Type	Properties	Solar Transmittance (%)	Visible Light Transmittance (%)	Solar Reflectance (%)	Visible Light Reflectance (%)
Curtain	Normal	50.66	50.34	48.44	49.64
	Designed for Natural Illumination	54.98	54.23	44.51	46.82
	Designed for Thermal Insulation	38.16	37.24	61.63	62.80
Shoji	Plastic	42.15	41.10	56.54	58.96
	Designed for Natural Illumination	44.28	43.03	54.50	56.76
	Designed for Thermal Insulation	21.30	20.15	75.14	79.02
Roller blind	Designed for Natural Illumination	34.92	34.52	62.52	64.23
	Designed for Light Shielding	0.01	0.00	69.10	83.97
Thermal Insulation Film	30 % Thermal Insulation	72.39	84.54	0.38	0.58
	80 % Thermal Insulation	14.31	18.02	1.91	2.27

The solar transmittance/reflectance and visual light transmittance/reflectance results calculated from spectra using solar transmittance software are shown in Table 2.* Comparing the samples, the transmittance of curtain is higher than shoji, but the reflectance of curtain is lower than shoji. The transmittance of roller blind is lower than both curtain and shoji, while the reflectance of roller blind is higher than both curtain and shoji. For the thermal insulation films, transmittance varies greatly depending on type, while reflectance is extremely low for all film types. There was no substantial difference between transmittance/reflectance in the visible light and near-infrared regions for curtains and shoji, but a difference between the visible light and near-infrared regions was observed in the reflectance of roller blinds designed for light shielding and the transmittance of thermal insulation film. Although these measurements are used as simple examples and do not produce defining characteristics for each sample material, they show that sample characteristics can be estimated based on spectral analysis and calculation of solar transmittance/reflectance.

Conclusion

Materials and products with energy-saving features are used all around us. The optical properties of these materials and products are described in JIS, and in this article we used a UV-3600 Plus with ISR-1503 attachment to measure the transmittance/reflectance spectra of commercially available curtains, shoji, roller blinds, and thermal insulation films. Using the ISR-1503 allowed us to obtain spectra with reduced steps between detectors. Using solar transmittance software also allowed us to calculate solar transmittance/reflectance based on the measurement results obtained. We anticipate that spectra and solar transmittance/reflectance data will be used to evaluate and check materials and products with improved functional features that will be developed in the future.

*: The solar transmittance software calculates solar transmittance/reflectance in the range of 300 nm to 2100 nm. Employing the user settings function in the software, it can also calculate solar transmittance/reflectance in the range of 300 nm to 2500 nm.

BACK TO CONTENTS

First Edition: Aug. 2016

SHIMADZU

Shimadzu Corporation

www.shimadzu.com/an/

SHIMADZU
Excellence in Science

Application News

No. A562

Spectrophotometric Analysis

Measurement Examples of Glass in Various Shapes

BACK TO CONTENTS

Around us there are a multitude of parts which are processed into various shapes to best fit their intended applications. As such, the need is increasing to be able to appropriately hold cylindrical samples and thin samples to achieve accurate measurements.

This article introduces examples of utilizing two sample holders which can meet the above needs: a cylindrical sample holder and a glass/film holder for the standard sample compartment.

K. Sobue

Evaluating Circular Glass

Fig. 1 shows the cylindrical sample holder. There are three types to the cylindrical sample holder, each capable of holding a sample size of ϕ5 to 25 mm (D25 mm), ϕ30 to 50 mm (D50 mm), and ϕ40 to 110 mm (D110 mm) respectively. By holding a sample at its periphery with springs, this holder is capable of holding a sample so that the incident beam strikes the center of the sample.

Four pieces of ϕ20-mm fused quartz with differing thicknesses were prepared for measurement. A D25 mm cylindrical sample holder and a light beam diagram unit were set on a spectrophotometer and the samples were measured using the conditions listed in Table 1. Fig. 2 shows the obtained transmittance spectra which indicate absorption at 1387 nm. Table 2 and Fig. 3 indicate the relationship between the sample thickness and the absorbance at 1387 nm. We can see from Fig. 3 that absorbance is proportional to the sample thickness.

Fig. 1 Cylindrical Sample Holders for D25 mm, D50 mm, and D110 mm Respectively (in order from front to back)

Table 1 Measurement Conditions

Instrument Used	: UV-3600 Plus, MPC-603A, Cylindrical sample holder (D25 mm), Light beam diaphragm unit
Wavelength Range	: 1000 nm to 1600 nm (fused quartz sample)
Scan Speed	: Low speed
Sampling Interval	: 1.0 nm
Slit Width	: (12) nm

Table 2 Relationship between Sample Thickness and Absorbance (Transmittance) at 1387 nm

Thickness	Absorbance (Abs)	Transmittance (%T)
1 mm	0.03	93.97
3 mm	0.04	91.36
5 mm	0.05	88.92

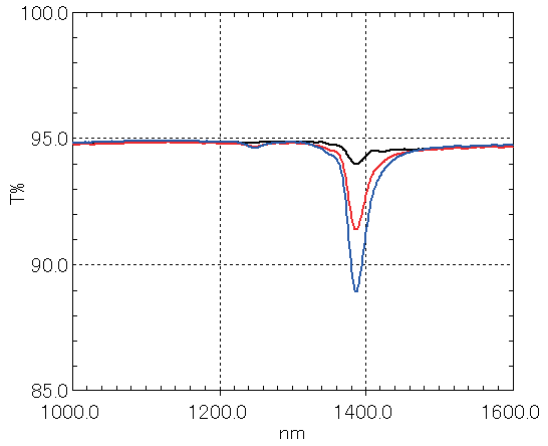

Fig. 2 Transmittance Spectra
Black: 1 mm, Red: 3 mm, Blue: 5 mm

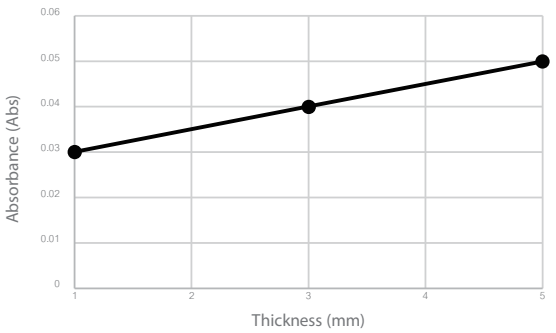

Fig. 3 Relationship between Sample Thickness and Absorbance at 1387 nm

Measurement Repeatability of a 15-mm Square Glass Sample

Fig. 4 shows the glass/film holder for the standard sample compartment. The holder is equipped with a grooved unit[*1] which enables precise holding of samples that are 15×15 mm (thickness: 1 mm) in size. Two types of 15-mm square glass plates (material: BK7 and quartz) were measured five times each by repositioning the sample for each measurement. Table 3 lists the measurement conditions and Figs. 5 and 6 show the measurement results.

Table 3 Measurement Conditions

Instrument Used	: UV-3600 Plus, Glass/film holder for standard sample compartment
Wavelength Range	: 300 nm to 800 nm (15-mm square sample) 500 nm to 1800 nm (anti-reflective coating sample)
Scan Speed	: Low speed
Sampling Interval	: 1.0 nm
Slit Width	: 2.0 nm (15-mm square sample) 5.0 nm (anti-reflective coating sample)
Detector Switching Wavelength	: 850/1650 nm
Grating Switching Wavelength	: 780 nm

BACK TO CONTENTS

Fig. 4 Glass/Film Holder for Standard Sample Compartment

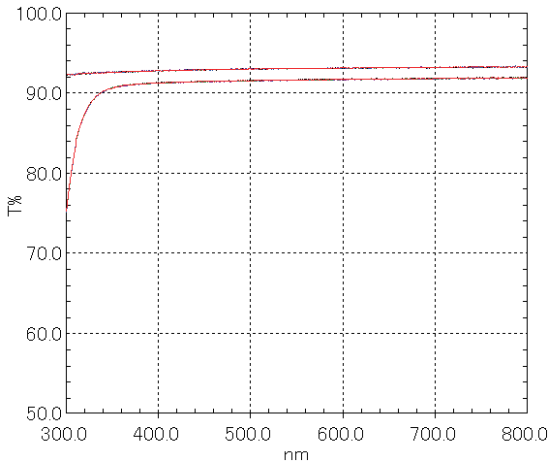

Fig. 5 Transmittance Spectra from Measurement by Repositioning Samples
Top: Quartz, Bottom: BK7
Black: 1st, Red: 2nd, Blue: 3rd, Green: 4th, Purple: 5th

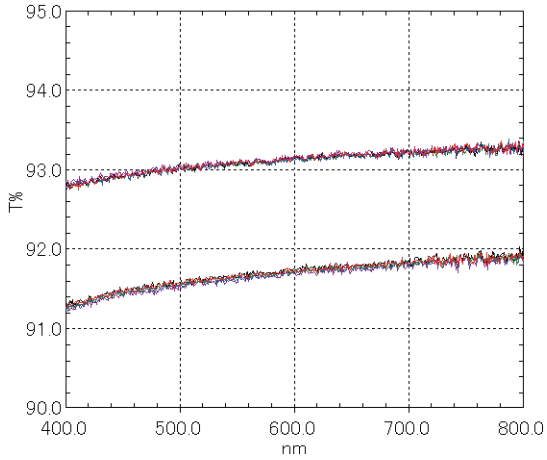

Fig. 6 Enlarged View of Fig. 5

Fig. 5 shows that when the glass material is BK7, transmittance is low in the ultraviolet range where wavelengths are shorter than 350 nm. When the glass material is quartz, transmittance is high at above 90 %T even in the ultraviolet range. Since both samples are set using the glass/film holder for the standard sample compartment, the repeatability of the spectra is favorable as shown in Fig. 6. Table 4 lists the photometric values obtained at 500 nm through the above measurements and the photometric values obtained at 500 nm by measuring the spectrum repeatedly without repositioning the sample. Both the average value and standard deviation are of the same level when the sample was repositioned and not repositioned.

Table 4 Repeatability of Transmittance at 500 nm

	BK7		Quartz	
	Repeat	Reposition	Repeat	Reposition
1st	91.499	91.563	93.053	93.026
2nd	91.503	91.550	93.072	93.041
3rd	91.519	91.531	93.085	93.028
4th	91.511	91.535	93.050	93.044
5th	91.511	91.510	93.077	93.049
Ave.	91.509	91.538	93.067	93.038
SD.	0.007	0.018	0.014	0.009

The glass/film holder for the standard sample compartment can also be used as an ordinary film holder. Fig. 7 shows the spectra obtained from a glass that is applied an anti-reflective coating (commercially available) using the conditions listed in Table 3. Anti-reflection is achieved by a dielectric multilayer film at 650 to 1050 nm and 750 to 1550 nm, and the transmittance in those ranges is near 100 %.

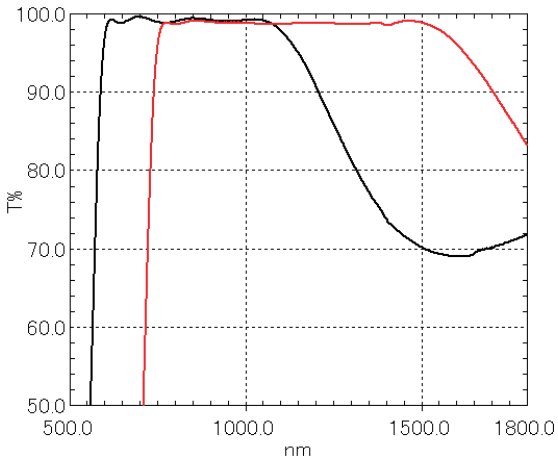

Fig. 7 Transmittance Spectra of Glass Sample with Anti-reflective Coating
Coating Wavelength Range
Black: 650 nm to 1050 nm, Red: 750 nm to 1550 nm

Conclusion

Measurement of a circular glass sample was done easily using the cylindrical sample holder which allowed to hold the sample centered with respect to the light beam. Also, the glass/film holder for the standard sample compartment enabled precise holding of a 15-mm square sample and data with favorable repeatability was obtained. Samples of various shapes and thickness can be held appropriately and measured with good precision by using accessories suitable for each specific sample.

*1 The size of the groove can be changed according to the size of the sample.

First Edition: Feb. 2018

Shimadzu Corporation
www.shimadzu.com/an/

SHIMADZU
Excellence in Science

Application News

No. A553

Spectrophotometric Analysis

Evaluation of Photonic Materials with Biomimetic Structural Coloration

BACK TO CONTENTS

Colors occur either as pigments that absorb certain colors while reflecting/scattering others or as structural coloration caused by microscopic structures. Many living things in the natural world produce this type of structural coloration that results in vivid colors, including morpho butterflies, peacocks, and jewel beetles. Biomimetics is gaining attention as a field that utilizes the functions and structures of these living things in the development of new technology and manufacturing processes by mimicking them.

In Application News No. A502, we confirmed the existence of structural coloration on a multi-layered film produced by mimicking the wing structure of morpho butterflies, in which the coloration was caused by interference.[1] The vivid colors observed on the wings of some birds are also structural coloration. For example, the structural coloration of peacock plumage is said to originate from the arrangement of melanin granules.[2] Michinari Kohri, Associate Professor at the Division of Applied Chemistry and Biotechnology at Chiba University's Graduate School of Engineering, has succeeded in producing highly visible structural coloration by controlling the size, blackness, refractive index, and arrangement of melanin-mimicking particles (PSt@PSA particles) created by coating the surface of polystyrene particles (PSt) with polydopamine (PDA), which is similar to melanin.[3]

This article introduces measurements of photonic materials with structural coloration performed in cooperation with Associate Professor Michinari Kohri.

K. Sobue, R. Fuji

Spectrum and Color Value Measurement of Samples

Fig. 1 shows an image of the samples captured from above. The samples on the left side were formed only from PSt particles. The diameter of PSt particles becomes smaller moving from the top row of samples to the bottom row. The samples down the center were thinly coated with PDA (iridescent) and the samples on the right side were thickly coated with PDA (non-iridescent). Differences in PSt particle diameter and PDA coating thickness change the colors that are visible. Fig. 2 shows an image of the samples captured at an angle. The color tone of the samples changes according to the viewing angle. Fig. 3 shows a conceptual diagram of a melanin-mimicking particle.

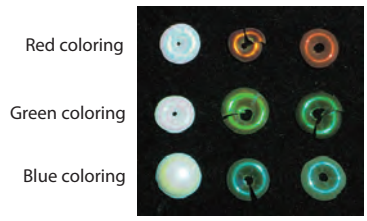

Fig. 1 Image of Samples Captured from Above

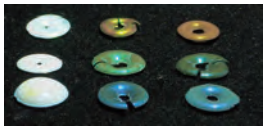

Fig. 2 Image of Samples Captured at an Angle

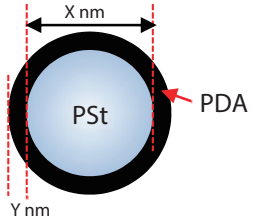

Fig. 3 Conceptual Diagram of a Melanin-Mimicking Particle
X: PSt Particle Diameter, Y: PDA Thickness

Fig. 4 shows inside the sample compartment of the SolidSpec-3700DUV with the variable angle absolute reflectance attachment installed. Use of the variable angle absolute reflectance attachment enables measurement with different angles of incident light with respect to the sample. For details on the variable angle absolute reflectance attachment, refer to Application News Nos. A390 and A394. Samples were set as shown in Fig. 4 and measurement was performed using the conditions listed in Table 1. Measurement was performed at incident angles of 5, 12, 30, and 45 degrees with the light beam reduced to a diameter of 1 mm by using the mask provided as an accessory with the SolidSpec-3700DUV.

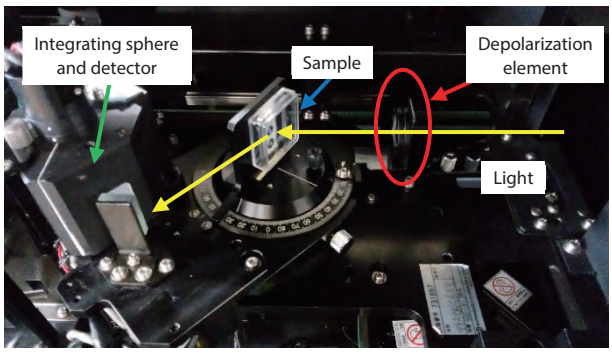

Fig. 4 Inside the Sample Compartment of the SolidSpec-3700DUV with the Variable Angle Absolute Reflectance Attachment Installed

Table 1 Measurement Conditions

Instrument	: SolidSpec-3700DUV, variable angle absolute reflectance attachment, quartz depolarizer *1
Measuring wavelength range	: 380 nm to 780 nm
Scan speed	: Low speed
Sampling interval	: 1.0 nm
Measurement light value	: Refractive index *2
Slit width	: 5 nm Light beam aperture mask ϕ1

*1: DEQ-2OP manufactured by SIGMAKOKI Co., Ltd. Produces artificially depolarized light.

*2: Since the refractive indices have mostly likely not been accurately measured due to the spherical shape of the samples, a.u. (arbitrary unit: unit for comparison as opposed to absolute values) was used as the reference value for the vertical axis.

BACK TO CONTENTS

Fig. 5 shows the reflectance spectra (5° incident angle) when the PSt particle diameter is constant and the PDA coating thickness is changed. We can see that a redshift occurs as the PDA thickness increases. Fig. 6 shows the color values calculated from the spectra plotted using commercially-available color analysis software. We can expect that as the PDA thickness increases, the color will shift from blue to green to yellow.

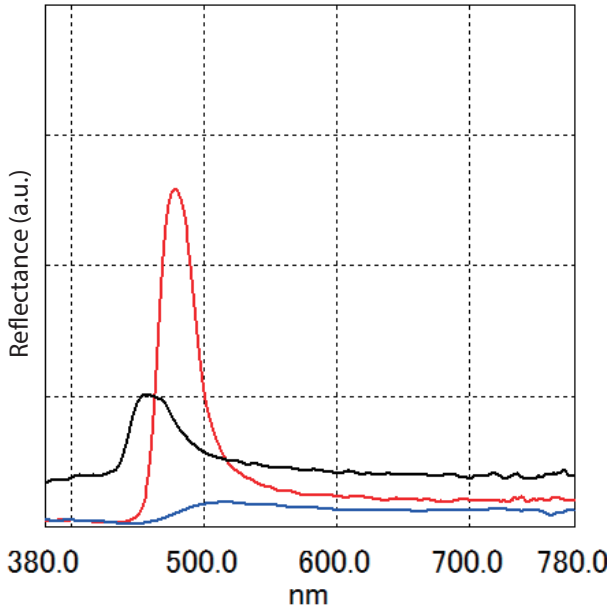

Fig. 5 Reflectance Spectra of Blue Coloring (5° Incident Angle)
Black: Uncoated PSt Particles,
Red: Thin PDA Coating (Iridescent),
Blue: Thick PDA Coating (Non-Iridescent)

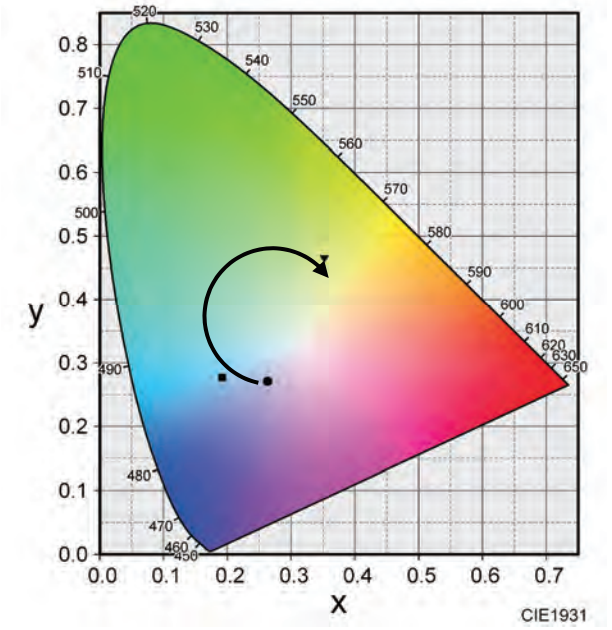

Fig. 6 Blue Coloring Color Values
Circle: Uncoated PSt Particles,
Square: Thin PDA Coating (Iridescent),
Triangle: Thick PDA Coating (Non-Iridescent)

Fig. 7 shows the reflectance spectra (5° incident angle) when only the PSt particle diameter is changed. A redshift occurs as the PSt particle diameter increases. Fig. 8 shows the reflectance spectra (5° incident angle) when each PSt particle sample is thinly coated with PDA. These cases also show the occurrence of a redshift.

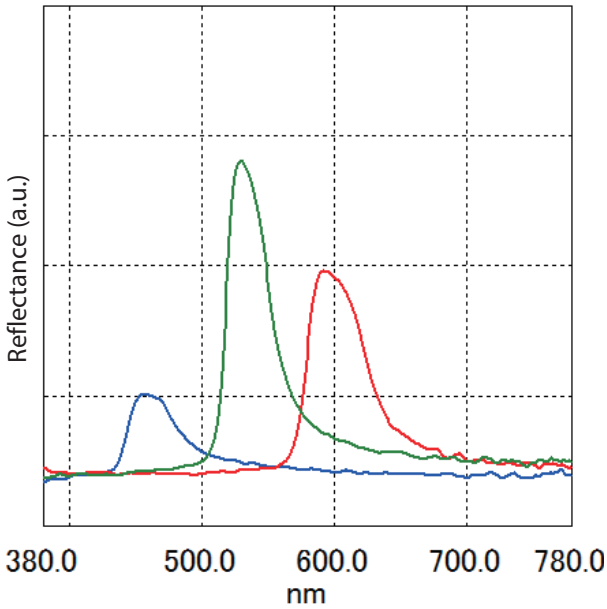

Fig. 7 Reflectance Spectra of PSt Particles with Differing Diameters (5° Incident Angle)
Blue: Blue Coloring (Uncoated PSt Particles),
Green: Green Coloring (Uncoated PSt Particles),
Red: Red Coloring (Uncoated PSt Particles)

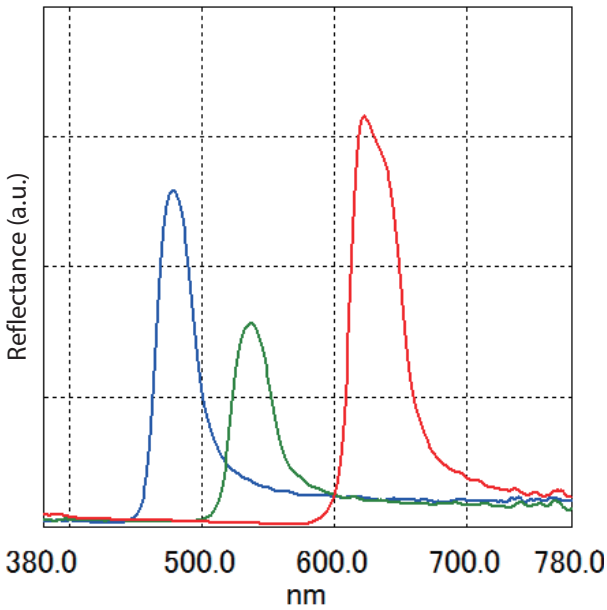

Fig. 8 Reflectance Spectra of PSt@PDA Particles with Thin PDA Coating (5° Incident Angle)
Blue: Blue Coloring (PSt@PDA Particles, Iridescent),
Green: Green Coloring (PSt@PDA Particles, Iridescent),
Red: Red Coloring (PSt@PDA Particles, Iridescent)

Fig. 9 shows the color values calculated from the spectra in Fig. 7 and Fig. 8 plotted using commercially-available color analysis software. This shows that the samples with PSt particles thinly coated with PDA exhibit a brighter color tone. Table 2 lists the color values and peak wavelength results.

Fig. 10 to Fig. 12 show the reflectance spectra resulting from light of differing incident angles striking the PSt@PDA particles thinly coated with PDA. A blueshift occurs as the incident angle increases for all of the samples. This is thought to be caused by incident angle differences in Bragg reflections.

Table 2 Color Values and Peak Wavelengths (5° Incident Angle)

Sample	x	y	Peak (nm)
Blue coloring (uncoated PSt particles)	0.263	0.271	454
Blue coloring (PSt@PDA particles, iridescent)	0.192	0.277	478
Blue coloring (PSt@PDA particles, non-iridescent)	0.352	0.466	517
Green coloring (uncoated PSt particles)	0.304	0.508	530
Red coloring (uncoated PSt particles)	0.447	0.359	593
Green coloring (PSt@PDA particles, iridescent)	0.323	0.612	536
Red coloring (PSt@PDA particles, iridescent)	0.647	0.298	624

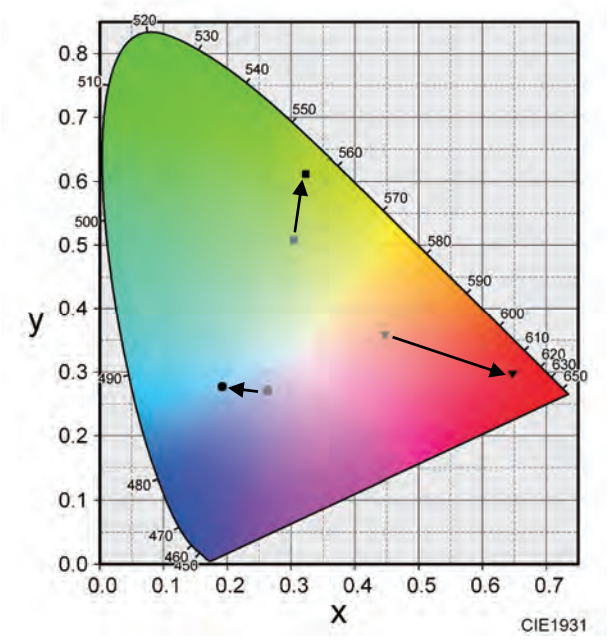

Fig. 9 Color Value Variation of Uncoated PSt Particles and PSt@PDA Particles (Iridescent)
Gray: Uncoated PSt Particles, Black: PSt@PDA Particles

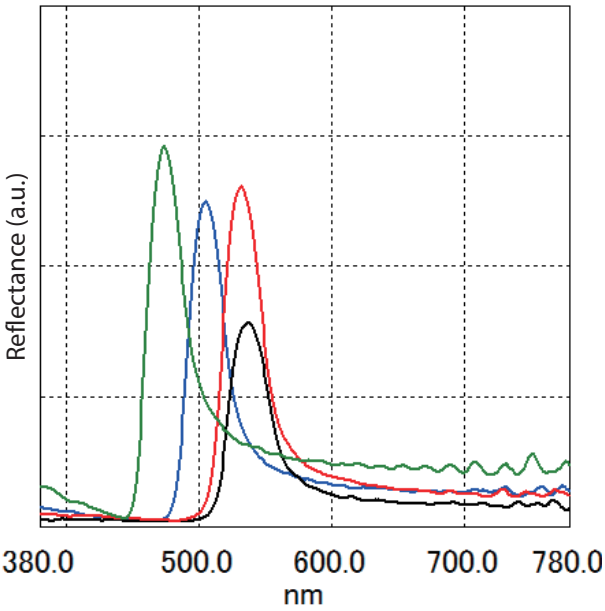

Fig. 11 Reflectance Spectra of Green Coloring (PSt@PDA, Iridescent)
Black: 5°, Red: 12°, Blue: 30°, Green: 45°

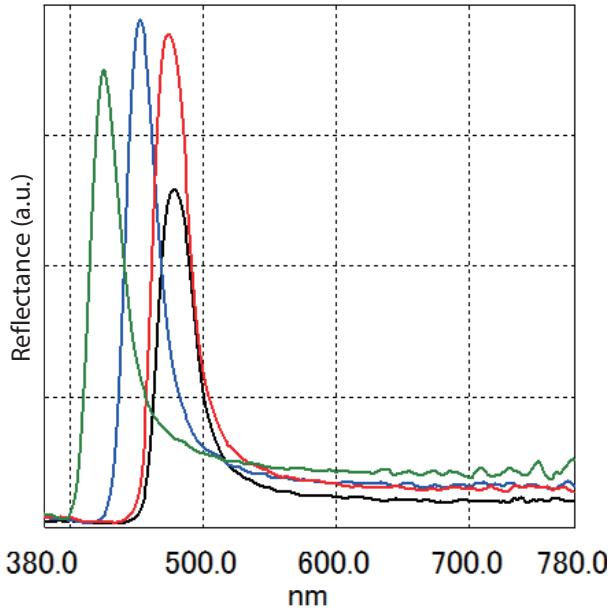

Fig. 10 Reflectance Spectra of Blue Coloring (PSt@PDA, Iridescent)
Black: 5°, Red: 12°, Blue: 30°, Green: 45°

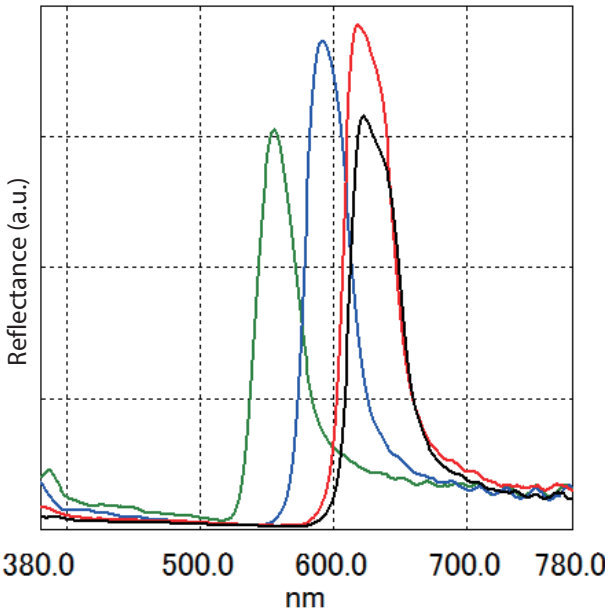

Fig. 12 Reflectance Spectra of Red Coloring (PSt@PDA, Iridescent)
Black: 5°, Red: 12°, Blue: 30°, Green: 45°

BACK TO CONTENTS

Observation of Particle Arrangement

Fig. 13 shows the SFT-4500 Nano Search Microscope that combines a laser microscope (LSM) and scanning probe microscope (SPM) to achieve high accuracy. The optical microscope and laser microscope were used to determine the observation position and the probe microscope was used to observe the arrangement of the green coloring particles. Fig. 14 to Fig. 16 show the 2D height images. The scanning range is 5.00 µm × 5.00 µm and the z range of the images is 300 nm. Fig. 14 and Fig. 15 show that the uncoated PSt particle sample and sample with a thin PDA coating have a regular arrangement of particles (colloidal crystal), whereas Fig. 16 shows that the sample with a thick PDA coating has an irregular arrangement of particles (amorphous structure). This difference in arrangement is considered to cause the differences in angular dependence and refractive index in the structural coloration of the samples.

Fig. 13 SFT-4500 Appearance

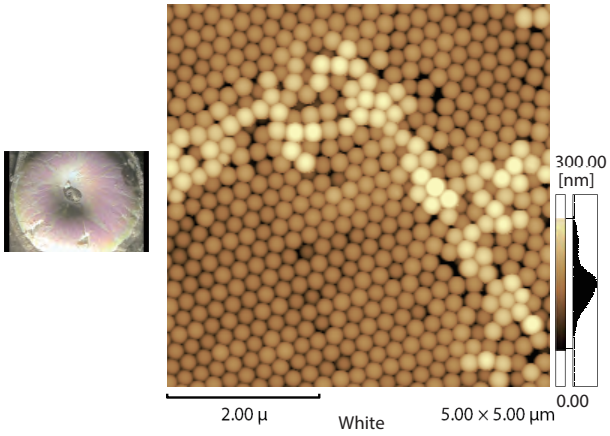

Fig. 14 Particle Arrangement of Green Coloring (Uncoated PSt Particles)

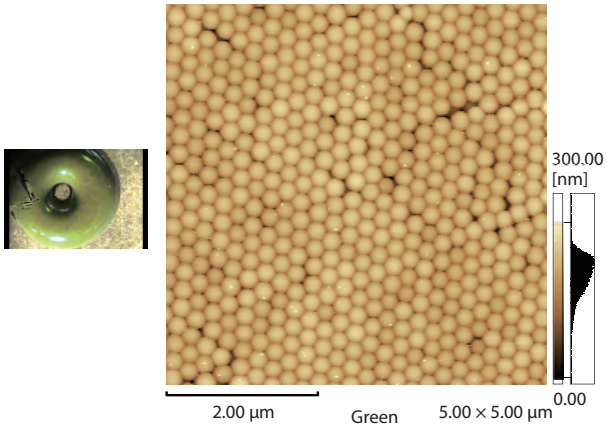

Fig. 15 Particle Arrangement of Green Coloring (PSt@PDA Particles, Iridescent)

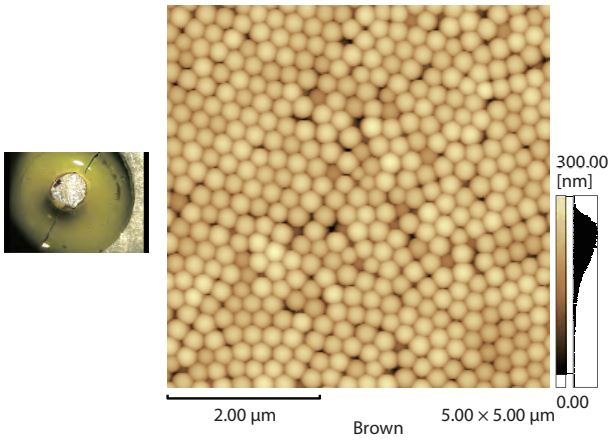

Fig. 16 Particle Arrangement of Green Coloring (PSt@PDA Particles, Non-Iridescent)

Conclusion

We conducted evaluation and observation of photonic materials with structural coloration using a spectrometer and the Nano Search Microscope. Using the spectrometer, we confirmed a shift in peak wavelength in the reflectance spectra that occurs according to the diameter of the PSt particles and the PDA coating thickness. We also confirmed a shift in peak wavelength in the reflectance spectra that occurs by changing the incident angle of light. Using the Nano Search Microscope, we confirmed a variation in particle arrangement that depends on the PDA coating thickness.

Since the color tone and angular dependence of structural coloration can be changed by controlling the size, blackness, refractive index, and arrangement of melanin-mimicking particles, it is expected this will lead to the development of ink materials with new types of color. The field of biomimetics is anticipated to allow manufacturing of efficient and environmentally-friendly materials such as these.

<Acknowledgments>
We would like to thank Associate Professor Michinari Kohri of the Division of Applied Chemistry and Biotechnology at Chiba University's Graduate School of Engineering for providing the samples used in these measurements and knowledge regarding biomimetics.

<References>
1) Shimadzu Corporation website
New World Opened Up by Biomimetics
http://www.shimadzu.com/csr/2016_f1.html
2) Yoshioka, S. & Kinoshita S, Effect of Macroscopic Structure in Iridescent Color of the Peacock Feathers, Forma, **17**, 169 (2002)
3) Kawamura, A., Kohri, M., Morimoto, G., Nannichi, Y., Taniguchi, T. & Kishikawa, K. Full-Color Biomimetics Photonic Materials with Iridescent and Non-Iridescent Structural Colors, Sci. Rep. **6**, 33984 (2016)

First Edition: Oct. 2017

Shimadzu Corporation
www.shimadzu.com/an/

SHIMADZU
Excellence in Science

Application News

No.A494

Spectrophotometric Analysis

Simplified Measurement of Coumarin in Diesel Oil

BACK TO CONTENTS

Introduction

In Japan, diesel oil is subject to a consumption tax (national tax) and a diesel oil delivery tax (regional tax). However, kerosene and low-sulfur / high-sulfur A fuel oil are not subject to the delivery tax. Therefore, to avoid the tax, some vendors have been known to sell fraudulent diesel oil that has been mixed with kerosene or fuel oil. As a countermeasure, starting in March 1991, the then Ministry of Trade and Industry required addition of a 1 ppm concentration of coumarin to commercial kerosene and low-sulfur / high-sulfur A fuel oil products, so that they can be easily identified. Consequently, local tax bureaus have been using this marker for inspecting diesel oil by random sampling. If coumarin is detected, it means kerosene or low-sulfur / high-sulfur A fuel oil was mixed in with the diesel oil and legal measures or other actions are taken against the violator.
Therefore, on December 10, 2010, the Japan Petroleum Institute (Testing and Analysis sub-committee of the Product committee) established standard JPI-5S-71-2010 as the official method for analyzing coumarin. In this example, we used Method A of the standard to measure the fluorescence spectrum of coumarin.

Analytical Procedure

The procedure for analyzing coumarin is summarized below and a photograph of the RF-6000 spectrofluorophotometer used to identify the coumarin diesel oil marker substance is shown in Fig. 1. Equipment and reagents required for the analysis are listed in Table 1.

Analytical Procedure

(1) Prepare various solutions.
(2) Prepare a standard sample for creating a calibration curve.
(3) Prepare sample for quantitative analysis.
(4) Shake and isomerize (UV irradiation).
(5) Prepare calibration curve.
(6) Measure unknown sample.

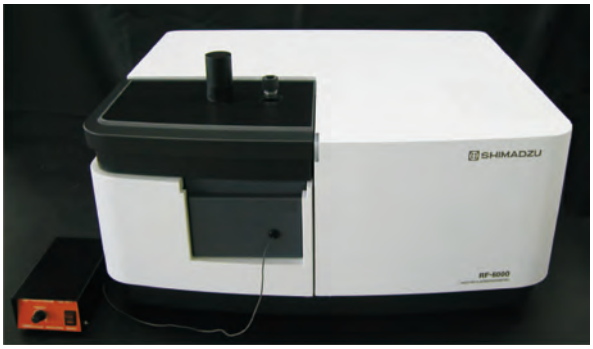

Fig. 1 RF-6000 Spectrofluorophotometer Coumarin (Diesel Oil Marker) Identification System

Table 1 Equipment and Reagents Required for Coumarin Analysis

(1)	RF-6000 spectrofluorophotometer system
(2)	Coumarin analysis kit (test tube holder with stirrer)
(3)	Dedicated coumarin measurement test tube (with stirrer)
(4)	Volumetric flasks (100 mL, 200 mL, and 500 mL)
(5)	Volumetric pipettes (1 mL, 2 mL, 5 mL, 6 mL, 8 mL, and 10 mL)
(6)	Measuring pipettes (0.5 mL, 1 mL, 2 mL, and 10 mL)
(7)	Test tube stand for 23 mm diameter tubes
(8)	Disposable gloves
(9)	Coumarin
(10)	Toluene
(11)	n-Dodecane
(12)	Sodium hydroxide and sodium nitrate for preparing alkaline aqueous solutions
(13)	1-Butanol and ethanol reagents for preparing alcohol solutions

Note: Items (9), (12), and (13) can be substituted with the Shimadzu RF Quantitation Reagent Kit.
A test tube shaker would also be helpful.

BACK TO CONTENTS

Preparing Solutions

Prepare each solution according to steps (a) to (e) below.

(a) Coumarin standard stock solution (10,000 mg/L)
(Can be stored for 3 months in a sealed container in a cool dark location)
Accurately weigh 1.0 ±0.005 g of coumarin into a 100 mL volumetric flask and fill to volume with toluene.

(b) Coumarin standard solution (100 mg/L)
Measure 5 mL of the coumarin standard stock solution (a) with a volmetric pipette and place it in a 500 mL volumetric flask. Then fill to volume with n-dodecane.

(c) Coumarin standard solution (1 mg/L)
Measure 5 mL of coumarin standard solution (b) with a volmetric pipette and place it in a 500 mL volumetric flask. Then fill to volume with n-dodecane.

(d) Alkaline aqueous solution (can be stored sealed for 1 month in a cool dark location)
Weigh 10 ±0.1 g sodium hydroxide and 20 ±0.1 g sodium nitrate and place them in a 100 mL volumetric flask. Then fill to volume with water.

(e) Alcohol solution (can be stored sealed for 1 month in a cool dark location)
Mix 80 mL 1-butanol and 60 mL ethanol.

Preparing Measurement Samples and Standard Samples for Creating a Calibration Curve

Insert stirrers in five test tubes used for creating the calibration curve. Then dispense the solutions indicated in Table 2. Prepare the measurement sample by inserting the stirrer in the test tube and then dispensing 1 mL of the measurement sample, 6 mL n-dodecane, 5 mL alkaline aqueous solution, and 8 mL alcohol solution.

Shaking and Isomerization

Install each test tube in the shaker and shake for three minutes at 240 rpm or faster. If a shaker is not available, shake by hand. Let stand for five minutes after shaking. Then confirm that the contents have separated into three layers, as shown in Fig. 2. From the top, these layers are the dodecane, alcohol solution, and alkaline aqueous solution layers.

Next, place the test tubes in the cell holder of the RF-6000 spectrofluorophotometer coumarin diesel oil marker identification system. Isomerize the coumarin by irradiating with 360 nm UV excitation wavelength (10 nm bandwidth) for three minutes while stirring with the stirrer. The isomerization progress can be checked by setting the fluorescence wavelength to 500 nm (10 nm bandwidth) and confirming the change in fluorescence intensity over time. Analytical conditions are indicated in Table 3. A time-course graph is shown in Fig. 3, with elapsed time on the horizontal axis and fluorescence intensity on the vertical axis. Irradiating samples with UV light causes the fluorescence intensity to increase with elapsed time. When the fluorescence intensity becomes constant isomerization is considered stabilized.

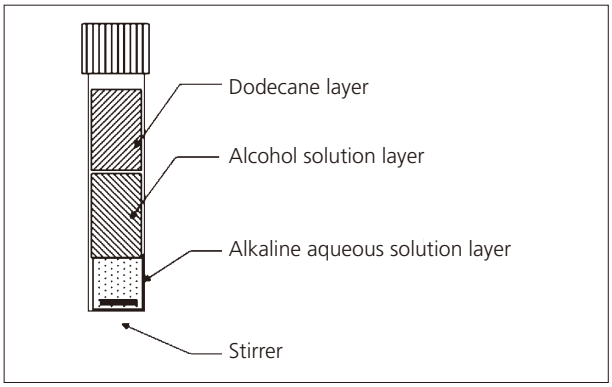

Fig. 2 Diagram of Test Tube Contents Separated into Three layers

Table 3 Analytical Conditions

Measurement mode	: Time course
Excitation wavelength	: 360 nm
Emission wavelength	: 500 nm
Bandwidth	: Ex: 10 nm, Em: 10 nm

Table 2 Preparing Standard Samples for Creating Calibration Curve

Types of Calibration Curves	Mixture Ratio (%)	0.0	10.0	40.0	80.0	120.0
	Coumarin Content (mg/L)	0.00	0.10	0.40	0.80	1.20
Reagent Acquisition Quantity (mL)	Coumarin Standard Solution (1.0 mg/L)	0	0.10	0.40	0.80	1.20
	n-Dodecane	7.0	6.9	6.6	6.2	5.8
	Alkaline Aqueous Solution	5.0	5.0	5.0	5.0	5.0
	Alcohol Solution	8.0	8.0	8.0	8.0	8.0

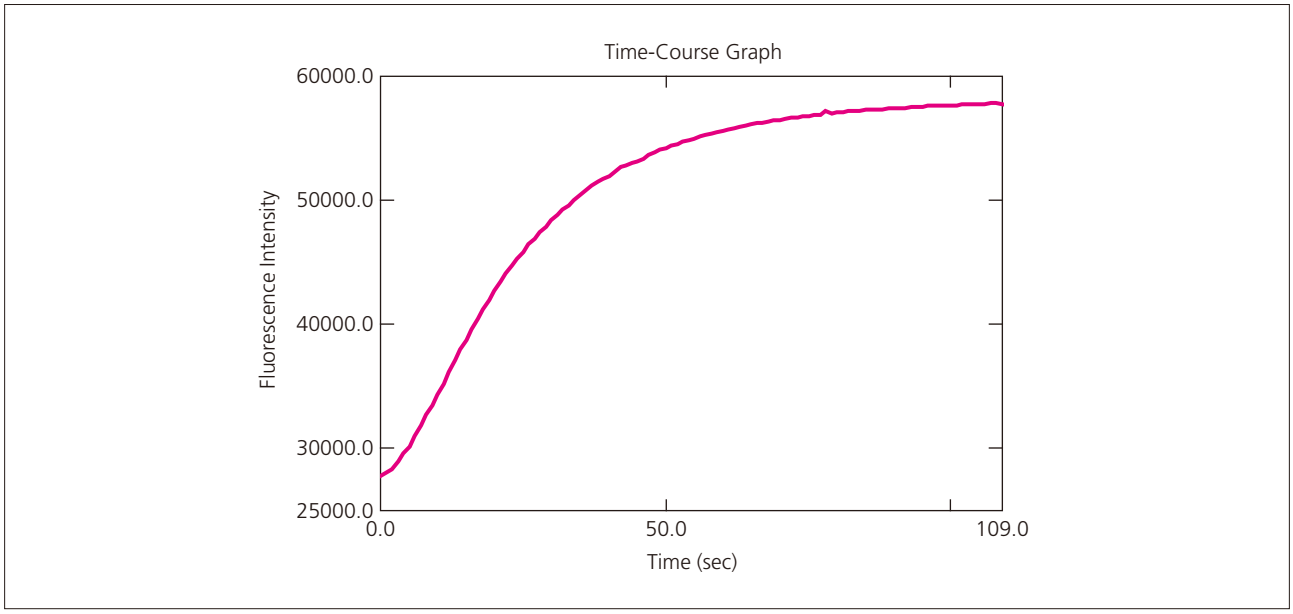

Fig. 3 Change in Fluorescence Intensity Due to Coumarin Isomerization

Isomerization Reaction of Coumarin

In an alkaline solution, coumarin breaks down by hydrolysis to form *cis*-*o*-hydroxycinnamic acid. If additionally irradiated with UV rays, it is isomerized to form *trans*-*o*-hydroxycinnamic acid. The structure of these isomers are shown in Fig. 4. When coumarin changes to *trans*-*o*-hydroxycinnamic acid, it emits fluorescent light. Coumarin can be quantitated by measuring the associated fluorescence intensity.

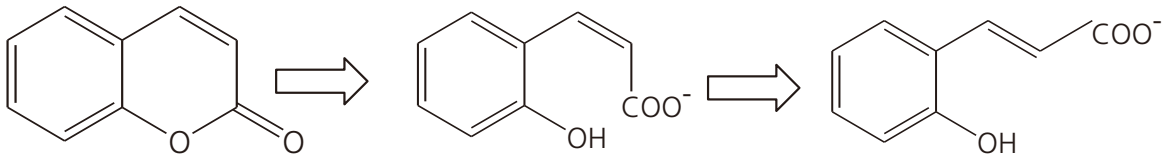

Coumarin *Cis*-*o*-hydroxycinnamic acid *Trans*-*o*-hydroxycinnamic acid

Fig. 4 Isomerization Reaction of Coumarin

Preparing a Calibration Curve and Measuring Coumarin Added to Diesel Oil

After irradiation with UV light, samples are measured using the analytical conditions indicated in Table 4. The fluorescence spectrum measured from the standard sample is shown in Fig. 5. The calibration curve is shown in Fig. 6. The squared correlation coefficient of the calibration curve, r^2, was 0.99965.

Results from measuring the measurement sample prepared by adding 0.5 ppm coumarin to commercial diesel oil are shown in Table 5. The quantitative results were approximately equivalent to the added quantity.

Table 4 Analytical Conditions

Excitation wavelength	: 360 nm
Emission wavelength	: 500 nm (390 to 630 nm when scanning spectra)
Bandwidth	: EX: 10 nm, EM: 10 nm

BACK TO CONTENTS

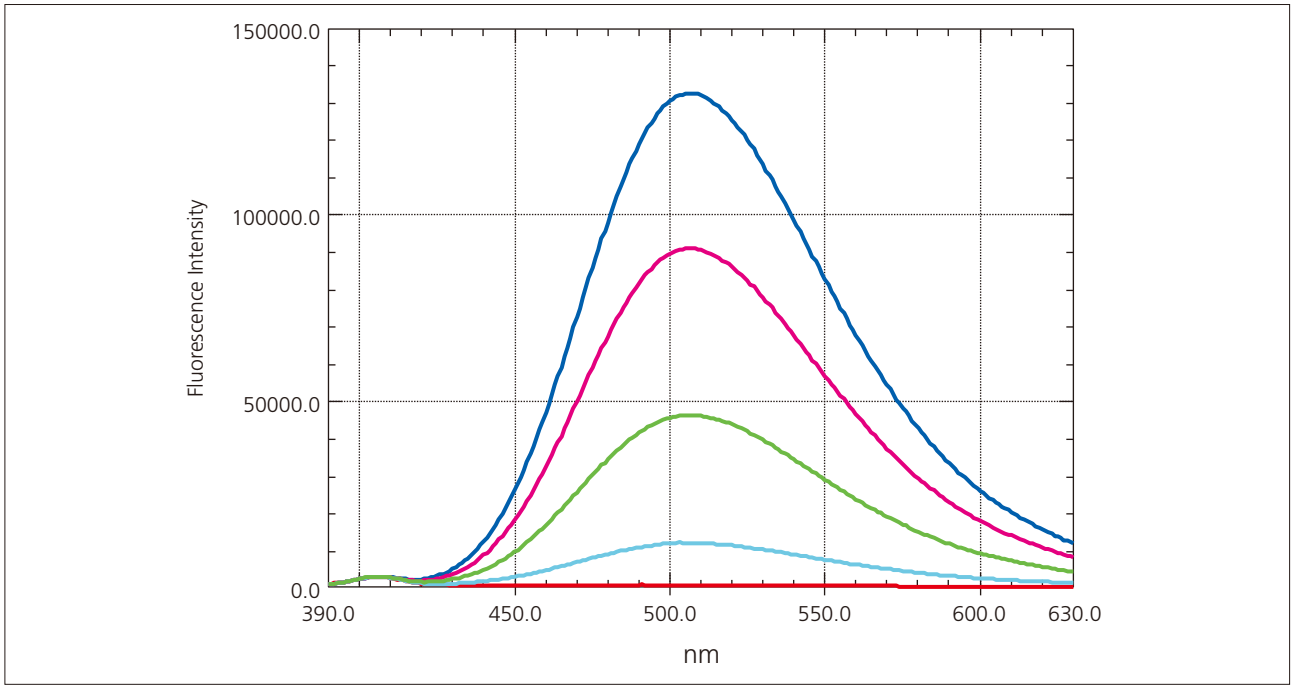

Fig. 5 Fluorescence Spectra of Standard Samples
In order of fluorescence intensity, with the highest intensity first, the corresponding concentrations are 1.2 ppm, 0.8 ppm, 0.4 ppm, 0.1 ppm, and 0 ppm.

	Sample Name	Concentration (ppm)	Fluorescence Intensity (500 nm)
1	0 ppm	0	470
2	0.1 ppm	0.1	11603
3	0.4 ppm	0.4	45767
4	0.8 ppm	0.8	90144
5	1.2 ppm	1.2	131583

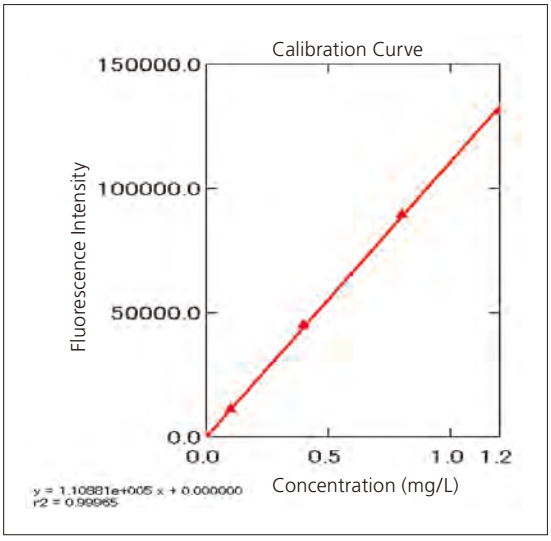

Fig. 6 Calibration Curve

Table 5 Measurement Results for Coumarin Added to Diesel Oil

Quantity Added (ppm)	Fluorescence Intensity	Measurement Result (ppm)
0.50	57440	0.514

Conclusion

This example showed that the Shimadzu RF-6000 spectrofluorophotometer can be used to easily and accurately measure coumarin according to Method A of the standard specified by the Japan Petroleum Institute.

First Edition: Oct. 2015

SHIMADZU
Shimadzu Corporation
www.shimadzu.com/an/

SHIMADZU
Excellence in Science

Application News

No.A497

Spectrophotometric Analysis

Measurement of Emission Spectra of LED Light Bulbs

BACK TO CONTENTS

Light sources that emit visible light, such as fluorescent lamps and LED light bulbs, have specific emission spectra. The hue of the light emitted by these light sources is determined by what extent to which different wavelengths of light are emitted. When a light source such as a light bulb is developed, measuring the emission spectra of the light source is very important for examining what kind of light the light source emits.
Emission spectra are usually measured with a UV-visible spectrophotometer (UV) or a spectrofluorophotometer (RF). When a UV instrument is used, the emission spectra that are measured incorporate some characteristics of the measurement instrument (instrument function), and are different spectra to those actually observed by a person. Shimadzu's RF-6000 spectrofluorophotometer system includes a function that automatically removes this instrument function (an automatic spectrum correction function). Therefore, using the RF-6000 allows for acquisition of accurate emission spectra that are not affected by the instrument function.
In this article, we present measurements of emission spectra of LED light bulbs using the RF-6000.

LED Light Bulbs

We measured commercially available LED light bulbs. We obtained eight bulbs in total, four different warm white color bulbs (A to D) and four different daylight white color bulbs (E to H), with each bulb in each group being from a different manufacturer. Warm white bulb A and daylight white bulb E are shown in Fig. 1, for example. The warm white color bulb has a yellowish hue, and the daylight white color bulb is white without any hue.
Fig. 2 shows the sample compartment of the RF-6000. LED light bulbs were fixed in place in a light bulb socket, connected to an external power source by routing the power cord through a hole in the lid of the sample compartment. Seven layers of mesh filter (wire mesh) were placed in front of the spectrofluorophotometer inlet port to reduce the intensity of the light from the LED bulbs. A blackout cloth was laid on top of the instrument as shown in Fig. 3 to ensure no external light entered the instrument during measurement.
There was no need to illuminate the sample with excitation light since the sample itself was the light emitter. For this reason, the shutter on the excitation light side was shut so no excitation light could incident onto the light bulb, and so only light emitted by the LED bulb was measured by the spectrofluorophotometer. The RF-6000 has a large sample compartment that allowed light bulbs to be installed inside the compartment without other adjustments.

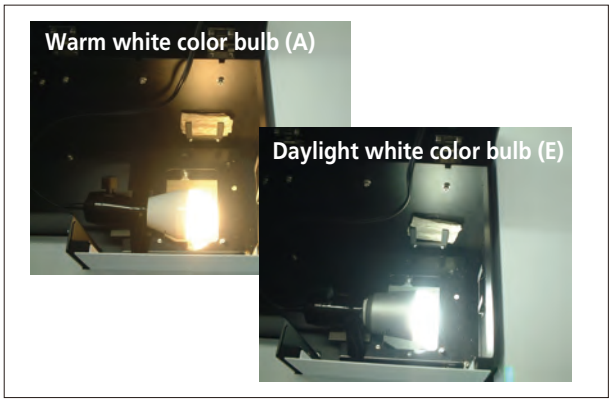

Fig. 1 LED Light Bulbs

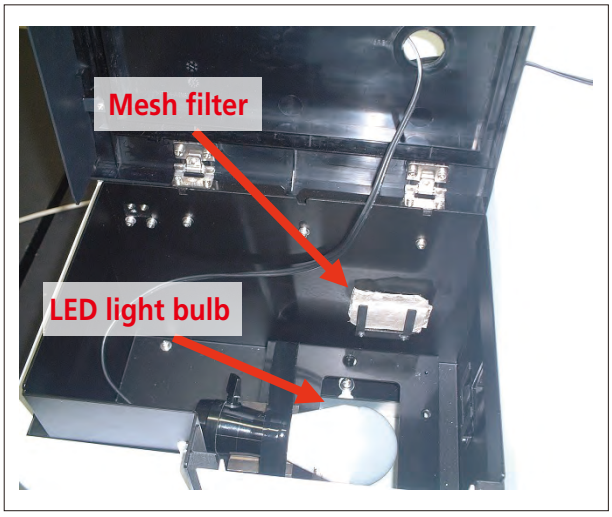

Fig. 2 LED Light Bulb Installed in the Sample Compartment

Fig. 3 Measurements with Sample Compartment Covered with Blackout Cloth

BACK TO CONTENTS

Measurement of Emission Spectra of LED Light Bulbs

The emission spectra of the warm white color bulbs and daylight white color bulbs measured under the conditions described in Table 1 are shown in Fig. 4 and Fig. 5, respectively. Measurements were taken twice while leaving the sample installed in the sample compartment. Fig. 4 shows that the high intensity of visible light emitted from the warm white color LED bulbs occurred in the green band (500 to 600 nm) and the red band (600 to 700 nm), showing that the yellowish hue emitted from the warm white bulbs was a mixture of light in these green and red bands. Fig. 5 shows that for the daylight white color LED bulbs the area under the graph is approximately equal across blue (400 to 500 nm), green, and red bands of light, and the hueless white light emitted from the daylight white bulb was a mixture of these bands. Fig. 4 and Fig. 5 also show that there are differences in peak wavelength and peak profile even between the LED light bulbs of the same color type. This demonstrates that different LED light bulb products of the same color type emit slightly different colors.

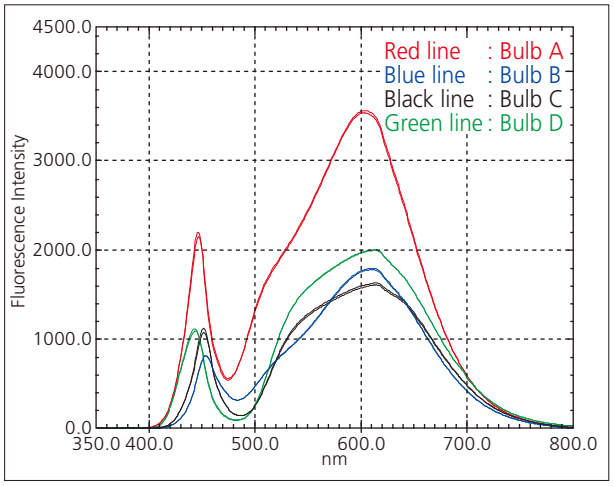

Fig. 4 Emission Spectra of Warm White Color Bulbs

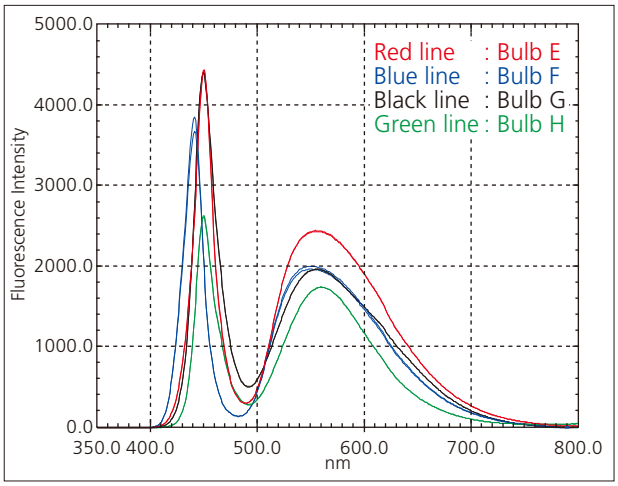

Fig. 5 Emission Spectra of Daylight White Color Bulbs

Table 1 Analytical Conditions

Measuring Instrument	: RF-6000 spectrofluorophotometer
Spectrum Type	: Emission spectrum
Excitation Wavelength	: 350 nm
Measured Wavelength Range	: 350 nm to 800 nm
Data Interval	: 1.0 nm
Scanning Speed	: 600 nm/min
Bandwidth	: Ex 5 nm, Em 5 nm
Sensitivity	: Auto

Comparison of Corrected Spectrum and Uncorrected Spectrum

The RF-6000 records the corrected spectrum after removing the instrument function as well as the uncorrected spectrum without the instrument function removed. Fig. 6 shows a comparison of the corrected spectrum and the uncorrected spectrum measured from a warm white color light bulb (sample A). This comparison shows the large discrepancy between the corrected spectrum and the uncorrected spectrum. A corrected spectrum is needed to be able to understand the correct status of light emission.

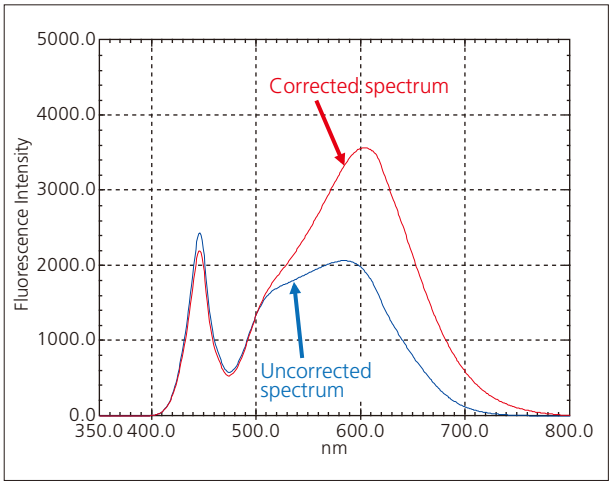

Fig. 6 Corrected Spectrum and Uncorrected Spectrum of Warm White Color Bulb (Sample A)

Conclusion

The RF-6000 has a large sample compartment that allows large samples such as light sources to be installed inside the compartment without other adjustments. The RF-6000 also has an automatic spectrum correction function that allows for automatic acquisition of measured spectra with the instrument function removed. The RF-6000 enables the collection of accurate emission spectra from light sources including LED light bulbs.

First Edition: Oct. 2015

SHIMADZU

Shimadzu Corporation

www.shimadzu.com/an/

SHIMADZU
Excellence in Science

Application News

No.A516

Spectrophotometric Analysis

Fluorescence Measurement of Organic Electroluminescent Material

BACK TO CONTENTS

Screens, lighting, and other products that incorporate organic electroluminescent (EL) materials are being developed on a daily basis in the electrical and electronic goods sector. Organic EL material development involves the synthesis of new substances and verification of their optical properties using photoluminescence (PL) technique. Researching the PL allows us to find materials that emit light with high efficiency, and we can elucidate the mechanism of its fluorescence in solution. Organic EL materials are developed through this process to meet specific criteria that can include hue, low energy consumption, or high luminous efficiency.
In order to evaluate organic EL materials, fluorescence must be measured quickly and accurately over a wide range of wavelengths.
Introduced here are the measurements of porphyrin solution (solvent: chloroform), an organic EL material, using an RF-6000 spectrofluorophotometer, with the help of the Institute for Basic Science, Pohang University of Science and Technology (POSTECH), South Korea.

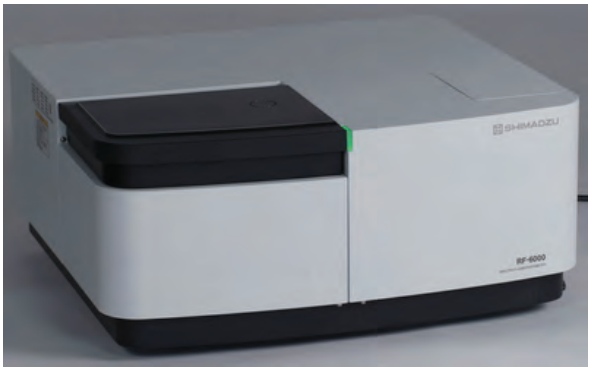

Fig. 1 RF-6000 Spectrofluorophotometer

Three-Dimensional (3D) Spectra Measurement

Fig. 1 shows the RF-6000. To first verify which fluorescence wavelength(s) appear at which excitation wavelength(s), the 3D spectra of porphyrin solution were measured using the analytical conditions shown in Table 1.
Fig. 2 shows the 3D spectra obtained, with excitation wavelength (Ex) is shown on the vertical axis, fluorescence wavelength (Em) is shown on the horizontal axis, and fluorescence intensity represented by different colors. The RF-6000 performs spectral correction in real time, allowing for the acquisition of corrected spectra with the factors due to instrument characteristics removed as soon as sample analysis is complete. Intense fluorescence of the analyzed sample was observed at around Em 660 nm and Em 720 nm. This fluorescence appeared at many excitation wavelengths, though results show the strongest fluorescence appeared at Ex 390 nm, followed by Ex 520 nm.

Table 1 Measurement Conditions

Instrument used	: RF-6000
Spectrum Type	: 3D spectrum
Measured Wavelength Range	: Ex 300-600 nm, Em 500-800 nm
Scanning Speed	: 6000 nm/min
Wavelength Interval	: Ex 10.0 nm, Em 2.0 nm
Bandwidth	: Ex 5.0 nm, Em 5.0 nm
Sensitivity	: Low
Measurement Time	: Approximately 2 minutes

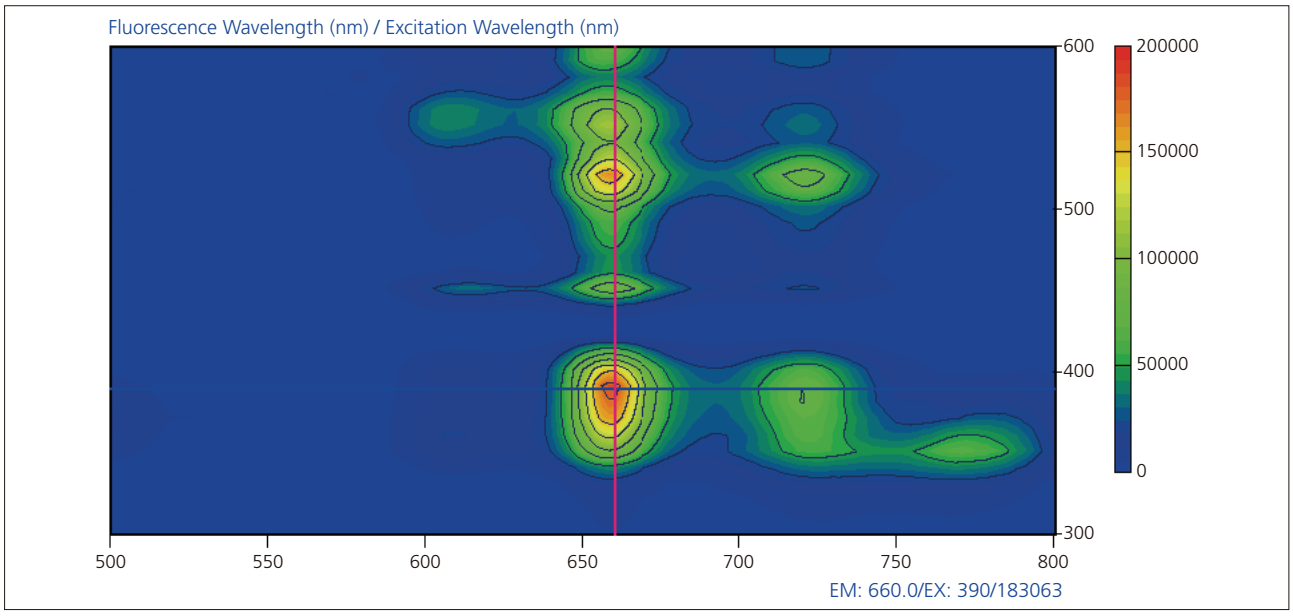

Fig. 2 Three-Dimensional Spectra of Porphyrin

Fluorescence Spectra Measured at Different Excitation Wavelengths

The 3D spectra in Fig. 2 shows fluorescence peaks at multiple excitation wavelengths. To observe fluorescence peaks in more detail, fluorescence spectra measurements were performed using the conditions in Table 2.
Fig. 3 shows fluorescence spectra at various excitation wavelengths, and that fluorescence peaks at 658 nm and 720 nm are present for all excitation wavelengths used. Fig. 3 also shows that the 658 nm fluorescence peak appears strongest at an excitation wavelength of 390 nm, and the 720 nm fluorescence peak appears strongest at an excitation wavelength of 520 nm.

Table 2 Measurement Conditions

Instrument used	: RF-6000
Spectrum Type	: Fluorescence spectrum
Measured Wavelength Range	: 390/420/520 nm for Ex, Ex to 800 nm for Em
Scanning Speed	: 200 nm/min
Wavelength Interval	: 1.0 nm
Bandwidth	: Ex 5.0 nm, Em 5.0 nm
Sensitivity	: Low

Conclusion

As the development of various organic EL materials continues, there will be a demand for spectra of higher sensitivity over a broader wavelength range to use in organic EL material evaluation. The RF-6000 is able to acquire 3D spectra quickly and accurately, and simultaneously acquire spectra with high sensitivity up to 900 nm. Using an optional integrating sphere with the RF-6000 also allows the measurement of quantum efficiency (absolute quantum yield).
In this study, using the RF-6000 spectrofluorophotometer, we successfully verified the 3D spectra and fluorescence spectra of an organic EL material.

<Acknowledgments>
The sample used in these measurements was provided by Professor Kyeng Park, the Institute for Basic Science, Pohang University of Science and Technology, South Korea. We are sincerely grateful to Professor Park for his help.

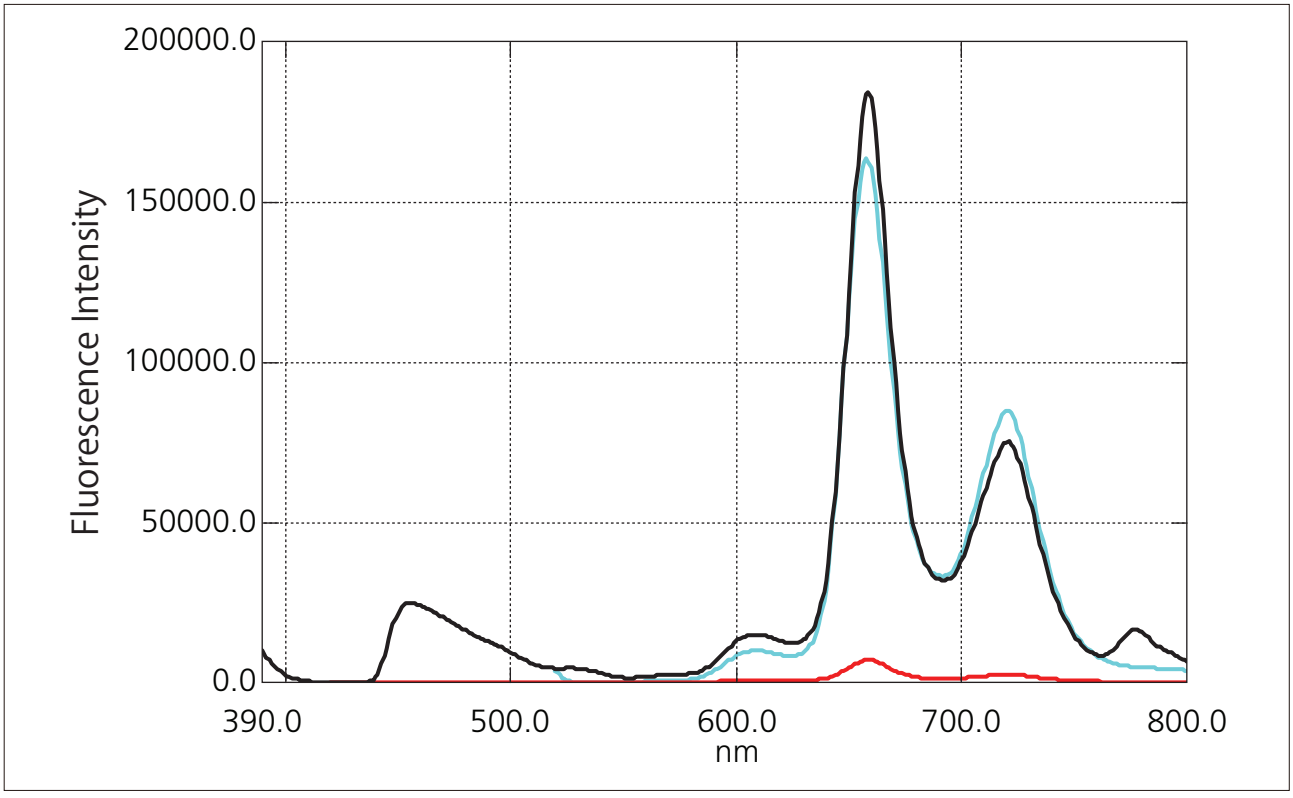

Fig. 3 Fluorescence Spectra of Porphyrin
Black line: Ex 390 nm, Red line: Ex 420 nm, Blue line: Ex 520 nm

First Edition: Oct. 2016

Shimadzu Corporation
www.shimadzu.com/an/

BACK TO CONTENTS

SHIMADZU
Excellence in Science

Application News

No. A561

Spectrophotometric Analysis

Light Emission Measurement at Low Temperature - Utilizing the Low-temperature Measurement Unit -

BACK TO CONTENTS

Light emission such as fluorescence occurs at transitions from the excited state to the ground state. The efficiency (η) of such emissions is expressed by the following equation based on the ratio of radiative transitions (W_R) and non-radiative transitions (W_{NR}).

$$\eta = W_R / (W_R + W_{NR})$$

Transitions from the excited state are greatly affected by the surrounding environment and heat has a substantial influence on emissions. Greater influences from heat increase non-radiative transitions, which in turn lowers emission efficiency and results in lower emission intensities. Therefore, to avoid the influence of heat, many measurements are done by lowering the sample temperature such as by using liquid nitrogen.

This article introduces measurements of liquid and powder samples cooled down to liquid nitrogen temperature (77 K) using a low-temperature measurement unit[*1] combined with the RF-6000 spectrofluorophotometer.

K. Sobue

Low-temperature Measurement of Liquid

Fig. 1 shows a cross-section of the low-temperature measurement unit. The low-temperature measurement unit holds a Dewar vessel in the sample chamber. The vessel is filled with liquid nitrogen and by setting a sample rod containing the sample in the vessel, the sample is cooled down to about liquid nitrogen temperature (77 K). As shown in Fig. 2, an observation window is designed on the front side of the sample chamber for sample observation, allowing operators to visually check if the sample is being irradiated with excitation light, or if the sample is emitting light.

Figs. 3 and Figs. 4 show the results of measuring naphthalene solutions (solvent: ethanol) with two differing concentrations (1.0×10^{-5} mol/L and 5.0×10^{-5} mol/L) at room temperature (300 K) and at liquid nitrogen temperature (77 K). The measurement conditions are listed in Table 1.

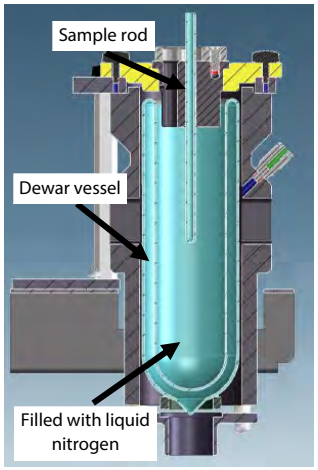

Fig. 1 Cross-section of the Low-temperature Measurement Unit

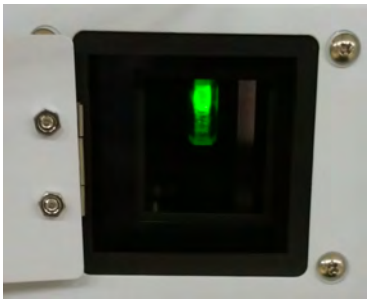

Fig. 2 The Sample Chamber from the Observation Window (Excitation light irradiated)

Table 1 Measurement Conditions

Instrument	: RF-6000, low-temperature measurement unit
Excitation Wavelength	: 275 nm
Measurement Wavelength Range	: 290 nm to 530 nm
Scan Speed	: 200 nm/min
Data Interval	: 1.0 nm
Bandwidth	: Ex 3.0 nm, Em 5.0 nm
Sensitivity	: Low

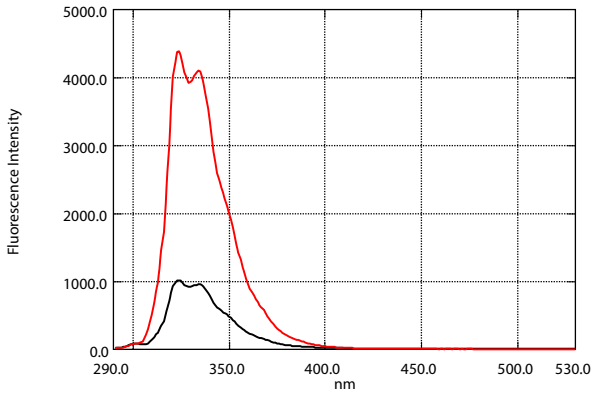

Fig. 3 Spectra at Room Temperature (300 K) Black: 1.0×10^{-5} mol/L, Red: 5.0×10^{-5} mol/L

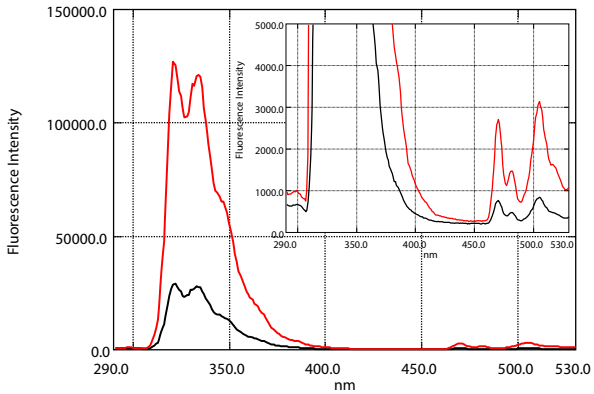

Fig. 4 Spectra at Liquid Nitrogen Temperature (77 K) Black: 1.0×10^{-5} mol/L, Red: 5.0×10^{-5} mol/L

Since the emission efficiency increased with the measurement at low temperature, signals were detected in the long-wavelength range near 500 nm in addition to the peaks near 325 nm and 335 nm which were observed at room temperature.

Fig. 5 shows the view from the observation window of the sample being irradiated with excitation light and the same view about one second after closing the shutter. Emission with a long lifetime (phosphorescence) can also be observed.

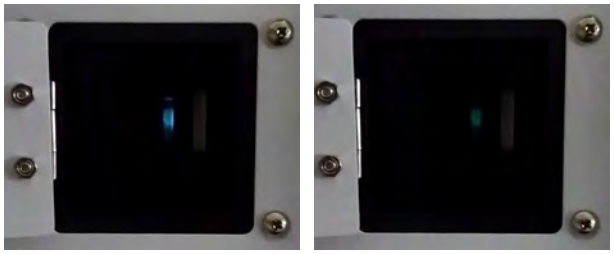

Fig. 5 Left: With Excitation Light Irradiation, Right: About One Second after Closing the Shutter

Low-temperature Measurement of Powder

Fig. 6 shows a sample rod for low-temperature measurement of powder or minute amounts of liquid. Composed of three acrylic plates, the sample is filled in a space 1-mm thick. The sample is cooled by immersing the projection on the right side of the rod (shown in Fig. 6) in liquid nitrogen, thereby allowing low-temperature measurement.

Fig. 7 shows the results of measuring benzophenone powder at room temperature (300 K) and at liquid nitrogen temperature (77 K). The measurement conditions are listed in Table 2.

Compared to room temperature, the low-temperature measurement yielded more sharp signals. This can expected to be because whereas there is an energy deactivation process relating to heat at room temperature, the process decreases at low temperature.

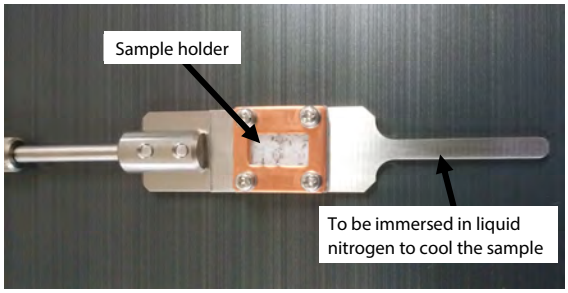

Fig. 6 Sample Rod for Powder or Minute Amounts of Liquid

Table 2 Measurement Conditions

Instrument	: RF-6000, low-temperature measurement unit
Excitation Wavelength	: 350 nm
Measurement Wavelength Range	: 370 nm to 660 nm
Scan Speed	: 200 nm/min
Data Interval	: 1.0 nm
Bandwidth	: Ex 3.0 nm, Em 5.0 nm
Sensitivity	: Low

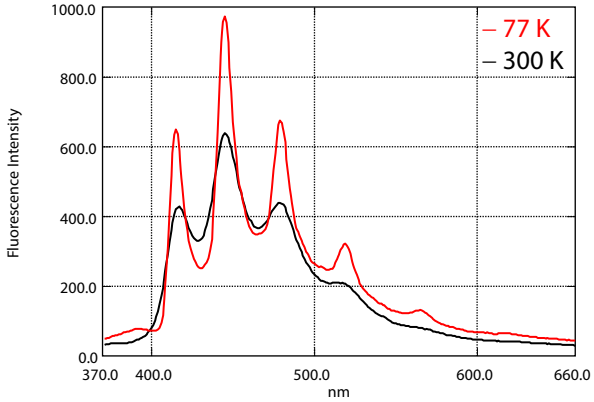

Fig. 7 Spectra of Benzophenone Powder Black: Room Temperature (300 K), Red: Liquid Nitrogen Temperature (77 K)

Conclusion

The light emission properties of liquid and powder at low temperature were successfully examined using the RF-6000 spectrofluorophotometer and low-temperature measurement unit.

With naphthalene solutions (solvent: ethanol), emissions which could not be observed at room temperature appeared in the spectra and also were observed visually from the observation window of the low-temperature measurement unit. Regarding the low-temperature measurement of benzophenone powder, sharper signals were obtained compared to the room temperature spectrum.

Reference
Organized and edited by the Phosphor Research Society: Phosphor Handbook (Ohmsha, Ltd.) (in Japanese)

*1 This unit is a semi-custom made product. Please contact Shimadzu for further details.

First Edition: Mar. 2018

Shimadzu Corporation
www.shimadzu.com/an/

SHIMADZU
Excellence in Science

Application News

No. X266

X-Ray Analysis

Quantitative Analysis of Film Thicknesses of Multi-Layer Plating Used on Cards

BACK TO CONTENTS

A three-layer plating of gold (Au), nickel (Ni), and copper (Cu) is often applied to the contact areas of electronic devices and IC chips. The amount of plating material deposited (film thickness) can be measured non-destructively by using X-ray fluorescence (XRF) spectrometry.
This article introduces a simple quantitative analysis of Au, Ni, and Cu film of a three-layer plating by employing the thin-film fundamental parameter (FP) method without using standard samples.

S. Ueno, K. Hori

Sample

1. Certified Reference Material:
   NMIJ CRM 5208-a, 20 mm × 20 mm
2. IC chip, SIM card

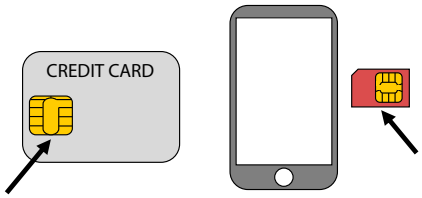

Fig. 1 IC Chip (Left) and SIM Card (Right)

Elements and Layers of Plating

The elements and layers of the plating are shown in Fig. 2.

Fig. 2 Elements and Layers of Plating

Sample Pretreatment

The samples were directly set on the sample stage without any pretreatment.

Quantitative Analysis of Film Thickness and Amount of Deposition

The layer of each metal, Au, Ni, and Cu, was quantitated by the thin-film FP method. The analysis diameter was set to 1 mmϕ.

1. Certified Reference Material NMIJ
   The analysis results of each layer's central point are shown in Table 1. A good result was obtained that the error of the quantitative value of each layer was within 5 % of the certified value.

Table 1 Results of the Quantitative Analysis of NMIJ CRM 5208-a

[μg/cm²]

Element/Layer	Au	Ni	Cu
Quantitative Value	192	862	852
Certified Value	184	869	880
(Uncertainty)	(5)	(17)	(14)

2. IC Chip (IC) and SIM Card (SIM)
   The analysis results of one central point on the IC and the SIM are shown in Table 2.

Table 2 Quantitation Results of IC and SIM

[μg/cm²]

Element/Layer	Au	Ni	Cu
IC	71.0	1,700	25,275
SIM	76.3	1,673	23,941

<Formula for the Amount of Deposition and Film Thickness>
In XRF spectrometry, the analysis result is quantitated as the amount of deposition and then the film thickness is calculated by the following formula using an assumed density.

$$\text{Film thickness } [\mu m] = \frac{\text{Amount of deposition } [\mu g/cm^2]}{\text{Density } [g/cm^3]} \times 10^{-2}$$

In this measurement test, the density [g/cm³] of Au, Ni, and Cu was assumed as 19.3, 8.90, and 8.94, respectively. Table 3 shows the film thicknesses calculated from the values of Table 2.

Table 3 Film Thickness of IC and SIM

[μm]

Element/Layer	Au	Ni	Cu
IC	0.037	1.91	28.3
SIM	0.040	1.88	26.8

With a thickness of approx. 30 μm, the Cu layer was the thickest among the three layers. Sufficient quantitation accuracy cannot be obtained in such a thick layer area as this Cu layer (see the next section for details), so we re-calculated the film thickness of the Au and Ni layers on the assumption that the the thickness of Cu layer was infinite. The results are shown in Table 4 as the final results of the amount of deposition and the film thickness.

Table 4 Amount of Deposition and Film Thickness at a Central Point with the Cu Layer Having an Infinite Thickness

Element/Layer	Au	Ni	Cu
	Amount of deposition [μg/cm²]		
IC	70.9	1,782	∞
SIM	76.3	1,756	∞
	Film thickness [μm]		
IC	0.037	2.00	∞
SIM	0.040	1.97	∞

3. Spectra
   Spectra of the analytical lines of each layer are shown in Fig. 3. While the thickness of the Au layer was thin at a few dozen nm, the peak was clear, demonstrating the high sensitivity of the analysis.
   Standard X-ray emission lines were used for analytical lines: AuLα, NiKα, and CuKα. Kβ and Lβ lines could be used when the analytical lines of each layer's element are close to each other.

BACK TO CONTENTS

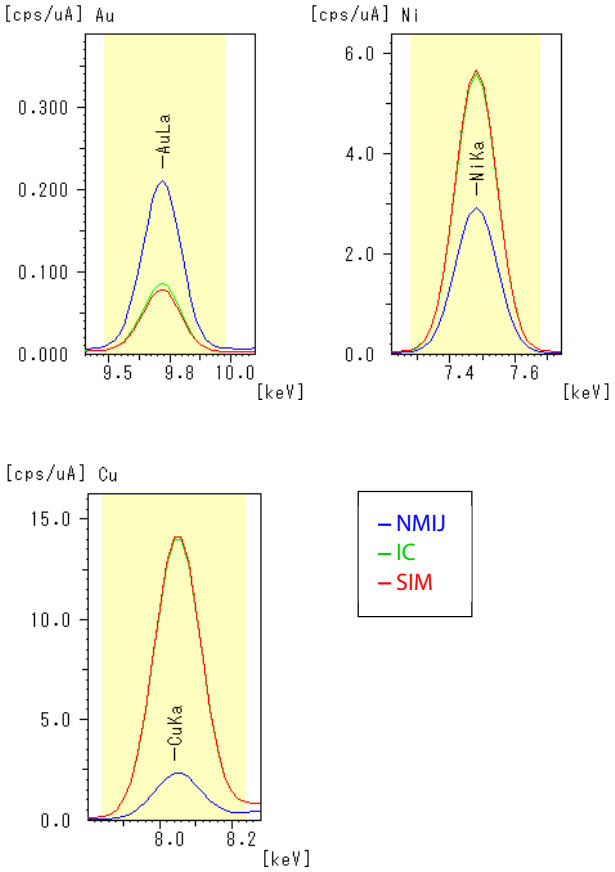

Fig. 3 Spectra of Analytical Lines

Repeatability

A repeatability test was performed by analyzing the IC chip repeatedly for 10 times with an analysis diameter of 1 mmϕ and 3 mmϕ. The amount of deposition of Au and Ni layer were analyzed on the assumption that the the thickness of Cu layer was infinite. The results are shown in Table 5.

Table 5 IC Chip Quantitation Repeatability [μg/cm²]

	Au	Ni	Analysis Diameter
Average	70.0	1,709	1 mmϕ
Standard Deviation	0.38	3.2	
Coefficient of Variation [%]	0.55	0.19	
Average	69.5	1,723	3 mmϕ
Standard Deviation	0.41	3.0	
Coefficient of Variation [%]	0.59	0.17	

Relationship between Theoretical X-ray Intensity and Thickness of Cu Film

The relationship between the theoretical X-ray intensity and the thickness [μm] of Cu film is shown in Fig. 4. When the intensity of the saturation thickness is defined as 90 % of the saturation intensity that is obtained when the Cu film has an infinite thickness (JIS H 8501), the upper quantitation limit is about 18 μm.

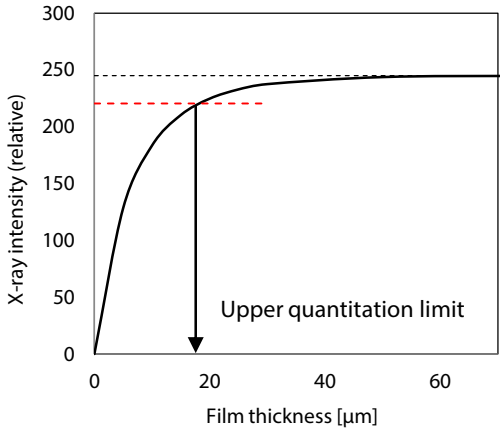

Fig. 4 Relationship between X-ray Intensity and Thickness [μm] of Cu Film

Conclusion

Film thicknesses of a three-layer plating of gold, nickel, and copper were analyzed with ease, high sensitivity and precision in the order of nm to μm using small analysis diameters of 1 mmϕ and 3 mmϕ. Quantitation of even thinner areas may be possible by using the standard analysis diameter of 10 mmϕ. As demonstrated in this research, XRF spectrometry is effective for film thickness measurement.

Furthermore, XRF spectrometry can also easily analyze the elements and their amounts used in the material. For example, it can be employed to manage the used amount and grasp the recovered amount on recycling of precious metals such as gold, platinum (Pt), palladium (Pd) and rhodium (Rh) that are used in films of plating and physical vapor deposition.

(Reference)
Estimated mass and price of gold used for the plating of the SIM card measured in this study

Mass 80 μg (80 μg/cm² × area 1 cm²)

Price Approx. 0.37 yen (USD 1,302.3 per troy ounce)
(London Metal Exchange price, Oct. 13, 2017)

Measurement Conditions

Instrument	: EDX-8000 / (7000)
Element - Analytical Line	: AuLα, NiKα, CuKα
Analysis Method	: Thin-film FP method
X-Ray Tube	: Rh Target
Detector	: SDD
Tube Voltage - Current	: 50 [kV] - Auto [μA]
Collimator	: 1, 3 [mmϕ]
Primary Filter	: None
Measurement Atmosphere	: Air
Integration time	: 100 [s]
Dead Time	: Max. 30 [%]

Acknowledgments
We would like to thank Shuichiro Terada who is majoring in Industrial Chemistry at the Tokyo University of Science Graduate School of Engineering for his collaboration in conducting measurements and preparing this article.

First Edition: May 2018

SHIMADZU
Shimadzu Corporation
www.shimadzu.com/an/

SHIMADZU
Excellence in Science

Application News

No. X267

X-Ray Analysis

X-Ray Fluorescence Analysis of Light Elements in Liquid Samples – EDX-8100 and Helium Purge Unit –

BACK TO CONTENTS

Shimadzu's EDX-8100 is an energy dispersive X-ray fluorescence spectrometer with high sensitivity for light elements and can be configured with an optional helium purge unit. The helium purge unit enables high-sensitivity analysis of light elements in samples that cannot be depressurized to a vacuum state such as solutions and samples that generate gas. As one effect, detection of fluorine (F) in liquid samples is possible with the EDX-8100, whereas it was not possible with the conventional EDX-8000.

The detection limits of the elements F to K in liquid samples in a He atmosphere and differences depending on the film used to hold the samples were evaluated.

S. Yada, N. Ichimaru

Elements and Samples

The samples are shown in Table 1. Pure water was used to calculate the background intensity.

Table 1 Elements, Contents, and Solutions

Element	Content [ppm]	Solution
F	94,962	Preparation
Na	20,000	Preparation
Mg	20,000	Preparation
Al	20,000	Preparation
Si, P, S, Cl, K	1,000	Atomic Absorption Standard Solution
-	-	Pure Water

Sample Pretreatment

Approximately 5 mL of each sample was introduced directly into a film-covered sample container. The three films shown in Table 2 were used.

Table 2 Sample Holder Films

Name	Thickness (μm)	Compositional Formula
Prolene™ (Chemplex)	4	C_3H_6
Polypropylene	5	C_3H_6
PET	6	$C_{10}H_8O_4$

Detection Limits

(1) Atmosphere: Air/He

Fig. 1 (next page) shows the measured spectra in air and a He atmosphere when using the polypropylene film. Table 3 shows the detection limits[*1] calculated from the intensity and measurement conditions (current and integration time). The He atmosphere enabled detection of F and Na, and improved detection of Mg by 40 times, Al and Si by 8 times, and P and S by approximately 2 times.

(2) Differences Depending on Film

Three types of films were used in measurements in a He atmosphere. Fig. 2 (next page) shows the spectra, and Table 4 shows the detection limits. Prolene (Chemplex Inc.) with a thickness of 4 μm displayed the highest sensitivity, and the influence of the film thickness and composition on absorption increased with lighter elements.

Conclusion

Measurements of liquid samples by EDX are possible regardless of conditions such as concentration, organic or inorganic material, suspension, and viscosity.

This technique is not limited to solutions, but is also effective with samples such as the following, which are difficult or impossible to depressurize to a vacuum.

- Teeth and other biomaterials (fracture, alteration) (Care is necessary in handling, for example, considering infection.)
- Porous materials such as zeolite (time required to reach measurement vacuum)
- Fibers and clothing (porous, wet)
- Ultrafine particles such as graphite powder (scattering)
- Sealed and enclosed materials (bursting)

This technique is effective for quickly determining the presence and content of light elements in the above-mentioned materials.

Measurement Conditions

Instrument	: EDX-8100
X-ray tube	: Rh target
Detector	: SDD
Tube voltage	: 50 [kV]
Tube current	: 260 to 483 [μA] (Auto)
Primary filter	: None (F to S) / #2 (Cl, K)
Collimator	: 10 [mmφ]
Measurement atmosphere	: Air/He
Integration Time	: 100 [sec]
Dead time	: 30 max. [%]

Table 3 Detection Limits (1) Differences Depending on Atmosphere [ppm]

Atmosphere	$_{9}$F	$_{11}$Na	$_{12}$Mg	$_{13}$Al	$_{14}$Si	$_{15}$P	$_{16}$S	$_{17}$Cl	$_{19}$K
Air	-	-	3,300	210	91	25	16	23	6.3
He	41,000	680	84	26	11	11	7.8	15	5.1

Table 4 Detection Limits (2) Differences Depending on Film [ppm]

Film	$_{9}$F	$_{11}$Na	$_{12}$Mg	$_{13}$Al	$_{14}$Si	$_{15}$P	$_{16}$S	$_{17}$Cl	$_{19}$K
Prolene™ (Chemplex)	18,000	480	72	22	10	9.7	7.5	14	4.7
Polypropylene	41,000	680	84	26	11	11	7.9	15	5.1
PET	-	5,400	340	55	54	25	24	18	5.8

BACK TO CONTENTS

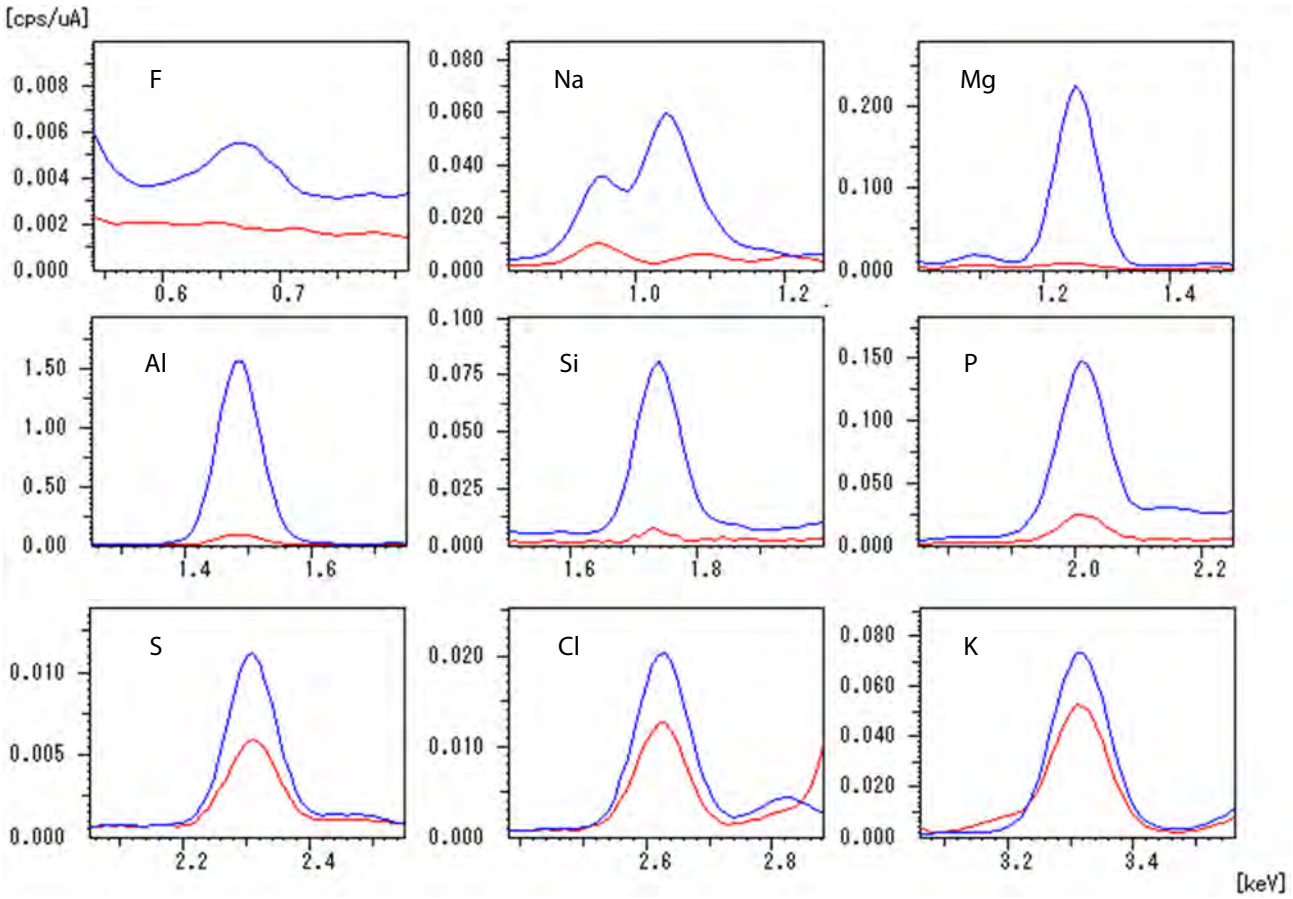

Fig. 1 X-Ray Fluorescence Spectra for F to K [Blue: He Atmosphere, Red: Air]

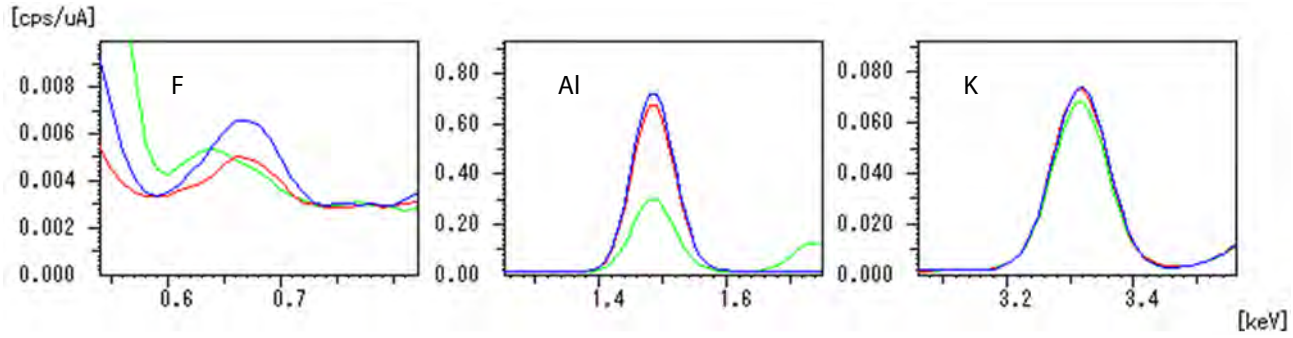

Fig. 2 X-Ray Fluorescence Spectra for F, Al, and K [Blue: Prolene (Chemplex), Red: Polypropylene, Green: PET]

*1 Calculation of detection limit

$$\text{Detection limit} = 3 \times \frac{\text{Content}}{\text{X–ray fluorescence intensity}} \times \frac{\sqrt{\text{Background intensity} \times \text{Integration time} \times \text{Current}}}{\text{Integration time} \times \text{Current}}$$

$$\text{(Example: Case of Table 3, P in He atmosphere)} = 3 \times \frac{1{,}000_{[ppm]}}{1.217437_{\left[\frac{cps}{\mu A}\right]}} \times \frac{\sqrt{0.536691_{\left[\frac{cps}{\mu A}\right]} \times 100_{[\text{sec}]} \times 283_{[\mu A]}}}{100_{[\text{sec}]} \times 283_{[\mu A]}} = 10.73_{[ppm]} \fallingdotseq 11_{[ppm]}$$

First Edition: Jun. 2018

SHIMADZU

Shimadzu Corporation

www.shimadzu.com/an/

SHIMADZU
Excellence in Science

Application Data Sheet

No.128

GC-MS
Gas Chromatograph Mass Spectrometer

Analysis of Resin Using the OPTIC-4 Multimode Inlet in Thermal Assisted Hydrolysis and Methylation Mode

BACK TO CONTENTS

The OPTIC-4 multimode inlet can be used for the thermal assisted hydrolysis and methylation-GC/MS (THM-GC/MS) method. In the THM-GC/MS method, the sample is subjected to alkaline hydrolysis while being heated. The resulting products are subjected to methylation derivatization, and the derivatized compounds are then measured with a GC/MS. THM-GC/MS is an effective method for measuring resin samples that produce polar compounds due to pyrolysis. The OPTIC-4 allows derivatization reactions within inert glass micro vials.

Experiment

An approximately 0.1 mg of polycarbonate resin sample clipped with a cutter knife was placed in a micro vial. Then, 4 μl of tetramethylammonium hydroxide (25 % in methanol) was added to the sample in the micro vial. The micro vial was placed in a liner, which was then passed through the O-ring for sealing the inlet. After both ends were capped, the liner was placed into the rack for the AOC-6000.
Table 1 shows the analytical conditions. For thermal assisted hydrolysis, measurements are generally performed with the temperature set to between 300 °C and 400 °C[*1, *2]. This is lower than the temperature used for typical pyrolysis-GC measurements without using a reaction reagent (500 °C to 600 °C). Accordingly, the inlet temperature was raised to 420 °C prior to the analysis.

Table 1: Analytical Conditions

Instrument	
Injection Port:	OPTIC-4
Liner:	L100011, DMI liner with taper
GC-MS:	GCMS-QP2020
Autosampler:	AOC-6000 (LINEX-2 and CDC Station included)
Column:	SH-Rxi-5SilMS (0.25 mm × 30 m, df = 0.25 μm)

Injector	
Vent Time:	1 min
Method Type:	Split
Equilibration Time:	5 sec
End Time:	60 min
Injector Temperature:	
40 °C (10 sec) → (60 °C/sec) → 420 °C (3 min) → 320 °C (hold)	
Carrier Gas:	Helium
Carrier Control Mode:	Flow control
Start Column Flow:	1.5 mL/min
End Column Flow:	1.5 mL/min
Initial Split Flow:	150 mL/min
Split Flow:	450 mL/min
Septum Purge Flow:	10 mL/min

MS	
Interface Temperature:	250 °C
Ion Source Temperature:	200 °C
Data Acquisition Time:	5 to 50.0 min
Measurement Mode:	Scan
Event Time:	0.3 sec
Mass Range:	*m/z* 29 to 600
Detector Voltage:	Relative to the Tuning Result 0 kV

GC
Column Oven Temperature:
40 °C (2 min) → (4 °C/min) → 230 °C → (10 °C/min) → 320 °C (1 min)

Results

The figures show the total ion current chromatogram (TICC) obtained, and the mass spectra for the compounds detected. When the ester bonds were hydrolyzed, bisphenol A was produced. As shown in Fig. 1, a derivative of bisphenol A with one hydroxyl group methylated and a derivative with two hydroxyl groups methylated were detected.

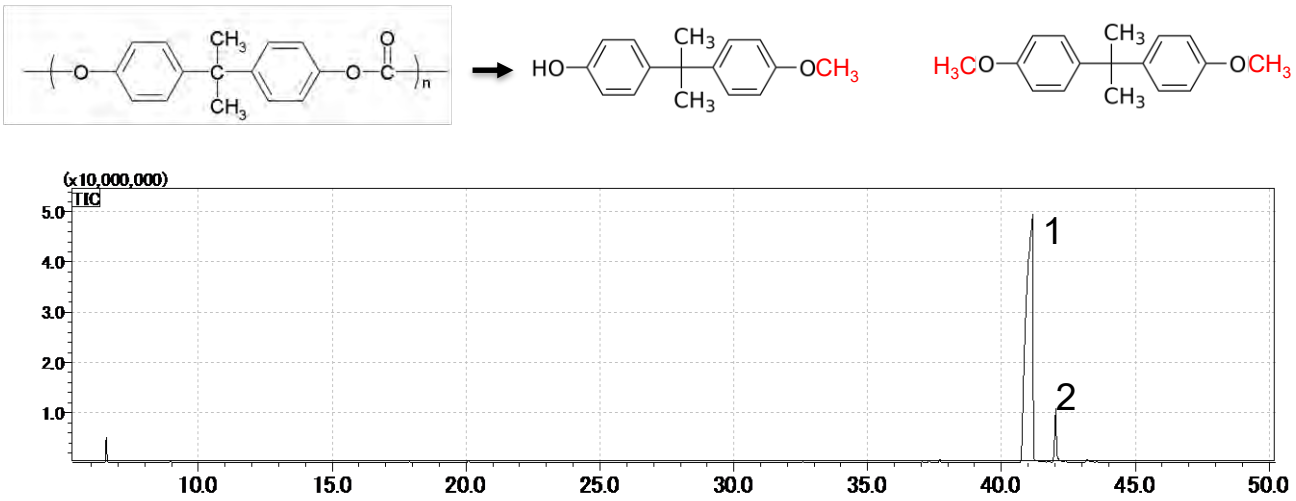

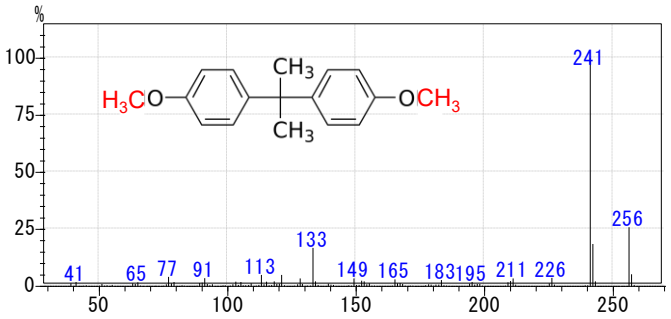

Peak 1
Derivative of Bisphenol A with Both Two -OH Groups Methylated (- OMe and –OMe)

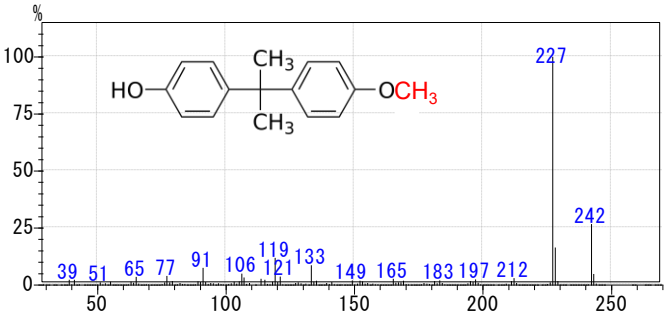

Peak 2
Derivative of Bisphenol A with One –OH Group Methylated (- OH and –OMe)

Fig. 1: Total Ion Current Chromatogram of Polycarbonate and Mass Spectra for Peaks Detected

Conclusions

The OPTIC-4 is equipped with sample injection modes that are indispensable for the evaluation of polymer materials. In addition to THM-GC/MS, these include pyrolysis, difficult matrix introduction (DMI), and thermal desorption. As a result, it is effective for the multifaceted evaluation of materials. Furthermore, using it with the AOC-6000 enables consecutive analyses to be performed automatically.

*1: S. Tsuge, H. Ohtani, C. Watanabe: Pyrolysis-GC/MS Data Book of Synthetic Polymers –Pyrograms, Thermorgams and MS of Pyrolyzers-, 1st Edition, Elsevier, 420 (2011)
*2: H. Ohtani and T. Takarazaki edited: Synthetic Polymer Chromatography, Ohmsha, Ltd., 401, 2013

First Edition: March, 2017

Shimadzu Corporation
www.shimadzu.com/an/

SHIMADZU
Excellence in Science

Application Data Sheet

No.129

GC-MS
Gas Chromatograph Mass Spectrometer

Analysis of Resin Using the OPTIC-4 Multimode Inlet in Pyrolysis Mode

BACK TO CONTENTS

The OPTIC-4 can be used for pyrolysis analysis of polymers. With the pyrolysis method, a small amount of a resin (a few dozen μg or less) is heated rapidly in a helium gas environment. The pyrolysates are then analyzed using a GC/MS. The structure of the resin can in turn be analyzed from the pyrolysates. The OPTIC-4 is capable of rapid heating up to 600 °C at 60 °C/sec, so data equivalent to that from a dedicated pyrolysis system can be obtained. This article describes the analysis of a polycarbonate resin using the OPTIC-4 in pyrolysis mode.

Experiment

An approximately 0.1 mg of polycarbonate resin sample clipped with a cutter knife was placed in a micro vial. The micro vial was placed in a liner, which was then passed through the O-ring for sealing the inlet. After both ends were capped, the liner was placed into the rack for the AOC-6000.
Table 1 shows the analytical conditions.

Table 1: Analytical Conditions

Instrument	
Injection Port:	OPTIC-4
Liner:	L100011, DMI liner with taper
GC-MS:	GCMS-QP2020
Autosampler:	AOC-6000 (LINEX-2 and CDC Station included)
Column:	SH-Rxi-5SilMS (0.25 mm × 30 m, df = 0.25 μm)

Injector	
Vent Time:	1 min
Method Type:	Split
Equilibration Time:	5 sec
End Time:	60 min
Injector Temperature:	
40 °C (10 sec) → (60 °C /sec) → 600 °C (3 min) → 320 °C (hold)	
Carrier Gas:	Helium
Carrier Control Mode:	Flow control
Transfer Column Flow:	0.7 mL/min
Start Column Flow:	1.5 mL/min
End Column Flow:	1.5 mL/min
Split Flow:	150 mL/min
Septum Purge Flow:	10 mL/min

MS	
Interface Temperature:	250 °C
Ion Source Temperature:	200 °C
Data Acquisition Time:	5 to 50.0 min
Measurement Mode:	Scan
Event Time:	0.3 sec
Mass Range:	*m/z* 29 to 600
Detector Voltage:	Relative to the Tuning Result 0 kV

GC
Column Oven Temperature:
40 °C (2 min) → (4 °C/min) → 230 °C → (10 °C/min) → 320 °C (1 min)

Results

Fig. 1 shows the total ion current chromatogram (TICC) obtained, and the mass spectra for the major pyrolysates. In the obtained TICC, bisphenol A is detected as peak 10; a number of other phenol compounds are also detected. In other words, a typical pyrogram for a polycarbonate resin, which has already been reported*1, was obtained.

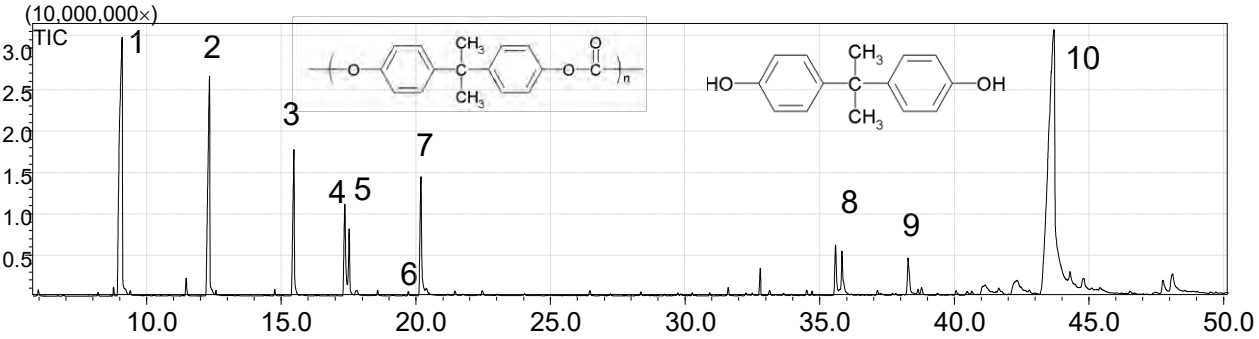

1=phenol, 2=*p*-cresol, 3=*p*-ethylphenol, 4=*p*-vinylphenol, 5=*p*-isopropylphenol, 6=*p*-*tert*-butylphenol, 7=*p*-isopropenylphenol, 8=*p*-hydroxy-2,2-diphenylpropane, 9=*p*-hydroxy-3-methyl-2,2-diphenylpropane, 10=bisphenol A

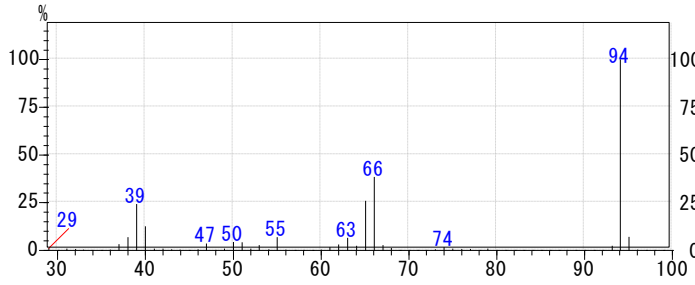

Peak 1: phenol

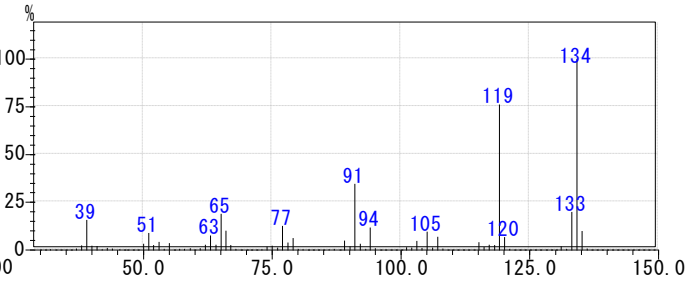

Peak 7: *p*-isopropenylphenol

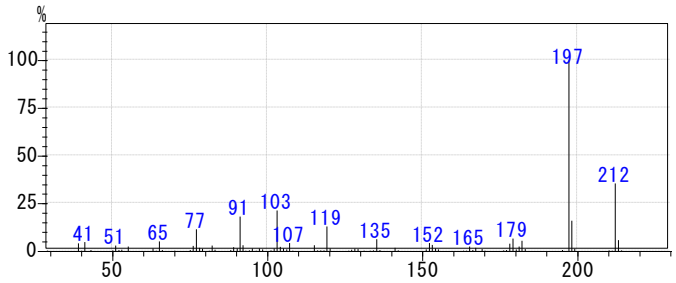

Peak 8: *p*-hydroxy-2,2-diphenylpropane

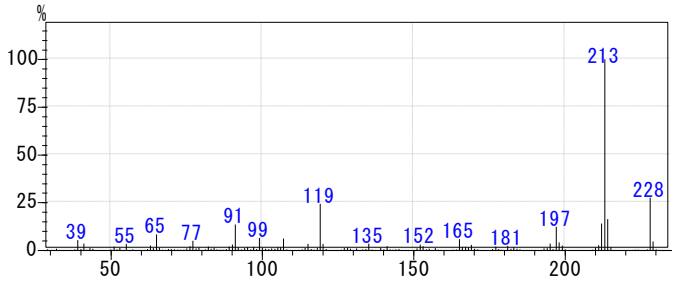

Peak 10: bisphenol A

Fig. 1: Total Ion Current Chromatogram of Polycarbonate, and Mass Spectra for its Pyrolysates

Conclusions

In addition to the pyrolysis of resins, the OPTIC-4 is equipped with sample injection modes that are indispensable for the evaluation of high polymer materials, including difficult matrix introduction (DMI) and thermal desorption. As a result, it is an effective system for the multifaceted evaluation of materials. Furthermore, consecutive analyses can be performed automatically by combining it with the AOC-6000.

*1: S. Tsuge, H. Ohtani, C. Watanabe: Pyrolysis-GC/MS Data Book of Synthetic Polymers –Pyrograms, Thermorgams and MS of Pyrolyzers-, 1st Edition, Elsevier, 420 (2011)

First Edition: March, 2017

Shimadzu Corporation

www.shimadzu.com/an/

SHIMADZU
Excellence in Science

Application Data Sheet

No. 122

GC-MS

Gas Chromatograph Mass Spectrometer

Estimation of Elemental Composition of Additives in Polymers Using Quick-CI and MassWorks™

BACK TO CONTENTS

GC-MS offers a wealth of fragmentation data and a thorough, highly useful mass spectral library, so it is used for identifying unknown compounds. To identify unknown compounds, searches using a mass spectral library are commonly used. However, considerable difficulties with compound identification can be encountered if a compound detected is not registered in the mass spectral library.
The Mass Works™ software from cerno BIOSCIENCE mathematically calculates the accurate mass from the quadrupole MS mass profile. It then outputs candidate composition formulas using the accurate mass and isotopic ratios.
This application sheet introduces the results of composition estimation using MassWorks for data acquired by means of the EI and CI methods with Quick-CI when analyzing additives in polymers.

* MassWorks™ is a trademark of cerno BIOSCIENCE.

Quick-CI

When estimating compositions, it is necessary to make use of molecular ions. However, with some compounds, molecular ions cannot be detected using the EI method. For this reason, in order to acquire information about molecular ions from protonated molecules, the positive chemical ionization (CI) method has been used. However, this requires an exchange of ion sources when switching between the EI and CI methods. By employing Quick-CI, which is included with the GCMS-QP2020, it is now possible to switch between the EI and CI methods without exchanging ion sources. Moreover, it is also possible to acquire data while switching between the EI and CI methods in a continuous analysis situation.

Sample Preparation

The ultrasonic solvent extraction method was used for pretreating the polymer sample. The sample for evaluation was finely pulverized, and approximately 300 mg was weighed and placed in a 40 mL vial. Then, 10 mL THF was added, a stopper was inserted, and it was processed for 60 minutes using ultrasound. The sample was then dissolved in solvent. After acclimatizing to room temperature, 20 mL of acetonitrile was instilled to precipitate the polymer, and then it was left at room temperature for 30 minutes. 1 mL of the supernatant was measured and placed into a GC vial, and then made the sample to be measured using GC-MS.

Output of Mass Profile Data

Mass profile data is required in order to use the MassWorks software. In GCMSsolution Ver4.42, a setting allows the export of mass profile data to be enabled/disabled (Fig. 1) in the analysis method. For the same measurement, both GC/MS data and mass profile data can be exported. By performing a search of the mass spectral library using GC/MS data, and using mass profile data for compounds that are difficult to identify, an estimation of the composition can be accomplished using MassWorks.

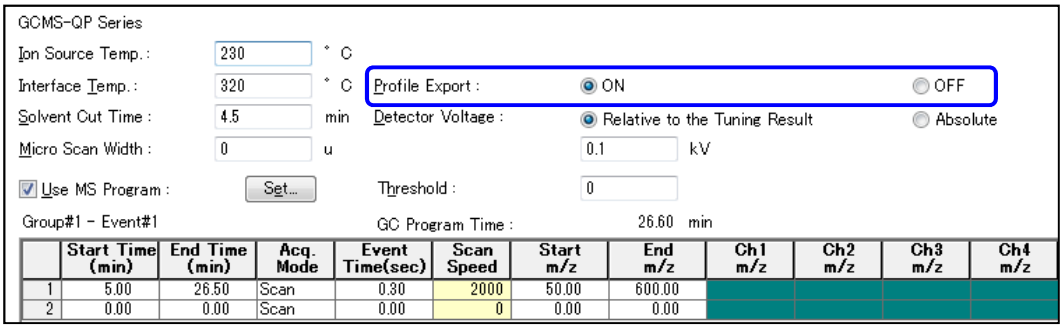

Fig. 1: Example of Settings for Profile Export

Analytical Conditions and Settings for Mass Calibration

To use MassWorks, it is necessary to use mass calibration data in order to calculate the theoretical accurate mass. This mass calibration data can be acquired automatically by means of PFTBA, which is used for tuning after analysis of a sample. The analytical conditions pertaining to this Application Data Sheet are shown in Table 1. An oven program was set so that the temperature was lowered to 60 °C to reduce the effect of column bleeding after the column's rise in temperature for the purpose of analyzing the sample (Fig. 2). Also, the MS time program needed to acquire mass correction data was set as shown in Fig. 3. Measurement is possible by setting some additions to the analytical conditions ordinarily used.

Table 1: Analytical Conditions

GC-MS	: GCMS-QP2020
Workstation	: GCMSsolution Ver4.42
Glass insert	: Deactivated splitless glass insert with wool (PN: 221-48876-03)
[GC]	
Column	: SH-Rxi™-5Sil MS (length 30 m, 0.25 mm I.D., df=0.25 μm)
Injection temp.	: 300 ˚C
Column oven temp.	: 110 ˚C (0.5 min) → (20 ˚C /min) → 110 ˚C (1 min) → (20 ˚C /min) → 320 ˚C (5 min) → (-100 ˚C /min) → 60 ˚C (7 min)
Injection mode	: Splitless
Flow control mode	: Linear velocity (45.8 cm/sec)
Initial column flow	: 1.5 mL/min
[MS]	
Interface temp.	: 300 ˚C
Ion source temp.	: 230 ˚C
Acquisition mode	: Scan
Scan event time	: 0.3 sec
MS program	: Refer to Fig. 3
EI	
Scan range	: *m/z* 50 to 600
CI	
Scan range	: *m/z* 120 to 600
Reagent gas	: Isobutane (80 kPa)

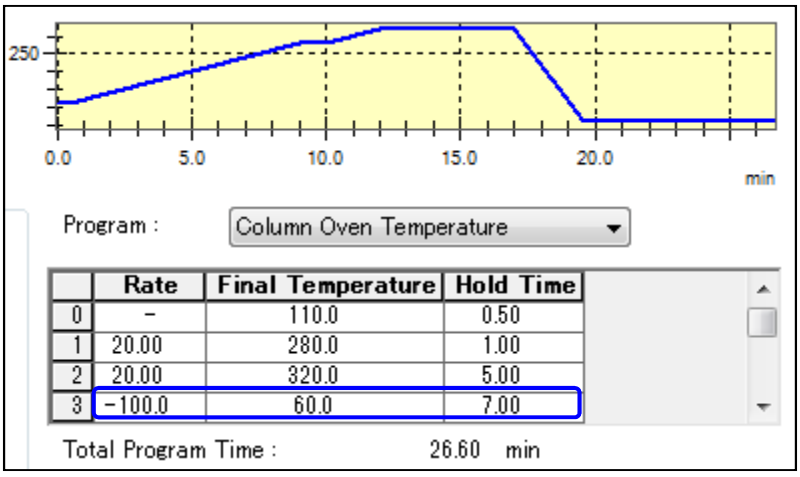

Fig. 2: Setting Example of Column Oven Program

	Time (min)	Command	Value
1	20.10	FilamentOFF	
2	20.60	PFTBAOpen	
3	20.60	DetectorGain=	1.2
4	21.10	FilamentON	
5	26.10	FilamentOFF	

Fig. 3: Setting Window for MS Program to Acquire Mass Calibration Data

Analysis Results

The total ion current chromatogram (TICC) for polymer sample A acquired using the EI and CI methods with Quick-CI is shown in Fig. 4. Concerning peak A, even though the mass spectral library was searched, identification was difficult. An observation of the mass spectrum (Fig. 5) acquired using the EI and CI methods reveals that the molecular weight of the compound is 410. The results of the analysis of an EI method mass profile using MassWorks is shown in Fig. 6. The first candidate was this composition formula: C24H27O4P (mass error 6.8527 mDa). In that vicinity, phosphoric acid triisopropyl phenyl ester, which has similar fragment ions, was detected; therefore, it could be assumed that it was phosphoric acid diisopropyl (phenyl) ester.

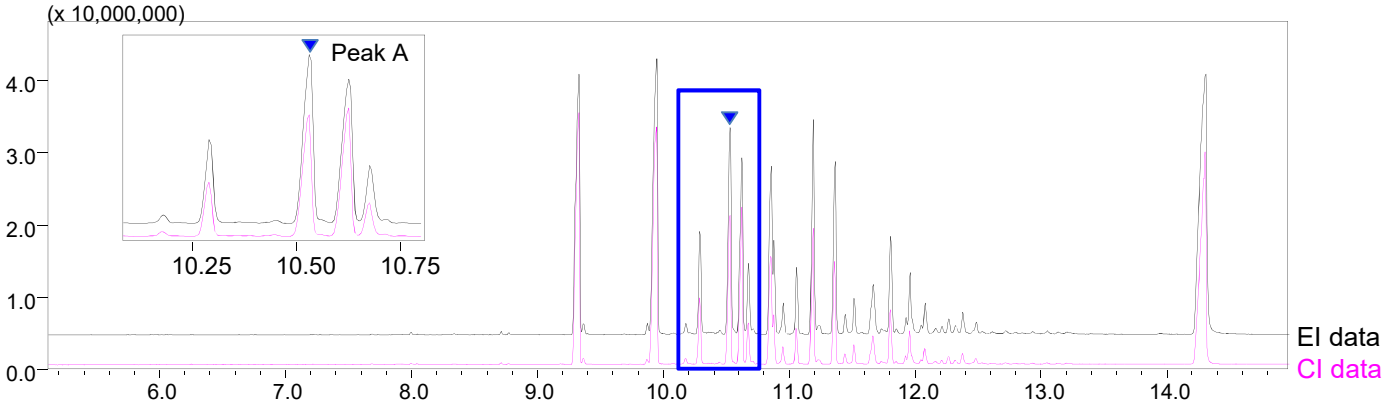

Fig. 4: Total Ion Current Chromatogram for Polymer Sample A Acquired with EI and CI Methods

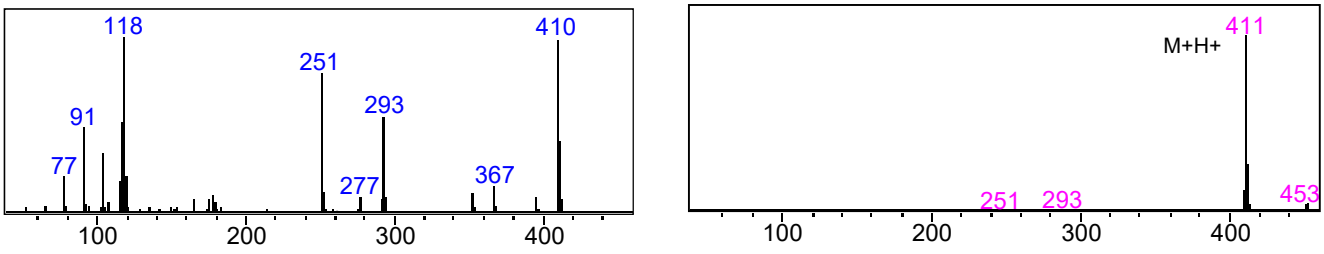

Fig. 5: Peak A Mass Spectrum (Left: EI Mass Spectrum, Right: CI Mass Spectrum)

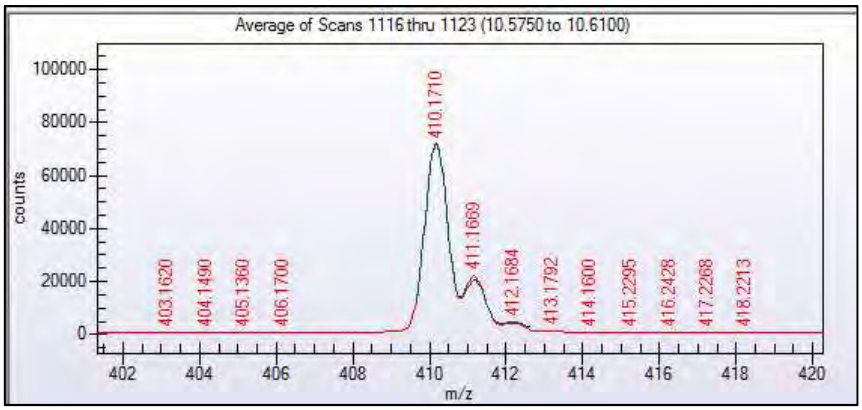

CLIPS Results

	Formula	Mono Isotope	Mass Error (mDa)	Mass Error (PPM)	Spectral Accuracy	RMSE	DBE
1	C24H27O4P	410.1641	6.8527	16.7070	97.6453	726	12.0
2	C24H26O6	410.1724	-1.3900	-3.3888	97.5311	761	12.0
3	C21H31O6P	410.1853	-14.2767	-34.8066	95.4464	1,403	7.0
4	C21H30O8	410.1935	-22.5194	-54.9024	95.3327	1,438	7.0
5	C20H27O7P	410.1489	22.1088	53.9015	94.6506	1,649	8.0
6	C20H26O9	410.1571	13.8661	33.8058	94.5344	1,684	8.0
7	C17H31O9P	410.1700	0.9795	2.3880	92.4341	2,332	3.0
8	C17H30O11	410.1783	-7.2632	-17.7078	92.3145	2,369	3.0
9	C16H26O12	410.1419	29.1223	71.0003	91.5159	2,615	4.0
10	C14H35O11P	410.1911	-20.1499	-49.1256	90.2238	3,013	-2.0
11	C14H34O13	410.1994	-28.3926	-69.2214	90.1002	3,051	-2.0
12	C13H31O12P	410.1548	16.2356	39.5825	89.4302	3,257	-1.0
13	C13H30O14	410.1630	7.9929	19.4868	89.3045	3,296	-1.0

Fig. 6: MassWorks Processed Results for Peak A
(Top: Mass Profile of *m/z* 410 of Peak A, Bottom: List of Candidates for Compositional Formula)

BACK TO CONTENTS

The total ion current chromatogram (TICC) for polymer sample B acquired using the EI and CI methods with Quick-CI is shown in Fig. 7. Concerning peak B, a search of the mass spectral library resulted in a large number of hits for similar compositions, which made identification very difficult. An observation of the mass spectrum (Fig. 8) acquired using the EI and CI methods reveals that no molecular ions were detected using the EI method, and that the molecular weight of the compound is 370, based on protonated molecules of the CI mass spectrum. Since in some cases no molecular ions can be detected using the EI method, it is essential that CI method data be evaluated in order to estimate the composition.
The results of the analysis of a CI method mass profile using MassWorks is shown in Fig. 9. The first candidate is this composition formula: C22H43O4 (mass error -0.7863 mDa). Considering the search results of the library using EI data, it was possible to infer and presume that it was diethylhexyl adipate (C22H42O4, protonation taken into consideration). Even with detection peaks that cannot be identified with a mass spectral library, the combination of CI molecular weight data and theoretical accurate mass data from MassWorks analysis allows for an expansion of qualitative analysis.

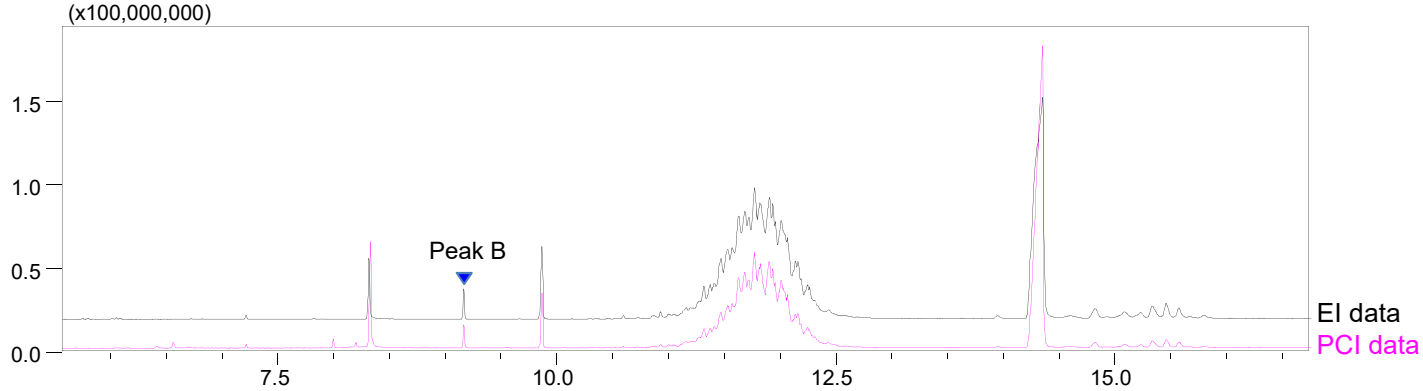

Fig. 7: Total Ion Current Chromatogram for Polymer Sample B Acquired with EI and CI Methods

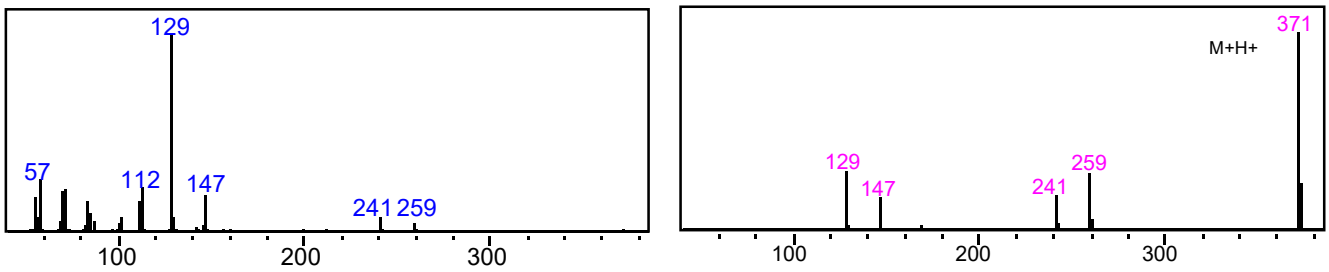

Fig. 8: Peak B Mass Spectrum (Left: EI Mass Spectrum, Right: CI Mass Spectrum)

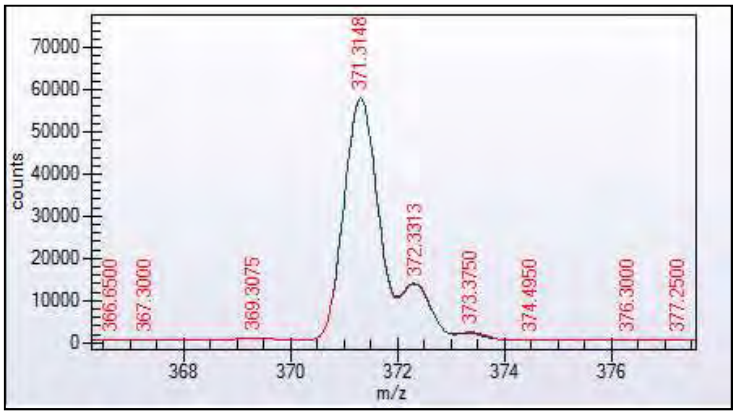

CLIPS Results

	Formula	Mono Isotope	Mass Error (mDa)	Mass Error (PPM)	Spectral Accuracy	RMSE	DBE
1	C22H43O4	371.3156	-0.7863	-2.1176	98.9772	256	1.5
2	C19H50P3	371.3120	2.8124	7.5743	98.7149	321	-3.5
3	C19H48O2PS	371.3107	4.0856	11.0030	97.8758	531	-3.5
4	C19H47O4S	371.3190	-4.1571	-11.1956	97.6479	588	-3.5
5	C19H49O2P2	371.3202	-5.4303	-14.6244	98.8709	282	-3.5
6	C22H44O2P	371.3073	7.4564	20.0811	98.8498	287	1.5
7	C19H49P2S	371.3025	12.3283	33.2017	98.0966	476	-3.5
8	C19H47O2S2	371.3012	13.6014	36.6305	95.1422	1,214	-3.5

Fig. 9: MassWorks Processed Results for Peak B
(Top: Mass Profile of *m/z* 371 of Peak B, Bottom: List of Candidates for Compositional Formula)

First Edition: April, 2016

SHIMADZU
Shimadzu Corporation
www.shimadzu.com/an/

BACK TO CONTENTS

SHIMADZU
Excellence in Science

Application News

No.A488

Spectrophotometric Analysis

Analysis of Inorganic Additives in Resin by FTIR and EDX

BACK TO CONTENTS

Additives enhance the quality of products by improving the functionality, workability, and stability of the materials used in the product. They are utilized in a wide range of products, including electronics, foods, pharmaceuticals, cosmetics, plastics, etc., and play an important role by adding value to products.
The approach taken in the analysis of additives is dependent on whether the additive is organic or inorganic. Organic additives are typically identified by first extracting the additives using a suitable pretreatment procedure, and after chromatographic separation of the extracted components, a suitable analytical instrument is used for qualitative analysis. On the other hand, comprehensive identification of inorganic additive components is typically based on the results obtained using elemental analysis, infrared spectroscopy or morphologic observation, etc[1)].
Here, we introduce examples of FTIR analysis to obtain useful information regarding some typical inorganic additives, in addition to an example of analysis of a resin containing an inorganic additive using FTIR and EDX.

Analysis of Inorganic Additives by FTIR

FTIR is used mainly for organic analysis, but useful information can also be obtained by applying FTIR to the analysis of some inorganic additives.
Here, we conducted single-reflection ATR measurement using a diamond prism. Table 1 shows the analytical conditions using FTIR, and the infrared spectra and peak positions of the four substances used as additives (aluminum silicate, aluminum hydroxide, magnesium silicate, and calcium carbonate) are shown in Fig. 1 to 4.
A spectral characteristic of inorganic additives is the appearance of a relatively wide peak in the lower wavenumber region. In addition, as is clearly evident in Fig. 1 to 3, a characteristic peak is sometimes present in the higher wavenumber region. In such cases, qualitative identification is possible by FTIR alone.

Table 1 Analytical Conditions

Instruments	: IR Tracer-100, Quest, Diamond
Resolution	: 4.0 cm^{-1}
Accumulation	: 40
Apodization	: Happ-Genzel
Detector	: DLATGS

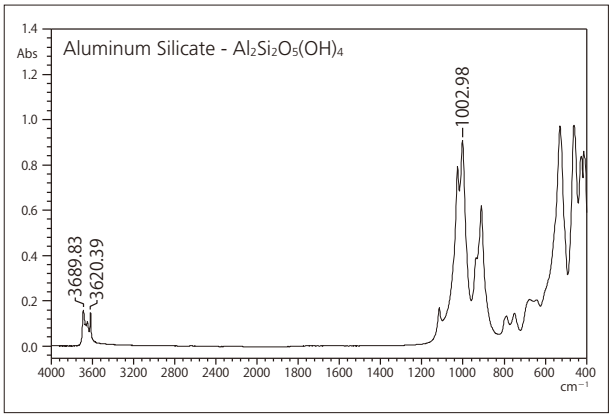

Fig. 1 IR Spectrum and Peak Position of $Al_2Si_2O_5(OH)_4$

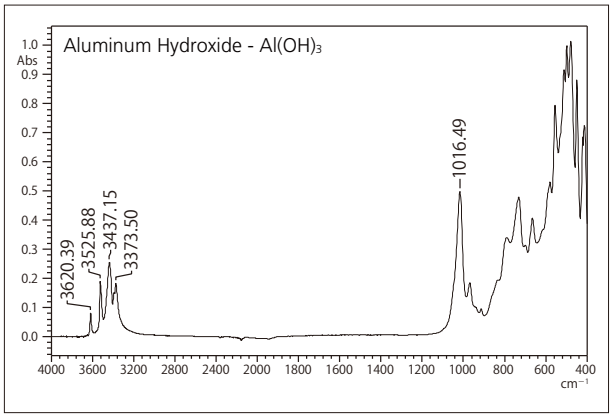

Fig. 2 IR Spectrum and Peak Position of $Al(OH)_3$

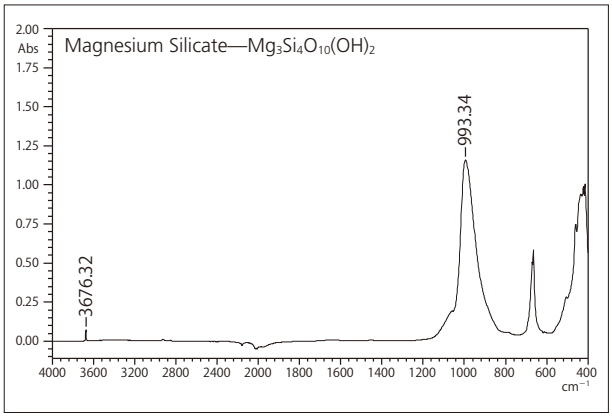

Fig. 3 IR Spectrum and Peak Position of $Mg_3Si_4O_{10}(OH)_2$

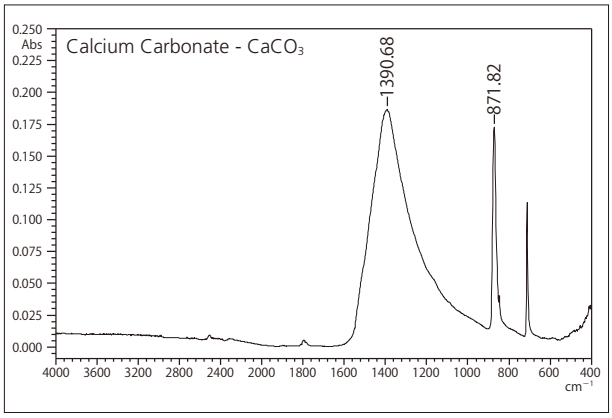

Fig. 4 IR Spectrum and Peak Position of $CaCO_3$

BACK TO CONTENTS

Analysis of Inorganic Additives in Resin

FTIR was used for the analysis of a connector cover as a sample that contains an inorganic additive. Fig. 5 shows a photograph of the sample, and Fig. 6 shows the results of analysis.

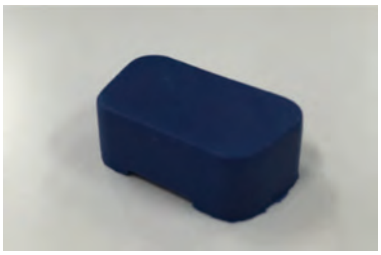

Fig. 5 Connector Cover

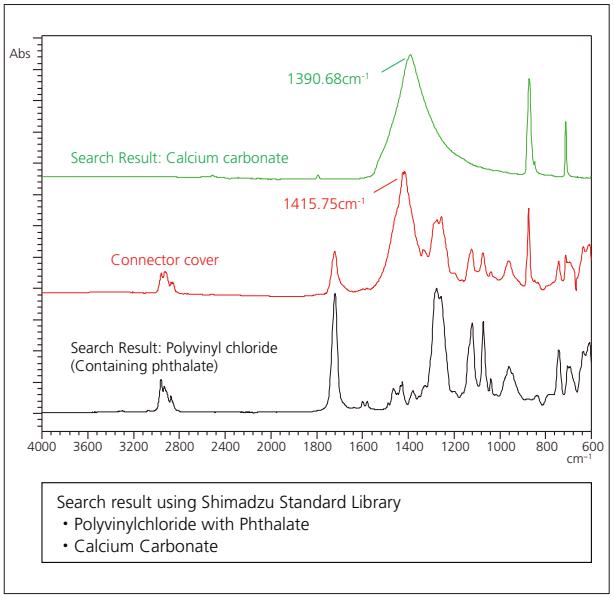

Fig. 6 IR Spectra and FTIR Search Results

From the infrared spectra and search results of Fig. 6, the principal component of the connector cover was determined to be polyvinylchloride (PVC). Also, the peak in the vicinity of 1415 cm^{-1} in the infrared spectrum suggests the presence of calcium carbonate ($CaCO_3$).

However, a comparison of the connector cover peak at 1415 cm^{-1} with the peak at 1390 cm^{-1} of calcium carbonate alone indicates a peak position shift of 25 cm^{-1}. Therefore, there is clearly insufficient basis to irrefutably conclude that calcium carbonate is included as an additive from the infrared spectrum alone.

Thus, we followed up this result by conducting EDX analysis to reconcile this discrepancy. The analytical conditions used are shown in Table 2, and the qualitative analytical results are shown in Fig. 7. Table 3-1 and Table 3-2 show the quantitative analytical results by the FP method[2].

Table 2 EDX Analytical Conditions

Instrument	: EDX-7000
X-ray Tube	: Rh target
Voltage / Current	: 15 kV(Na-Sc), 50 kV(Ti-U) / Auto
Atmosphere	: Vacuum
Measurement Diameter	: 10 mmφ
Integration Time	: 100 sec

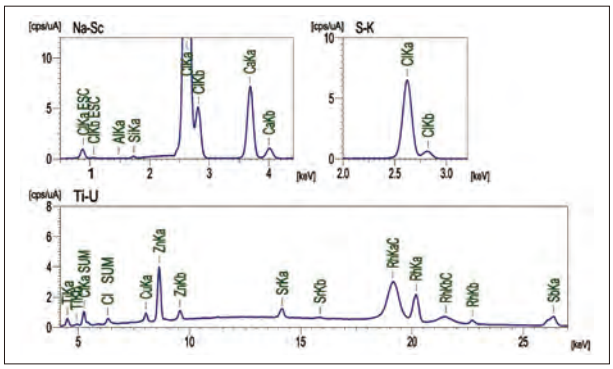

Fig. 7 Results of Qualitative Analysis of Connector Cover by EDX

Table 3-1 Results A of Quantitative Analysis of Connector Cover by EDX

[%]

Element	Cl	Ca	Sb	Zn	Ti	Si	Al	Cu	Sr
Quantitation Value	72.56	26.11	0.40	0.31	0.23	0.21	0.096	0.054	0.030

Table 3-2 Results B of Quantitative Analysis of Connector Cover by EDX

[%]

Element	C_2H_3Cl	$CaCO_3$	SiO_2	Sb_2O_3	TiO_2	ZnO	Al_2O_3	CuO	SrO
Quantitation Value	73.14	25.55	0.31	0.30	0.25	0.25	0.13	0.046	0.024

As clearly indicated in Table 3-1, chlorine (Cl) and calcium (Ca) are the principal constituent elements. This is consistent with the polyvinyl chloride results obtained by FTIR, supporting the presence of calcium carbonate. Table 3-2 shows the quantitative analytical results for specific compounds identified from the results of both FTIR and EDX. It should be noted that other detected elements are assumed to be oxides[3]. Thus, the combination of FTIR and EDX has provided sufficient evidence that calcium carbonate is present as an additive.

Conclusion

By applying a combination of FTIR and EDX, we were able to more accurately identify the additives included in an actual sample. Such an analysis is applicable to contaminant analysis and confirmation testing, and should be considered an effective means for conducting such confirmation testing in a wide range of fields, including electrical and electronic, chemical, pharmaceutical, and foods, etc.

1) Toshikatsu Nishioka, Tatsuya Housaki: (2011) "A Guide on Plastic Analysis," Maruzen Publishing Co., Ltd.
2) Hirotomo Ochi, Hideo Okashita: Shimadzu Review, 45 (1-2), 51 (1988)
3) Sachio Murakami, et.al: Shimadzu Review, 69 (1-2), 133 (2012)

First Edition: May. 2015

SHIMADZU
Shimadzu Corporation
www.shimadzu.com/an/

Find us on

LinkedIn

ResearchGate

Contact us

https://www.shimadzu.com/an/contact/index.html

First Edition: March, 2019

SHIMADZU

Shimadzu Corporation

www.shimadzu.com/an